University of Alberta

Mathematical programming for sequence optimization in block cave mining

By
Yashar Pourrahimian

A thesis submitted to the Faculty of Graduate Studies and Research in partial fulfillment of the requirements for the degree of Doctor of Philosophy

in

Mining Engineering

Department of Civil and Environmental Engineering

Spring 2013
Edmonton, Alberta

This Thesis is lovingly dedicated:

To my wonderful parents, Mahmoudeh and Hashem
Who have stood by me in my best and worst times

To my lovely wife, Rozhin
Who gave life to my living

To my sister and brother, Aylar and Elyar
Who are my best friends & I'm proud to have them

And to Rozhin's family, Naser, Malak and Kaveh
For their support and patience

ABSTRACT

Production scheduling of any mining system has an enormous effect on the operation's economics. The economics of today's mining industry are such that the major mining companies are increasing the use of massive mining methods. Among the mining methods available, caving methods are favored because of their low cost and high production rates. Caving methods have become the underground bulk mining method of choice and are expected to continue as such in the foreseeable future.

The objective of this study is to develop, implement, and verify a theoretical optimization framework based on a mixed-integer linear programming (MILP) model for block-cave long-term production scheduling, whereby a mineral is extracted and prepared at a desired market specification, with the maximum economic return measured by NPV, and within acceptable technical and operational constraints. In this research, three MILP formulations are introduced for three levels of problem resolution (i) cluster level, (ii) drawpoint level, and (iii) drawpoint-and-slice level. These formulations can be used in two ways: (i) as a single-step method in which each of the formulations is used independently; (ii) as a multi-step method in which the solution of each step is used to reduce the number of variables in the next level and consequently to generate a practical block cave schedule in a reasonable amount of CPU runtime for large-scale problems.

The main scientific contribution of this research on the body of knowledge is the development, implementation, and verification of a theoretical framework for long-term production schedule optimization of block-cave mines using MILP. This research directly contributes to creating new knowledge, understanding, and innovative technologies that are required to generate near-optimal life-of-mine production schedules for block-cave mining operations. The main industrial contribution of this research includes development and testing of a prototype open-source software application with the graphical user interface, DSBC.

ACKNOWLEDGMENT

Working on the PhD was a wonderful and often overwhelming experience. I am indebted to many people for making the time working on my PhD an unforgettable experience.

First of all, I am deeply grateful to my advisors, Dr. Hooman Askari-Nasab and Dr. Dwayne Tannant for their continuous help and support in all stages of this thesis. I would also like to thank Dr. Hooman for being an open person to ideas, and for encouraging and helping me to shape my interest and ideas. I admire your ability to balance research interests and personal pursuits. Furthermore, I am very grateful to my advisory committee members – Dr. Jozef Szymanski, Dr. Jeffery Boisvert, Dr. Ming J. Zuo, and Dr. Alexandra M. Newman. Your comments and corrections are appreciated.

I am grateful for the insight and encouragement from my colleagues Messrs Behrang Koushavand, Eugene Ben-Awuah, Mohammad Tabesh, Mohammad Mahdi Badiozamani Tari, Hesameddin Eivazy, Shiv Prakash Upadhyay, Marclus Mwai, and Ms Samira Kalantari and Ms Elmira Torkamani. My gratitude also goes to all my friends in Edmonton for the support they offered me whilst pursuing this research.

I would like to thank my parents, Mahmoudeh and Hashem for their infinite support throughout everything. They have given their unconditional support, knowing that doing so contributed greatly to my absence these last five years. They were strong enough to let me go easily, to believe in me, and to let slip away all these years. I also would like to thank my sister and brother, Aylar and Elyar, who I always respect them for being a wonderful sister and brother. I would also like to thank my wife's family Malak, Naser and Kaveh for their patience and support they provided us during my research.

I would like to thank the most wonderful person who has chosen to spend her life with me as my soul mate. It is not possible to summarize Rozhin and her

influence on me in one paragraph, but I will try. Her love, intelligence, honesty, goodness, healthiness, humor, taste, liveliness, patience and beauty have given me something to live for. She is the most balanced and well-adjusted person I have ever known. The fact of her existence is a continual miracle to me. Without her encouragement and inspiration, I would not be able to accomplish my thesis.

Yashar Pourrahimian, January 2013

TABLE OF CONTENTS

ABSTRACT

AKNOWLEDGMENT

LIST OF FIGURES

LIST OF TABLES

LIST OF ABBREVIATIONS

NOMENCLATURE

CHAPTER 1: INTRODUCTION 1

1.1 Introduction 2

1.2 Statement of the Problem 4

1.3 Summary of Literature Review 8

1.4 Objective of the Study 10

1.5 Context and Scope of Work 11

1.6 Research Methodology 12

1.7 Scientific Contributions and Industrial Significance of the Research 19

1.8 Organization of Thesis 21

CHAPTER 2: LITERATURE REVIEW 23

2.1 Introduction 24

2.2 Caving Production System 26

2.3 Geotechnical Parameters Affecting the Planning of the Block Cave 28

2.4 Mine Production Scheduling 30

2.4.1 Open-Pit Production Scheduling 31

2.4.2 Underground Mines Production Scheduling 35

2.5 Application of Clustering in Mine-Production Scheduling 41

2.6 Rationale for PhD Research 43

2.7 Summary and Conclusions 44

CHAPTER 3: THEORETICAL FRAMEWORK: BLOCK-CAVE PRODUCTION SCHEDULING 46

3.1 Introduction 47

3.2 Planning a Block-Cave Mine 47

3.3 Clustering 52

3.3.1 Draw Columns Aggregation Using Hierarchical Clustering 53

3.4 Mathematical Programming Formulation 55
3.4.1 Models Assumption 56
3.4.2 Formulation of MILP Models 57
3.4.3 Objective Function at Three Level of Resolution 59
3.4.4 Constraints 59
3.4.4.1 Mining Capacity 60
3.4.4.2 Grade Blending 60
3.4.4.3 Maximum Number of Active Clusters or Drawpoints 60
3.4.4.4 Number of New Clusters or Drawpoints 60
3.4.4.5 Continuous Mining 61
3.4.4.6 Mining Precedence 61
3.4.4.7 Reserves 66
3.4.4.8 Draw Rate 66
3.4.5 MILP Formulations at Three Level of Resolution 66
3.4.5.1 Cluster-Level Model 66
3.4.6 Drawpoint-Level Model 72
3.4.7 Drawpoint-and-Slice Level Model 77
3.5 Multiple Mines 84
3.6 Summary and Conclusion 85
CHAPTER 4: MILP FORMULATION IMPLEMENTATION 86
4.1 Introduction 87
4.2 Numerical Modeling 88
4.3 General Formulation 88
4.3.1 The MILP Models Objective Function 89
4.3.2 The Constraints of the MILP Models 91
4.3.2.1 Mining capacity 95
4.3.2.2 Average Grade of Production 96
4.3.2.3 Opening, Closing, and Continuous Mining 97
4.3.2.4 Maximum Number of Active Clusters and Drawpoints 104
4.3.2.5 Mining Precedence 107
4.3.2.6 Number of New Clusters and Drawpoints 115
4.3.2.7 Draw rate 117
4.3.2.8 Reserves 120
4.3.3 Multiple Mines 121
4.4 Implementation of an Efficient MILP Model 122
4.4.1 Implementation of MILP Model with Fewer Binary Decision Variables 123

4.5 Summary and Conclusion 126
CHAPTER 5: VERIFICATION, EXPERIMENTS, AND DISCUSSION OF RESULTS 127
5.1 Introduction 128
5.2 Main Dataset 128
5.3 Application of the MILP Models using the Single-step Method 129
5.3.1 Application of the Single-step Method at the Cluster Level 132
5.3.2 Application of the Single-Step Method at the Drawpoint Level 144
5.3.3 Application of the Single-Step Method at the Drawpoint-and-Slice Level 151
5.3.4 Summary and Comparison of Results of Three Different Levels of Resolution 155
5.4 Application of the MILP Models using the Multi-Step Method 157
5.4.1 Summary of the Multi-Step Method 180
5.4.2 Sensitivity Analysis 181
5.4.3 Effectiveness of Multi-Step Method 189
5.5 Summary and Conclusion 192
CHAPTER 6: SUMMARY, CONCLUSIONS AND RECOMMENDATIONS 195
6.1 Summary of Research 196
6.2 Conclusions 202
6.3 Contributions of PhD Research 204
6.4 Recommendations for Future Research 205
BIBLIOGRAPHY 206
APPENDIX 216

LIST OF TABLES

Table 3.1. Calculating best height of draw (BHOD) 51
Table 4.1. Size of the coefficient vector of objective function for each model 90
Table 4.2. Size of the decision variables' vector and its order for each model..... 91
Table 4.3. Number of rows in constraint' coefficient matrix for different models..... 94
Table 5.1. Production scheduling parameters at cluster level..... 137
Table 5.2. Number of variables and constraints for cluster level with 17 clusters 137
Table 5.3. Numerical result for cluster level formulation with 17 clusters..... 138
Table 5.4. Production scheduling parameters at drawpoint level 145
Table 5.5. Numerical results for the drawpoint level formulation..... 145
Table 5.6. Number of variables and constraints at the drawpoint-and-slice level formulation with 102 drawpoints and 2,058 slices 151
Table 5.7. Numerical result for the drawpoint-and-slice level formulation with 102 drawpoints and 2,058 slices 151
Table 5.8. Comparison of results of the three levels of resolution for the single-step method..... 157
Table 5.9. Production scheduling parameters at cluster level..... 164
Table 5.10. Number of variables and constraints for cluster level with 35 clusters 164
Table 5.11. Numerical result for cluster level formulation with 35 clusters..... 164
Table 5.12. Number of variables and constraints at the drawpoint level with 298 drawpoints..... 171
Table 5.13. Numerical result for drawpoint level formulation with 298 drawpoints..... 172
Table 5.14. Number of variables and constraints at the drawpoint-and-slice level formulation with 298 drawpoints and 5,539 slices 176
Table 5.15. Numerical result for the drawpoint-and-slice level formulation with 298 drawpoints and 5,539 slices 176
Table 5.16. Results of the three levels of resolution for the multi-step method 181
Table 5.17. Production scheduling parameters for main scenario 182
Table 5.18. Different scenarios according to changes in draw rate 183
Table 5.19. Different scenarios according to changes in the maximum number of active clusters or drawpoints 183

Table 5.20. Different scenarios according to changes in the maximum number of new clusters or drawpoints 184
Table 5.21. Comparison of the results of MILP formulations for multi-step and single-step methods..... 190
Table 6.1. Summary of results from numerical application for single-step and multi-step methods 201

LIST OF FIGURES

Figure 1.1. Schematic representation of the problem definition 7
Figure 1.2. Summary of research methodology 15
Figure 1.3. Proposed clustering steps for block cave in west to east (WE) or vice versa (EW) with dots representing individual drawpoints 17
Figure 2.1. Isometric view of a caving operation at Henderson mine (Doepken, 1982) .. 25
Figure 2.2. Undercutting methods (Barraza and Crorkan, 2000)..... 28
Figure 3.1. Required steps for block-cave production scheduling using MILP..... 49
Figure 3.2. Defined phases based on advancement directions and their boundaries for west to east (WE) and east to west (EW) mining directions, with dots representing individual drawpoints..... 53
Figure 3.3. Clustering without phases for the west to east direction 54
Figure 3.4. Three different levels of resolution for block-cave production scheduling with dots representing individual drawpoints 58
Figure 3.5. Determination of the number of active clusters or drawpoints in each period. The green line shows the periods in which the related cluster or drawpoint is active 61
Figure 3.6. Determination method of the predecessor cluster based on the advancement direction 63
Figure 3.7. Offset herringbone extraction level layout (Brown, 2003)..... 65
Figure 3.8. Determination method of the predecessor drawpoints among the adjacent drawpoints based on the advancement direction..... 65
Figure 3.9. Determination method of the predecessor drawpoints based on the advancement direction 65

Figure 4.1. Order of constraints in the constraint' coefficient matrix for the cluster level and drawpoint level formulations 93
Figure 4.2. Order of constraints in the constraint' coefficient matrix for the drawpoint-and-slice level formulation..... 93
Figure 4.3. Divisions of the constraints' coefficient matrix according to the decision variables at the drawpoint-and-slice level formulation 94
Figure 4.4. The structure of each variable in the constraints coefficient matrix and decision variables vector..... 95
Figure 4.5. The structure of each variable in the constraint coefficient matrix and decision variable vector for multiple mines problem 122
Figure 4.6. Elimination of the variables related to the slices 125
Figure 5.1. Plan view of 298 drawpoints 128
Figure 5.2. Draw columns tonnage distribution..... 129
Figure 5.3. Height profile based on the main database 130
Figure 5.4. Grade profile based on the average grade of each draw column 130
Figure 5.5. Plan view of 102 drawpoints 131
Figure 5.6. 3D view of draw columns after applying the BHOD (102 draw columns) .. 132
Figure 5.7. Defined advancement lines to create clustering phases: (a) west to east or east to west direction, and (b) north to south or south to north direction..... 133
Figure 5.8. Available tonnage within each phase for different advancement directions: (a) WE/EW, and (b) NS/SN 134
Figure 5.9. Clusters and their information in WE and EW directions 135
Figure 5.10. Clusters and their information in NS and SN directions 136
Figure 5.11. Production tonnage for different directions at the cluster level over the mine life 138
Figure 5.12. Number of active clusters for different directions at the cluster level over the mine life 139
Figure 5.13. Number of active drawpoints for different directions at the cluster level over the mine life 139
Figure 5.14. Number of new clusters that must be opened for different directions at the cluster level over the mine life..... 140

Figure 5.15. Amount of depletion from clusters 8 and 17 in the WE and EW directions 142
Figure 5.16. Amount of depletion from clusters 8 and 17 in the NS and SN directions. 142
Figure 5.17. Discounted cash flow and cumulative DCF for different directions at the cluster level over the mine life 143
Figure 5.18. Opening pattern using the cluster-level formulation in the WE direction .. 144
Figure 5.19. Production tonnage for different directions at the drawpoint level over the mine life 146
Figure 5.20. Number of active drawpoints for different directions at the drawpoint level over the mine life 146
Figure 5.21. Number of new drawpoints that must be opened for different directions at the drawpoint level over the mine life 147
Figure 5.22. Amount of depletion from drawpoints 96 and 80 in the WE and EW directions 148
Figure 5.23. Amount of depletion from drawpoints 57 and 80 in the NS and SN directions 149
Figure 5.24. Discounted cash flow and cumulative DCF for different directions at the drawpoint level over the mine life 150
Figure 5.25. Opening pattern using the drawpoint level formulation in the WE direction 150
Figure 5.26. Production tonnage in the WE and SN directions at the drawpoint-and-slice level over the mine life 152
Figure 5.27. Number of active drawpoints in the WE and SN directions at the drawpoint-and-slice level over the mine life 153
Figure 5.28. Number of new drawpoints that must be opened in the WE and SN directions at drawpoint-and-slice level over the mine life 153
Figure 5.29. Average grade of production in the WE and SN directions at the drawpoint-and-slice level over the mine life 154
Figure 5.30. Opening pattern using the drawpoint-and-slice level formulation in the WE direction 154
Figure 5.31. Opening pattern using the drawpoint-and-slice level formulation in the SN direction 155

Figure 5.32. 3D view of the draw columns after applying the BHOD (298 draw columns) 158
Figure 5.33. Defined advancement lines to create clustering phases: (a) west to east or east to west direction (WE/EW), and (b) north to south or south to north direction (NS/SN)..... 160
Figure 5.34. Available tonnage within each phase for different advancement directions: (a) WE/EW, and (b) NS/SN..... 161
Figure 5.35. Clusters and their information in the WE and EW directions 162
Figure 5.36. Clusters and their information in the NS and SN directions..... 163
Figure 5.37. Production tonnage for different directions at the cluster level over the mine life 165
Figure 5.38. Number of active clusters for different directions at the cluster level over the mine life 166
Figure 5.39. Number of new clusters that must be opened for different directions at the cluster level over the mine life..... 166
Figure 5.40. Amount of depletion from clusters 10, 20, 22, and 35 in the WE and EW directions..... 167
Figure 5.41. Amount of depletion from clusters 16, 20, 28, and 33 in NS and SN directions..... 168
Figure 5.42. Discounted cash flow and cumulative DCF for different directions at the cluster level over the mine life..... 169
Figure 5.43. Opening pattern using the cluster level formulation in the WE direction for 298 drawpoints..... 170
Figure 5.44. Opening pattern using the cluster level formulation in the SN direction for 298 drawpoints..... 170
Figure 5.45. Production tonnage for WE and SN directions at the drawpoint level over the mine life 172
Figure 5.46. Number of active drawpoints in WE and SN directions at the drawpoint level over the mine life 173
Figure 5.47. Number of new drawpoints that must be opened in the WE and SN directions at the drawpoint level over the mine life..... 173
Figure 5.48. Amount of depletion from drawpoint 123 in the WE and SN directions ... 174

Figure 5.49. Opening pattern using the drawpoint level formulation in the WE direction for 298 drawpoints (multi-step method) 175
Figure 5.50. Opening pattern using the drawpoint level formulation in the SN direction for 298 drawpoints (multi-step method) 175
Figure 5.51. Satisfied constraints and opening pattern of drawpoints based on the drawpoint-and-slice level solution for the west to east direction..... 178
Figure 5.52. How to extract from drawpoint 56: (a) draw rate, and (b) percentage extraction from each slice within draw column associated with drawpoint 56..... 179
Figure 5.53. Comparison of the discounted cash flow for three levels of resolution in the west to east direction using the multi-step method 180
Figure 5.54. Impact of changes in the draw rate on the NPV and CPU time at the cluster level..... 184
Figure 5.55. Impact of changes in the draw rate on the NPV and CPU time at the drawpoint level..... 185
Figure 5.56. Impact of changes in the draw rate on the NPV and CPU time at the drawpoint-and-slice level..... 185
Figure 5.57. Impact of changes in the maximum number of active clusters on the NPV and CPU time at the cluster level..... 186
Figure 5.58. Impact of changes in the maximum number of active drawpoints on the NPV and CPU time at the drawpoint level 187
Figure 5.59. Impact of changes in the maximum number of active drawpoints on the NPV and CPU time at the drawpoint-and-slice level..... 187
Figure 5.60. Impact of changes in the maximum number of allowable new clusters on the NPV and CPU time at the cluster level..... 188
Figure 5.61. Impact of changes in the maximum number of allowable new drawpoints on the NPV and CPU time at the drawpoint level 188
Figure 5.62. Impact of changes in the maximum number of allowable new drawpoints on the NPV and CPU time at the drawpoint-and-slice level..... 189
Figure 5.63. Schematic comparison of the methods and levels of resolutions in terms of solution time and solution quality..... 191
Figure 6.1. Summary of the research methods..... 198

LIST OF ABBREVIATIONS

Parameters

BHOD	Best Height of Draw
DCF	Discounted Cash Flow
DSBC	Drawpoint Scheduling in Block-Caving
EPGAP	Relative MIP Gap Tolerance
GP	Goal Programming
LP	Linear Programming
MILP	Mixed Integer Linear Programming
MIP	Mixed Integer Programming
NPV	Net Present Value
QP	Quadratic Programming

LIST OF NOMENCLATURE

Sets

S^{cl}	For each cluster, *cl*, there is a set, S^{cl}, defining the predecessor clusters that must be started prior to extracting cluster *cl*.
S^{d}	For each drawpoint, *d*, there is a set, S^{d}, defining the predecessor drawpoints that must be started prior to extracting drawpoint *d*.
S^{ds}	For each drawpoint, *d*, there is a set S^{ds} defining the slices in the draw column associated with drawpoint *d*.
S^{dls}	For each drawpoint, *d*, there is a set S^{dls} defining the lowest slice within the draw column associated with drawpoint *d*.
S^{s}	For each slice, *s*, there is a set S^{s} defining the predecessor slices that must be extracted prior to extracting slice *s*.

Indices

$cl \in \{1,...,CL\}$	Index for clusters.
$d \in \{1,...,D\}$	Index for drawpoints.
$e \in \{1,...,E\}$	Index for elements of interest in each slice.
k	Index for a cluster belonging to set S^{cl}.
l	Index for a drawpoint belonging to set S^{d}.
n	Index for a slice belonging to set S^{ds}.
p	Index for a slice belonging to set S^{dls}.
q	Index for a slice belonging to set S^{s}.
$s \in \{1,...,S\}$	Index for slices.
$t \in \{1,....,T\}$	Index for scheduling periods.

Decision variables

Cluster level model

$A_{cl,t} \in \{0,1\}$ Binary decision variable equal to 1 if cluster *cl* is active in period *t*; otherwise it is 0.

$U_{cl,t} \in [0,1]$ Continuous decision variable, representing the portion of cluster *cl* to be extracted in period *t*.

$Z_{cl,t} \in \{0,1\}$ Binary variable controlling the precedence of extraction of clusters. It is equal to 1 if extraction from cluster *cl* is started in period *t*; otherwise it is 0.

Drawpoint level model

$A_{d,t} \in \{0,1\}$ Binary decision variable equal to 1 if drawpoint *d* is active in period *t*; otherwise it is 0.

$U_{d,t} \in [0,1]$ Continuous decision variable, representing the portion of drawpoint *d* to be extracted in period *t*.

$Z_{d,t} \in \{0,1\}$ Binary variable controlling the precedence of extraction of drawpoints. It is equal to 1 if extraction from drawpoint *d* is started in period *t*; otherwise it is 0.

Drawpoint-and- slice level model

$B_{s,t} \in \{0,1\}$ Binary variable controlling the precedence of the extraction of slices. It is equal to 1 if the extraction of slice *s* has started by or in period *t*; otherwise it is 0.

$C_{d,t} \in \{0,1\}$ Binary variable controlling the closing period of drawpoints. It is equal to 1 if the extraction of drawpoint *d* has finished by or in period *t*; otherwise it is 0.

$E_{d,t} \in \{0,1\}$ Binary variable controlling the starting period of drawpoints and precedence of extraction of drawpoints. It is equal to 1 if the extraction of drawpoint *d* has started by or in period *t*; otherwise it is 0.

$X_{s,t} \in [0,1]$ Continuous decision variable representing the portion of slice s to be extracted in period t.

Parameters

CL Maximum number of clusters in the model.

$CLEV_{cl}$ Economic value of cluster cl.

D Maximum number of drawpoints in the model.

DC Direct mining cost.

DEV_d Economic value of the draw column associated with drawpoint d.

D_{ij} Distance value between draw columns i and j.

$\widetilde{D}_{ij}$ Normalized distance value between draw columns i and j.

$\underline{DR}_{d,t}$ Minimum possible draw rate of drawpoint d in period t.

$\overline{DR}_{d,t}$ Maximum possible draw rate of drawpoint d in period t.

$\underline{DR}_{k,t}$ Minimum possible draw rate of drawpoints belonging to set S^{cl} in period t.

$\overline{DR}_{k,t}$ Maximum possible draw rate of drawpoints belonging to set S^{cl} in period t.

G_{es} Average grade of element e in the ore portion of slice s.

$\overline{G}_{e,t}$ Upper limit of the acceptable average head grade of element e in period t.

$\underline{G}_{e,t}$ Lower limit of the acceptable average head grade of element e in period t.

G_{ij} Grade difference between draw columns i and j.

$\widetilde{G}_{ij}$	Normalized grade difference between draw columns i and j.
gr_e	Grade of the element e.
i	Discount rate.
$\underline{M}_t$	Lower limit of mining capacity in period t.
$\overline{M}_t$	Upper limit of mining capacity in period t.
MC	Milling cost.
$N_{Acl,t}$	Maximum allowable number of active clusters in period t.
$N_{Ad,t}$	Maximum allowable number of active drawpoints in period t.
$\underline{N}_{Ncl,t}$	Lower limit for the number of new clusters, the extraction from which can start in period t.
$\overline{N}_{Ncl,t}$	Upper limit for the number of new clusters, the extraction from which can start in period t.
$\underline{N}_{Nd,t}$	Lower limit for the number of new drawpoints, the extraction from which can start in period t.
$\overline{N}_{Nd,t}$	Upper limit for the number of new drawpoints, the extraction from which can start in period t.
NDP_{cl}	Number of draw columns within cluster cl.
Ns_d	Number of slices within the draw column associated with drawpoint d.
OC	Overhead costs.
S	Maximum number of slices in the model.

SEV_s	Economic value of slice *s*.
T	Maximum number of scheduling periods.
T_{ij}	Tonnage difference between draw columns *i* and *j*.
$\tilde{T}_{ij}$	Normalized tonnage difference between draw columns *i* and *j*.
Ton_{cl}	Total tonnage of material within cluster *cl*.
Ton_d	Total tonnage of material within the draw column associated with drawpoint *d*.
Ton_s	Total tonnage of material within slice *s*.
$U\,\mathrm{Re}v_e$	Revenue factor per unit of the element *e*.
WD	Weighting factor for distance.
WG	Weighting factor for grade.
WT	Weighting factor for tonnage.

CHAPTER 1

INTRODUCTION

This chapter is a general overview of the research. It discusses the background of the study; the problem statement; the study's objectives, context and scope; the proposed methodology; and the contributions of the research.

1.1 Introduction

Mine planning consists of defining the source, destination and extraction time of ore and waste during the mine-life. Production scheduling of any mining system has an enormous effect on the operation's economics. Nowadays, production scheduling is one of the key components in determining mine viability, because the mining industry faces lower grade and marginal reserves (Burgher and Erickson, 1984; Dagdelen and Johnson, 1986; Chanda, 1990). Production scheduling defines the tonnages and grades to be mined throughout the mine-life. The scheduling problems are usually complex due to the nature and variety of the constraints on the system. A production schedule must provide a mining sequence that takes into account the physical limitations of the mine and, to the extent possible, meets the demanded quantities of each raw ore type at each time period throughout the mine-life.

The economics of today's mining industry are such that the major mining companies are increasing the use of massive mining methods. Among the mining methods available, caving methods are favored because of their low cost and high production rates. Caving methods have become the underground bulk mining method of choice and are expected to continue in the foreseeable future. One of these methods is block caving, which has gained popularity due to its low operating cost and high productivity. Laubscher (1994) defines block caving as:

> Cave mining refers to all mining operations in which the ore-body caves naturally after under cutting its base. The caved material is recovered using drawpoints.

Some of this method's advantages include low cost, centralized production, simple ventilation control, and high production rates. Block cave mine planning poses complexities in different areas such as safety, environment, ground control and production scheduling. As the mining industry is faced with more marginal resources, it is becoming essential to generate production schedules which will

provide optimal operating strategies while meeting technical and environmental constraints.

Improvements in computing power and scheduling algorithms over the past years have allowed planning engineers to develop models to schedule even more complex mining systems (Alford et al., 2007; Caccetta, 2007). Consequently, it is now possible to formulate a mixed-integer linear programming (MILP) scheduling model that captures the essential components of a caving mine to generate a robust, practical, near-optimal schedule. The caving industry is now moving towards the next generation of caving geometries and scenarios: super caves (Chitombo, 2010). This requires a new approach in looking at the scheduling of block-cave operations, and this is what this research seeks to introduce.

There are three time horizons for production scheduling: long, medium and short-term. The long-term mine production scheduling provides a strategic plan for the mining operations, whereas the medium-term mine production schedule provides a monthly operational scheme for mining while tracking the strategic plan. Medium-term schedules include more detailed information that allows for a more accurate design of ore extraction from a special area of the mine, or information that would allow for necessary equipment substitution or the purchase of needed equipment and machinery. The medium-term schedule is also divided into short-term periods (Osanloo et al., 2008). A long-term production schedule contains fewer details than a short-term plan. However a long-term plan includes clear definitions related to mining reserves, production sequence, and production rate.

A production scheduling methodology that is based on a limited number of influential parameters will lead to optimistic production schedules. In addition, the geotechnical behavior of the rockmass must be considered for production scheduling. Currently, production targets are the result of production schedules computed with mine planning parameters that do not evolve as a function of the operational performance, and are not linked to the geotechnical behavior of rock

mass. Also, relying only on manual planning methods or computer software that is based on heuristic algorithms will lead to mine schedules that are not the optimal global solution.

In this research, the main focus will be on long-term production planning in block cave mines. Long-term production planning determines the distribution of cash flows over the mine-life and the feasibility of the project; and it is also a very important prerequisite for medium- and short-term scheduling. One of the main goals of long-term production planning is to integrate internal and external mine planning factors that affect the mine operation's performance. Mines use the schedules as short-term operational guides, and as long-term strategic planning tools to determine when to start mining a production area.

1.2 Statement of the Problem

The proposed research lies within the area of applied operations research. The research problem is classified as production scheduling in the context of mine planning.

In the case of a block-cave mine, the production schedule mainly defines the amount of the material to be mined from the drawpoints in every period of production, to achieve a given planning objective. The mine plan also defines the number of new drawpoints that need to be constructed, and their sequence, to support a given production target. In other words, scheduling a block-cave mine is a matter of finding the goal that better represents the strategic planning vision subject to the following constraints: mine design, geomechanical, operational, and environmental. The production schedule is subject to a variety of physical and economic constraints. The constraints enforce the production target, draw rate, mining precedence, maximum number of active drawpoints, number of new drawpoints in each period, continuous mining, and complete extraction of reserves.

The following research question drives this dissertation.

Can a strategic long-term production schedule for block-cave mines be generated that will result in the near-optimal net present value for the mining operation while honoring all the operational and technical constraints, such as development rate, vertical mining rate, lateral mining rate, mining capacity, maximum number of active drawpoints, and advancement direction?

The block-cave long-term production schedule must:

- Determine the best advancement direction.
- Determine the order, time, and tonnage of extraction of material from drawpoints over the mine life that maximizes the net present value (NPV) of the operation.
- Determine the long-term production schedule for a block-cave mine at different levels of resolutions: (i) cluster level, (ii) drawpoint level, and (iii) drawpoint-and-slice level.
- Generate a robust practical near-optimal schedule in a reasonable amount of CPU time using a multi-stage approach incorporating the models at different levels of resolutions.

In this research, the block-cave long-term production scheduling problem is studied based on the following assumptions:

- The ore-body is represented by a geological block model, which is a three-dimensional array of rectangular or cubical blocks.
- The column of rock above each drawpoint, which is referred to as a draw column, is divided into slices which match the vertical spacing of the geological block model. The slices are stored in a slice file.
- The draw columns, which are vertical, are created based on the block model.

- Numerical data are used to represent each attribute of the ore-body, such as tonnage, density, grade of elements, elevation, percentage of dilution, and economic data for each slice.

- It is assumed that the physical layout of the production level is offset herringbone (Brown, 2003).

- The model is used for multi-period optimization.

- There is no material mixing between blocks as a function of draw, meaning that the source model is assumed to be static over time.

- The dilution is taken into account in the slice-file, which is the input into the production scheduling optimization model.

- The draw columns are aggregated by being grouped into clusters based on similarities between their physical location, average grade, and tonnage.

- The portion scheduled to be extracted from each cluster is assumed to be taken from all the drawpoints, based on the ratio of each draw column's tonnage in the cluster (Pourrahimian et al., 2012a).

Figure 1.1 illustrates the scheduling of a block-cave mine containing D draw columns. Each draw column d is made up of N_{sd} slices. The material in each draw column is scheduled over T periods respecting the constraints associated with mining operation and geomechanical conditions. The parameters ton_t and g_t represent the amount of material scheduled to be extracted and average grade of material scheduled in each period, respectively. The indices indicate the periods. The amount of ton_t and g_t must be computed so that (a) all constraints are satisfied, and (b) the NPV is maximized. If there are multiple mines, the same concept is applied. For multiple mines, the value of the discounted cash flow (DCF) is obtained from all mines for each period. For instance, if there are four mines, the value of the DCF for period t is equal to the summation of the DCF values for four mines in period t.

The long-term production schedules to be developed are subject to a variety of technical and physical constraints. The constraints control the development rate, vertical mining rate (production rate per drawpoint), lateral mining rate (rate of opening new drawpoints), mining capacity, maximum number of active drawpoints, cave draw strategies, and advancement direction.

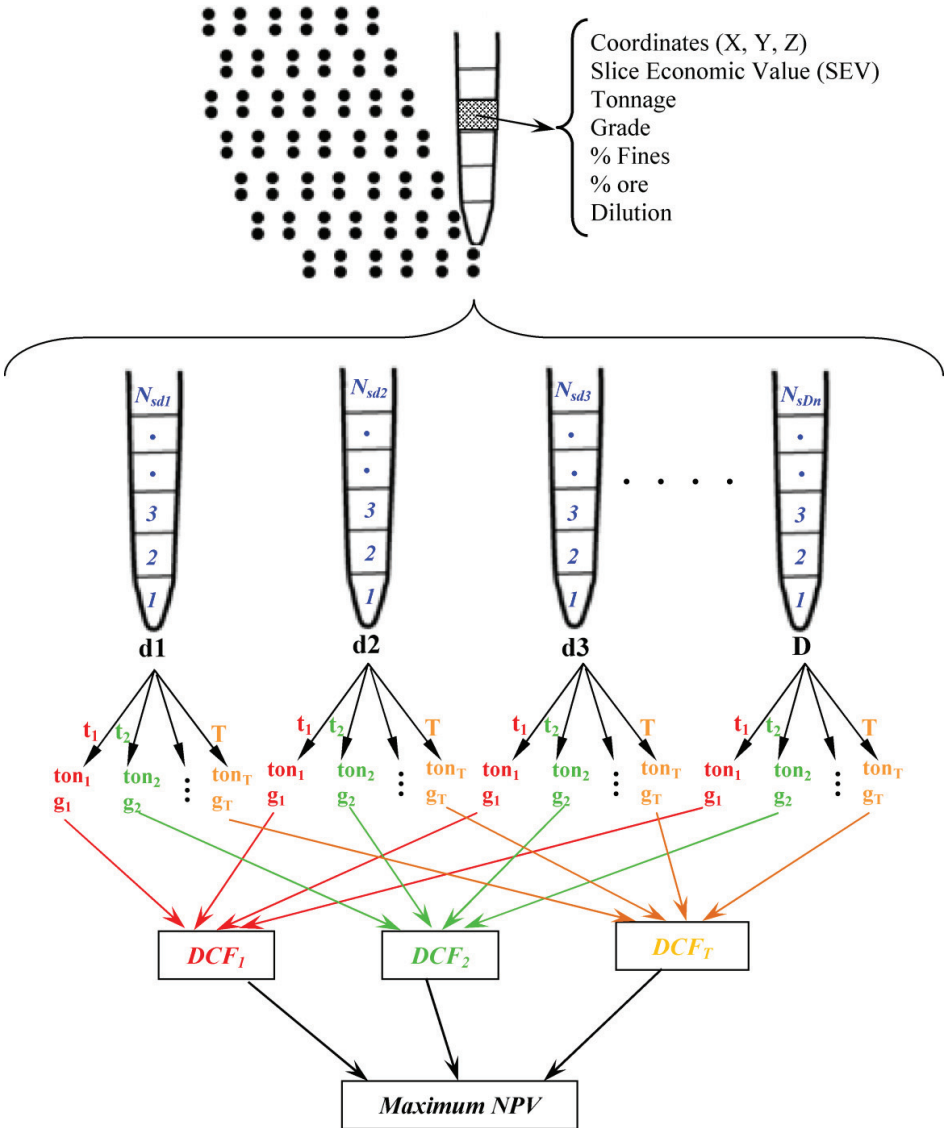

Figure 1.1. Schematic representation of the problem definition

1.3 Summary of Literature Review

Using mathematical programming optimization with exact solution methods to solve the long-term production planning problem has proved to be robust and results in answers within known limits of optimality. As the solution gets closer to optimality, it leads to production schedules that generate higher NPV than those obtained from heuristic optimization methods. This has led to extensive research on the application of mathematical programming models to the long-term production planning problem. When these models are applied to the long-term production planning problem, they result in large-scale optimization problems with numerous binary and continuous variables which become difficult to solve with the current state of hardware and software and may have lengthy solution times.

The majority of the scheduling publications to date have been concerned with open-pit mining applications. Underground mining is more complex in nature than surface mining (Kuchta et al., 2004). Underground mining is less flexible than surface mining due to the geotechnical, equipment, and space constraints (Topal, 2008). As a result, many of the scheduling concepts and algorithms developed for surface mining have found their way into underground applications.

Current practice in underground mine scheduling has tended toward the use of simulation and heuristic software to determine feasible rather than optimal schedules. A compromise between schedule quality and problem size has forced the use of mine design and planning models which incorporate the essential characteristics of the mining system while remaining mathematically tractable. Different types of scheduling methods have been applied to underground mine scheduling. Production scheduling algorithms and formulations in literature can be divided into two main research areas: 1) heuristic methods and 2) exact solution methods for optimization. In addition to these categories, other methods such as queuing theory (Su, 1986; Huang and Kumar, 1994), network analysis (Russell, 1987; Brazil et al., 2000; Brazil et al., 2003), and dynamic programming

(Sherer and Gentry, 1982; Muge et al., 1992) have been used to schedule production and/or material transport.

The mathematical programming models that have been used for underground mine production scheduling include: linear programming (LP), mixed-integer programming (MIP), mixed-integer linear programming (MILP), goal programming (GP), and quadratic programming (QP) (Song, 1989; Chanda, 1990; Trout, 1995; Winkler, 1998b; Guest et al., 2000; Carlyle and Eaves, 2001; Rubio, 2002; Rahal et al., 2003; Smith et al., 2003; Diering, 2004; Newman and Kuchta, 2007; Rahal, 2008; Weintraub et al., 2008; Diering, 2012; Parkinson, 2012; Pourrahimian et al., 2012a; Pourrahimian et al., 2012c). Most of these methods are faced with the practical implementation due to numerous constraints and size of the optimization problem. Therefore, various methods of aggregation have been used to reduce the number of integer variables that are required to formulate the mine planning problem with MILP techniques (Epstein et al., 2003; Newman and Kuchta, 2007; Weintraub et al., 2008; Askari-Nasab et al., 2011; Tabesh and Askari-Nasab, 2011; Pourrahimian et al., 2012a).

In a block-caving method, a production scheduling methodology that is based on a limited number of influential parameters will lead to optimistic production schedules. In addition, the geotechnical behavior of the rock mass must be considered for production scheduling. Currently, production targets are the result of production schedules computed with mine planning parameters that do not evolve as a function of the operational performance, and are not linked to the geotechnical behavior of rock mass. Also, relying only on manual planning methods or computer software that is based on heuristic algorithms will lead to mine schedules that do not represent optimal global solution.

The limitations in the current production scheduling optimization in block caving are: (i) limitations in solving large-scale problems. These come about as a result of significant computer overhead, in terms of memory and speed, required to solve the large-scale problems; (ii) treatment of stochastic variables such as grade,

commodity price, and production cost as deterministic processes. This can generate suboptimal results; (iii) trial-and-error process to find the mining start point and advancement direction; (iv) integration of fewer geotechnical constraints into real-scale production scheduling. These limitations can affect the viability as well as other aspects of mining projects, emphasizing the need for optimization tools that take into consideration these deficiencies. Consequently, it is important that robust models are developed to address these challenges.

The lack of a mathematical block-cave production schedule model for long-term production scheduling that takes more number of detail constraints into account with the ability to find the best starting point and advancement direction of mining, is worrisome. This research will introduce a MILP mine scheduling framework for block-caving in which from the mentioned limitations, solving a large-scale problem in a reasonable CPU time, the mining starting point and advancement direction will be addressed to generate a near-optimal production schedule with higher NPV compared to heuristic methods.

1.4 Objective of the Study

The objective of this study is to develop, implement, and verify a theoretical optimization framework for block-cave long-term production scheduling, whereby a mineral is extracted and prepared at a desired market specification, with the maximum economic return measured by NPV, and within acceptable technical and operational constraints.

The resultant methodology generates practical near-optimal production schedules that honor the following operational constraints: the development rate, vertical mining rate (production rate per drawpoint), lateral mining rate (rate of opening new drawpoints), mining capacity, maximum number of active drawpoints, cave draw strategies, and advancement direction.

To achieve the objectives, this work includes the development and testing of a theoretical and conceptual framework using mixed-integer linear mathematical programming that focuses on:

- Maximizing the NPV of the mining operations considering the effect of technical and operational conditions on mine-production schedules.

- Developing techniques and methodologies that can generate strategic schedules for large block-cave projects.

- Developing computer code and tools that implement the formulated model for block-cave operations.

- Developing techniques that can generate near-optimal realistic mine plans in a reasonable amount of CPU time that has practical merit and is accepted as an implementable mine plan by practitioners and end-users.

- Evaluating the generated results in terms of mining-practice feasibility and optimality of the solution on large-scale real-world problems.

1.5 Context and Scope of Work

The study addresses the development of a mixed-integer programming model for long-term production scheduling in a block-caving operation in the presence of operational and geomechanical constraints. Meanwhile, the approach in which tonnages are depleted from the draw columns is scalable from long-term to short-term applications. The algorithm's objective is to maximize the NPV of block-caving operations subject to geological, operating, and marketing requirements and constraints. A comprehensive problem definition and mathematical modeling are carried out to define and develop the MILP models, which comply with the objectives of the study.

It should be noted that the study will have limitations due to the assumptions and methodologies incorporated.

- Gemcom's GEMS and PCBC (Gemcom Software International, 2012) are used to build geologic and economic block models, assigning the drawpoint locations, converting the geological and grade information from being block-

model-based to drawpoint-based, computing drawpoint reserves, and creating slice files.

- A production schedule for a block-cave mine is generated using developed MILP models.

It is assumed that data from the geologic block models are deterministic; no attribute uncertainties will be considered. Another assumption is that the size of the layout is fixed.

The input data into the long-term production scheduler, such as geological block model, grades, costs, prices, recoveries, and practical mining constraints, are based on the best point estimates available at the time of optimization. Any change in the input data requires a re-optimization of the production schedule with the new input parameters. This is aligned with the mining industry practice of updating yearly, quarterly, monthly, and weekly mine plans, as new data become available and uncertainty is reduced over time. In other words, the limitation of this approach is similar to any deterministic model in capturing uncertainty. Detail parameters such as drilling, blasting, and ventilation are not considered.

1.6 Research Methodology

The main motivation for conducting this research is to improve long-term block-cave production schedules with a focus on operational constraints using a MILP mine-planning framework. The MILP is suitable for scheduling mine production because it is a well known operations research technique that exploits the strengths of modern linear programming algorithms while allowing the representation of production decisions (yes/no) as binary values. The objective is to maximize the expected NPV. The first part of this study involves a thorough literature survey on block-cave mining method, mine-production scheduling optimization, including surface and underground mining methods, and clustering algorithms.

The following is a summary of the research tasks that must be completed to achieve the study's objectives:

- Propose and develop a theoretical framework using mathematical programming, specifically MILP, for production scheduling of block-cave mines without considering a flow model for the material.
- Test, calibrate and verify the formulations and analyze the results in relation to the expected and inherent behavior of the theoretical and practical aspects of the formulations.
- Implement these formulations for block-cave-mine case studies to generate life-of-mine production schedules. For large mines, clustering algorithms will be used to combine draw columns to decrease both the number of variables in the model and the solution time.
- Assess the results of the case studies in terms of feasibility from a mining-practice point of view. Also, test the methodology to confirm that the results are within an acceptable range of the theoretical optimum and acceptable CPU runtime to be considered practical from the end-users' point of view.
- Quantify the impact of the use of the MILP formulations and the developed workflow on the block-caving operation with respect to NPV.
- Provide complete documentation on the workflow and parameter calibration.

Appropriate mining concepts, and mathematical and numerical models were formulated to define the inputs and outputs of the MILP mine-planning framework. The research focuses on developing, analyzing and implementing a theoretical framework to address the long-tem production scheduling problem of block-cave mines.

Figure 1.2 illustrates a summary of the research methodology. All stages before scheduling, from creating a block model to converting slice file, are done using GEMS and PCBC (Gemcom Software International, 2012). After creating the

slice file, all the optimization steps are done using our developed software for drawpoint scheduling in block-caving (DSBC). The separated steps based on each software include:

- GEMS and PCBC

    1. Creating a block model using GEMS
    2. Importing drawpoints data such as coordinates, dip, and azimuth
    3. Creating a slice file using PCBC
    4. Calculating the best height of draw (BHOD)

- DSBC

    1. Importing the slice file, the BHOD file, and coordinates of drawpoints in DSBC
    2. Creating all required databases and sets to use in the developed MILP models
    3. Clustering the draw columns based on the similarity of the draw column's tonnage, average grade, and physical location
    4. Defining the scheduling parameters
    5. Creating an objective function and constraints for each model
    6. Solving the problem using one of the methods: either single-step or multi-step
    7. Discussing the results

The first step is to create a block model, using GEMS, to provide a quantitative description of the rockmass, including and surrounding the cave zone. Then, drawpoint locations are defined and PCBC is used to convert block-model data into drawpoint-based data. Afterwards, the slices are constructed for each drawpoint. These slices represent the draw column above each drawpoint before any extraction begins. The best height of draw (BHOD) for each draw column is estimated. The BHOD is the height that produces the best economic value.

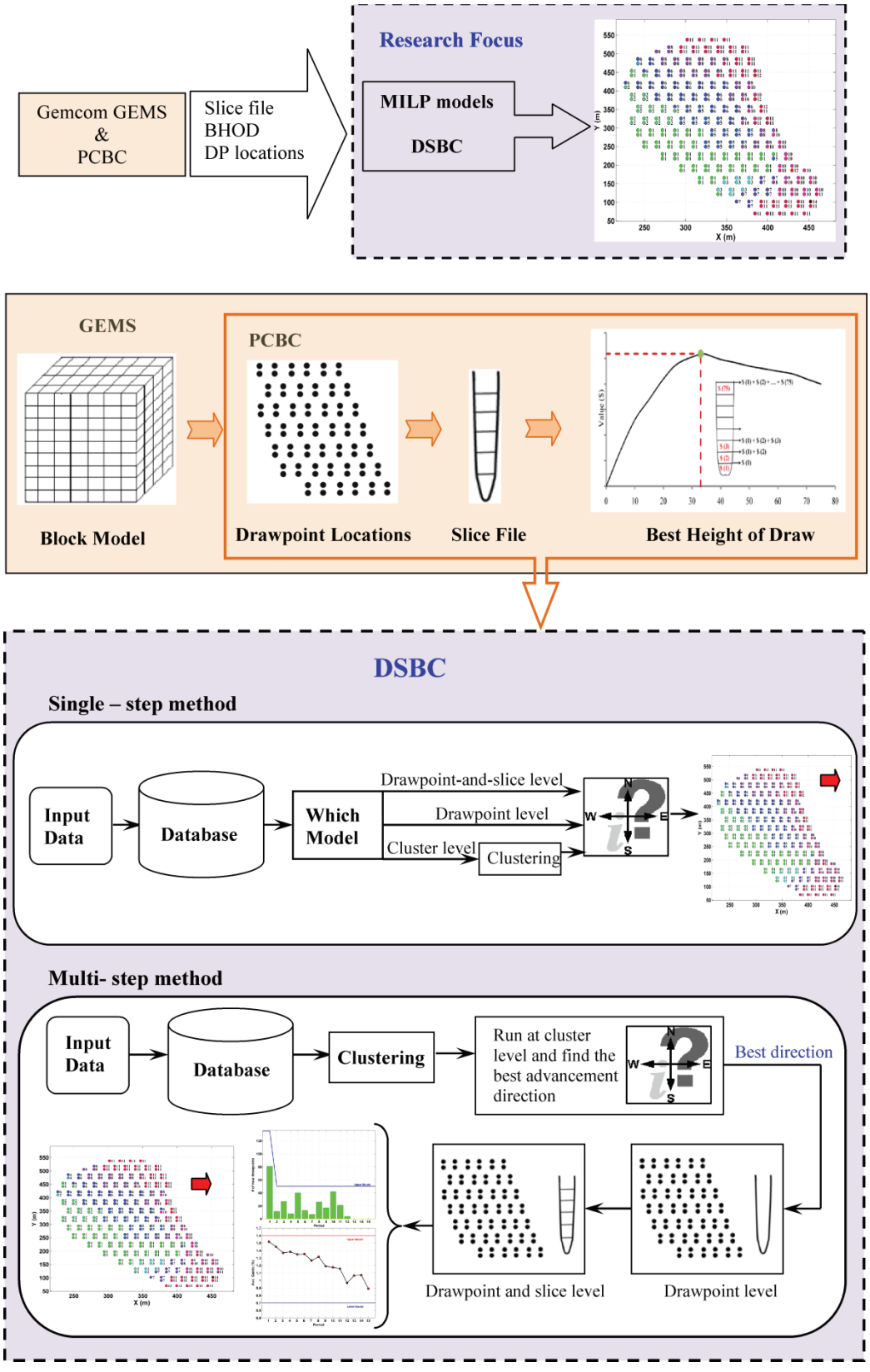

Figure 1.2. Summary of research methodology

Usually, it is not discounted with time (Diering and Villa, 2007). Afterwards, a block cave mine's production schedule can be optimized using the MILP formulations. There are two different approaches for production schedule optimization: single-step and multi-step.

After importing the output of the PCBC in the DSBC, the BHOD is applied to the original draw columns and the final height of draw is obtained for each draw column. It must be mentioned that, the BHOD can also be calculated by the MILP models. For this purpose the obtained BHOD from the PCBC is not applied to the original draw columns and optimization is done using the original draw columns. Afterwards, slices within the same draw column are grouped and the total tonnage, draw column economic value, and average weighted grade are calculated for each draw column to use at the drawpoint level model. Then, all required sets, and the precedence and database are created. A MATLAB (2011) application is used as the programming platform to define the MILP model. A TOMLAB/CPLEX (Holmstrom, 2011) solver, which uses a branch-and-cut optimization algorithm, is employed to solve the MILP problem. This algorithm is a hybrid of branch-and-bound and cutting-plane methods (Horst and Hoang, 1996; Wolsey, 1998). The user sets an optimization termination criterion in CPLEX known as the gap tolerance (EPGAP). The EPGAP, which is a measure of optimality, sets an absolute tolerance on the gap between the best integer objective and the objective of the best node remaining in the branch-and-cut algorithm. It instructs CPLEX to terminate once a feasible integer solution within the set EPGAP has been found. As the solution gets closer to optimality, it leads to production schedules that generate a higher NPV than those obtained from heuristic optimization methods.

In the single-step method, which is better for use with small mines, the problem can be solved separately, at different levels of resolution. To solve the problem at the cluster-level, the drawpoints are first grouped into clusters based on similarities between their physical location and tonnage and average grade of draw column above each drawpoint. For this purpose, the planner divides the

mine into phases based on advancement directions. Figure 1.3a shows phases and their boundaries for west to east (WE) and east to west (EW) mining directions.

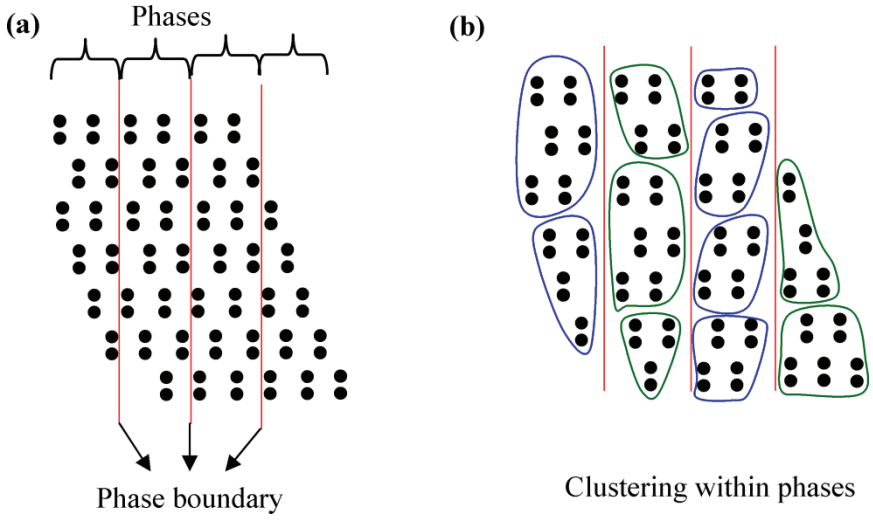

Figure 1.3. Proposed clustering steps for block cave in west to east (WE) or vice versa (EW) with dots representing individual drawpoints

Then, the draw columns within each phase are aggregated into practical scheduling units, using modified hierarchical clustering algorithms based on an algorithm presented by Tabesh and Askari-Nasab (2011) (see Figure 1.3b). Similar to drawpoints, each cluster has coordinates representing the center of the cluster and its coordinates. We assume that the portion scheduled to be extracted from each cluster is taken from all the drawpoints, based on the ratio of each draw column's tonnage in the cluster (Pourrahimian et al., 2012a). Then, using the MILP formulation at the cluster level, the optimal life-of-mine multi-period block-cave production schedule is generated for different advancement directions. The number of practical directions that we can use is limited based on geotechnical constraint. The direction with the maximum NPV is chosen as the mining direction. This is the strategic yearly production schedule with the objective of NPV maximization. The strategic plan honors the mining capacity and uniform feed to the processing plant.

To solve the problem at the drawpoint level, the related MILP formulation is used and the optimal long-term block-cave production schedule at the drawpoint level

is generated for different advancement directions. The direction with the maximum NPV is chosen as the mining direction. At the drawpoint-and-slice level, the related MILP formulation can be used to generate the optimal medium-term plan at the drawpoint level including slices. The time horizon for this detailed 3D model could vary as a subset of the time horizons chosen in the drawpoint level or the life of the mine. It should be mentioned that at the cluster and drawpoint level formulations, the precedence between clusters or drawpoints is controlled in a horizontal direction, but at the drawpoint-and-slice level formulation, the precedence between drawpoints and slices is controlled in horizontal and vertical directions, respectively.

To overcome the size problem of mathematical programming models and to generate a robust practical near-optimal schedule, the multi-step method for long-term production scheduling of block caving is used. After clustering, the problem is solved using the related MILP formulation at the cluster level for different possible advancement directions based on geotechnical constraints. Then, according to the value of the NPV and the practicality of the schedule, the best advancement direction is chosen among the assessed directions. The problem is only solved for the best direction at the two other levels of resolution. The solution of the cluster level is used to eliminate the variables to reduce the computational time at the drawpoint-level model. After solving the drawpoint-level model, the solution is used to eliminate the variables at the drawpoint-and-slice level. The time horizon for this detailed 3D model could vary as a subset of the time horizons chosen in the drawpoint level or life-of-the-mine.

In general, the development and implementation of the MILP optimization models framework was undertaken in three major stages. The first stage involved introducing the MILP model and how it can be applied for mine production scheduling (Pourrahimian and Askari-Nasab, 2009a; Pourrahimian and Askari-Nasab, 2009b; Pourrahimian et al., 2009c; Pourrahimian and Askari-Nasab, 2010a; Pourrahimian and Askari-Nasab, 2010b). The second stage included

extending the MILP models for different level of resolutions (Pourrahimian and Askari-Nasab, 2011; Pourrahimian et al., 2012a; Pourrahimian et al., 2012c).

Finally, an efficient form of the MILP models was deployed. Based on the size of the mine, production scheduling can be achieved by two methods: single-step or multi-step (Pourrahimian et al., 2012c). These approaches were used to facilitate continuous feedback from the research community and industry experts in an effort to improve the model.

1.7 Scientific Contributions and Industrial Significance of the Research

The main scientific contribution of this research on the body of knowledge is the development, implementation, and verification of a theoretical framework for long-term production schedule optimization of block-cave mines using MILP. This research directly contributes to creating new knowledge, understanding, and innovative technologies that are required to generate near-optimal life-of-mine production schedules for block-cave mining operations.

The proposed formulation and methodology developed offers the following significant improvements over the previous research in the context of mathematical programming models for block-cave production scheduling:

- Proposition of three MILP production scheduling models at three levels of detailed resolution.
- Consideration of a multistage solution methodology using the three above-mentioned MILP models to generate a practical block-cave schedule in a reasonable amount of CPU runtime.
- Consideration of a multistage solution methodology using the three above-mentioned MILP models to generate a practical block-cave schedule in a reasonable CPU runtime.
- Proposition of using a hierarchical clustering algorithm based on the cave advancement direction to aggregate drawpoints into selective mining-units of

scheduling. The contribution of drawpoint aggregation is twofold: (a) it generates a practical mining schedule that follows a selective mining-unit, and (b) reduces the number of variables, especially binary variables in the MILP formulation, to make it computationally tractable.

- Introduction of the concept of different cave advancement directions to find the best single operation direction or combination thereof, and the best starting location. Since the caving industry is now moving towards the next generation of caving geometries and scenarios, super caves, this concept will be useful.

The main industrial contribution of this research includes development and testing of a prototype open-source software application with the graphical user interface, DSBC. The prototype software contributes to transferring knowledge and optimization technology developed in this research to practitioners and end-users in the field of block-cave production scheduling.

DSBC allows block-cave mine planners to generate practical near-optimal life-of-mine production schedules while controlling:

1. Mining capacity
2. Draw rate
3. Grade blending
4. Continuous mining
5. Reserves
6. Mining precedence
7. Maximum number of active drawpoints
8. Number of new drawpoints in each period

1.8 Organization of Thesis

Chapter 1 is a general overview of the research. It discusses the background of the study, followed by the problem statement, objectives, context, scope, proposed methodology and contributions of the research.

Chapter 2, the literature review, provides an overview of production scheduling in mining operations. It presents the difference between production scheduling in surface and underground operations. It provides background about the block-cave mining system, as well as planning methodologies used in block caving. Clustering algorithms and their applications in mine planning are also highlighted. The chapter concludes with the rationale for this PhD research.

Chapter 3 contains the theoretical framework for the MILP formulations for block-cave production-scheduling optimization. It contains the mixed integer linear programming (MILP) formulations for three levels of resolution: (i) cluster level, (ii) drawpoint level, and (iii) drawpoint-and-slice level. This chapter describes how the production models can be used in practice. To overcome the size problem of mathematical programming models and to generate a robust, practical, near-optimal schedule, a clustering method for long-term production scheduling of block caving is presented. The production scheduler aims to maximize the net present value of the mining operation while the mine planner has control over the development rate, vertical mining rate, lateral mining rate, mining capacity, maximum number of active drawpoints, and advancement direction. To support a given production target, the production scheduler defines the opening and closing time for each drawpoint and cluster, the draw rate from each drawpoint and cluster, the number of new drawpoints and clusters that need to be constructed, and the sequence of extraction from the drawpoints and clusters.

Chapter 4 discusses the mixed-integer linear programming (MILP) models' implementation. The chapter describes the numerical modeling of the MILP models' different components and how they can be set in a MATLAB

(MathWorksInc, 2011) programming environment for a TOMLAB/CPLEX optimization solver (Holmstrom, 2011). This includes the numerical modeling of the objective function and constraints. The chapter concludes with an elaboration on techniques for implementing an efficient MILP model framework.

Chapter 5 presents experimentation with the MILP model framework and DSBC software. This includes case studies and verification of the models. The models for different levels of the resolution cluster level, drawpoint level, and drawpoint-and-slice level are discussed separately. A modified hierarchical clustering algorithm based on the algorithm presented by Tabesh and Askari-Nasab (2011) for long-term production scheduling of block caving is applied to the data. A multi-step case study is carried out to verify the models and generate a near-optimal realistic mine plan in a reasonable amount of CPU time.

Chapter 6, the last chapter, contains the thesis summary and concluding statements. The benefits and contributions of this research are highlighted, as well as recommendations for future work in integrated mine planning and production scheduling.

CHAPTER 2

LITERATURE REVIEW

Chapter 2 provides an overview of production scheduling in mining operations. It presents the difference between production scheduling in surface and underground operations. It provides background about the block-cave mining system, as well as planning methodologies used in block caving. Clustering algorithms and their applications in mine planning are also highlighted. The chapter concludes with the rationale for this PhD research.

2.1 Introduction

The economics of today's mining industry are such that major mining companies are increasing the use of massive mining methods. Of the methods available, caving mines are favored because of their low cost and high production rates.

Caving is most often applied to low-grade, massive deposits. In this method, the full block or an approximately equi-dimensional block is fully undercut to initiate caving. The undercut is drilled and blasted progressively and some broken ore is withdrawn to create a void into which initial caving of the overlying material can take place. As material is extracted from drawpoints located on the production level, the caving propagates upwards throughout the ore-body until the overlying rock also caves and surface subsidence occurs. The area required to establish a cave depends on the strength of the rock mass, but the lateral extend of the ore-body must be large enough to insure that a cave can be established (Julin, 1992). In addition to the size and shape of the deposit, the rock mass characteristics must be considered. The deposit should be neither very soft nor extremely tough (Tobie and Julin, 1982). The current trend in caving is moving toward harder and tougher ore deposits, as experts have recognized that caving can be initiated in harder rock if it has a suitable structure (Laubscher, 1994). The caving industry is now moving towards the next generation of caving geometries and scenarios: super caves (Chitombo, 2010). Based on the size of broken material, different handling systems can be used. For fine ore fragmentation, the full gravity system (Grizzly) is most suitable. For somewhat coarse material, a slusher system should be implemented. For coarse material, the Load-Haul-Dump (LHD) system might be the best option. Figure 2.1 shows a typical caving layout.

Caving methods have become the underground bulk mining methods of choice, a trend that is expected to continue into the foreseeable future. One of these methods, block caving, has been shown to be promising and has gained popularity in the last years due to its low operating cost and high productivity. The conceptual and practical definition of block caving as stated by Laubscher (1994) is that "cave mining refers to all mining operations in which the ore-body caves

naturally after undercutting its base. The caved material is recovered using drawpoints." Some of the advantages of this method include low cost, centralized production, simple ventilation control, and high production rates.

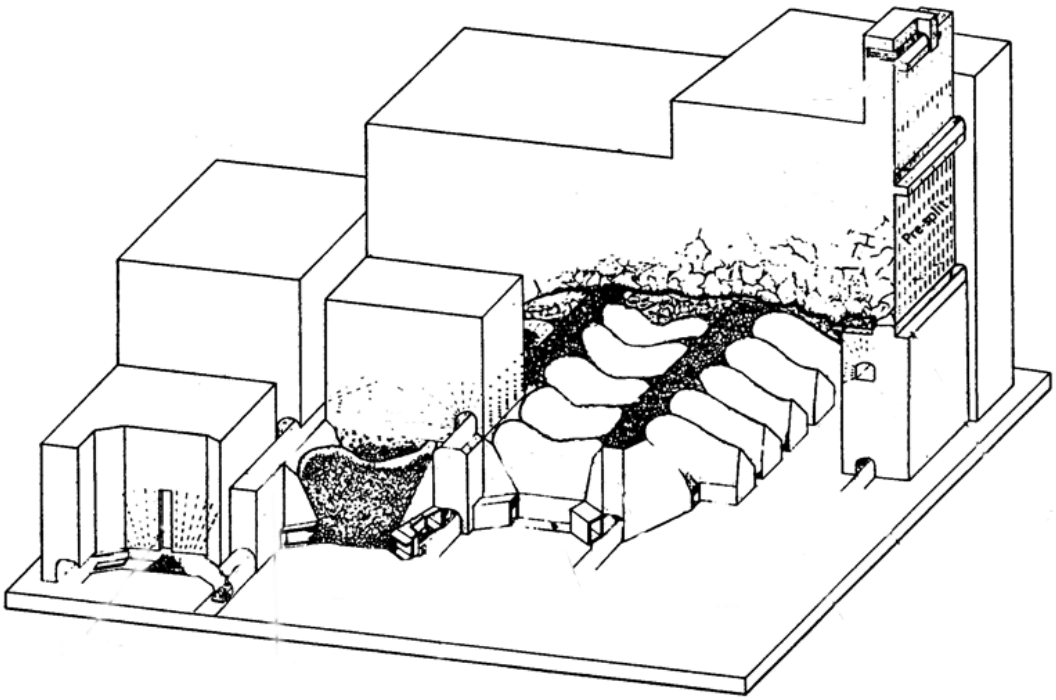

Figure 2.1. Isometric view of a caving operation at Henderson mine (Doepken, 1982)

Laubscher (1994) identified 25 parameters that should be considered before the implementation of any caving operation. The following parameters are common to all cave mining methods: capability, fragmentation, production level layout, draw-zone spacing, draw control, dilution entry, undercutting sequence, and support requirements.

Caving has been used successfully for mining of a wide range of deposits such as porphyry copper, molybdenite, diamond, asbestos, nickel, and magnetite (De Wolfe, 1981; Guest et al., 2000). The first block-caving operation recognized as such was the Pewabic mine, Menominee Range, Michigan (Peele, 1941). The only similarity to present-day operations was the ore handling. The production level was conditioned as a room and pillar mine in which the pillars were reduced in size to induce the caving. Since 1950, De Beers has used block-cave methods

for its operations in South Africa (Owen and Guest, 1994). Not all methods introduced at the De Beers operations were successfully initiated, and often plans had to be reviewed and modified according to the mine's performance. Mechanized panel caving was introduced at the Premier diamond mine in 1990 (Barlett, 1992). The Henderson mine was the first block-cave operation to introduce fully mechanized equipment (Rech et al., 2000). The El Teniente mine first used LHDs in the early 1980s (Chacon et al., 2004) and introduced a novel way of designing the production level layout that is now known as the El Teniente layout (Rojas et al., 2000).

Even though the technology and methods applied in block caving have evolved dramatically over the years, concepts for mine planning have not evolved along the same path. Mine planning and production scheduling for any mining system have an enormous effect on the operation's economics. In recent years, much attention has been given to understanding the principles of gravity flow and rock mechanics, but without considering mine planning as an important part of the mining system. The caving methods present many advantages, such as low cost, centralized production, simple ventilation control, high production rate, and increased safety for production workers (Julin and Tobie, 1973; Tobie and Julin, 1982; Owen and Guest, 1994). However, the successful application of this method depends not just on its advantages, but on correctly designing the production level, and establishing an accurate and well-organized draw-control system (Butcher, 1999).

2.2 Caving Production System

Block caving is a mining method that relies on natural processes for its success. Therefore, it requires more detailed geotechnical investigations of the ore-body than do other methods in which conventional drilling and blasting are employed as part of the mine production (Rubio, 2006). In the case of caving, the draw control is concerned with extracting ore in such a way as to achieve production targets while minimizing waste entry, and preventing the transfer of stress onto mine workings. It is important to ensure that this draw management system is in

place before production begins, to prevent resource loss due to production pressures during cave initiation (Pretorius and Ngidi, 2008).

The physical layout of the production level is critical to the success of a caving operation. Therefore, the first consideration in developing a caving draw-control system is the operation's physical design. Among the different existing panel layouts in active use at caving operations, the Herringbone and El Teniente layouts appear to be preferred designs, as they are used at more than 90% of current operations (Flores et al., 2004).

Undercutting is also one of the most important aspects of caving operations, as it initiates caving and reduces stresses (Laubscher, 1994). The speed of the undercut advance is important and the yearly cave line must move at a reasonable velocity (De Wolfe, 1981). The magnitude of stress-induced damage on the production level can be controlled with the speed of the undercut (Butcher, 1999). According to Brown (2003), there are several methods by which the undercut may be advanced across a panel cave:

- Henderson "Just-In Time" undercutting: a method in which the drawbells are blasted from the undercut level just before the undercut is fired.
- Post-undercutting: undercut drilling and blasting takes place after the production level has been developed.
- Pre-undercutting: no development or construction takes place on the production level before the undercut has been blasted.
- Advance undercutting: the production level is developed in advance of the blasting of the undercut. This method was introduced to reduce the drawpoints' exposure to the abutment stress zones, which were induced as a result of the undercutting process.

Figure 2.2 illustrates pre-undercutting and advance undercutting methods.

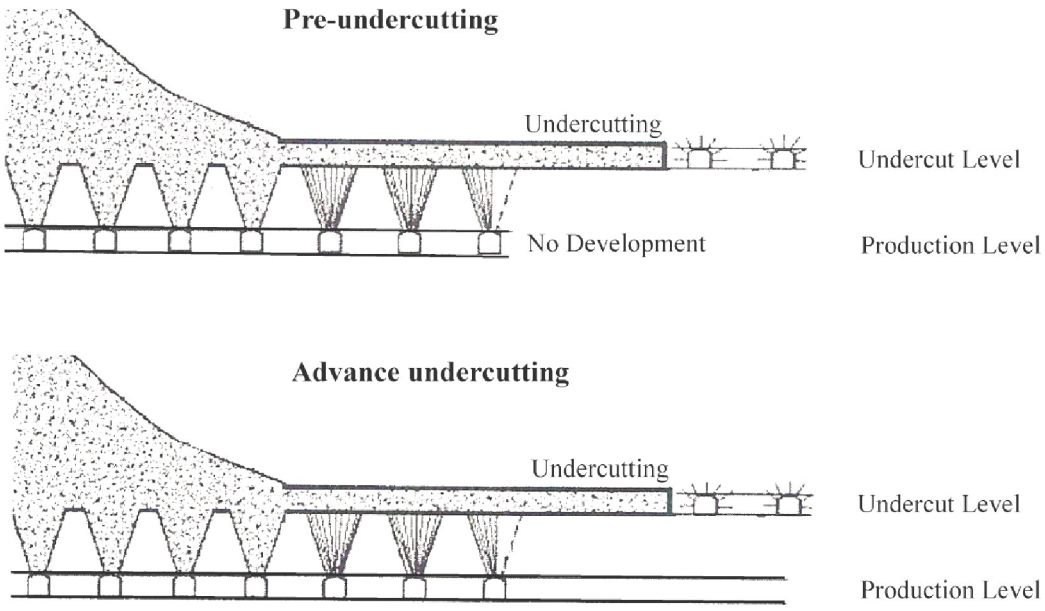

Figure 2.2. Undercutting methods (Barraza and Crorkan, 2000)

Butcher (1999) recommended five guidelines to reduce damage to the production level in caving operations:

- Use advanced undercutting where possible.
- Minimize horizontal irregularities in the undercut front.
- Ensure that the undercut advance rate is high enough to de-stress the production level.
- Place the undercut level as high above the production level as practically possible.
- Advance undercutting from the weakest ground toward the strongest to ensure that cave propagation occurs.

2.3 Geotechnical Parameters Affecting the Planning of the Block Cave

The properties of rock mass have a significant impact on mine design and production. The ability to represent the variability of the geotechnical parameters throughout the ore-body results in decreasing the risk of the mining methods as

well as increasing the ability to forecast production (Summers, 2000). The main geotechnical parameters affecting the planning of the block cave can be grouped into four categories: (i) cavability, (ii) stress, (iii) fragmentation, and (iv) flow and mixing (Rahal, 2008).

Rubio (2004b) proposed an illustrated representation of the link between the geotechnical and the mine planning parameters of block caving. He introduced four fundamental models to determine mine-planning parameters such as draw rate, undercut sequence, development rate, tonnage, draw method, and production targets. These models are (i) fragmentation, (ii) geomechanical, (iii) geological, and (iv) reconciliation.

The first task in block-cave planning is to determine the cavability of an ore-body. For a good caving action, generally the ore body should have fractures in three orientations (Julin, 1992). Cavability, in the context of draw control, is primarily concerned with balancing caving rates and production. Production should be high enough to prevent re-compaction of the broken material in the cave while allowing the cave to propagate upward through the rock mass (Julin and Tobie, 1973). The effect of stress on draw horizon stability must be reduced by mine planning. Stress-induced damage is normally proportional to a number of mining related factors, such as depth below surface, undercut height, distance between the undercut and draw horizon, rock mass strength, and pillar size on the extraction level (Butcher, 1999). Fragmentation affects drawpoint productivity and the ingress of diluting materials (Laubscher, 1994; Rubio et al., 2004b). Drawpoint productivity is affected by fragmentation because the frequency and severity of "hang-ups" dictate the production rate (Rahal, 2008). An understanding of broken ores is of particular importance in caving operations. Current research in flow and mixing falls into three categories: (i) numerical flow studies, (ii) physical modeling, and (iii) full-scale flow experiments (Heslop and Laubscher, 1981; Pretorius and Ngidi, 2008; Rahal, 2008; Van As and Van Hout, 2008).

2.4 Mine Production Scheduling

Mining is the process of extracting a beneficial, naturally occurring resource from the earth. The historical assessment of mineral resource evaluations has demonstrated that project profitability is sensitive to mine-planning decisions (Askari-Nasab and Awuah-Offei, 2009; Newman et al., 2010). Production scheduling for any mining system has an enormous effect on the operation's economics. As the mining industry is faced with more marginal resources, it is becoming essential to generate production schedules that will provide optimal operating strategies while meeting practical, technical, and environmental constraints (Burgher and Erickson, 1984; Dagdelen and Johnson, 1986; Chanda, 1990). Some of the benefits expected from better production schedules include increased equipment utilization, optimum recovery of marginal ores, reduced costs, steady production rates, and consistent product quality (Dagdelen and Johnson, 1986; Chanda, 1990; Wooller, 1992; Chanda and Dagdelen, 1995; Winkler, 1996).

The majority of the scheduling publications to date have been concerned with open-pit mining applications. Underground mining is more complex in nature than surface mining (Kuchta et al., 2004). Underground mining is less flexible than surface mining due to the geotechnical, equipment, and space constraints (Topal, 2008). As a result, many of the scheduling concepts and algorithms developed for surface mining have found their way into underground applications.

There are three time horizons for production scheduling: long-, medium- and short-term. Long-term mine-production scheduling provides a strategic plan for mining operations, whereas medium-term mine-production scheduling provides a monthly operational scheme for mining while tracking the strategic plan. Medium-term schedules include more detailed information that allows for a more accurate design of ore extraction from a special area of the mine, or information that allows for necessary equipment substitution or the purchase of necessary equipment and machinery. The medium-term schedule is also divided into short-term periods (Osanloo et al., 2008). A long-term production schedule contains

fewer details than a short-term plan. However, a long-term plan includes clear definitions related to mining reserves and the production sequence and production rate.

A wide range of packages are available for mine scheduling, the majority of which are devoted to surface-mining operations. The development of software for underground operations is slower than that for surface mining. Despite this slow uptake in underground applications, improvements in computing power and scheduling algorithms over the past few years have allowed planning engineers to develop models to schedule even complex mining systems (Alford et al., 2007; Caccetta, 2007).

2.4.1 Open-Pit Production Scheduling

For nearly 30 years, research in surface-mine scheduling has focused on developing the optimum ultimate pit-limit algorithm rather than solving for the optimum open-pit production sequence. The ultimate pit-limit method is relatively easy to solve, but it does not directly constrain production other than to impose limits on the pit slope. Since mining companies have been forced to account for a wider range of production constraints, different methods have been used to optimize mine production (Kim and Zhao, 1994).

Recent production scheduling algorithms and formulations in literature have been developed along two main research areas: 1) heuristic methods and 2) exact solution methods for optimization (Askari-Nasab and Awuah-Offei, 2009).

Most of the commercial software has been developed based on heuristic methods. Commercial mine-scheduling software such as XPAC Auto Scheduler (RungeLimited, 2009), Whittle (Gemcom Software International Inc., 2012), and NPV Scheduler (Datamine Corporate Limited, 2008) use heuristic methods to generate long-term production schedules. Heuristic methods iterate over different alternatives leading to the generation of the ultimate pit limit, with each alternative having a different discounted cash flow and, hence, different NPV. Due to this, the solution generated may be sub-optimal in terms of NPV.

Authors including Denby and Schofield (1994) and Askari-Nasab (2006) have conducted extensive research using artificial intelligence techniques to solve the problem of long-term production planning. Denby and Schofield (1995) used multi-objective optimization to deal with an ore-grade variance. Using genetic algorithms, they tried to maximize value and minimize risk in open-pit production planning. Askari-Nasab (2006) also developed and implemented an intelligence-based theoretical framework for open-pit production planning. The drawback in applying these techniques is that the solution is not reproducible or optimal.

In recent years, there has been an increase in the use of operations research techniques for scheduling problems. A variety of operations research, including linear programming (LP) and mixed-integer linear programming (MILP), has been applied to the mine-production scheduling problem. Newman et al. (2010) presented a comprehensive review of operations research in mine planning. Using different methods, they summarized authors' attempts to develop methodologies to optimize production scheduling in underground and surface mines.

Exact solution methods for optimization with mathematical programming models have proved to be robust in solving the long-term production planning problem. Using exact solution methods results in solutions within known limits of optimality. As the solution gets closer to optimality, it leads to production schedules that generate higher NPVs than those obtained from heuristic optimization methods.

The pioneering work of Johnson (1969) used an LP model, which led to the mixed-integer programming (MIP) formulations by Gershon (1983) for the production scheduling problem. The LPs' suitability for mine scheduling relies on the fact that non-linear functions can be approximated by a series of piecewise linear functions. In other words, it is often possible that under a weak assumption, integer programming problems be reformulated as an equivalent linear problem (Jordi and Curin, 1979; Smith, 1999). These characteristics have made it possible to use LP for optimizing ore blending (Chanda and Dagdelen, 1995), quality

control (Maitra et al., 1994), and economic optimization (Winkler and Griffin, 1998). The classical LP formulation has two major shortcomings. The first is that only one objective function is permitted at a time (Chanda and Dagdelen, 1995). The second is that LP is unable to restrict variables to integer values. The first problem can be overcome by using goal programming (GP) to allow the use of multiple objectives during optimization. The second problem may be overcome by using MILP (Barbaro and Ramani, 1986). MILP mathematical optimization models have the capability to consider multiple ore processors and multiple elements during optimization. This flexibility of mathematical programming models results in production schedules generating significantly higher NPVs than those generated by other traditional methods (Askari-Nasab et al., 2011). When MILP models are applied, production schedules generate near theoretical optimal NPVs. MILP is an extension of LP in which all constraints remain linear but variables may be continuous or integer values.

Various models based on MILP mathematical optimization have been used to solve the long-term open-pit scheduling problem (Caccetta and Hill, 2003; Ramazan and Dimitrakopoulos, 2004b; Dagdelen and Kawahata, 2007; Boland et al., 2009; Askari-Nasab et al., 2011).

An integer programming formulation that was developed by Dagdelen and Johnson (1986) uses Lagrangian relaxation and subgradient optimization algorithms to solve the long-term production planning problem. Subsequent integer programming models developed by Akaike and Dagdelen (1999) and Caccetta and Hill (2003) use 4D-network relaxation and subgradient optimization, and branch-and-cut, respectively to solve the long-term production planning optimization problem. These authors noted that implementation on large-scale problems or with dynamic cut-off grades was a challenge.

MIP formulations developed by Ramazan and Dimitrakopoulos (2004a) attempted to reduce the number of binary variables and solution times by setting certain variables as binary and others as continuous. This resulted in partial mining of

blocks that have the same ore value affecting the generated NPV. Ramazan et al. (2005) and Ramazan (2007) developed an MIP model that used an aggregation method to reduce the number of integer variables in scheduling. This formulation was solved based on a fundamental tree algorithm and was used in scheduling a case with 38,457 blocks within the final pit limit. The problem was broken down into four push-backs based on the nested pit approach using Whittle (Gemcom Software International Inc., 2012) and formulated as separate MIP models. This may not guarantee a global optimum solution of the problem. Caccetta and Hill (2003) presented an MILP model and Boland et al. (2009) presented an LP approach to generate mine production schedules with block processing selectivity. However, they did not present enough information on the generated schedules to enable an assessment of the practicality of the solutions from a mining operation point of view.

Recent research work by Askari-Nasab et al. (2011) on applying exact solution methods of optimization to the long-term production planning problem has led to the development of MILP models that use block-clustering techniques to address the problem of having a large number of decision variables. With a combination of their MILP models and a block clustering algorithm, Askari-Nasab et al. (2011) applied their models to a large-scale problem. The formulations use a combination of continuous and binary variables. The continuous variables control the portion of a block to be extracted in each period. Binary variables control the order of block extraction or precedence of mining cuts through a dependency-directed graph using a depth-first search algorithm. The concept of mining cuts using clustering techniques is reinforced as an option for solving MILP problems for large-scale deposits. The formulation was implemented on an iron-ore-mine intermediate scheduling case study over 12 periods in TOMLAB/CPLEX (Holmstrom, 2011) environment. This model does not consider multiple material types or waste disposal planning.

2.4.2 Underground Mines Production Scheduling

The majority of the scheduling publications to date have been concerned with open-pit mining applications. Underground mining is more complex in nature than surface mining (Kuchta et al., 2004). As a result, the development of software for underground operations has been delayed and many of the scheduling concepts and algorithms developed for surface mining have found their way into underground mining. Underground mining methods are characterized by complex decision combinations, conflicting goals and interaction between production constraints. Current practice in underground-mine scheduling has tended toward using simulation and heuristic software to determine feasible, rather than optimal, schedules. A compromise between schedule quality and problem size has forced the use of mine design and planning models, which incorporate the essential characteristics of the mining system while remaining mathematically tractable. Different types of methods have been applied to underground mine scheduling. Similar to open-pit mines, production scheduling algorithms and formulations in literature can be divided into two main research areas: 1) heuristic methods and 2) exact solution methods for optimization.

In addition to these categories, other methods such as queuing theory (Su, 1986; Huang and Kumar, 1994), network analysis (Russell, 1987; Brazil et al., 2000; Brazil et al., 2003), and dynamic programming (Sherer and Gentry, 1982; Muge et al., 1992) have been used to schedule production and/or material transport.

Heuristic methods are generally used to generate a good solution in a reasonable amount of time. These methods are used when there is no known method to find an optimal solution under the given constraints. Despite shortcomings such as frequently required intervention, and the lack of a way to prove optimality, simulation and heuristics are able to handle non-linear relationships as part of the scheduling procedure.

One of the earlier successful applications of simulation in underground mining was developed for room-and-pillar mining (Hanson and Selim, 1975). The model

was event-oriented, with all event times treated as stochastic variables. Mine simulation incorporated drilling, blasting, mucking and roof bolting into a system that reported equipment utilization, production tonnage, and the number of holes drilled. The authors made no claim that this system could be used to optimize the production system. Maxwell (1978) used a simulation system to estimate mill-feed grades given a predicted drawpoint production rate. This application highlighted the ability of simulation to address non-linear effects in the underground mining system. In this case, the flow of material in the cave was simulated based on scraper production from the finger raise. As in the previous example, this system made no claim that the schedule produced was optimal. Gerling and Helmz (1986) used the simulation to handle different components within the mining system. The proposed model used a series of sub-models to deal with the deposit reserves, the drift system, the development drifting operations, and the stoping operations. This integrated heuristic produced a schedule based on maximizing the NPV over the mine-life. The authors found that the heuristic sometimes produced schedules that were technically and operationally unrealistic.

Gershon (1987) proposed that the sequence of mining that yields the largest NPV return is the one that should be chosen from a group of candidate schedules. He described two heuristic methods that were appropriate for surface and underground mining. The first of these was based on scheduling decisions regarding blending criteria, while the second was most appropriate for commodities that have difficult blending requirements. In the first method, the assumption is made that the best long-term schedule is one that allows the blending specifications to be met for the longest period time. The second method proposed that a block should be mined if it enables the extraction of additional material. Gershon concluded that the schedules produced with heuristic algorithms must only be regarded as a useful guide.

Unlike surface mining, in underground mining, such as caving, the resource model changes with time. Because the draw history affects the current contents of

the cave by allowing the influx of waste or by eliminating sections of the reserves when insitu stresses collapse, production drifts. One of the leading candidates in the block-caving method is a simulation system called PCBC (Gemcom Software International, 2012). Diering (2000) presented the principles behind the commercial tool PCBC to compute production schedules using several case studies with different draw methods. PCBC is a simulation tool to prepare and evaluate various production schedules. The program is capable of modeling the material mixing model using two mixing mechanisms: vertical mixing and horizontal mixing. Vertical mixing allows materials to migrate vertically at different rates in each draw column while horizontal mixing allows horizontal migration based on relative draw rates. The software simply simulates extraction from each active drawpoint on a period-by-period basis subject to various draw constraints. The developers of PCBC have also given PCBC the ability to solve incremental periods using linear and integer programming (Rubio and Diering, 2004a). In PCBC, the mining sequence is controlled manually using the trial-and-error process to find the mining start point and advancement direction. Consequently, it cannot yield an optimum solution for the problem.

Mathematical models can provide a mathematically provable optimum schedule. The LP method has been used most extensively. Scheduling underground mining operations is primarily characterized by discrete decisions to mine blocks of ore, along with complex sequencing relationships between blocks. Since LP models cannot capture the discrete decisions required for scheduling, MIPs are generally the appropriate mathematical programming approach to scheduling. The advantage of using these methods for production scheduling is that they can provide a mathematically provable optimum schedule. These methods are able to approximate some non-linear systems, but they are not as flexible as simulation. In the MILP method, any feasible schedule produced has an associated gap that provides a measure of how far the feasible schedule is from its linear relaxation. This gap is based on the difference between the best node and best integer feasible value found within the branch-and-bound search tree.

The early sequencing models for underground operations use a combination of simulation and optimization. They use simulation to assess production schedules and linear programming to make decisions regarding the extracted ore (Newman et al., 2010). Chanda (1990) implemented an algorithm to write daily orders and developed the interface between mathematical programming and simulation by integrating the two into a short-term planning system for a continuous block cave. The objective function was defined to minimize the fluctuation in the average grade drawn between shifts. The production schedule given by the integer program was used as input to a simulation model that considered constraints such as production capacity. Winkler (1998b) described a production-scheduling model to determine the amount of ore to mine in each period from each production block. He used linear programming to solve a corresponding single-period model, and simulation to fix the current period's decisions and optimize over the successive period. Song (1989) also attempted to account for material movement within the panel by using simulation with mathematical programming. However, unlike Chanda (1990), he used simulation to determine the effect of undercut parameters, drawpoint spacing, caving probability, and drift stability on production. A MILP formulation was then developed using regression equations for the restrictions revealed within the simulation study. The resulting MILP optimized the draw by enforcing the geometrical and operational limitations which satisfy cavability and stability demands in the block cave. The author does not give any indication of solvable problem size or solution time.

Trout (1995) implemented the first attempt to optimize underground mine production schedules using integer programming. The objective was to maximize the NPV subjected to the constraints on stope sequencing, stope extraction and backfill quantities, equipment capacities, and production grade. He used binary variables to control the timing of extraction from or backfilling of a stope and used continuous variables to track the material extracted from or backfilled into a stope in a given period. The model was run over a 17-period horizon in which the last four periods were aggregated into durations that were three times longer than

the previous 13. Trout's model ran out of memory, but it yielded a 25 percent improvement over the NPV generated by current operational policies.

Guest et al. (2000) applied mathematical programming to long-term scheduling in block caving. In this case, the objective function was explicitly defined to maximize draw-control behavior. However, the author stated that the implicit objective was to optimize net present value (NPV). There are two problems with this approach. The first is that maximizing tonnage or mining reserves will not necessarily lead to maximum NPV. The second is that draw control is a planning constraint and not an objective function. The objective function in this case would be to maximize tonnage, minimize dilution, or maximize mine life.

Carlyle and Eaves (2001) presented a model that maximized revenue from Stillwater's sublevel stoping platinum and palladium mine. They used integer variables to schedule the timing of various expansion-planning activities. There were three constraints in their model: sequencing of operations and stope preparation, production limits of stopes, and bounds on the change in crew size between periods. They obtained near-optimal solutions for a variety of scenarios over a 10-quarter time horizon (Newman et al., 2010). Smith et al. (2003) formulated a large-scale, time-dynamic, life-of-complex mixed-integer program production schedule to optimize lead/zinc cash flow based on a detailed life-of-project production-scheduling study. The objective was to maximize NPV subject to operational constraints such as ore availability, mill capacity, mine-infrastructure production capacity, grade limits, continuous production rules, and precedence relationship between production blocks. The authors were unable to solve all instances of their problem in a reasonable amount of time (Newman et al., 2010).

Rubio (2002) developed a methodology that would enable mine planners to compute production schedules in block-cave mining. He proposed new production process integration and formulated two main planning concepts as potential goals

to optimize the long-term planning process, thereby maximizing NPV and mine life.

Rahal et al. (2003; 2008) described a mixed-integer goal program. The model had the dual objectives of minimizing the deviation from the ideal draw. This algorithm assumes that the optimal draw strategy is known. The authors developed life-of-mine draw profiles for notional scenarios and showed that by using the results from their integer program, they greatly reduced deviation from ideal drawpoint depletion rates while adhering to a production target.

Diering (2004) presented a non-linear optimization method to minimize the deviation between a current draw profile and the target defined by the mine planner. He emphasized that this algorithm could also be used to link the short-term plan with the long-term plan. The long-term plan is represented by a set of surfaces that are used as a target to be achieved based on the current extraction profile when running the short-term plans. Rubio and Diering (2004a) described the application of mathematical programming to formulate optimization problems in block-cave production planning. They formulated two main planning strategies: maximization of NPV and maximization of mine life. They used the operational constraints presented by Rubio (2002).

Newman and Kuchta (2007) formulated a multi-period mixed-integer program for iron ore production at Kiruna, Sweden. They designed a heuristic method based on solving a smaller and more tractable model. For this purpose, they aggregated periods and then solved the original model using information gained from the aggregated model. Weintraub et al. (2008) developed and used successfully MIP models for El Teniente, a large Chilean block-caving mine. They used *a priori* and *a posteriori* aggregation procedures to reduce the model size in their model.

Parkinson (2012) developed three integer programming models: Basic, Malkin, and 2Cone. All of the models share three basic constraints. The start-once constraint ensures that each drawpoint is opened once and only once. The global-

capacity constraint ensures that the number of active drawpoints does not exceed the downstream-processing capacity. The last constraint, that the opened draw points must form a single, contiguous group, or cave, is the source of the model variations.

2.5 Application of Clustering in Mine-Production Scheduling

The applications of MILP models result in production schedules generating near theoretical optimal NPVs. In practice, formulating a real-size mine production planning problem by including all the blocks as integer variables will simply exceed the capacity of the current commercial mathematical optimization solvers.

An efficient way of overcoming the large number of decision variables and constraints is by applying a clustering technique. Clustering can be referred to as the task of grouping similar entities together so that maximum intracluster similarity and intercluster dissimilarity are achieved. This can be modeled and solved as a mathematical programming problem, but will require more resources and time. Therefore, non-exact algorithms have been developed in the literature to solve these problems. These algorithms are usually implemented by defining a measure of similarity or dissimilarity among the objects. There are two main categories: partitional and hierarchical clustering. Partitional clustering is done by partitioning data objects into a number of groups. Hierachical clustering, on the other hand, is performed by creating a hierarchy of clusters. In comparison, hierarchical clustering creates better clusters, though more CPU time is required (Johnson, 1967; Feng et al., 2010; Tabesh and Askari-Nasab, 2011).

Various methods of aggregation have been used to reduce the number of integer variables that are required to formulate the mine-planning problem with MILP techniques (Epstein et al., 2003; Newman and Kuchta, 2007; Weintraub et al., 2008; Askari-Nasab et al., 2011; Tabesh and Askari-Nasab, 2011; Pourrahimian et al., 2012a).

Epstein et al. (2003) used aggregation for underground block-sequencing operations and embeded it in an optimization-based heuristic. Newman and

Kuchta (2007) formulated a mixed-integer program to schedule iron-ore production over multiple time periods. To overcome the size problem, they designed a heuristic based on solving a smaller, more tractable model. In this model, they aggregated time periods and then solved the original model using information gained from the aggregated model. Askari-Nasab et al. (2011) developed and implemented a deterministic MILP formulation for a long-term large-scale open-pit production scheduling problem capable of solving real-size open-pit production optimization problems in a reasonable time frame. To reduce the number of binary variables in the formulation, the blocks within the same level or mining bench were grouped into clusters based on their attributes, spatial location, rock type, and grade distribution. Askari-Nasab et al. divided the major decision variables into two categories: continuous variables representing the portion of a block which is going to be extracted and processed in each period, and binary variables controlling the order of extraction of blocks or the precedence of mining-cuts through a dependency-directed graph. Tabesh and Askari-Nasab (2011) presented a two-stage clustering approach based on an agglomerative hierarchical algorithm and tabu search. Their algorithm aggregates blocks into selective mining units based on a similarity index which is defined based on rock types, ore grades, and distances between blocks. Weintraub et al. (2008) used *a priori* and *a posteriori* aggregation procedures to reduce the model size in their MIP models developed for El Teniente, a large Chilean block-caving mine. They divided the mine into sectors and sub-sectors. Each sector was divided into columns of extraction points which were composed of blocks, and these blocks were the basic units of extraction. The planning process considered a 25-year horizon. Weintraub et al. used *a priori* and *a posteriori* methods to aggregate the blocks and columns, respectively. They reported that the percentage error in the value of the objective function for the original model with the disaggretion of the aggregate model was 3.62%. The execution time was reduced by 73.68%. The model dimension was reduced by 90%.

2.6 Rationale for PhD Research

The economics of today's mining industry are such that the major mining companies are increasing the use of massive mining methods. Among the mining methods available, caving methods are favored because of their low cost and high production rates. Caving methods have become the underground bulk mining methods of choice, a trend expected to continue in the foreseeable future.

Scheduling a block-cave mine is a matter of finding the goal that better represents the strategic planning vision. The scheduling process is subject to mine design, geomechanical, operational, and environmental constraints.

Although simulation and heuristics are able to handle non-linear relationships and effects as a part of the scheduling procedure, they cannot guarantee the optimal solution. Applying mathematical programming models such as LP and MILP with exact solution methods for optimization has proved to be robust. Solving these models with exact solution methods, results in solutions within known limits of optimality. As the solution gets closer to optimality, it results in production schedules that generate higher NPV than those obtained from heuristic optimization methods. The literature has shown that both surface and underground mining systems are adaptable to formulations as set of linear constraints. This has resulted in extensive research on the application of mathematical programming models to the long-term production planning problem. The inherent difficulty in applying these models to the long-term production planning problem is that they result in large-scale optimization problems containing many binary and continuous variables. These are difficult to solve with the current available computing software and hardware, and may require lengthy solution times.

The literature review showed that in a block-caving method, a production scheduling methodology that is based on a limited number of influential parameters will lead to optimistic production schedules. In addition, the geotechnical behavior of the rockmass must be considered for production scheduling. Currently, production targets are the result of production schedules

computed with mine planning parameters that do not evolve as a function of the operational performance, and are not linked to the geotechnical behavior of rock mass. Also, relying only on manual planning methods or computer software that is based on heuristic algorithms will lead to mine schedules that are not the optimal global solution.

The lack of a mathematical block-cave production scheduling model for long-term production scheduling that takes more number of detail constraints into account with the ability to find the best starting point and advancement direction of mining, is worrisome. This research will introduce a MILP mine scheduling framework for block-caving which will determine the mining starting point, advancement direction, and generate a near-optimal production schedule with higher NPV compared to heuristic methods in a reasonable time.

2.7 Summary and Conclusions

A review of the relevant literature for this research has shown that production scheduling of any mining system has an enormous effect on the operation's economics, and that deviations from the optimal mine plan can have a great impact on mine economics. Over the last 50 years, continuous attempts have been made to address the pit limit and production scheduling optimization problems. However, the literature on underground mining is more recent, partially because of the complicated nature of underground operations. The current practice in underground mine scheduling has tended toward the use of simulation and heuristic software to determine feasible rather than optimal draw schedules.

This reliance on heuristic methods to find usable, rather than optimal schedules was necessitated by the great computational expense required to find a provable optimum. In other words, a compromise between schedule quality and problem size has forced the use of mine design and planning models which embody the essential characteristics of the mining system while remaining mathematically tractable. As a result, many types of scheduling methods have been applied to underground mine scheduling. A summary includes: (i) queuing theory; (ii)

network analysis; (iii) dynamic programming; (iv) simulation; (v) LP; (vi) MILP; and (vii) goal programming.

The literature review showed that in a block-caving method, a production scheduling methodology that is based on a limited number of influential parameters will lead to optimistic production schedules. In addition, the geotechnical behavior of the rockmass must be considered for production scheduling. Also, relying only on manual planning methods or computer software that is based on heuristic algorithms will lead to mine schedules that are not the optimal global solution.

The limitations in the current production scheduling optimization in block caving are: (i) limitations in solving large-scale problems. These come about as a result of significant computer overhead, in terms of memory and speed, required to solve the large-scale problems; (ii) treatment of stochastic variables such as grade, commodity price, and production cost as deterministic processes. This can generate suboptimal results; (iii) trial-and-error process to find the mining start point and advancement direction; (iv) integration of fewer geotechnical constraints into real-scale production scheduling. These limitations can affect the viability as well as other aspects of mining projects, emphasizing the need for optimization tools that take into consideration these deficiencies. Consequently, it is important that robust models are developed to address these challenges.

CHAPTER 3

THEORETICAL FRAMEWORK: BLOCK-CAVE PRODUCTION SCHEDULING

Chapter 3 contains the mixed integer linear programming (MILP) formulations for three levels of resolution: (i) cluster level, (ii) drawpoint level, and (iii) drawpoint-and-slice level. This chapter describes how the production models can be used in practice. To overcome the size problem of mathematical programming models and to generate a robust, practical, near-optimal schedule, a clustering method for long-term production scheduling of block caving is presented. The production scheduler aims to maximize the net present value of the mining operation while the mine planner has control over the development rate, vertical mining rate, lateral mining rate, mining capacity, maximum number of active drawpoints, and advancement direction. To support a given production target, the production scheduler defines the opening and closing time for each drawpoint and cluster, the draw rate from each drawpoint and cluster, the number of new drawpoints and clusters that need to be constructed, and the sequence of extraction from the drawpoints and clusters.

3.1 Introduction

The goal of long-term mine production scheduling is to determine the mining sequence, which optimizes the company's strategic objective while honoring the operational and geotechnical limitations over the mine life. There are a number of strategic objectives common in the industry. Usually, the target is to maximize the net present value (NPV) of mining operations within the existing economic, technical, and environmental constraints. However, other objectives such as cost minimization or reserve maximization could also be considered. The production schedule defines the management investment strategy. An optimal plan in mining projects will result in cost reduction, increasing equipment utilization, optimum recovery of marginal ores, steady production rates, and consistent product quality.

This chapter describes steps in planning a block cave mine. Also, it focuses on the modified clustering method for block caving, formulating, and developing the MILP models for block-cave production-scheduling optimization. The production scheduler aims to maximize the mining operation's NPV, while the mine planner has control over: (i) mining capacity, (ii) draw rate, (iii) mining precedence, (iv) maximum number of active drawpoints, (v) number of new drawpoints in each period, (vi) continuous mining, and (vii) total reserves. The production scheduler defines the opening and closing time of each drawpoint and cluster, the draw rate from each drawpoint and cluster, the number of new drawpoints and clusters that need to be constructed, and the sequence of extraction from the drawpoints and clusters to support a given production target.

3.2 Planning a Block-Cave Mine

Scheduling a block-cave mine is a matter of finding the goal that best represents the strategic planning vision subject to several mine design, geomechanical, operational, and environmental constraints. The production schedule is subject to a variety of physical and economic constraints. To compute this production schedule, many decisions need to be made with regard to accessibility and infrastructure, mining capacity, mining sequence, grade target, etc. Strategic

planning defines the project goal. Figure 3.1 shows the workflow that has to be followed to schedule a block-cave mine using the developed MILP models in this research. These steps include:

1. Creating a block model using GEMS software (Gemcom Software International, 2012).
2. Importing drawpoint data including coordinates, dip, and azimuth.
3. Creating a slice file using PCBC software (Gemcom Software International, 2012).
4. Calculating the best height of draw (BHOD).
5. Importing a slice file, the BHOD file, and coordinates of drawpoints into the software that we have developed for drawpoint scheduling in block-caving (DSBC).
6. Creating all required databases and sets to use in the developed MILP models. The sets are used to define the predecessor clusters, drawpoints, and slices.
7. Clustering the draw columns based on the similarity of the draw column's tonnage, average grade, and physical location.
8. Defining the input scheduling parameters.
9. Creating the objective function and constraints at each level of resolution: (i) cluster level, (ii) drawpoint level, and (iii) drawpoint-and-slice level.
10. Solving the problem using one of the methods: either single-step or multi-step.
11. Discussing the results

The first step is creating the resource model. The resource model is a block model in which each block represents an attribute of the geological deposit. The second step is to find the mining unit that will properly represent the mining method. In a block-caving method, the caved material is extracted from a drawpoint. A disturbance zone called the ellipsoid of draw can be observed above the drawpoint. When the height of this ellipsoid is large enough, the disturbance zone

is called the draw column. Thus, these draw columns will be modeled in a block-cave mine. Every column represents a drawpoint. Then, the total column is divided into slices, which match the vertical spacing of the geological block model. Afterwards, the BHOD (Diering, 2000) for each draw column is calculated.

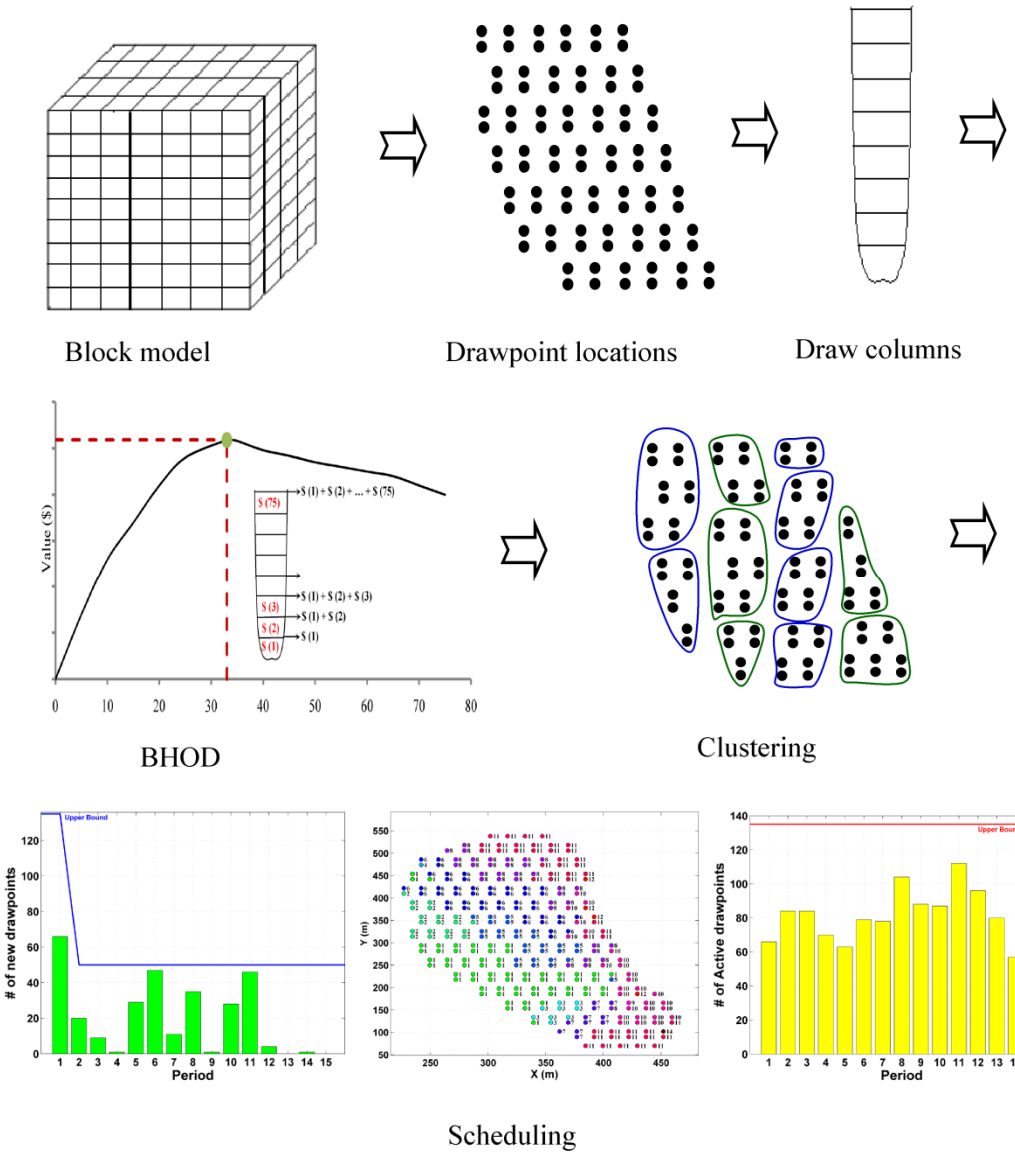

Figure 3.1. Required steps for block-cave production scheduling using MILP

Table 3.1 shows the calculation for one draw column of copper and gold. The revenue per ton is calculated using the revenue factors per unit of grade material

(e.g., $ per gram of gold or $ percent of copper) and the mining cost, which includes per ton overheads and per ton milling costs (see Equation (3.1)).

$$\text{Revenue} = \left(\sum_{e=1}^{n} \left(U\text{Rev}_e \times gr_e \right) \right) - (DC + MC + OC) \tag{3.1}$$

Where

- $U\text{Rev}_e$ is the revenue factor per unit of the element e,
- gr_e is the grade of the element e,
- DC is the direct mining cost, and
- MC and OC are milling cost and overhead costs, respectively.

In Table 3.1, it is assumed that copper and gold revenue factors, and mining cost, are $28/t, $13/t, and $22/t, respectively. The number of possibilities for finding the optimal height is equal to the number of slices above each drawpoint. A simple comparison of the dollar value for each combination (slice 1; then slices 1 and 2; then slices 1, 2, and 3) allows the best height to be found. The maximum value in this case is obtained for slice number 14. If the height of each slice is 10m, the BHOD for this draw column is 140m. After applying the BHOD, the final height of draw is obtained. Afterwards, the production schedule of a block-cave mine can be optimized using the MILP formulation.

Although not an optimal way to calculate the BHOD, this is the method used in current industrial practice and commercial software such as PCBC (Gemcom Software International, 2012). Using our MILP models, this height of draw can be calculated as part of the optimization problem with setting the reserve constraint less than or equal to one.

Table 3.1. Calculating best height of draw (BHOD)

Slice No.	Cu%	Au%	Current value	Maximum Cumulative value
25	0.04	0.01	-20.75	90.54
24	0.05	0.01	-20.47	111.29
23	0.07	0.02	-19.78	131.76
22	0.10	0.02	-18.94	151.54
21	0.14	0.03	-17.69	170.48
20	0.19	0.04	-16.16	188.17
19	0.25	0.06	-14.22	204.33
18	0.33	0.08	-11.72	218.55
17	0.42	0.1	-8.94	230.27
16	0.53	0.12	-5.6	239.21
15	0.64	0.15	-2.13	244.81
14	0.77	0.18	1.9	246.94
13	0.89	0.21	5.65	245.04
12	1.01	0.24	9.4	239.39
11	1.11	0.26	12.46	229.99
10	1.20	0.29	15.37	217.53
9	1.28	0.31	17.87	202.16
8	1.34	0.32	19.68	184.29
7	1.39	0.33	21.21	164.61
6	1.43	0.34	22.46	143.4
5	1.46	0.34	23.3	120.94
4	1.48	0.34	23.86	97.64
3	1.49	0.35	24.27	73.78
2	1.48	0.36	24.12	49.51
1	1.53	0.35	25.39	25.39

3.3 Clustering

In mathematical programming using MILP formulations, usually the size of the branch-and-cut tree becomes so large that insufficient memory remains to solve the LP sub-problems. The size of the branch-and-cut tree can actually be affected by the specific approach one takes in performing the branching and by the structure of each problem. So, there is no way to determine the size of the tree before solving the problem. Attempts have been made to overcome the curse of dimensionality using aggregation, which causes difficulties for long-term production scheduling combinatorial optimization in open pit and underground mines (Epstein et al., 2003; Newman and Kuchta, 2007; Weintraub et al., 2008; Askari-Nasab et al., 2011; Tabesh and Askari-Nasab, 2011).

Clustering is defined as the process of grouping similar entities together so that maximum intra-cluster similarity and inter-cluster dissimilarity are achieved. The clustering problem is proven to be NP-Hard (Gonzalez, 1982). Therefore, a wide range of non-exact algorithms has been developed in the literature. These algorithms are usually performed by defining a measure of similarity or dissimilarity between the objects. These techniques can be categorized into two major groups: hierarchical and partitional clustering. The hierarchical clustering is performed by creating a hierarchy of clusters. It is known to result in better clusters compared to partitional algorithms, but it does so by taking more CPU time (Feng et al., 2010).

Hierarchical clustering algorithms are divided into two main groups: agglomerative versus divisive clustering. In the former group, clusters are formed by merging smaller ones. This means that at the beginning, the number of clusters is the same as the number of objects. As the algorithm goes on, more similar clusters are merged together until the stopping criteria are met or all the objects fall into the same cluster. The procedure is the other way around for the divisive clustering techniques: i.e., all the objects are considered to belong to the same cluster in the beginning of the algorithm, and clusters are divided into two in each step of the algorithm. Finding the target cluster to split and the way they are

divided is a tricky step. That is the reason this method of clustering has not attracted as much attention as the other groups.

3.3.1 Draw Columns Aggregation Using Hierarchical Clustering

To overcome the size problem of mathematical programming models, the draw columns are aggregated into practical scheduling units using clustering algorithms. For this purpose, the algorithm by Tabesh and Askari-Nasab (2011) was modified for its application in block-cave mining. Draw column aggregation is required for two reasons: (i) to generate a practical mining schedule that follows a selective mining unit, and (ii) to reduce the number of variables, especially binary variables in the MILP formulation to make it computationally tractable. The planner has to divide the mine into phases based on advancement directions. These phases will control practical cave advancement. Clustering is done within each phase. This means two drawpoints that are located within two different phases cannot be in the same cluster (Figure 3.2).

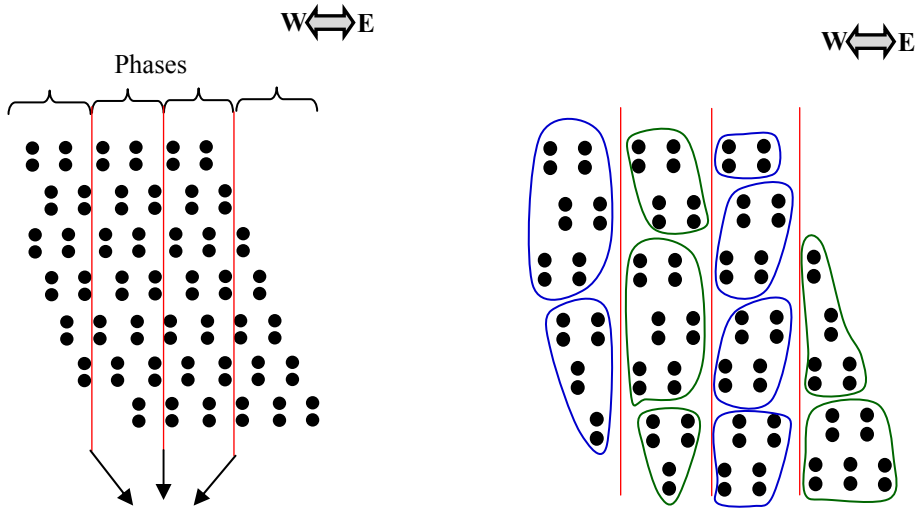

Figure 3.2. Defined phases based on advancement directions and their boundaries for west to east (WE) and east to west (EW) mining directions, with dots representing individual drawpoints.

Figure 3.3 shows an example of impractical clusters for west to each direction when the phases are not defined. It is obvious that defining precedence between clusters and controlling practical cave advancement are impossible.

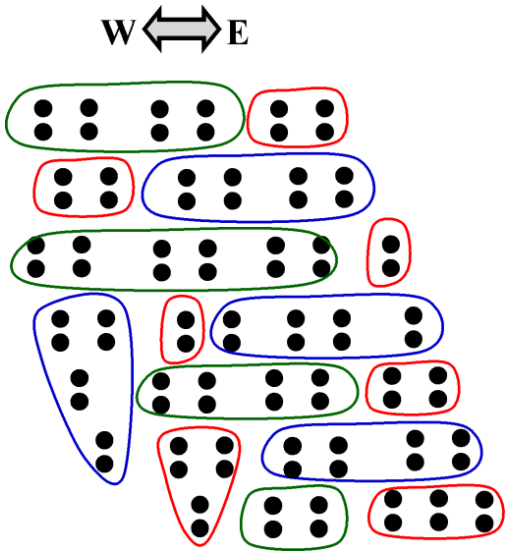

Figure 3.3. Clustering without phases for the west to east direction

The general procedure of the algorithm is as follows:

1. Define the maximum number of required clusters and the maximum number of allowed draw columns within each cluster.
2. Each draw column is considered a cluster, so if there are D draw columns, then there are D clusters. The similarities between clusters are the same as the similarities between the objects they contain.
3. Similarity values are calculated.
4. The most similar pair of clusters is merged into a single cluster.
5. The similarity between the new cluster and the rest of the clusters is calculated. Steps 2 and 3 are repeated until the maximum number of clusters is reached or there is no pair of clusters to merge because of the maximum number of allowed draw columns within each cluster.

The similarity value between draw columns i and j is defined by Equation (3.2), Where $\widetilde{D_{ij}}$ represents the normalized distance value between draw columns i and

j, $\widetilde{G_{ij}}$ represents the normalized grade difference between draw columns i and j, and $\widetilde{T_{ij}}$ represents the normalized tonnage difference between draw columns i and j. WD, WG, and WT are weighting factors for distance, grade, and tonnage, respectively.

$$S_{ij} = \frac{1}{\widetilde{D}_{ij}^{WD} \times \widetilde{G}_{ij}^{WG} \times \widetilde{T}_{ij}^{WT}} \tag{3.2}$$

A mine with D draw columns has a $D \times D$ distance matrix. The matrix is normalized by dividing all of its elements by the maximum value. The calculated normalized distance factor is then raised to the power of W_D. The same approach is taken for grade and tonnage differences. To avoid infinite numbers in similarity indices, the grade and tonnage difference values are considered equal to a very small number wherever these values for two draw columns are the same. The mine planner defines the weights.

3.4 Mathematical Programming Formulation

In this section, the MILP formulations are presented for three levels of problem resolution: (i) cluster level, (ii) drawpoint level, and (iii) drawpoint-and-slice level. The production scheduler aims to maximize the NPV of the mining operation, while the mine planner has control over the development rate, vertical mining rate, lateral mining rate, mining capacity, maximum number of active drawpoints, and advancement direction. To support a given production target, the production scheduler defines the opening and closing time for each drawpoint and cluster, the draw rate from each drawpoint and cluster, the number of new drawpoints and clusters that need to be constructed, and the sequence of extraction from the drawpoints and clusters. The MILP models can be used in two ways. In the single-step method, the problem is solved at each level of resolution independently. This means the objective function and constraint are set up for each level and then the problem is solved. In the multi-step method, the cluster level results are used for variable elimination in the drawpoint level. The

drawpoint level results are used for variable elimination in the drawpoint-and-slice level formulation.

3.4.1 Models Assumption

Several major assumptions are used in the MILP formulations. These assumptions are all valid at different resolution levels:

1. For planning and operational purposes, the geological configuration of the deposit is expressed by a block model. Each block is uniquely identified with its geological characteristic, in particular the ore grades. A draw column, which is vertical, is created based on the block model. The total column is divided into slices, which match the vertical spacing of the geological block model. Numerical data are used to represent orebody attributes in each slice, such as tonnage, density, grade of elements, elevation, percentage of dilution, and economic data.

2. The model is used for multi-period optimization. There is no material mixing between blocks as a function of draw. The source model is assumed to be static with time. The dilution modeling is carried out in PCBC (Gemcom Software International, 2012) at the slice level, prior to using this static model.

3. To create the clusters, the draw columns are grouped into clusters based on similarities between their physical location, average grade, and tonnage.

4. The portion scheduled to be extracted from each cluster is assumed to be taken from all the drawpoints, based on the ratio of each draw column's tonnage in the cluster.

5. Models are solved in different advancement directions which are limited based on geotechnical constraints. Thus, the extraction precedence among clusters and drawpoints should be known and given as an input to the algorithm. These are handled in the models using binary parameters that

control which cluster, drawpoint, or slice are preferred over others based on the advancement direction.

6. The rate of the undercutting and subsequent cluster, drawpoint, or slice opening periods is handled in the models using binary parameters that regulate whether or not a cluster, drawpoint, or slice is available for production.

7. The models are used to determine a long-term production schedule at three different levels of resolution: (i) aggregated draw columns (cluster level), (ii) drawpoint level, and (iii) drawpoint-and-slice level. The models do not provide guidance for short-term planning.

3.4.2 Formulation of MILP Models

In a typical block-cave long-term scheduling problem, the number of integer and continuous decision variables, and the number of constraints formulating a problem exceed the capacity of the current state of hardware and software to solve the problem in a reasonable time. To overcome the size problem of mathematical programming models and generate a robust, practical, near-optimal schedule, a multi-step method for long-term production scheduling of block caving is presented. There are three levels of resolution, each with a formulation that can be used individually (see Figure 3.4). The three levels of resolution for the MILP models are: a) cluster level model, b) drawpoint level model, and c) drawpoint-and-slice level model.

In the cluster-level model, the draw columns are aggregated into practical scheduling units using a hierarchical clustering algorithm. Aggregation is necessary to generate near-optimal realistic mine plans in a reasonable CPU time that could be considered useful in real-world mine planning. At this level, the optimal life-of-mine multi-period block-cave production schedule is generated at the cluster level. This is the strategic yearly production schedule with the objective of NPV maximization. The strategic plan honors mining capacity and uniform feed to the processing plant.

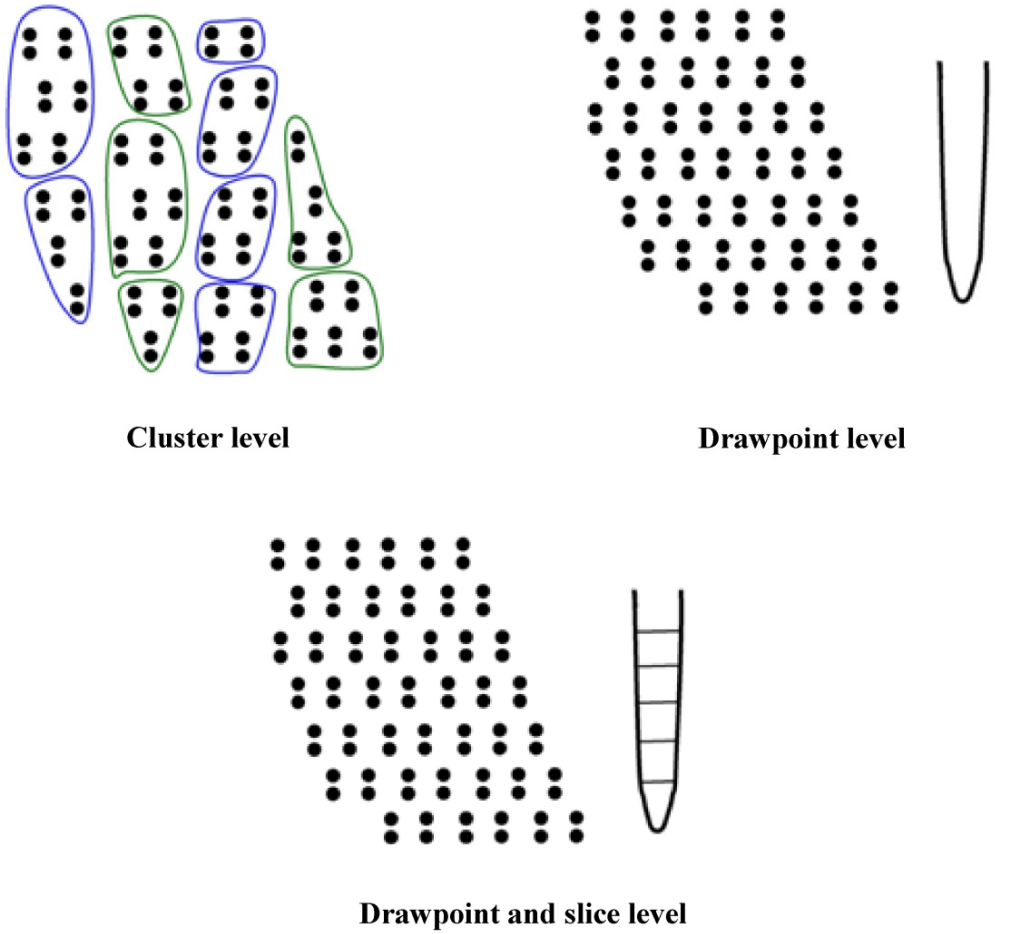

Figure 3.4. Three different levels of resolution for block-cave production scheduling with dots representing individual drawpoints

The drawpoint-level model, in which the slices within each draw column are grouped without considering the grade of slices, uses draw columns to optimize the production schedule.

At the drawpoint-and-slice level, the model uses drawpoints and slices. At this level, precedence between slices and between drawpoints and grades of slices, are also involved. The time horizon for this detailed 3D model could vary as a subset of the time horizons chosen in the previous models.

At the cluster and drawpoint levels, the precedence between clusters or drawpoints is controlled in a horizontal direction. In other words, we treat the

problem at these levels as a strategic long-term plan, and the slices are not used in the formulations.

3.4.3 Objective Function at Three Level of Resolution

There are a number of strategic objectives common in industry. Usually, the target is to maximize the mining operations' NPV within the existing economic, technical, and environmental constraints. However, other objectives, such as cost minimization or reserve maximization, could also be considered.

One of the main goals of planning a block-cave mine is to maximize the mine's value. In this research, the MILP formulations' objective functions are to maximize the mining operation's NPV. According to the level of resolution, the strategy is to mine the clusters, drawpoints, or slices with higher economic value early in order to maximize the NPV.

At the drawpoint-and-slice level formulation, profit from mining a drawpoint depends on the value of the slices and the costs incurred in mining, while at the drawpoint level, profit from mining a drawpoint depends on the value of the material within the related draw column. At the cluster level, profit from mining a cluster depends on the economic value of the draw columns located within the cluster.

3.4.4 Constraints

The following set of constraints is included in the formulation at three levels of resolution:

- Mining capacity
- Grade blending
- Maximum number of active clusters or drawpoints
- Number of new clusters or drawpoints

- Continuous mining
- Mining precedence
- Reserves
- Draw rate

3.4.4.1 Mining Capacity

This constraint forces a mining system to achieve its desired production target. It ensures that the total tonnage of material extracted from clusters, drawpoints, or slices in each period is within the acceptable range that allows flexibility for potential operational variations. This constraint is applied to all levels of resolution.

3.4.4.2 Grade Blending

This constraint forces the mining system to achieve the desired grade. It ensures that the average grade of production is within the desired range in each period. This constraint is only used at drawpoint-and-slice-level model.

3.4.4.3 Maximum Number of Active Clusters or Drawpoints

This constraint controls the maximum number of active clusters or drawpoints at any given period in the schedule. In each period, the number of active clusters or drawpoints must not exceed the allowable number and has to be constrained according to the size of the ore-body, available infrastructure, and equipment availability. A large number of active clusters or drawpoints might lead to serious operational problems. Figure 3.5 illustrates how the number of active clusters or drawpoints is calculated in each period. This number in each period is equal to the summation of the lines under that period.

3.4.4.4 Number of New Clusters or Drawpoints

This constraint defines the maximum feasible number of clusters or drawpoints to be opened at any given time within the scheduled horizon. This constraint is

usually based on the footprint geometry, the geotechnical behavior of the rock mass, and the existing infrastructure of the mine, which will typically define available mining faces.

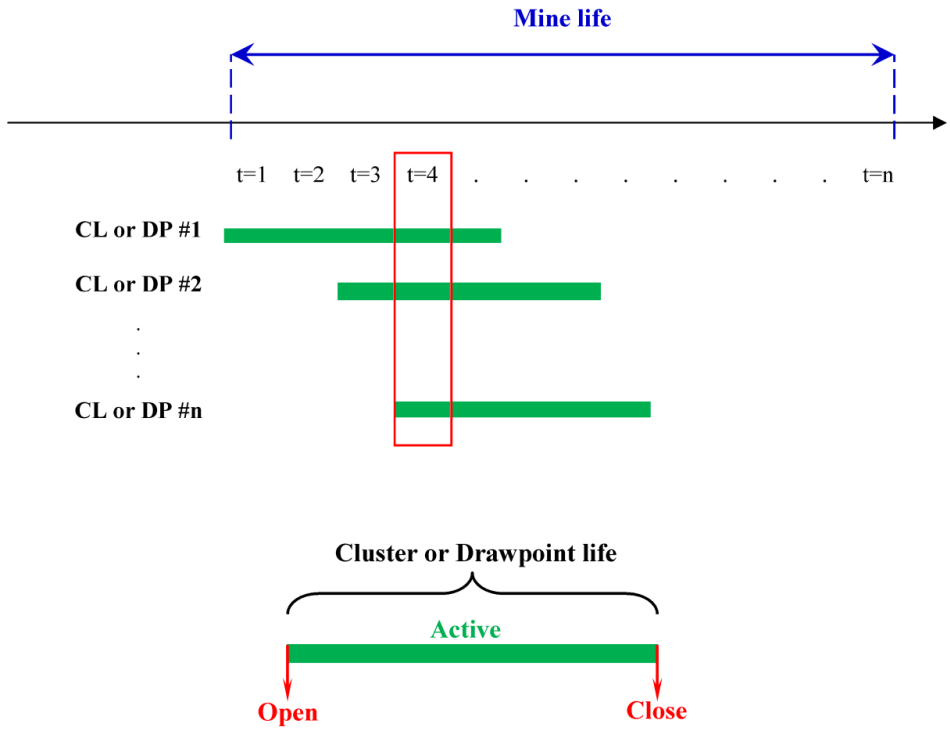

Figure 3.5. Determination of the number of active clusters or drawpoints in each period. The green line shows the periods in which the related cluster or drawpoint is active

3.4.4.5 Continuous Mining

This constraint forces the mining system to extract material from clusters, drawpoints, or slices continuously after opening until closing. In other words, after starting the extraction from a cluster, drawpoint, or slice, at least the acceptable minimum portion of them must be extracted in each period during the life of them.

3.4.4.6 Mining Precedence

This constraint defines where to start the caving within the layout and how to progress. The planner gives the advancement direction to the model. There are different methods to define the advancement direction. Barlett (1992) recommended starting the caving where the weak rock is located. This method has

two advantages: (i) the hydraulic ratio can be reached earlier in the life of the mine, which shortens the time needed to recover the investment; (ii) the mine can reach a steady production earlier since adequate fragmentation is achieved. Another method consists of starting where the high grade ore is located. This method leads to early payback of the investment or high NPV.

Because of the continuous advancement of the cave front in block caving, the production schedules using the MILP formulation are implemented for different advancement directions. The mining precedence is defined based on the level of resolution. At the cluster level, according to the advancement direction, for each cluster there are some clusters among adjacent clusters that must be started before the considered one is extracted. Also, it is possible that there is no predecessor cluster. The same concept is applied to the drawpoints and the slices at other levels of resolution.

At the cluster level, to determine the clusters that extraction from them must be started before the considered cluster, the three steps below must be followed.

1. The boundary drawpoints of the considered cluster are determined. These boundary drawpoints are located behind an imaginary line perpendicular to the desired advancement direction at the cluster's center point.

2. All clusters that have at least one adjacent drawpoint with the boundary drawpoints are determined.

3. Clusters whose center point is behind the center point of the considered cluster are defined as clusters from which extraction must be started before the considered cluster in the considered advancement direction out of selected clusters in the previous step.

For instance, Figure 3.6 shows four clusters which have been created for the south to north (SN) advancement direction. The boundary drawpoints of cluster 25, which are located behind of the red imaginary line, are d17, d24, d31, and d37. Clusters 23 and 26 have at least one adjacent drawpoint with the boundary

drawpoints of cluster 25. Therefore, they have the potential to be considered clusters from which extraction must be started before extracting from cluster 25. Since the center point of cluster 23 is behind the center point of cluster 25 in the considered direction (SN), it is only selected as a cluster from which extraction must be started before extracting from cluster 25.

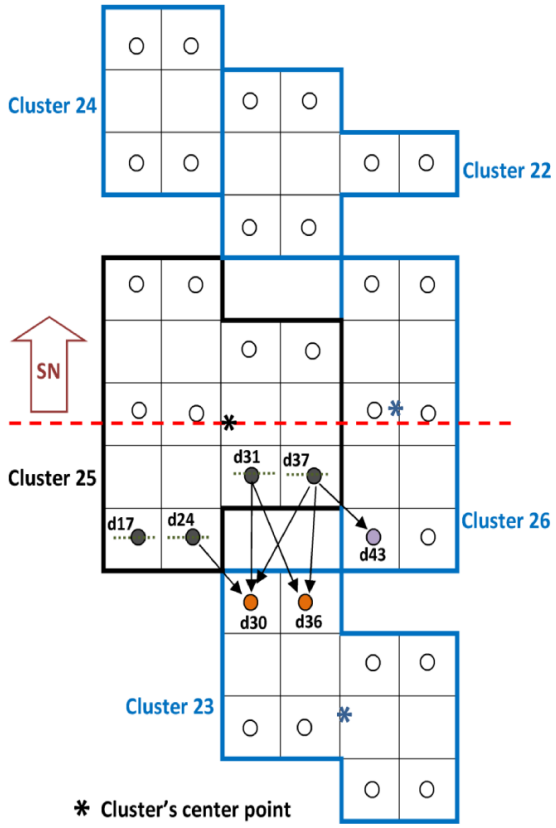

Figure 3.6. Determination method of the predecessor cluster based on the advancement direction

At the drawpoint level, the drawpoints from which extraction must be started before extracting from the considered drawpoint are determined based on clusters and drawpoints within clusters. For this purpose, the two steps below must be followed:

1. Each drawpoint belongs to a cluster that has its predecessor clusters. Therefore, members of the predecessor clusters are considered as

drawpoints from which extraction must be started before extracting from the considered drawpoint.

2. Imagine a line perpendicular to the desired advancement direction at the location of the considered drawpoint. All adjacent drawpoints located in the same cluster and behind the imaginary line are considered drawpoints from which extraction must be started before extracting from the considered drawpoint.

In the offset herringbone layout (Brown, 2003), each drawpoint is surrounded by a maximum of seven drawpoints (see Figure 3.7). Figure 3.8 shows the procedure to determine the precedence between the adjacent drawpoints. The adjacent drawpoints for drawpoint d4 include d1, d2, d3, d5, d6, d7, and d8. In the advancement direction of north to south (NS), the extraction of drawpoints d1, d2, and d3 has to be started prior to extracting from drawpoint d4. Figure 3.8b shows the advancement direction of south west to north east (SW to NE). The extraction of drawpoints d1, d6, and d7 has to be started prior to extracting from drawpoint d4.

Figure 3.9 illustrates the above-mentioned steps. Drawpoint d30 belongs to cluster CL32. So, extraction from all drawpoints within clusters CL20 and CL15 must be started before d30. In addition to this, among adjacent drawpoints for drawpoint d30 within cluster CL32, the extraction of drawpoints d37, d43, and d44 has to be started prior to extracting from drawpoint d30. Consequently, extraction from d30 can be started if only if extraction from the determined 19 drawpoints has been started.

The precedence between drawpoints or clusters is controlled in a horizontal direction. At the drawpoint-and-slice level model, in addition to the horizontal direction, the precedence between slices in a vertical direction must be controlled as well. Extraction from a slice can be started only if the slice below the slice in question has been extracted completely.

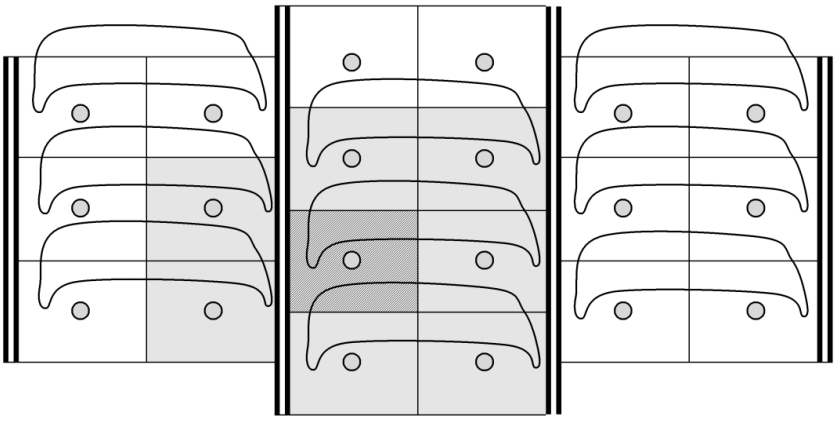

Figure 3.7. Offset herringbone extraction level layout (Brown, 2003)

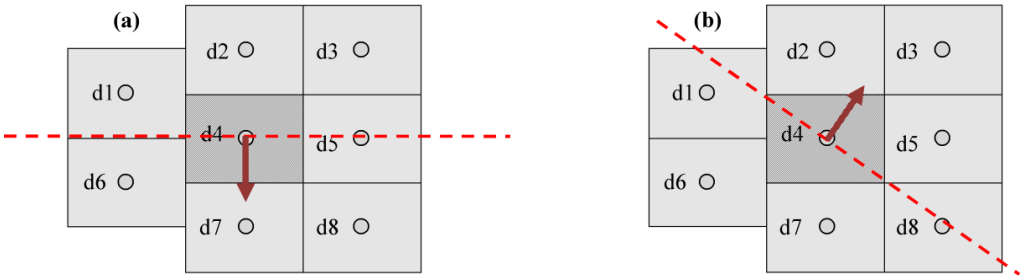

Figure 3.8. Determination method of the predecessor drawpoints among the adjacent drawpoints based on the advancement direction.

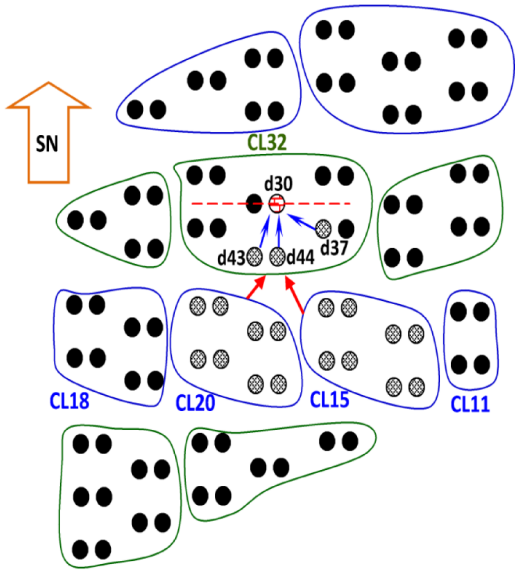

Figure 3.9. Determination method of the predecessor drawpoints based on the advancement direction

3.4.4.7 Reserves

This constraint ensures that the fractions of the cluster or draw column that are extracted over the scheduling periods sum to one, which means there is no selective mining, and thereby all the material in the cluster or draw column must be extracted. The all material must be extracted because the BHOD, which is the maximum cumulative value along the draw column, has already been calculated for all draw columns. If this constraint be set less than or equal one, there is no need to use the calculated BHOD by PCBC, because in this case the BHOD draw is calculated for each draw column during the optimization.

3.4.4.8 Draw Rate

This constraint controls the maximum and minimum tonnage that can be drawn from a drawpoint in a period of time. This rate should be fast enough to avoid compaction and slow enough to avoid air gaps. The fragmentation process usually determines the maximum limit to the draw rate, since time is required to achieve good fragmentation. However, sometimes the maximum rate may be dictated by the LHD productivity. It is important to notice that the draw rate is a function of the planning horizon.

3.4.5 MILP Formulations at Three Level of Resolution

3.4.5.1 Cluster-Level Model

At the cluster level, profit from mining a cluster depends on the economic value of the draw columns located within the cluster. The economic value of each cluster (CLEV) is equal to the summation of the economic value of the draw columns within the cluster and the costs incurred in mining. The CLEV is a constant value for each cluster. To solve the problem at the cluster level, three sets of decision variables are employed: one continuous decision variable and two binary variables. The continuous decision variable indicates the portion of extraction from each cluster in each period. Two binary variables control the number of active clusters, precedence of extraction between clusters, opening and closing time of each cluster, draw rate from each cluster, and the number of new

clusters that need to be constructed in each period. At the cluster level formulation, binary variables are defined to identify at what period a given cluster is started and active. At this level of resolution, the objective function tries to mine the cluster with a higher CLEV earlier than others.

The notation used to formulate the problem at the cluster level is classified as sets, indices, parameters and decision variables.

Sets

S^{cl}	For each cluster, *cl*, there is a set, S^{cl} , defining the predecessor clusters that must be started prior to extracting cluster *cl*.

Indices

$cl \in \{1,...,CL\}$	Index for clusters.
k	Index for a cluster belonging to the set S^{cl}.
$t \in \{1,....,T\}$	Index for scheduling periods.

Parameters

CL	Maximum number of clusters in the model.
$CLEV_{cl}$	Economic value of cluster *cl*.
$\underline{DR}_{d,t}$	Minimum possible draw rate of drawpoint *d* in period *t*.
$\overline{DR}_{d,t}$	Maximum possible draw rate of drawpoint *d* in period *t*.
$\underline{DR}_{k,t}$	Minimum possible draw rate of drawpoints belonging to set S^{cl} in period *t*.
$\overline{DR}_{k,t}$	Maximum possible draw rate of drawpoints belonging to set S^{cl} in period *t*.
i	Discount rate.

$\underline{M}_t$ Lower limit of mining capacity in period *t*.

$\overline{M}_t$ Upper limit of mining capacity in period *t*.

$N_{Acl,t}$ Maximum allowable number of active clusters in period *t*.

$\underline{N}_{Ncl,t}$ Lower limit for the number of new clusters, the extraction from which can start in period *t*.

$\overline{N}_{Ncl,t}$ Upper limit for the number of new clusters, the extraction from which can start in period *t*.

NDP_{cl} Number of draw columns within cluster *cl*.

T Maximum number of scheduling periods.

Ton_{cl} Total tonnage of material within cluster *cl*.

Decision variables

$A_{cl,t} \in \{0,1\}$ Binary decision variable equal to 1 if cluster *cl* is active in period *t*; otherwise it is 0.

$U_{cl,t} \in [0,1]$ Continuous decision variable, representing the portion of cluster *cl* to be extracted in period *t*.

$Z_{cl,t} \in \{0,1\}$ Binary variable controlling the precedence of extraction of clusters. It is equal to 1 if extraction from cluster *cl* is started in period *t*; otherwise it is 0.

Objective function:

$$\text{Maximize} \quad \sum_{t=1}^{T}\sum_{cl=1}^{CL}\left[\frac{CLEV_{cl}}{(1+i)^t}\right]U_{cl,t} \tag{3.3}$$

Constraints:

$$\underline{M}_t \le \sum_{cl=1}^{CL} U_{cl,t} \times \left(Ton_{cl}\right) \le \overline{M}_t$$

$$\forall t \in \{1,...,T\} \quad (3.4)$$

$$A_{cl,t} \le L.U_{cl,t}$$

$$L \ge \left(\frac{\max\left\{Ton_{cl}\right\}}{\min\left\{\text{number of drawpoints within a cluster}\right\} \times \text{minimum draw rate}} \right)$$

$$\forall t \in \{1,...,T\}, \quad cl \in \{1,...,CL\} \quad (3.5)$$

$$U_{cl,t} \le A_{cl,t}$$

$$\forall t \in \{1,...,T\}, \quad cl \in \{1,...,CL\} \quad (3.6)$$

$$\sum_{cl=1}^{CL} A_{cl,t} \le N_{Acl,t}$$

$$\forall t \in \{1,...,T\} \quad (3.7)$$

$$Z_{cl,t} - \sum_{j=1}^{t} U_{k,j} \le 1 - \left(\frac{\min\left\{\text{number of drawpoints within a cluster}\right\} \times \text{minimum draw rate}}{\max\left\{Ton_{cl}\right\}} \right)$$

$$\forall cl \in \{1,...,CL\}, \quad t \in \{1,...,T\}, \quad k \in S^{cl} \quad (3.8)$$

$$\sum_{t=1}^{T} Z_{cl,t} = 1$$

$$\forall cl \in \{1,...,CL\} \quad (3.9)$$

$$A_{cl,t} - A_{cl,(t-1)} \le Z_{cl,t}$$

$$\forall cl \in \{1,...,CL\}, \quad t \in \{2,...,T\} \quad (3.10)$$

$$A_{cl,1} - Z_{cl,1} \le 0.5$$

$$\forall cl \in \{1,...,CL\} \quad (3.11)$$

$$A_{cl,t} \times \left(NDP_{cl} \times \underline{DR}_{k,t} \right) \le U_{cl,t} \times \left(Ton_{cl} \right) \le \left(NDP_{cl} \times \overline{DR}_{k,t} \right)$$

$$\forall cl \in \{1,...,CL\}, \quad t \in \{1,...,T\}, \quad k \in S^{cl} \qquad (3.12)$$

$$\underline{N}_{Ncl,t} \le \sum_{cl=1}^{CL} Z_{cl,t} \le \overline{N}_{Ncl,t}$$

$$\forall t \in \{2,...,T\} \qquad (3.13)$$

$$\sum_{cl=1}^{CL} Z_{cl,1} \le N_{Acl,1} \qquad (3.14)$$

$$\sum_{t=1}^{T} U_{cl,t} = 1$$

$$\forall cl \in \{1,...,CL\} \qquad (3.15)$$

The objective function, Equation (3.3), is composed of the CLEV, discount rate, and a continuous decision variable that indicates the portion of a cluster, which is extracted in each period. The most profitable clusters will be chosen as part of the production in order to optimize the NPV. The total tonnage and draw rate of each cluster, and the cluster economic value, are all a function of the number of draw columns within the cluster. The constraints are presented by Equations (3.4) to (3.15).

Equation (3.4) represents the mining capacity, which ensures that the total tonnage of material extracted from clusters in each period is within the acceptable range that allows flexibility for potential operational variations. The constraints are controlled by the continuous variable $U_{cl,t}$. There is one constraint per period. Equations (3.5) to (3.7), control the maximum number of active clusters at any given period of the schedule. During the mine life, each cluster can be in three different situations: open, active, and closed. Equation (3.5) forces variable $A_{cl,t}$ to be zero if a portion of cluster *cl* is not extracted in period *t*, while Equation (3.6) changes variable $A_{cl,t}$ to 1 when a portion of cluster *cl* is extracted in period *t*.

The MILP formulation is implemented for different advancement directions based on the precedence between clusters. According to the advancement direction, for each cluster *cl* there is a set S^{cl} which defines the predecessor clusters among adjacent clusters that must be started before cluster *cl* is extracted. The number of datasets is equal to the number of advancement directions defined for each cluster.

To control the precedence of extraction, a binary decision variable, $Z_{cl,t}$, is employed. Equation (3.8) is applied to all members of set S^{cl}. If the summation of extracted portions from each cluster belonging to set S^{cl} until the considered period, *t*, is equal to or greater than the minimum allowable draw rate for the cluster, then extraction from cluster *cl* can be started. It should be mentioned that at the right side of Equation (3.8), the required percentage of the extraction for the predecessor clusters can be defined for each cluster. Equation (3.9) ensures that cluster *cl* is opened once during the mine life.

Extraction from each cluster must be continuous. Equation (3.10) ensures that if extraction from cluster *cl* is started during or after period two, at least a portion of the cluster is extracted until all of the material within that cluster has been extracted; otherwise the cluster must be closed. The minimum portion of extraction must be equal or greater than the minimum allowable draw rate of the cluster. Equation (3.11) is used for period one. It ensures that if extraction from cluster *cl* is started in period one, the related variable $A_{cl,1}$ for the cluster is equal to 1.

Equation (3.12) controls the maximum and minimum rate of draw from the cluster. The draw rate of each cluster is a function of the number of draw columns within the cluster. When cluster *cl* is not active, variable $A_{cl,t}$ is equal to zero and this relaxes the lower bound of Equation (3.12).

The number of new clusters opened in each period is controlled by Equation (3.13). Variable $Z_{cl,t}$ is equal to 1 if the extraction from cluster *cl* is started in period *t*. Therefore, the summation of this variable for all clusters in each period indicates the number of new clusters opened in that period. At the beginning and

in period one, the number of new clusters is equal to the maximum number of active clusters.

Equation (3.15) ensures that the fractions of each cluster that are extracted over the scheduling periods sum to one, which means that all the material within the cluster is going to be extracted. To solve the problem without considering the obtained BHOD form the PCBC, this equation must be less than or equal to 1. Using this method, the best height of draw for each cluster can be obtained.

3.4.6 Drawpoint-Level Model

At the drawpoint level formulation, profit from mining a drawpoint depends on the value of the material within the related draw column. The economic value of each draw column (DEV) is equal to the summation of the economic value of the slices within the draw column and the costs incurred in mining. The DEV is a constant value for each drawpoint. At this level of resolution, the objective function, Equation (3.16), seeks to mine draw columns with higher DEV earlier than others. The objective function is composed of the DEV, discount rate, and a continuous decision variable that indicates the portion of a draw column, which is extracted in each period. The most profitable drawpoints will be chosen as part of the production in order to optimize the NPV. Two binary variables control the number of active drawpoints, precedence of extraction between drawpoints, opening and closing time of each drawpoint, draw rate from each drawpoint, and the number of new drawpoints that need to be constructed in each period. At the drawpoint level formulation, binary variables are defined to identify at what period a given drawpoint is started and active. The total tonnage and the draw column economic value are all a function of the number of slices within the draw column. The DEV is the summation of economic value of slices within the draw column and is a constant value for each drawpoint.

The notation used to formulate the problem at the drawpoint level has classified as sets, indices, parameters and decision variables.

Sets

S^d	For each drawpoint, d, there is a set S^d defining the predecessor drawpoints that must be started prior to extraction of drawpoint d.

Indices

$d \in \{1,...,D\}$	Index for drawpoints.
l	Index for a drawpoint belonging to set S^d.
$t \in \{1,....,T\}$	Index for scheduling periods.

Parameters

D	Maximum number of drawpoints in the model.
DEV_d	Economic value of the draw column associated with drawpoint d.
$\underline{DR}_{d,t}$	Minimum possible draw rate of drawpoint d in period t.
$\overline{DR}_{d,t}$	Maximum possible draw rate of drawpoint d in period t.
$N_{Ad,t}$	Maximum allowable number of active drawpoints in period t.
$\underline{N}_{Nd,t}$	Lower limit for the number of new drawpoints, the extraction from which can start in period t.
$\overline{N}_{Nd,t}$	Upper limit for the number of new drawpoints, the extraction from which can start in period t.
Ton_d	Total tonnage of material within the draw column associated with drawpoint d.

Decision variables

$A_{d,t} \in \{0,1\}$	Binary decision variable equal to 1 if drawpoint d is active in period t; otherwise it is 0.
$U_{d,t} \in [0,1]$	Continuous decision variable, representing the portion of drawpoint d to be extracted in period t.

$Z_{d,t} \in \{0,1\}$ Binary variable controlling the precedence of extraction of drawpoints. It is equal to 1 if extraction from drawpoint *d* is started in period *t*; otherwise it is 0.

Objective function:

$$\text{Maximize} \quad \sum_{t=1}^{T}\sum_{d=1}^{D}\left[\frac{DEV_d}{(1+i)^t}\right]U_{d,t} \tag{3.16}$$

Constraints:

$$\underline{M}_t \le \sum_{d=1}^{D} U_{d,t} \times (Ton_d) \le \overline{M}_t$$

$$\forall t \in \{1,...,T\} \tag{3.17}$$

$$A_{d,t} \le L.U_{d,t} \quad , L \ge \frac{\max\{Ton_d\}}{\text{minimum draw rate}}$$

$$\forall t \in \{1,...,T\}, \quad d \in \{1,...,D\} \tag{3.18}$$

$$U_{d,t} \le A_{d,t}$$

$$\forall t \in \{1,...,T\}, \quad d \in \{1,...,D\} \tag{3.19}$$

$$\sum_{d=1}^{D} A_{d,t} \le N_{Ad,t}$$

$$\forall t \in \{1,...,T\} \tag{3.20}$$

$$Z_{d,t} - \sum_{j=1}^{t} U_{l,j} \le 1 - \left(\frac{\text{minimum draw rate}}{\max\{Ton_d\}}\right)$$

$$\forall d \in \{1,...,D\}, \quad t \in \{1,...,T\}, \quad l \in S^d \tag{3.21}$$

$$\sum_{t=1}^{T} Z_{d,t} = 1$$

$$\forall d \in \{1,...,D\} \qquad (3.22)$$

$$A_{d,t} - A_{d,(t-1)} \le Z_{d,t}$$

$$\forall t \in \{1,...,T\}, \quad d \in \{1,...,D\} \qquad (3.23)$$

$$A_{d,1} - Z_{d,1} \le 0.5$$

$$\forall d \in \{1,...,D\} \qquad (3.24)$$

$$A_{d,t} \times \underline{DR}_{d,t} \le U_{d,t} \times (Ton_d) \le \overline{DR}_{d,t}$$

$$\forall t \in \{1,...,T\}, \quad d \in \{1,...,D\} \qquad (3.25)$$

$$\underline{N}_{Nd,t} \le \sum_{d=1}^{D} Z_{d,t} \le \overline{N}_{Nd,t}$$

$$\forall t \in \{2,...,T\} \qquad (3.26)$$

$$\sum_{d=1}^{D} Z_{d,1} \le N_{Ad,1} \qquad (3.27)$$

$$\sum_{t=1}^{T} U_{d,t} = 1$$

$$\forall d \in \{1,...,D\} \qquad (3.28)$$

The constraints are presented by Equations (3.17) to (3.28). Equation (3.17) represents the mining capacity, which ensures that the total tonnage of material extracted from drawpoints in each period is within the acceptable range that allows flexibility for potential operational variations. The constraints are controlled by the continuous variable $U_{d,t}$. There is one constraint per period. Equations (3.18) to (3.20), control the maximum number of active drawpoints at any given period in the schedule. Similar to the cluster level formulation, each drawpoint can be in three different situations during the mine life: open, active,

and closed. Equation (3.18) forces variable $A_{d,t}$ be zero if a portion of drawpoint d is not extracted in period t, while Equation (3.19) changes variable $A_{d,t}$ to 1 when a portion of drawpoint d is extracted in period t.

The MILP formulation is implemented for different advancement directions based on the precedence between drawpoints. According to the advancement direction, for each drawpoint d there is a set S^d, which defines the predecessor drawpoints among adjacent drawpoints that must be started before drawpoint d is extracted. The number of datasets is equal to the number of advancement directions defined for each drawpoint. To control the precedence of extraction, a binary decision variable, $Z_{d,t}$, is employed. Equation (3.21) is applied to all members of set S^d. If the summation of extracted portions from each drawpoint which belongs to set S^d until the considered period, t, is equal to or greater than the minimum allowable draw rate, then extraction from drawpoint d can be started. It should be mentioned that at the right side of Equation (3.21), the required percentage of the extraction for the predecessor drawpoints can be defined for each drawpoint. Equation (3.22) ensures that drawpoint d is opened once during the mine life.

Extraction from each drawpoint must be continuous. Equation (3.23) ensures that if extraction from drawpoint d is started during or after period two, at least a portion of the draw column is extracted until all of the material within the draw column associated with the drawpoint has been extracted; otherwise the drawpoint must be closed. The minimum portion of extraction must be equal to or greater than the minimum allowable draw rate. Equation (3.24) is used for period one. It ensures that if extraction from drawpoint d is started in period one, the related variable $A_{d,1}$ for the drawpoint is equal to 1.

Equation (3.25) controls the maximum and minimum rate of draw from each drawpoint. When drawpoint d is not active, variable $A_{d,t}$ is equal to zero and this relaxes the lower bound of Equation (3.25).

The number of new drawpoints in each period is controlled by Equation (3.26). Variable $Z_{d,t}$ is equal to 1 if the extraction from drawpoint d is started in period t.

Therefore, the summation of this variable for all drawpoints in each period indicates the number of new drawpoints opened in that period. At the beginning and in period one, the number of new drawpoints is equal to the maximum number of active drawpoints.

Equation (3.28) ensures that the fractions of the draw column extracted over the scheduling periods are going to sum up to one, which means that all the material within the draw column is going to be extracted. To solve the problem without considering the obtained BHOD form the PCBC, this equation must be less than or equal to 1. Using this method, the best height of draw for each draw column can be obtained based on the optimization.

3.4.7 Drawpoint-and-Slice Level Model

At the drawpoint-and-slice level, profit from mining a drawpoint depends on the value of the slices and the costs incurred in mining. The objective function, Equation (3.29), is composed of the slice economic value (SEV), discount rate, and a continuous decision variable that indicates the portion of the slice extracted in each period. The objective function seeks to mine slices with higher SEV earlier than other slices. The SEV is a constant value for each slice.

To solve the problem at this level of resolution, one continuous decision variable and one binary variable for slices, and two binary variables for drawpoints, are employed. The continuous decision variable indicates the portion of extraction from each slice in each period. The binary decision variable for slices controls precedence of extraction between slices. The binary decision variables for drawpoints control the number of active drawpoints, precedence of extraction between drawpoints, opening and closing time of each drawpoint, draw rate from each drawpoint, and number of new drawpoints that need to be constructed in each period. For the drawpoint-and-slice level formulation, instead of using binary variables to define explicitly at what period a drawpoint is started or is active, the binary variables specify whether a drawpoint is started by a certain

period, because the "*by period"* formulations tend to be solved faster than those the *"at period"* formulations.

The notation used to formulate the problem at the drawpoint-and-slice level is classified as sets, indices, parameters and decision variables.

Sets

S^d	For each drawpoint, d, there is a set, S^d, defining the predecessor drawpoints that must be started prior to extracting drawpoint d.
S^{ds}	For each drawpoint, d, there is a set S^{ds} defining the slices in the draw column associated with drawpoint d.
S^{dls}	For each drawpoint, d, there is a set S^{dls} defining the lowest slice within the draw column associated with drawpoint d.
S^s	For each slice, s, there is a set S^s defining the predecessor slices that must be extracted prior to extracting slice s.

Indices

$e \in \{1,...,E\}$	Index for elements of interest in each slice.
l	Index for a drawpoint belonging to set S^d.
n	Index for a slice belonging to set S^{ds}.
p	Index for a slice belonging to set S^{dls}.
q	Index for a slice belonging to set S^s.
$s \in \{1,...,S\}$	Index for slices.
$t \in \{1,....,T\}$	Index for scheduling periods.

Parameters

G_{es}	Average grade of element e in the ore portion of slice s.
$\overline{G}_{e,t}$	Upper limit of the acceptable average head grade of element e in period t.

$\underline{G}_{e,t}$ Lower limit of the acceptable average head grade of element *e* in period *t*.

Ns_d Number of slices within the draw column associated with drawpoint *d*.

S Maximum number of slices in the model.

SEV_s Economic value of slice *s*.

Ton_s Total tonnage of material within slice *s*.

Decision variables

$B_{s,t} \in \{0,1\}$ Binary variable controlling the precedence of the extraction of slices. It is equal to 1 if the extraction of slice *s* has started by or in period *t*; otherwise it is 0.

$C_{d,t} \in \{0,1\}$ Binary variable controlling the closing period of drawpoints. It is equal to 1 if the extraction of drawpoint *d* has finished by or in period *t*; otherwise it is 0.

$E_{d,t} \in \{0,1\}$ Binary variable controlling the starting period of drawpoints and precedence of extraction of drawpoints. It is equal to 1 if the extraction of drawpoint *d* has started by or in period *t*; otherwise it is 0.

$X_{s,t} \in [0,1]$ Continuous decision variable representing the portion of slice *s* to be extracted in period *t*.

Objective function:

$$\text{Maximize} \quad \sum_{t=1}^{T}\sum_{s=1}^{S}\left(\frac{SEV_s}{(1+i)^t}\right)\times X_{s,t} \tag{3.29}$$

Constraints:

$$\underline{M}_t \le \sum_{s=1}^{S} (Ton_s) \times X_{s,t} \le \overline{M}_t$$

$$\forall t \in \{1,...,T\} \qquad (3.30)$$

$$\sum_{s=1}^{S} \left(Ton_s \times \left(\underline{G}_{e,t} - G_{es} \right) \right) \times X_{s,t} \le 0$$

$$\forall t \in \{1,...,T\}, \quad e \in \{1,...,E\} \qquad (3.31)$$

$$\sum_{s=1}^{S} \left(Ton_s \times \left(G_{es} - \overline{G}_{e,t} \right) \right) \times X_{s,t} \le 0$$

$$\forall t \in \{1,...,T\}, \quad e \in \{1,...,E\} \qquad (3.32)$$

$$X_{p,t} - E_{d,t} \le 0$$

$$\forall t \in \{1,...,T\}, \quad d \in \{1,...,D\}, \quad p \in S^{dls} \qquad (3.33)$$

$$E_{d,t} - E_{d,(t+1)} \le 0$$

$$\forall t \in \{1,...,T\}, \quad d \in \{1,...,D\} \qquad (3.34)$$

$$E_{d,t} - C_{d,t} \le L \times \sum X_{n,t} \quad , \quad L \ge \left(\frac{\max \{ Ton_d \}}{\text{minimum draw rate}} \right)$$

$$\forall t \in \{1,...,T\}, \quad d \in \{1,...,D\}, \quad n \in S^{ds} \qquad (3.35)$$

$$C_{d,t} - C_{d,(t+1)} \le 0$$

$$\forall t \in \{1,...,T\}, \quad d \in \{1,...,D\} \qquad (3.36)$$

$$\sum_{d=1}^{D} (E_{d,t} - C_{d,t}) \le N_{Ad,t}$$

$$\forall t \in \{1,...,T\} \qquad (3.37)$$

$$E_{l,t} - E_{d,t} \le 0$$

$$\forall d \in \{1,...,D\}, \quad t \in \{1,...,T\}, \quad l \in S^d \qquad (3.38)$$

$$\sum_{j=1}^{t} X_{s,j} - B_{s,t} \leq 0$$

$$\forall s \in \{1,...,S\}, \quad t \in \{1,...,T\} \qquad (3.39)$$

$$B_{s,t} - \sum_{j=1}^{t} X_{q,j} \leq 0$$

$$\forall s \in \{1,...,S\}, \quad t \in \{1,...,T\}, \quad q \in S^s \qquad (3.40)$$

$$B_{s,t} - B_{s,(t+1)} \leq 0$$

$$\forall s \in \{1,...,S\}, \quad t \in \{1,...,T\} \qquad (3.41)$$

$$\frac{\sum X_{n,t}}{Ns_d} \leq E_{d,t} - C_{d,t}$$

$$\forall d \in \{1,...,D\}, \quad t \in \{1,...,T\}, \quad n \in S^{ds} \qquad (3.42)$$

$$\underline{N}_{Nd,t} \leq \sum_{d=1}^{D} E_{d,t} - \sum_{d=1}^{D} E_{d,(t-1)} \leq \overline{N}_{Nd,t}$$

$$\forall t \in \{2,...,T\} \qquad (3.43)$$

$$\sum_{d=1}^{D} E_{d,1} \leq N_{Ad,1} \qquad (3.44)$$

$$\left(E_{d,t} - C_{d,t}\right).\underline{DR}_{d,t} \leq \sum \left(Ton_n\right).X_{n,t} \leq \overline{DR}_{d,t}$$

$$\forall d \in \{1,...,D\}, t \in \{1,...,T\}, n \in S^{ds} \qquad (3.45)$$

$$\sum_{t=1}^{T} X_{s,t} = 1$$

$$\forall s \in \{1,...,S\} \qquad (3.46)$$

The constraints are presented by Equations (3.30) to (3.45). Equation (3.30) represents the mining capacity which ensures that the total tonnage of material extracted from slices in each period is within the acceptable range that allows flexibility for potential operational variations. The constraints are controlled by the continuous variable $X_{s,t}$. There is one constraint per period.

Equations (3.31) and (3.32) control the production's average grade. They force the mining system to achieve the desired grade. The average grade of the element of interest has to be within the acceptable range and between the certain values.

Each draw column is divided into slices. The lowest slice controls the starting period of extraction from each drawpoint. This means that the extraction from the draw column associated with drawpoint d is started by the extraction from the relevant lowest slice. Equation (3.33) controls this concept and forces variable $E_{d,t}$ to change to 1 when a portion of the lowest slice of the draw column is extracted in period t. Equation (3.34) ensures that when variable $E_{d,t}$ changes to 1, it remains 1 until the end of the mine life.

When the extraction of the last portion of a slice is finished in period t, extraction of the slice above can start in period t or $t+1$. In other words, the extraction of a slice can start if the slice below has been totally extracted. If the extraction of a slice is not started after finishing the extraction of the slice below in period t or $t+1$, the relevant drawpoint must be closed. The concept is applied using Equation (3.35). This ensures that when drawpoint d is open, at least a portion of one of the slices within the draw column associated with drawpoint d is extracted; otherwise, the drawpoint must be closed. This means extraction must be continuous; otherwise, the drawpoint will be closed. Equation (3.36) ensures that when variable $C_{d,t}$ changes to 1, it remains 1 until the end of the mine life.

As mentioned, when variables $E_{d,t}$ and $C_{d,t}$ change to 1, they remain 1 until the end of the mine life. This helps us to control the maximum number of active drawpoints in each period using Equation (3.37).

At the drawpoint-and-cluster level formulation, the mining precedence is controlled in vertical and horizontal directions. The precedence between drawpoints is controlled in a horizontal direction while the precedence between slices is controlled in a vertical direction. Equation (3.38) ensures that all drawpoints belonging to the relevant set, S^d, are started before drawpoint d is extracted. This set is defined based on the selected mining advancement direction. The set can be empty, which means the considered drawpoint can be extracted in any time period in the schedule. Equation (3.38) also ensures that only the set of the immediate predecessor drawpoints needs to start prior to starting the drawpoint under consideration.

Extraction of slice s can be started if the slice below it has been totally extracted. For each slice within the draw column except the lowest, there is a set S^s defining the predecessor slice that must be extracted prior to the extraction of slice s. The extraction precedence of the slices within each draw column is controlled by Equations (3.39), (3.40) and (3.41). Equation (3.39) forces variable $B_{s,t}$ changes to 1 if extraction from slice s is started in period t. Equation (3.40) ensures that variable $B_{s,t}$ can change to 1 only if the slice below it has been extracted totally. In other words, this ensures that the extraction of the slice belonging to the relevant set, S^s, has been finished prior to the extraction of slice s. Equation (3.41) ensures that when variable $B_{s,t}$ changes to 1, it remains 1 until the end of the mine life. Equation (3.42) guarantees that slice s is extracted when the relevant drawpoint is active.

The drawpoint opening is controlled by the variable, $E_{d,t}$, which takes a value of 1 from the opening period to the end of the mine life. From period two to the end of the mine life, the difference between the summation of opened drawpoints until and including period t, and the summation of opened drawpoints until and including previous period t-1, indicates the number of new drawpoints that need to be opened in each period. Equation (3.43) ensures that the number of new drawpoints opened in each period except period one is within the acceptable

range. At the beginning and in period one, the number of new drawpoints is equal to the maximum number of active drawpoints.

Equation (3.45) ensures that the draw rate from each drawpoint is within the desired range in each period. Equation (3.45) imposes upper and lower bounds for the draw rate. When drawpoint d is not active, $(E_{d,t} - C_{d,t})$ is equal to zero and this relaxes the lower bound of the equation.

Equation (3.46) ensures that the fractions of the slice extracted over the scheduling periods sum to one and thereby all the material in the draw column must be extracted. To solve the problem without considering the obtained BHOD form the PCBC, this equation must be less than or equal to 1. Using this method, the best height of draw for each draw column can be obtained based on the optimization.

3.5 Multiple Mines

All the mentioned equations at three levels of resolution were only for a single mine. To solve the problem at the cluster level, drawpoint level, or drawpoint-and-slice level models for multiple mines, similar objective functions and constraints are applied. The only difference is that everything must be controlled for all mines. For example, the discounted cash flow (DCF) for each period is equal to summation of the DCF of the mines in that particular period. For the constraints, for instance the production target, the total production of each period is calculated based on the production of each mine in that particular period. To generate a production schedule, a different mining precedence can be applied to each mine.

3.6 Summary and Conclusion

This chapter has presented the MILP models that are suitable for life-of-mine production scheduling in block-caving operations. The models provide an optimum, tactical production schedule. The production scheduler aims to maximize the NPV of the mining operation while the mine planner has control

over the development rate, vertical mining rate, lateral mining rate, mining capacity, maximum number of active drawpoints, and advancement direction. To support a given production target, the production scheduler defines the opening and closing time for each drawpoint and cluster, the draw rate from each drawpoint and cluster, the number of new drawpoints and clusters that need to be constructed, and the sequence of extraction from the drawpoints and clusters.

The introduced modified clustering method based on an algorithm presented by Tabesh and Askari-Nasab (2011) brings two advantages that will help solve the problem. First, it reduces the number of variables, especially binary variables in the MILP formulation to make it computationally tractable. The second advantage of clustering lies in generating a practical mining schedule.

The models may be used for two purposes. They can be used for mine planning and feasibility studies, or production scheduling. Mine planning and feasibility studies are normally carried out prior to production. For this purpose, MILP allows the investigation of a wide range of production schedules and development strategies. The models can be used individually for small mines. But they can be used successively to help large mines overcome the size problem of mathematical programming and generate a robust, practical, near-optimal schedule. For this purpose, the output of each model is used as the input for the other model.

CHAPTER 4

MILP FORMULATION IMPLEMENTATION

Chapter 4 discusses the mixed-integer linear programming (MILP) models' implementation. The chapter describes the numerical modeling of the MILP models' different components and how they can be set in a MATLAB programming environment for a TOMLAB/CPLEX optimization solver. This includes the numerical modeling of the objective function and constraints. The chapter concludes with an elaboration on techniques for implementing an efficient MILP model framework.

4.1 Introduction

The mathematical formulations and theoretical architecture development resulted in the mixed-interger linear programming (MILP) formulations discussed in Chapter 3. This chapter focuses on the development and application of numerical models using a set of procedural instructions and methods in order to achieve the research objectives. The formulation and application of the MILP model begins with considering its main subcomponents: (i) objective function, and (ii) constraints.

The MILP formulation development starts with identifying the appropriate numerical modeling platform that can be used in setting up the problem and solving it in a reasonable time. MATLAB (Math Works Inc, 2011) was used as the numerical modeling platform and TOMLAB/CPLEX (Holmstrom, 2011) as the optimization solver. MATLAB is a high-level language and interactive environment for numerical computation, visualization, and programming. Using MATLAB, the user can analyze data, develop algorithms, and create models and applications. The language, tools, and built-in math functions enable users to explore multiple approaches and reach a solution faster than with spreadsheets or traditional programming languages, such as C/C++ or Java. TOMLAB is a general-purpose development and modeling environment in MATLAB for research and teaching about, and finding practical solutions to optimization problems. TOMLAB/CPLEX integrates the solver package CPLEX with MATLAB and TOMLAB. The CPLEX solver is a large-scale mixed-integer linear and quadratic programming solver. The package includes simplex and barrier solvers for linear, quadratic, and conic programming.

The generalized structure that TOMLAB/CPLEX uses to solve a MILP problem was identified and used as the basis for the numerical modeling of the MILP formulations. With this in mind, MATLAB was used to create the numerical model of the main subcomponent of the MILP formulations to be passed on to TOMLAB/CPLEX for optimization. This chapter includes a discussion about further numerical modeling techniques used to implement an efficient, practical

MILP model for block-cave production planning. The chapter also includes discussions about the numerical implementation of the MILP model, and explanations about the techniques deployed to make the MILP model efficient.

4.2 Numerical Modeling

Using mathematical programming models like the MILP formulation for mine optimization usually results in large-scale optimization problems. A commercial optimization solver capable of handling such problems is CPLEX (IBM, 2009). This optimization solver uses a branch and cut algorithm and makes it possible for the MILP model to solve large-scale problems. Branch and cut is a method of combinatorial optimization for solving integer-programming problems. This algorithm is a hybrid of branch-and-bound and cutting plane methods (Horst and Hoang, 1996; Wolsey, 1998).

The MILP model solver in this research was TOMLAB/CPLEX (Holmstrom, 2011). The user sets an optimization termination criterion in CPLEX known as the gap tolerance (EPGAP). The EPGAP, which is a measure of optimality, sets an absolute tolerance on the gap between the best integer objective and the objective of the best node remaining in the branch-and-cut algorithm. It instructs CPLEX to terminate once a feasible integer solution within the set EPGAP has been found.

The numerical modeling techniques for the MILP formulation, together with strategies in developing a MILP problem that can be compiled efficiently, are discussed here. This includes compiling the matrices for the objective function and constraints. These matrices are compiled using the format as outlined in the TOMLAB/CPLEX user's guide (Holmstrom, 2011).

4.3 General Formulation

TOMLAB generalizes an MILP problem in the form stated by Equations (4.1) to (4.3). These were reorganized to the generalized structure of a MILP problem.

$$\min f(x) = \mathbf{c}^T \mathbf{x} \qquad (4.1)$$

Subject to:

$$\mathbf{x}_L \leq \mathbf{x} \leq \mathbf{x}_U \tag{4.2}$$

$$\mathbf{b}_L \leq \mathbf{A}\mathbf{x} \leq \mathbf{b}_U \tag{4.3}$$

Where

- $\mathbf{c}$ is the linear objective function coefficients of the MILP model; a vector j×1.
- $\mathbf{x}$ is the decision variable of the MILP model: a vector j×1.
- $\mathbf{x}_L$ and $\mathbf{x}_U$ define the lower and upper bounds on the decision variables: vectors j×1.
- $\mathbf{A}$ represents the coefficients of the constraints of the MILP model: a matrix i×j.
- $\mathbf{b}_L$ and $\mathbf{b}_U$ define the lower and upper bounds on the constraints vectors j×1. Equality constraints are defined by setting the lower bounds equal to the upper bounds for the respective elements of vectors $\mathbf{b}_L$ and $\mathbf{b}_U$.

4.3.1 The MILP Models Objective Function

The objective of the block-cave production planning as defined by the Equations (3.3), (3.16), and (3.29) is to maximize the NPV of the mining operation. As shown by Equation (4.1), the general form of the MILP model in TOMLAB is to minimize the objective function. Therefore, the objective function coefficient vector for Equations (3.3), (3.16), and (3.29) must be multiplied by a negative sign changing it to minimize the –NPV of the mining operation. For notation simplification, the matrix vertical concatenation operator, ";" is used. This operator creates a matrix or vector by concatenating them along the vertical dimension of the matrix or vector. The MILP models' objective function, as

represented by Equations (3.3), (3.16), and (3.29), has a coefficient vector, $\mathbf{c}$. Table 4.1 shows the size and structure of these vectors for each model. In the third column of Table 4.1, $\mathbf{D}_{CLEV}$ is a $(CL \times T) \times 1$ vector holding the discounted cluster economic values (CLEV) shown by Equation (3.3), and $\mathbf{0}_{cl}$ is a $(2 \times CL \times T) \times 1$ vector with all elements equal to zero; CL is the maximum number of clusters and T is the number of scheduling periods. $\mathbf{D}_{DEV}$ is a $(D \times T) \times 1$ vector holding the discounted drawpoint economic values (DEV) shown by Equation (3.16), and $\mathbf{0}_{d}$ is a $(2 \times D \times T) \times 1$ vector with all elements equal to zero; D is the maximum number of drawpoints. $\mathbf{D}_{SEV}$ is a $(S \times T) \times 1$ vector holding the discounted slice economic values (SEV) shown by Equation (3.29), and $\mathbf{0}_{s}$ is a $((S + 2D) \times T) \times 1$ vector with all elements equal to zero; S is the maximum number of slices.

Table 4.1. Size of the coefficient vector of objective function for each model

Model	Size of the coefficient vector	Coefficient vector
Cluster level	$(3 \times CL \times T) \times 1$	$[\mathbf{D}_{CLEV}; \mathbf{0}_{cl}]$
Drawpoint level	$(3 \times D \times T) \times 1$	$[\mathbf{D}_{DEV}; \mathbf{0}_{d}]$
Drawpoint and slice level	$(2 \times (S + D) \times T) \times 1$	$[\mathbf{D}_{SEV}; \mathbf{0}_{s}]$

The objective function coefficient vector and constraints' coefficient matrices have different units and orders of magnitude. It therefore becomes important to transform them to unitless vectors and matrices. This is done by normalizing the vectors and matrices by dividing them by norm(s) of their multiplier vector(s). Table 4.2 represents the size of the decision variables' vector and its order for each model. At the cluster level, $\mathbf{U}_{cl}$ is a $(CL \times T) \times 1$ vector holding the continuous decision variables controlling the portion of the cluster to be extracted in each period: $U_{cl,t} \in [0,1]$. $\mathbf{A}_{cl}$ is a $(CL \times T) \times 1$ vector holding the binary decision

variables controlling the cluster's activity in each period: $A_{cl,t} \in \{0,1\}$. $\mathbf{Z}_{cl}$ is a $(CL \times T) \times 1$ vector holding the binary decision variables controlling the precedence of the clusters' extraction in each period: $Z_{cl,t} \in \{0,1\}$. At the drawpoint level, $\mathbf{U}_d$ is a $(D \times T) \times 1$ vector holding the continuous decision variables controlling the portion of drawpoints to be extracted in each period: $U_{d,t} \in [0,1]$. $\mathbf{A}_d$ is a $(D \times T) \times 1$ vector holding the binary decision variables controlling the activity of drawpoints in each period: $A_{d,t} \in \{0,1\}$. $\mathbf{Z}_d$ is a $(D \times T) \times 1$ vector holding the binary decision variables controlling the precedence of extraction of drawpoints in each period: $Z_{d,t} \in \{0,1\}$. At the drawpoint-and-slice level, $\mathbf{X}_s$ is a $(S \times T) \times 1$ vector holding the continuous decision variables controlling the portion of the slice to be extracted in each period: $X_{s,t} \in [0,1]$. $\mathbf{B}_s$ is a $(S \times T) \times 1$ vector holding the binary decision variables controlling the precedence of the extraction of slices: $B_{s,t} \in \{0,1\}$. $\mathbf{E}_d$ is a $(D \times T) \times 1$ vector holding the binary decision variables controlling the starting period of drawpoints and the precedence of extraction of drawpoints: $E_{d,t} \in \{0,1\}$. $\mathbf{C}_d$ is a $(D \times T) \times 1$ vector holding the binary decision variables controlling the closing period of drawpoints: $C_{d,t} \in \{0,1\}$.

Table 4.2. Size of the decision variables' vector and its order for each model

Model	Size of the decision variable vector	Structure
Cluster level	$(3 \times CL \times T) \times 1$	$[\mathbf{U}_{cl}; \mathbf{A}_{cl}; \mathbf{Z}_{cl}]$
Drawpoint level	$(3 \times D \times T) \times 1$	$[\mathbf{U}_d; \mathbf{A}_d; \mathbf{Z}_d]$
Drawpoint-and-slice level	$(2 \times (S + D) \times T) \times 1$	$[\mathbf{X}_s; \mathbf{B}_s; \mathbf{E}_d; \mathbf{C}_d]$

4.3.2 The Constraints of the MILP Models

We proceed to develop the numerical models for the inequality and equality constraints of the MILP models represented by Equations (3.4) to (3.15) for the

cluster level, Equations (3.17) to (3.28) for the drawpoint level, and Equations (3.30) to (3.46) for the drawpoint-and-slice level.

For cluster-level and drawpoint-level formulations, binary variables are defined to identify at what period a given cluster or drawpoint is started and active. For the drawpoint-and-slice level formulation, instead of using binary variables to define explicitly at what period a drawpoint or slice is started or is active, the binary variables specify whether a drawpoint or slice is started by a certain period. Caccetta and Hill (2003) employed this approach in their formulation of the open-pit mine-scheduling problem. Instances using the "*by period"* formulations tend to be solved faster than those using the *"at period"* formulations, because the resultant branch-and-bound tree is more balanced. Figure 4.1 and Figure 4.2 show the structure of the constraints' coefficient matrix for the different levels of resolution. The number of rows for each constraint at different levels of resolution is shown in Table 4.3.

In addition to the constraints, the constraints' coefficient matrix is divided into different areas according to the decision variables. Figure 4.3 shows these areas for the drawpoint-and-cluster-level formulation. The number of these areas is defined based on the number of the decision variables type for each model. Therefore, there are three areas at the cluster level and the drawpoint level formulations belonging to the related variables, and four areas at the drawpoint-and-slice level formulation. Each area itself is divided into sub-areas based on the number of scheduling periods. Figure 4.4 illustrates the structure of each variable in the constraint coefficient matrix and decision variable vector. The number of columns in each period depends on the level of resolution at which the problem is going to be solved. At the cluster level formulation, the number of columns in each period is equal to the maximum number of the clusters for all variables U, A, and Z. At the drawpoint-and-slice level formulation, the number of columns in each period for both variables X and B is equal to the maximum number of slices while for variables E and C, it is equal to the maximum number of drawpoints.

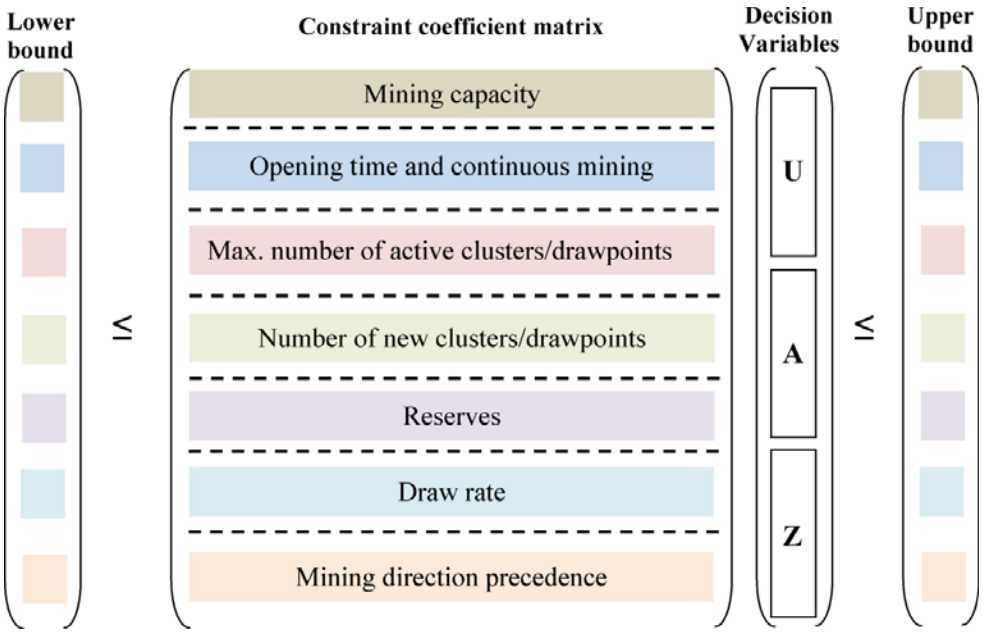

Figure 4.1. Order of constraints in the constraint' coefficient matrix for the cluster level and drawpoint level formulations

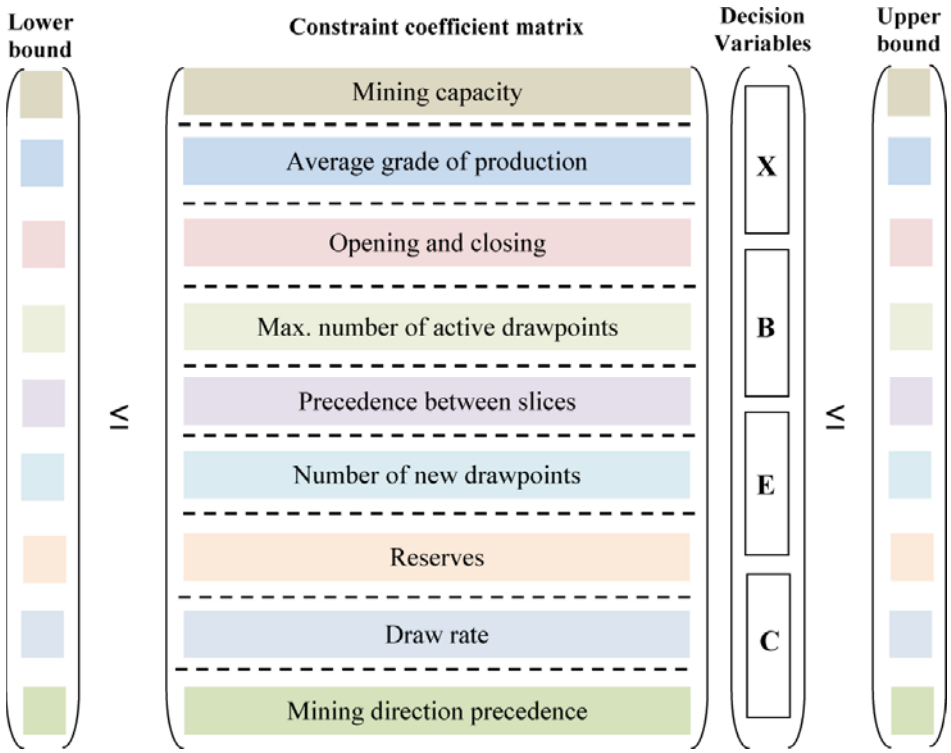

Figure 4.2. Order of constraints in the constraint' coefficient matrix for the drawpoint-and-slice level formulation

Table 4.3. Number of rows in constraint' coefficient matrix for different models

Constraint	Number of rows in coefficient matrix		
	CL level	DP level	DP & SL level
Mining capacity	T	T	T
Ave. grade of production	0	0	$2T$
Opening, closing, and continuous mining	$CL\times(1+T)$	$D\times(1+T)$	$D\times(5T-2)$
Max. number of active DP/CL	$(2CL+1)\times T$	$(2D+1)\times T$	T
Precedence between slices	0	0	Subject to change
Number of new CLs/DPs	T	T	T
Reserves	CL	D	S
Draw rate	$CL\times T$	$D\times T$	$2D\times T$
Mining direction precedence	Varies based on the advancement direction		

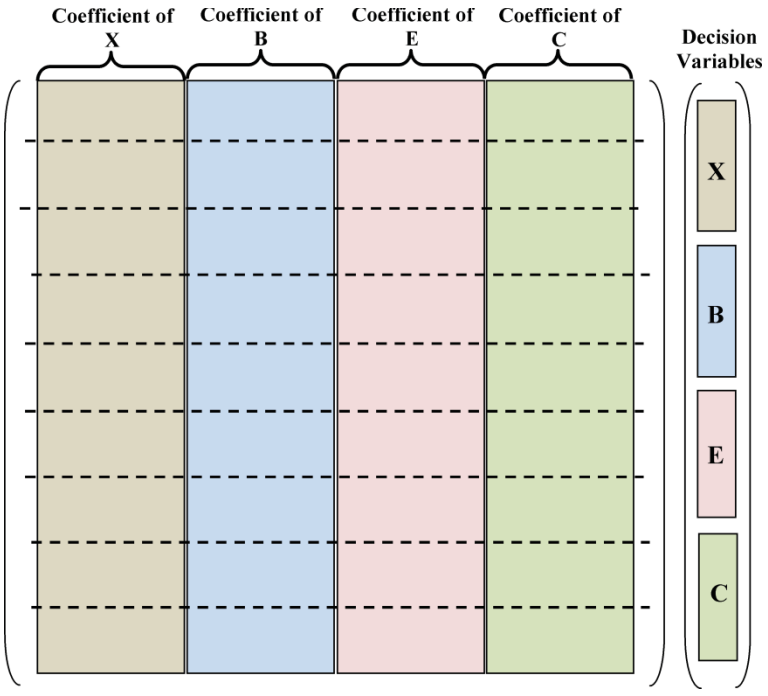

Figure 4.3. Divisions of the constraints' coefficient matrix according to the decision variables at the drawpoint-and-slice level formulation

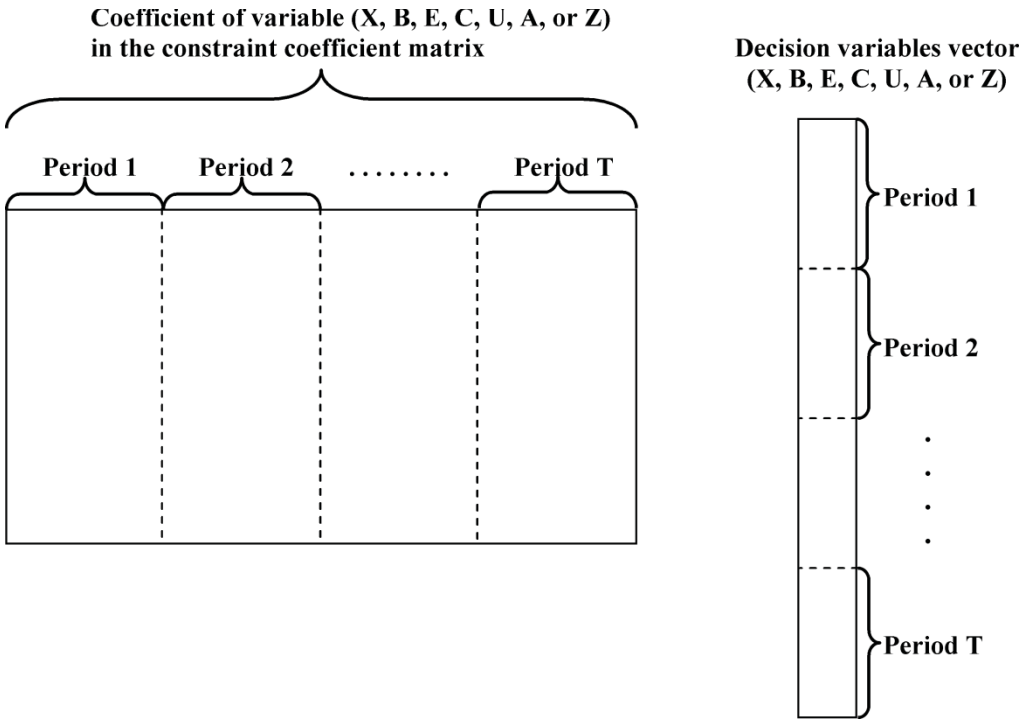

Figure 4.4. The structure of each variable in the constraints coefficient matrix and decision variables vector

It must be mentioned that the structure of the all constraints is explained in detail in this chapter. But when the constraints are created using the DSBC, in order to save memory space and handle the size of constraints' coefficient matrix, MATLAB's sparse function is used. This function converts a full matrix to sparse form by squeezing out any zero elements.

4.3.2.1 Mining capacity

In all models, this constraint forms T rows of the constraint coefficient matrix. Equation (4.4) shows the structure of this constraint. $\mathbf{U}_p$, $\mathbf{A}_p$, and $\mathbf{Z}_p$ are $T\times(CL\times T)$ and $T\times(D\times T)$ matrices at the cluster-level and drawpoint-level formulations, respectively. All the elements of $\mathbf{A}_p$ and $\mathbf{Z}_p$ matrices are equal to zero. Equation (4.5) shows the structure of the area related to the decision variable $\mathbf{U}_p$ in the coefficient matrix of the mining capacity constraint. $\mathbf{K}_{ton}^{t}$ is a $1\times CL$ row vector containing the tonnage of the clusters at the cluster-level formulation and a $1\times D$ row vector containing the tonnage of the drawpoints at the drawpoint level

formulation. $\mathbf{0}$ is a $1\times CL$ and $1\times D$ vector at the cluster level and the drawpoint level formulations, respectively. All the elements of these vectors are equal to zero. In this constraint, each row represents a period. Therefore, in each row the $\mathbf{K}_{ton}^{t}$ vector is placed in the corresponding period, t. For instance, to define this constraint for period 1, the $\mathbf{K}_{ton}^{1}$ vector must be in row 1 at period 1.

Equation (4.6) shows the structure of the mining capacity constraint at the drawpoint and slice level formulation. $\mathbf{X}_p$ and $\mathbf{B}_p$ are $T\times(S\times T)$ matrices while $\mathbf{E}_p$ and $\mathbf{C}_p$ are $T\times(D\times T)$ matrices. All elements of the $\mathbf{B}_p$, $\mathbf{E}_p$, and $\mathbf{C}_p$ matrices are equal to zero. The structure of matrix $\mathbf{X}_p$ is similar to that of matrix $\mathbf{U}_p$. But, here, $\mathbf{K}_{ton}^{t}$ is a $1\times S$ row vector containing the tonnage of the slices and $\mathbf{0}$ is a $1\times S$ vector with all elements equal to zero. The lower and upper bounds of the mining capacity constraint are $T\times 1$ vectors for all models. In all models, after creating the coefficient matrix and lower and upper bound vectors for the mining capacity constraint, each row of this matrix and vectors is divided by the norm of the same row of the coefficient matrix.

$$\left[\mathbf{Lb}_p\right]\le\left[\mathbf{U}_p \quad \mathbf{A}_p \quad \mathbf{Z}_p\right]\le\left[\mathbf{Ub}_p\right] \tag{4.4}$$

$$\mathbf{U}_p=\begin{bmatrix}\mathbf{K}_{ton}^{1} & \mathbf{0} & . & \mathbf{0}\\ \mathbf{0} & \mathbf{K}_{ton}^{2} & . & \mathbf{0}\\ . & . & . & \mathbf{0}\\ . & . & . & \mathbf{0}\\ \mathbf{0} & \mathbf{0} & . & \mathbf{K}_{ton}^{t}\end{bmatrix} \tag{4.5}$$

$$\left[\mathbf{Lb}_p\right]\le\left[\mathbf{X}_p \quad \mathbf{B}_p \quad \mathbf{E}_p \quad \mathbf{C}_p\right]\le\left[\mathbf{Ub}_p\right] \tag{4.6}$$

4.3.2.2 Average Grade of Production

This constraint, which is applied only to the drawpoint-and-slice-level formulation, forms $2T$ rows of the constraints' coefficient matrix. Each of constraints (3.31) and (3.32) form T rows of the constraints' coefficient matrix.

The first T rows represent the lower bound equation and the rest represent the upper bound equation. Equation (4.7) illustrates the structure of this constraint. $\mathbf{X}_g$ and $\mathbf{B}_g$ are $2T \times (S \times T)$ matrices while $\mathbf{E}_g$ and $\mathbf{C}_g$ are $2T \times (D \times T)$ matrices. All elements of the $\mathbf{B}_g$, $\mathbf{E}_g$, and $\mathbf{C}_g$ matrices are equal to zero. In Equation (4.8), $\mathbf{G}_l$ and $\mathbf{G}_u$ are $1 \times S$ row vectors. Each element of these vectors is calculated according to the period of extraction, tonnage of the slice, acceptable grade for the production in the considered period, and grade of the slice. The lower and upper bounds of grade constraint are $2T \times 1$ vectors. In the lower bound, all the elements are –infinity while in the upper bound all the elements are zero.

$$\left[\mathbf{Lb}_g\right] \le \left[\mathbf{X}_g \quad \mathbf{B}_g \quad \mathbf{E}_g \quad \mathbf{C}_g\right] \le \left[\mathbf{Ub}_g\right] \tag{4.7}$$

$$\mathbf{X}_g = \begin{bmatrix} \mathbf{G}_l & \mathbf{0} & . & \mathbf{0} \\ \mathbf{0} & \mathbf{G}_l & . & \mathbf{0} \\ . & . & . & . \\ . & . & . & . \\ \mathbf{0} & \mathbf{0} & . & \mathbf{G}_l \\ \mathbf{G}_u & \mathbf{0} & . & \mathbf{0} \\ \mathbf{0} & \mathbf{G}_u & . & \mathbf{0} \\ . & . & . & . \\ . & . & . & . \\ \mathbf{0} & \mathbf{0} & . & \mathbf{G}_u \end{bmatrix} \tag{4.8}$$

4.3.2.3 Opening, Closing, and Continuous Mining

At the cluster-level and drawpoint-level formulations, each cluster or drawpoint can be opened once during the mine life. After opening, the extraction from each level must be continuous. The related part in the coefficient matrix for the cluster level is created according to Equations (3.9), (3.10), and (3.11). At the drawpoint level, it is created using Equations (3.22), (3.23), and (3.24). Equations (3.9) and (3.22), form CL and D rows of the coefficient matrix in the related formulation. Equation (4.9) shows the structure of these constraints and their upper and lower

bounds at the cluster level and the drawpoint level formulations. Based on the considered formulation, index 1 is used for Equations (3.9) and (3.22) while index 2 is used for Equations (3.10), (3.11), (3.23), and (3.24). $\mathbf{U}_{oc1}$, $\mathbf{A}_{oc1}$, and $\mathbf{Z}_{oc1}$ are $T\times(CL\times T)$ and $T\times(D\times T)$ matrices at the cluster-level and drawpoint-level formulations, respectively. All the elements of the $\mathbf{U}_{oc1}$ and $\mathbf{A}_{oc1}$ matrices are equal to zero.

Equation (4.10) illustrates the structure of matrix $\mathbf{Z}_{oc1}$. $\mathbf{K}_r^t$ is a $1\times CL$ and $1\times D$ vector for the cluster-level and drawpoint-level formulations, respectively. In this vector, only the $r\,th$ element is equal to 1. The rest are zero. r represents the ID number of the cluster or drawpoint. For example, if there are 100 drawpoints, $\mathbf{K}_{43}^2$ is a 1×100 vector in which the 43rd element is 1 and the rest are zero. $\mathbf{K}_{43}^2$ is located under the column representing period 2. Equations (3.10) and (3.11) at the cluster level and Equations (3.23) and (3.24) at the drawpoint level form T rows for each cluster or drawpoint. Equations (3.11) and (3.24) are applied to the first row of T rows for each cluster or drawpoint. $\mathbf{U}_{oc2}$, $\mathbf{A}_{oc2}$, and $\mathbf{Z}_{oc2}$ are $(CL\times T)\times(CL\times T)$ and $(D\times T)\times(D\times T)$ matrices at the cluster-level and the drawpoint-level formulations, respectively. All elements of matrix $\mathbf{U}_{oc2}$ are equal to zero. In the $\mathbf{A}_{oc2}$ and $\mathbf{Z}_{oc2}$ matrices, each cluster or drawpoint allocates T rows to itself. The first line is created based on Equation (3.11) at the cluster level and Equation (3.24) at the drawpoint level.

$$\begin{bmatrix}\mathbf{Lb}_{oc1}\\ \mathbf{Lb}_{oc2}\end{bmatrix}\le\begin{bmatrix}\mathbf{U}_{oc1} & \mathbf{A}_{oc1} & \mathbf{Z}_{oc1}\\ \mathbf{U}_{oc2} & \mathbf{A}_{oc2} & \mathbf{Z}_{oc2}\end{bmatrix}\le\begin{bmatrix}\mathbf{Ub}_{oc1}\\ \mathbf{Ub}_{b2}\end{bmatrix} \tag{4.9}$$

$$\mathbf{Z}_{oc1}=\begin{bmatrix}\mathbf{K}_1^1 & \mathbf{K}_1^2 & . & \mathbf{K}_1^T\\ \mathbf{K}_2^1 & \mathbf{K}_2^2 & . & \mathbf{K}_2^T\\ . & . & . & .\\ \mathbf{K}_{r-1}^1 & \mathbf{K}_{r-1}^2 & . & \mathbf{K}_{r-1}^T\\ \mathbf{K}_r^1 & \mathbf{K}_r^2 & . & \mathbf{K}_r^T\end{bmatrix} \tag{4.10}$$

Equations (4.11) and (4.12) show the structure of the $\mathbf{A}_{oc2}$ and $\mathbf{Z}_{oc2}$ matrices. $\mathbf{K}_{r,1}^{t}$ and $\mathbf{K}_{r,-1}^{t}$ are $1\times CL$ and $1\times D$ vectors at the cluster-level and the drawpoint-level formulations, respectively. r represents the ID number of the cluster or drawpoint, and t is the period. $\mathbf{K}_{r,1}^{t}$ indicates that all elements of this vector are zero except the $r\,th$ element, which is equal to 1. $\mathbf{K}_{r,-1}^{t}$ indicates that all the elements of this vector are zero except the $r\,th$ element, which is equal to -1.

$$\mathrm{A}_{oc2}=\begin{bmatrix} \mathrm{K}_{1,1}^{1} & 0 & . & 0 & 0 \\ \mathrm{K}_{1,-1}^{1} & \mathrm{K}_{1,1}^{2} & . & 0 & 0 \\ . & . & . & . & . \\ 0 & . & \mathrm{K}_{1,-1}^{T-2} & \mathrm{K}_{1,1}^{T-1} & 0 \\ 0 & . & 0 & \mathrm{K}_{1,-1}^{T-1} & \mathrm{K}_{1,1}^{T} \\ . & . & . & . & . \\ . & . & . & . & . \\ \mathrm{K}_{r,1}^{1} & 0 & . & 0 & 0 \\ \mathrm{K}_{r,-1}^{1} & \mathrm{K}_{r,1}^{2} & . & 0 & 0 \\ . & . & . & . & . \\ 0 & . & \mathrm{K}_{r,-1}^{T-2} & \mathrm{K}_{r,1}^{T-1} & 0 \\ 0 & . & 0 & \mathrm{K}_{r,-1}^{T-1} & \mathrm{K}_{r,1}^{T} \end{bmatrix} \tag{4.11}$$

$$Z_{oc2}=\begin{bmatrix} \mathrm{K}_{1,-1}^{1} & 0 & . & 0 & 0 \\ 0 & \mathrm{K}_{1,-1}^{2} & . & 0 & 0 \\ . & . & . & . & . \\ 0 & 0 & . & \mathrm{K}_{1,-1}^{T-1} & 0 \\ 0 & 0 & . & 0 & \mathrm{K}_{1,-1}^{T} \\ . & . & . & . & . \\ . & . & . & . & . \\ \mathrm{K}_{r,-1}^{1} & 0 & . & 0 & 0 \\ 0 & \mathrm{K}_{r,-1}^{2} & . & 0 & 0 \\ . & . & . & . & . \\ 0 & 0 & . & \mathrm{K}_{r,-1}^{T-1} & 0 \\ 0 & 0 & . & 0 & \mathrm{K}_{r,-1}^{T} \end{bmatrix} \tag{4.12}$$

0 is a $1\times CL$ and $1\times D$ vector at the cluster-level and the drawpoint-level formulations, respectively. All the elements of these vectors are equal to zero. The lower and upper bounds of this constraint are $CL\times\left(1+T\right)$ and $D\times\left(1+T\right)$ vectors at the cluster- and the drawpoint-level formulations, respectively. In the lower bound, all the elements are –infinity. In the upper bound vector, all the elements are zero except at the location of the first period for each cluster or

drawpoint, where the elements are 0.5. For example, if there are 10 drawpoints in the model which has to be scheduled over three periods, the ID numbers of the elements of the upper bound vector for this constraint, which are equal to 0.5, include 1, 4, 7, and 10.

At the drawpoint-and-slice-level formulation, the opening and closing constraints are controlled using Equations (3.33), (3.34), (3.35), (3.36), and (3.42). Equation (4.13) illustrates the structure of these constraints. Indices 1 to 5 are associated with Equations (3.33), (3.34), (3.35), (3.36), and (3.42), respectively. X_1, B_1, X_3, B_3, X_5, and B_5 are $(D\times T)\times(S\times T)$ matrices. E_1, C_1, E_3, C_3, E_5, and C_5 are $(D\times T)\times(D\times T)$ matrices. X_2, B_2, X_4, and B_4 are $(D\times(T-1))\times(S\times T)$ matrices. E_2, C_2, E_4, and C_4 are $(D\times(T-1))\times(D\times T)$ matrices. All the elements of the B_1, C_1, X_2, B_2, C_2, B_3, X_4, B_4, E_4, and B_5 matrices are equal to zero. Equation (4.14) illustrates the structure of the matrix X_1. $\mathbf{K}^{t,1}_{d,ls_d}$ is a $1\times S$ vector with all the elements equal to zero except the $ls_d\,th$ element, which is equal to 1. ls_d is the ID of the lowest slice of the draw column associated with drawpoint d. In each row these vectors are placed in a column related to the considered period. $\mathbf{0}$ is a $1\times S$ vector with all the elements equal to zero.

Equation (4.15) illustrates the structure of matrix E_1. $\mathbf{K}^{t,-1}_{d}$ is a $1\times D$ vector with all the elements equal to zero except the $d\,th$ element, which is equal to -1. In each row these vectors are placed in a column related to the considered period. $\mathbf{0}$ is a $1\times D$ vector with all the elements equal to zero. Lb_1 and Ub_1 are $(D\times T)\times 1$ vectors. All the elements of Lb_1 and Ub_1 vectors are –infinity and zero, respectively. Equation (4.16) illustrates the structure of the matrix E_2. $\mathbf{K}^{t,1}_{d}$ and $\mathbf{G}^{t,-1}_{d}$ are $1\times D$ vectors with all the elements equal to zero except the d th element, which is equal to 1 and -1, respectively. d is the ID of the draw column associated with drawpoint d. In each row these vectors are placed in a column

related to the considered period. $\mathbf{0}$ is a $1\times D$ vector with all the elements equal to zero. Matrix C_4 is similar to matrix E_2. Lb_2, Lb_4, Ub_2, and Ub_4 are $\left(D\times\left(T-1\right)\right)\times 1$ vectors. All the elements of the lower bound and upper bound vectors are –infinity and zero, respectively.

$$\begin{bmatrix}\mathbf{Lb}_1\\ \mathbf{Lb}_2\\ \mathbf{Lb}_3\\ \mathbf{Lb}_4\\ \mathbf{Lb}_5\end{bmatrix}\le\begin{bmatrix}\mathbf{X}_1 & \mathbf{B}_1 & \mathbf{E}_1 & \mathbf{C}_1\\ \mathbf{X}_2 & \mathbf{B}_2 & \mathbf{E}_2 & \mathbf{C}_2\\ \mathbf{X}_3 & \mathbf{B}_3 & \mathbf{E}_3 & \mathbf{C}_3\\ \mathbf{X}_4 & \mathbf{B}_4 & \mathbf{E}_4 & \mathbf{C}_4\\ \mathbf{X}_5 & \mathbf{B}_5 & \mathbf{E}_5 & \mathbf{C}_5\end{bmatrix}\le\begin{bmatrix}\mathbf{Ub}_1\\ \mathbf{Ub}_2\\ \mathbf{Ub}_3\\ \mathbf{Ub}_4\\ \mathbf{Ub}_5\end{bmatrix} \tag{4.13}$$

$$\mathbf{X}_1=\begin{bmatrix}\mathbf{K}_{1,ls_1}^{1,1} & \mathbf{0} & \mathbf{0} & . & \mathbf{0}\\ \mathbf{0} & \mathbf{K}_{1,ls_1}^{2,1} & & . & \mathbf{0}\\ \mathbf{0} & \mathbf{0} & \mathbf{K}_{1,ls_1}^{3,1} & . & \mathbf{0}\\ \mathbf{0} & \mathbf{0} & \mathbf{0} & . & \mathbf{0}\\ \mathbf{0} & \mathbf{0} & \mathbf{0} & . & \mathbf{K}_{1,ls_1}^{T,1}\\ . & . & . & . & .\\ . & . & . & . & .\\ \mathbf{K}_{D,ls_D}^{1,1} & \mathbf{0} & \mathbf{0} & . & \mathbf{0}\\ \mathbf{0} & \mathbf{K}_{D,ls_D}^{2,1} & \mathbf{0} & . & \mathbf{0}\\ \mathbf{0} & \mathbf{0} & \mathbf{K}_{D,ls_D}^{3,1} & . & \mathbf{0}\\ . & . & . & . & .\\ \mathbf{0} & \mathbf{0} & \mathbf{0} & . & \mathbf{K}_{D,ls_D}^{T,1}\end{bmatrix} \tag{4.14}$$

Equation (4.17) illustrates the structure of matrix X_3. $\mathrm{K}_{d,S^{ds}}^{t,-L}$ is a $1\times S$ vector in which all the elements are zero except the elements whose indices are equal to indices of the slices within the draw column associated with drawpoint d. These elements are equal to $-L$. S^{ds} is a set which defines the slices in the draw column associated with drawpoint d. These vectors are placed in a column related to the considered period. 0 is a $1\times S$ vector with all the elements equal to zero. Equation (4.18) illustrates the structure of the matrix E_3. $\mathbf{K}_d^{t,1}$ is a $1\times D$ vector

with all the elements equal to zero except the *d th* element, which is equal to 1. Each vector is placed in the related column based on the considered period. *t* represents the considered period.

$$\mathbf{E}_1 = \begin{bmatrix} \mathbf{K}_1^{1,-1} & \mathbf{0} & \mathbf{0} & . & \mathbf{0} \\ \mathbf{0} & \mathbf{K}_1^{2,-1} & & . & \mathbf{0} \\ \mathbf{0} & \mathbf{0} & \mathbf{K}_1^{3,-1} & . & \mathbf{0} \\ \mathbf{0} & \mathbf{0} & \mathbf{0} & . & \mathbf{0} \\ \mathbf{0} & \mathbf{0} & \mathbf{0} & . & \mathbf{K}_1^{T,-1} \\ . & . & . & . & . \\ . & . & . & . & . \\ \mathbf{K}_D^{1,-1} & \mathbf{0} & \mathbf{0} & . & \mathbf{0} \\ \mathbf{0} & \mathbf{K}_D^{2,-1} & \mathbf{0} & . & \mathbf{0} \\ \mathbf{0} & \mathbf{0} & \mathbf{K}_D^{3,-1} & . & \mathbf{0} \\ . & . & . & . & . \\ \mathbf{0} & \mathbf{0} & \mathbf{0} & . & \mathbf{K}_D^{T,-1} \end{bmatrix} \tag{4.15}$$

$$\mathbf{E}_2 = \begin{bmatrix} \mathbf{K}_1^{1,1} & \mathbf{G}_1^{2,-1} & \mathbf{0} & . & \mathbf{0} \\ \mathbf{0} & \mathbf{K}_1^{2,1} & \mathbf{G}_1^{2,-1} & . & \mathbf{0} \\ . & . & . & . & . \\ \mathbf{0} & . & \mathbf{K}_1^{T-3,1} & \mathbf{G}_1^{T-2,-1} & \mathbf{0} \\ \mathbf{0} & . & \mathbf{0} & \mathbf{K}_1^{T-2,1} & \mathbf{G}_1^{T-1,-1} \\ . & . & . & . & . \\ . & . & . & . & . \\ \mathbf{K}_D^{1,1} & \mathbf{G}_D^{2,-1} & \mathbf{0} & . & \mathbf{0} \\ \mathbf{0} & \mathbf{K}_D^{2,1} & \mathbf{G}_D^{2,-1} & . & \mathbf{0} \\ . & . & . & . & . \\ \mathbf{0} & . & \mathbf{K}_D^{T-3,1} & \mathbf{G}_D^{T-2,-1} & \mathbf{0} \\ \mathbf{0} & . & \mathbf{0} & \mathbf{K}_D^{T-2,1} & \mathbf{G}_D^{T-1,-1} \end{bmatrix} \tag{4.16}$$

$$X_3 = \begin{bmatrix} K_{1,S^{ds}}^{1,-L} & 0 & 0 & . & 0 & 0 \\ 0 & K_{1,S^{ds}}^{2,-L} & 0 & . & 0 & 0 \\ . & . & . & . & . & . \\ 0 & 0 & 0 & . & K_{1,S^{ds}}^{T-1,-L} & 0 \\ 0 & 0 & 0 & . & 0 & K_{1,S^{ds}}^{T,-L} \\ . & . & . & . & . & . \\ . & . & . & . & . & . \\ K_{D,S^{ds}}^{1,-L} & 0 & 0 & . & 0 & 0 \\ 0 & K_{D,S^{ds}}^{2,-L} & 0 & . & 0 & 0 \\ . & . & . & . & . & . \\ 0 & 0 & 0 & . & K_{D,S^{ds}}^{T-1,-L} & 0 \\ 0 & 0 & 0 & . & 0 & K_{D,S^{ds}}^{T,-L} \end{bmatrix} \quad (4.17)$$

$\mathbf{0}$ is a $1 \times D$ vector with all the elements equal to zero. The structure of matrix C_3 is similar to matrix E_3 with the difference being that in matrix C_3 the $d\,th$ element is replaced with -1 instead of 1. Lb_3 and Ub_3 are $(D \times T) \times 1$ vectors. All the elements of the lower bound and upper bound vectors are –infinity and zero, respectively.

$$\mathbf{E}_3 = \begin{bmatrix} \mathbf{K}_1^{1,1} & \mathbf{0} & \mathbf{0} & . & \mathbf{0} \\ \mathbf{0} & \mathbf{K}_1^{2,1} & & . & \mathbf{0} \\ \mathbf{0} & \mathbf{0} & \mathbf{K}_1^{3,1} & . & \mathbf{0} \\ \mathbf{0} & \mathbf{0} & \mathbf{0} & . & \mathbf{0} \\ \mathbf{0} & \mathbf{0} & \mathbf{0} & . & \mathbf{K}_1^{T,1} \\ . & . & . & . & . \\ . & . & . & . & . \\ \mathbf{K}_D^{1,1} & \mathbf{0} & \mathbf{0} & . & \mathbf{0} \\ \mathbf{0} & \mathbf{K}_D^{2,1} & \mathbf{0} & . & \mathbf{0} \\ \mathbf{0} & \mathbf{0} & \mathbf{K}_D^{3,1} & . & \mathbf{0} \\ . & . & . & . & . \\ \mathbf{0} & \mathbf{0} & \mathbf{0} & . & \mathbf{K}_D^{T,1} \end{bmatrix} \quad (4.18)$$

Equation (4.19) illustrates the structure of matrix X_5. $K_{d,S^{ds}}^{T-1,\,1/Ns_D}$ is a $1 \times S$ vector in which all the elements are zero except the elements whose indices are equal to indices of the slices within the draw column associated with drawpoint d. These

elements are equal to $\left(1/Ns_d\right)$, in which Ns_d is the number of the slices within the draw column associated with drawpoint d. 0 is a $1\times S$ vector with all the elements equal to zero. These vectors are placed in a column related to the considered period. Matrix E_5 is similar to matrix C_3 while matrix C_5 is similar to matrix E_3. Lb_5 and Ub_5 are $\left(D\times T\right)\times 1$ vectors. All the elements of the lower bound and upper bound vectors are –infinity and zero, respectively. After creating the coefficient matrix and lower and upper bound vectors of Equation (4.13), each row of the matrix and vectors is divided by the norm of the same row of the coefficient matrix.

$$\mathrm{X}_5=\begin{bmatrix}
\mathrm{K}_{1,S^{ds}}^{1,\,1/Ns_1} & 0 & 0 & . & 0 & 0\\
0 & \mathrm{K}_{1,S^{ds}}^{2,\,1/Ns_1} & 0 & . & 0 & 0\\
. & . & . & . & . & .\\
0 & 0 & 0 & . & \mathrm{K}_{1,S^{ds}}^{T-1,\,1/Ns_1} & 0\\
0 & 0 & 0 & . & 0 & \mathrm{K}_{1,S^{ds}}^{T,\,1/Ns_1}\\
. & . & . & . & . & .\\
. & . & . & . & . & .\\
\mathrm{K}_{D,S^{ds}}^{1,\,1/Ns_D} & 0 & 0 & . & 0 & 0\\
0 & \mathrm{K}_{D,S^{ds}}^{2,\,1/Ns_D} & 0 & . & 0 & 0\\
. & . & . & . & . & .\\
0 & 0 & 0 & . & \mathrm{K}_{D,S^{ds}}^{T-1,\,1/Ns_D} & 0\\
0 & 0 & 0 & . & 0 & \mathrm{K}_{D,S^{ds}}^{T,\,1/Ns_D}
\end{bmatrix} \tag{4.19}$$

4.3.2.4 Maximum Number of Active Clusters and Drawpoints

This constraint is controlled using Equations (3.5), (3.6), and (3.7) at the cluster-level formulation, and Equations (3.17), (3.18), and (3.19) at the drawpoint-level formulation. Equation (4.20) shows the structure of this constraint at both formulations in which the indices indicate that there are three equations. Based on the considered formulation, index 1 is used for Equations (3.5) and (3.17), index 2 is used for Equations (3.6) and (3.18), and finally index 3 is used for Equations (3.7) and (3.19). $\mathbf{U}_1, \mathbf{U}_2$, $\mathbf{A}_1, \mathbf{A}_2$, $\mathbf{Z}_1$ and $\mathbf{Z}_2$ are $\left(CL\times T\right)\times\left(CL\times T\right)$ matrices at

the cluster-level and $(D\times T)\times(D\times T)$ matrices at the drawpoint-level formulations.

All the elements of matrices $\mathbf{Z}_1$ and $\mathbf{Z}_2$, are equal to zero. Equations (4.21) and (4.22) represent the structure of matrices $\mathbf{A}_1$ and $\mathbf{U}_1$, respectively. Matrix $\mathbf{U}_2$ is equal to matrix $\mathbf{A}_1$ and matrix $\mathbf{A}_2$ is equal to matrix $\mathbf{U}_1$ divided by L. $\mathbf{K}^t_{r,1}$ and $\mathbf{K}^t_{r,-1}$ are $1\times CL$ and $1\times D$ vectors at the cluster-level and drawpoint-level formulations, respectively. r represents the ID number of the cluster or drawpoint and t is the considered period. $\mathbf{K}^t_{r,1}$ indicates that all the elements of this vector are zero except the $r\,th$ element, which is equal to 1. $\mathbf{K}^t_{r,-1}$ indicates that all the elements in this vector are zero except the $r\,th$ element, which is equal to -1.

$$\begin{bmatrix}\mathbf{Lb}_1\\ \mathbf{Lb}_2\\ \mathbf{Lb}_3\end{bmatrix}\le\begin{bmatrix}\mathbf{U}_1 & \mathbf{A}_1 & \mathbf{Z}_1\\ \mathbf{U}_2 & \mathbf{A}_2 & \mathbf{Z}_2\\ \mathbf{U}_3 & \mathbf{A}_3 & \mathbf{Z}_3\end{bmatrix}\le\begin{bmatrix}\mathbf{Ub}_1\\ \mathbf{Ub}_2\\ \mathbf{Ub}_3\end{bmatrix} \tag{4.20}$$

$$\mathbf{U}_1 = L\times\begin{bmatrix}
\mathbf{K}^1_{1,-1} & \mathbf{0} & \mathbf{0} & \mathbf{0} & \cdots & \mathbf{0} & \mathbf{0}\\
\mathbf{0} & \mathbf{K}^2_{1,-1} & \mathbf{0} & \mathbf{0} & \cdots & \mathbf{0} & \mathbf{0}\\
\mathbf{0} & \mathbf{0} & \mathbf{K}^3_{1,-1} & \mathbf{0} & \cdots & \mathbf{0} & \mathbf{0}\\
\vdots & \vdots & \vdots & \vdots & \cdots & \vdots & \vdots\\
\mathbf{0} & \mathbf{0} & \mathbf{0} & \mathbf{0} & \cdots & \mathbf{0} & \mathbf{K}^T_{1,-1}\\
\vdots & \vdots & \vdots & \vdots & \cdots & \vdots & \vdots\\
\vdots & \vdots & \vdots & \vdots & \cdots & \vdots & \vdots\\
\mathbf{K}^1_{r,-1} & \mathbf{0} & \mathbf{0} & \mathbf{0} & \cdots & \mathbf{0} & \mathbf{0}\\
\mathbf{0} & \mathbf{K}^2_{r,-1} & \mathbf{0} & \mathbf{0} & \cdots & \mathbf{0} & \mathbf{0}\\
\mathbf{0} & \mathbf{0} & \mathbf{K}^3_{r,-1} & \mathbf{0} & \cdots & \mathbf{0} & \mathbf{0}\\
\vdots & \vdots & \vdots & \vdots & \cdots & \vdots & \vdots\\
\mathbf{0} & \mathbf{0} & \mathbf{0} & \cdots & \cdots & \mathbf{0} & \mathbf{K}^T_{r,-1}
\end{bmatrix} \tag{4.21}$$

$$\mathbf{A}_1 = \begin{bmatrix} \mathbf{K}_{1,1}^1 & \mathbf{0} & \mathbf{0} & \mathbf{0} & \cdots & \mathbf{0} & \mathbf{0} \\ \mathbf{0} & \mathbf{K}_{1,1}^2 & \mathbf{0} & \mathbf{0} & \cdots & \mathbf{0} & \mathbf{0} \\ \mathbf{0} & \mathbf{0} & \mathbf{K}_{1,1}^3 & \mathbf{0} & \cdots & \mathbf{0} & \mathbf{0} \\ \vdots & \vdots & \vdots & \vdots & \cdots & \vdots & \vdots \\ \mathbf{0} & \mathbf{0} & \mathbf{0} & \mathbf{0} & \cdots & \mathbf{0} & \mathbf{K}_{1,1}^T \\ \vdots & \vdots & \vdots & \vdots & \cdots & \vdots & \vdots \\ \vdots & \vdots & \vdots & \vdots & \cdots & \vdots & \vdots \\ \mathbf{K}_{r,1}^1 & \mathbf{0} & \mathbf{0} & \mathbf{0} & \cdots & \mathbf{0} & \mathbf{0} \\ \mathbf{0} & \mathbf{K}_{r,1}^2 & \mathbf{0} & \mathbf{0} & \cdots & \mathbf{0} & \mathbf{0} \\ \mathbf{0} & \mathbf{0} & \mathbf{K}_{r,1}^3 & \mathbf{0} & \cdots & \mathbf{0} & \mathbf{0} \\ \vdots & \vdots & \vdots & \vdots & \cdots & \mathbf{0} & \mathbf{0} \\ \mathbf{0} & \mathbf{0} & \mathbf{0} & \mathbf{0} & \cdots & \mathbf{0} & \mathbf{K}_{r,1}^T \end{bmatrix} \tag{4.22}$$

$\mathbf{U}_3, \mathbf{A}_3,$ and $\mathbf{Z}_3$ are $T \times (CL \times T)$ matrices at the cluster-level and $T \times (D \times T)$ matrices at the drawpoint-level formulations. All the elements of matrices $\mathbf{U}_3$ and $\mathbf{Z}_3$, are equal to zero. Equation (4.23) illustrates the structure of matrix $\mathbf{A}_3$. $\mathbf{K}_{one}^t$ is a $1 \times CL$ and $1 \times D$ vector of ones at the cluster-level and drawpoint-level formulations, respectively. t represents the considered period. Lb_1 and Lb_2 are $(CL \times T) \times 1$ and $(D \times T) \times 1$ vectors at the cluster-level and drawpoint-level formulations with the all the elements equal to –infinity. Ub_1 and Ub_2 are $(CL \times T) \times 1$ and $(D \times T) \times 1$ vectors at the cluster-level and drawpoint-level formulations with all the elements equal to zero. Lb_3 and Ub_3 are $T \times 1$ vectors at both the cluster- and drawpoint-level formulations. The elements of vector Lb_3 are equal to zero for both formulations. The elements of vector Ub_3 are equal to $N_{Acl,t}$ and $N_{Ad,t}$ at the cluster-level and the drawpoint-level formulations, respectively. After creating the coefficient matrix and lower and upper bound vectors, each row of the matrix and vectors is divided by the norm of the same row of the coefficient matrix.

$$\mathbf{A}_3 = \begin{bmatrix} \mathbf{K}_{one}^1 & \mathbf{0} & \mathbf{0} & \mathbf{0} & \mathbf{0} & \mathbf{0} & . & . & \mathbf{0} \\ \mathbf{0} & \mathbf{K}_{one}^2 & \mathbf{0} & \mathbf{0} & \mathbf{0} & \mathbf{0} & . & . & \mathbf{0} \\ \mathbf{0} & \mathbf{0} & \mathbf{K}_{one}^3 & \mathbf{0} & \mathbf{0} & \mathbf{0} & . & . & \mathbf{0} \\ . & . & . & . & . & . & . & . & \mathbf{0} \\ \mathbf{0} & \mathbf{0} & \mathbf{0} & \mathbf{0} & \mathbf{0} & \mathbf{0} & . & . & \mathbf{K}_{one}^T \end{bmatrix} \tag{4.23}$$

The maximum number of active drawpoints at the drawpoint-and-slice-level formulation is controlled using Equation (3.37). Equation (4.24) shows the structure of this constraint. $\mathbf{X}_{Act}$ and $\mathbf{B}_{Act}$ are $T \times (S \times T)$ matrices and $\mathbf{E}_{Act}$ and $\mathbf{C}_{Act}$ are $T \times (D \times T)$ matrices. All the elements of the $\mathbf{X}_{Act}$ and $\mathbf{B}_{Act}$ matrices are equal to zero. Equation (4.25) illustrates the structure of matrix $\mathbf{E}_{Act}$. $\mathbf{K}_{one}^t$ is a $1 \times D$ vector of ones and t represents the considered period. In each row, this vector is placed in a column related to the considered period.

Matrix $\mathbf{C}_{Act}$ has a structure similar to that of matrix $\mathbf{E}_{Act}$, with the difference being that all the members of vector $\mathbf{K}_{one}^t$ are equal to -1 instead of 1. Lb_{Act} and Ub_{Act} are $T \times 1$ vectors. All the elements of the Lb_{Act} and Ub_{Act} vectors are zero and $N_{Ad,t}$, respectively. After creating the coefficient matrix and lower and upper bound vectors of Equation (4.24), each row of the matrix and vectors is divided by the norm of the same row of the coefficient matrix.

4.3.2.5 Mining Precedence

At the cluster-level and the drawpoint-level formulations, the mining precedence is controlled in the horizontal direction based on the advancement direction. Equations (3.8) and (3.21) control this constraint for these formulations. Equation (4.26) illustrates the structure of this constraint at the cluster-level and the drawpoint-level formulations. Matrix $\mathrm{U}_{prec,r}$ represents the area of the coefficient matrix related to variable U for cluster or drawpoint r. The number of rows depends on the defined precedence in the advancement direction.

$$\left[\mathbf{Lb}_{Act}\right] \le \left[\mathbf{X}_{Act} \quad \mathbf{B}_{Act} \quad \mathbf{E}_{Act} \quad \mathbf{C}_{Act}\right] \le \left[\mathbf{Ub}_{Act}\right] \tag{4.24}$$

$$\mathbf{E}_{Act=}\begin{bmatrix} \mathbf{K}^{1}_{1,one} & \mathbf{0} & . & \mathbf{0} & \mathbf{0} \\ \mathbf{0} & \mathbf{K}^{2}_{1,one} & . & \mathbf{0} & \mathbf{0} \\ . & . & . & . & . \\ \mathbf{0} & \mathbf{0} & . & \mathbf{K}^{T-1}_{1,one} & \mathbf{0} \\ \mathbf{0} & \mathbf{0} & . & \mathbf{0} & \mathbf{K}^{T}_{1,one} \\ . & . & . & . & . \\ . & . & . & . & . \\ \mathbf{K}^{1}_{D,one} & \mathbf{0} & . & \mathbf{0} & \mathbf{0} \\ \mathbf{0} & \mathbf{K}^{2}_{D,one} & . & \mathbf{0} & \mathbf{0} \\ . & . & . & . & . \\ \mathbf{0} & \mathbf{0} & . & \mathbf{K}^{T-1}_{D,one} & \mathbf{0} \\ \mathbf{0} & \mathbf{0} & . & \mathbf{0} & \mathbf{K}^{T}_{D,one} \end{bmatrix} \tag{4.25}$$

The number of rows allocated to each cluster or drawpoint is calculated using Equation (4.27). The dimension of matrix A_{prec} in each row is same as the related U_{prec} and Z_{prec} matrices. All the elements of matrix A_{prec} are equal to zero. To better clarify the issue, this part continues using the cluster level formulation. The same concept must also be used at the drawpoint level formulation. Equation (4.28) illustrates the structure of matrix $\mathrm{Z}_{prec,1}$.

$$\begin{bmatrix} \mathbf{Lb}_{prec,1} \\ \mathbf{Lb}_{prec,2} \\ . \\ . \\ \mathbf{Lb}_{prec,r} \end{bmatrix} \le \begin{bmatrix} \mathbf{U}_{prec,1} & \mathbf{A}_{prec,1} & \mathbf{Z}_{prec,1} \\ \mathbf{U}_{prec,2} & \mathbf{A}_{prec,2} & \mathbf{Z}_{prec,2} \\ . & . & . \\ . & . & . \\ \mathbf{U}_{prec,r} & \mathbf{A}_{prec,r} & \mathbf{Z}_{prec,r} \end{bmatrix} \le \begin{bmatrix} \mathbf{Ub}_{prec,1} \\ \mathbf{Ub}_{prec,2} \\ . \\ . \\ \mathbf{Ub}_{prec,r} \end{bmatrix} \tag{4.26}$$

$$N_{Rows} = \begin{cases} T \times \text{number of members in set } S^{cl} & (\text{cluster level}) \\ T \times \text{number of members in set } S^{d} & (\text{drawpoint level}) \end{cases} \tag{4.27}$$

$$Z_{prec,1} = \begin{bmatrix} K_{1,1}^{1,1} & 0 & 0 & . & 0 \\ 0 & K_{1,1}^{2,1} & 0 & . & 0 \\ 0 & 0 & K_{1,1}^{3,1} & . & 0 \\ 0 & 0 & 0 & . & 0 \\ 0 & 0 & 0 & . & K_{1,1}^{T,1} \\ K_{2,1}^{1,1} & 0 & 0 & . & 0 \\ 0 & K_{2,1}^{2,1} & 0 & . & 0 \\ 0 & 0 & K_{2,1}^{3,1} & . & 0 \\ 0 & 0 & 0 & . & 0 \\ 0 & 0 & 0 & . & K_{2,1}^{T,1} \\ . & . & . & . & . \\ . & . & . & . & . \\ . & . & . & . & . \\ . & . & . & . & . \\ K_{n,1}^{1,1} & 0 & 0 & . & 0 \\ 0 & K_{n,1}^{2,1} & 0 & . & 0 \\ 0 & 0 & K_{n,1}^{3,1} & . & 0 \\ . & . & . & . & . \\ 0 & 0 & 0 & . & 0 \\ 0 & 0 & 0 & . & K_{n,1}^{T,1} \end{bmatrix} \quad (4.28)$$

$K_{n,cl}^{t,1}$ is a $1 \times CL$ vector with all the elements equal to zero except *cl th* element, which is equal to 1. n is the number of members for cluster cl in set S^{cl}. Equation (4.29) illustrates the structure of matrix $U_{prec,1}$. $K_{n,cl}^{t,-1}$ is a $1 \times CL$ vector with all the elements equal to zero except *n th* element, which is equal to -1. n is the ID number of the *n th* member for cluster cl in set S^{cl}.

For example, if there are 100 clusters in the model which must be scheduled over 15 periods, there will be 100 sections for each variable (e.g. $U_{prec,1}, U_{prec,2}, ..., U_{prec,100}$). $K_{8,45}^{t,-1}$ is a 1×100 vector in which all the elements are zero except the 8th element, which is equal to -1. This vector is placed under the t *th* column, which represents the considered period. The number 45 is the cluster's ID number. The size of the $U_{prec,45}$ or $Z_{prec,45}$ matrices depends on the number of members in set S^{45}. For instance, if the number of members in this set is nine, cluster 45 allocates 135 rows to itself. The elements of the lower bound vector of all sections are –infinity. But, for the upper bound, the elements can be changed from cluster to cluster based on geotechnical conditions.

$$U_{prec,1}=\begin{bmatrix} G_{1,1}^{1,-1} & 0 & 0 & . & 0 \\ G_{1,1}^{1,-1} & G_{1,1}^{2,-1} & 0 & . & 0 \\ G_{1,1}^{1,-1} & G_{1,1}^{2,-1} & G_{1,1}^{3,-1} & . & 0 \\ . & . & . & . & 0 \\ G_{1,1}^{1,-1} & G_{1,1}^{2,-1} & G_{1,1}^{3,-1} & . & G_{1,1}^{T,1} \\ G_{2,1}^{1,-1} & 0 & 0 & . & 0 \\ G_{2,1}^{1,-1} & G_{2,1}^{2,-1} & 0 & . & 0 \\ G_{2,1}^{1,-1} & G_{2,1}^{2,-1} & G_{2,1}^{3,-1} & . & 0 \\ . & . & . & . & 0 \\ G_{2,1}^{1,-1} & G_{2,1}^{2,-1} & G_{2,1}^{3,-1} & . & K_{2,1}^{T,-1} \\ . & . & . & . & . \\ . & . & . & . & . \\ . & . & . & . & . \\ . & . & . & . & . \\ G_{n,1}^{1,-1} & 0 & 0 & . & 0 \\ G_{n,1}^{1,-1} & G_{n,1}^{2,-1} & 0 & . & 0 \\ G_{n,1}^{1,-1} & G_{n,1}^{2,-1} & G_{n,1}^{3,-1} & . & 0 \\ . & . & . & . & . \\ . & . & . & . & 0 \\ G_{n,1}^{1,-1} & G_{n,1}^{2,-1} & G_{n,1}^{3,-1} & . & G_{n,1}^{T,-1} \end{bmatrix} \quad (4.29)$$

In other words, the required percentage of extraction from the predecessor clusters can be defined for each cluster separately. In equations (3.8) and (3.21), this amount is same for all clusters.

At the drawpoint-and-slice-level formulation, the mining precedence is controlled in both the horizontal and vertical directions. The precedence between drawpoints is controlled in a horizontal direction while the precedence between slices is controlled in a vertical direction. For this purpose, Equations (3.38), (3.39), (3.40), and (3.41) are used.

Equation (4.30) illustrates the structure of the coefficient matrix of this constraint. Matrices with index H are created using Equation (3.38), and matrices with index V are created using Equations (3.39), (3.40), and (3.41). Matrices X_{Hprec}, B_{Hprec}, E_{Hprec}, and C_{Hprec} have the same size, which depends on the defined precedence in the advancement direction. The number of rows in vectors Lb_{Hprec} and Ub_{Hprec} is similar to the number of rows in these matrices. All the elements of the X_{Hprec},

B_{Hprec}, and C_{Hprec} matrices are zero. The number of rows allocated to each drawpoint in matrix E_{Hprec} is calculated using the drawpoint part of Equation (4.27).

$$\begin{bmatrix} Lb_{Hprec} \\ Lb_{Vprec1} \\ Lb_{Vprec2} \\ Lb_{Vprec3} \end{bmatrix} \leq \begin{bmatrix} X_{Hprec} & B_{Hprec} & E_{Hprec} & C_{Hprec} \\ X_{Vprec1} & B_{Vprec1} & E_{Vprec1} & C_{Vprec1} \\ X_{Vprec2} & B_{Vprec2} & E_{Vprec2} & C_{Vprec2} \\ X_{Vprec3} & B_{Vprec3} & E_{Vprec3} & C_{Vprec3} \end{bmatrix} \leq \begin{bmatrix} Ub_{Hprec} \\ Ub_{Vprec1} \\ Ub_{Vprec2} \\ Ub_{Vprec3} \end{bmatrix} \tag{4.30}$$

Equation (4.31) illustrates the structure of matrix E_{Hprec}. $K_{n,d}^{t,-1,1}$ is a $1\times D$ vector with all the elements equal to zero, except the $n\,th$ and $d\,th$ elements, which are equal to -1 and 1, respectively. d represents the ID number of the drawpoint, and n is the ID number of the $n\,th$ member of set S^d which defines the predecessor drawpoints that must be started prior to extraction of drawpoint d. 0 is a $1\times D$ vector with all the elements equal to zero. The elements of the lower and upper bound vectors are –infinity and zero, respectively. As mentioned before, the indices 1, 2, and 3 in Equation (4.30) are related to Equations (3.39), (3.40), and (3.41) , respectively. X_{Vprec1}, E_{Vprec1}, and C_{Vprec1} and B_{Vprec1} are $(S\times T)\times(S\times T)$ matrices and E_{Vprec1} and C_{Vprec1} are $(S\times T)\times(D\times T)$ matrices. All the elements of the E_{Vprec1} and C_{Vprec1} matrices are zero. In matrices X_{Vprec1} and B_{Vprec1} , each slice allocates T rows to itself.

Equations (4.32) and (4.33) illustrate matrix X_{Vprec1} and B_{Vprec1}. $K_s^{t,1}$ and $K_s^{t,-1}$ are $1\times S$ vectors with all the elements equal to zero except the $s\,th$ element, which is equal to 1 and -1, respectively. Each vector is placed in a column related to the considered period. 0 is a $1\times S$ vector with all the elements equal to zero. Matrices X_{Vprec2}, B_{Vprec2}, E_{Vprec2}, and C_{Vprec2} have the same number of rows. All the elements of matrices E_{Vprec2} and C_{Vprec2} are zero. Matrices X_{Vprec2} and B_{Vprec2} should be prepared in a way to ensure that variable $B_{s,t}$ can change to 1, only if the slice below has been extracted totally. In matrices X_{Vprec2} and B_{Vprec2} each

slice allocates T rows to itself. On the other hand, it is obvious that there is no restriction for the lowest slices, so the size of these matrices is $\left(\left(S-D\right)\times T\right)\times\left(S\times T\right)$, in which D is the maximum number of the drawpoints that is equivalent to the number of the lowest slices.

$$\mathrm{E}_{Hprec}=\begin{bmatrix}
\mathrm{K}_{1,1}^{1,-1,1} & 0 & 0 & . & 0\\
0 & \mathrm{K}_{1,1}^{2,-1,1} & 0 & . & 0\\
0 & 0 & \mathrm{K}_{1,1}^{3,-1,1} & . & 0\\
. & . & . & . & .\\
0 & 0 & 0 & . & \mathrm{K}_{1,1}^{T,-1,1}\\
\mathrm{K}_{2,1}^{1,-1,1} & 0 & 0 & . & 0\\
0 & \mathrm{K}_{2,1}^{2,-1,1} & 0 & . & 0\\
0 & 0 & \mathrm{K}_{2,1}^{3,-1,1} & . & 0\\
. & . & . & . & .\\
0 & 0 & 0 & . & \mathrm{K}_{2,1}^{T,-1,1}\\
. & . & . & . & .\\
. & . & . & . & .\\
\mathrm{K}_{n,1}^{1,-1,1} & 0 & 0 & . & 0\\
0 & \mathrm{K}_{n,1}^{2,-1,1} & 0 & . & 0\\
0 & 0 & \mathrm{K}_{n,1}^{3,-1,1} & . & 0\\
. & . & . & . & .\\
0 & 0 & 0 & . & \mathrm{K}_{n,1}^{T,-1,1}\\
. & . & . & . & .\\
. & . & . & . & .\\
\mathrm{K}_{1,D}^{1,-1,1} & 0 & 0 & & 0\\
0 & \mathrm{K}_{1,D}^{2,-1,1} & 0 & & 0\\
0 & 0 & \mathrm{K}_{1,D}^{3,-1,1} & & 0\\
. & . & . & . & .\\
0 & 0 & 0 & . & \mathrm{K}_{1,D}^{T,-1,1}\\
. & . & . & . & .\\
. & . & . & . & .\\
\mathrm{K}_{n,D}^{1,-1,1} & 0 & 0 & . & 0\\
0 & \mathrm{K}_{n,D}^{2,-1,1} & 0 & . & 0\\
0 & 0 & \mathrm{K}_{n,D}^{3,-1,1} & . & 0\\
. & . & . & . & .\\
0 & 0 & 0 & . & \mathrm{K}_{n,D}^{T,-1,1}
\end{bmatrix} \tag{4.31}$$

$$X_{Vprec1} = \begin{bmatrix} K_1^{1,1} & 0 & 0 & . & 0 \\ K_1^{1,1} & K_1^{2,1} & 0 & . & 0 \\ K_1^{1,1} & K_1^{2,1} & K_1^{3,1} & . & 0 \\ . & . & . & . & . \\ K_1^{1,1} & K_1^{2,1} & K_1^{3,1} & . & K_1^{T,1} \\ K_2^{1,1} & 0 & 0 & . & 0 \\ K_2^{1,1} & K_2^{2,1} & 0 & . & 0 \\ K_2^{1,1} & K_2^{2,1} & K_2^{3,1} & . & 0 \\ . & . & . & . & . \\ K_2^{1,1} & K_2^{2,1} & K_2^{3,1} & . & K_2^{T,1} \\ . & . & . & . & . \\ . & . & . & . & . \\ K_s^{1,1} & 0 & 0 & . & 0 \\ K_s^{1,1} & K_s^{2,1} & 0 & . & 0 \\ K_s^{1,1} & K_s^{2,1} & K_s^{3,1} & . & 0 \\ . & . & . & . & . \\ K_s^{1,1} & K_s^{2,1} & K_s^{3,1} & . & K_s^{T,1} \\ . & . & . & . & . \\ . & . & . & . & . \\ K_S^{1,1} & 0 & 0 & . & 0 \\ K_S^{1,1} & K_S^{2,1} & 0 & . & 0 \\ K_S^{1,1} & K_S^{2,1} & K_S^{3,1} & . & 0 \\ . & . & . & . & . \\ K_S^{1,1} & K_S^{2,1} & K_S^{3,1} & . & K_S^{T,1} \end{bmatrix} \tag{4.32}$$

$$B_{Vprec1} = \begin{bmatrix} K_1^{1,-1} & 0 & 0 & . & 0 \\ 0 & K_1^{2,-1} & 0 & . & 0 \\ 0 & 0 & K_1^{3,-1} & . & 0 \\ . & . & . & . & . \\ 0 & 0 & 0 & . & K_1^{T,-1} \\ . & . & . & . & . \\ . & . & . & . & . \\ K_s^{1,-1} & 0 & 0 & . & 0 \\ 0 & K_s^{2,-1} & 0 & . & 0 \\ 0 & 0 & K_s^{3,-1} & . & 0 \\ . & . & . & . & . \\ 0 & 0 & 0 & . & K_s^{T,-1} \\ . & . & . & . & . \\ . & . & . & . & . \\ K_S^{1,-1} & 0 & 0 & . & 0 \\ 0 & K_S^{2,-1} & 0 & . & 0 \\ 0 & 0 & K_S^{3,-1} & . & 0 \\ . & . & . & . & . \\ 0 & 0 & 0 & . & K_S^{T,-1} \end{bmatrix} \tag{4.33}$$

Equations (4.34) and (4.35) illustrate matrices X_{Vprec2} and B_{Vprec2}. $K_s^{t,1}$ and $K_s^{t,-1}$ are $1 \times S$ vectors with all the elements equal to zero except the *s th* element, which

is equal to 1 and -1, respectively. Each vector is placed in a column related to the considered period. 0 is a $1\times S$ vector with all the elements equal to zero. Equation (4.36) illustrates the structure of matrix E_{Vprec3}. All the elements of the X_{Vprec3}, B_{Vprec3} and C_{Vprec3} matrices are zero. $\mathbf{K}_s^{t,1}$ and $\mathbf{G}_s^{t,-1}$ are $1\times S$ vectors with all the elements equal to zero except the s *th* elements which are equal to 1 and -1 respectively. s is the ID number of the slice. In each row, these vectors are placed in the columns related to the considered period. $\mathbf{0}$ is a $1\times S$ vector with all the elements equal to zero. In Equation (4.30), the size of the lower and upper bound vectors is defined based on the related sections in the coefficient matrix. All the elements of the lower and upper bound vectors are –infinity and zero, respectively.

$$\mathrm{X}_{Vprec2}=\begin{bmatrix}
\mathrm{K}_1^{1,-1} & 0 & 0 & . & 0\\
\mathrm{K}_1^{1,-1} & \mathrm{K}_1^{2,-1} & 0 & . & 0\\
\mathrm{K}_1^{1,-1} & \mathrm{K}_1^{2,-1} & \mathrm{K}_1^{3,-1} & . & 0\\
. & . & . & . & .\\
\mathrm{K}_1^{1,-1} & \mathrm{K}_1^{2,-1} & \mathrm{K}_1^{3,-1} & . & \mathrm{K}_1^{T,-1}\\
\mathrm{K}_2^{1,-1} & 0 & 0 & . & 0\\
\mathrm{K}_2^{1,-1} & \mathrm{K}_2^{2,-1} & 0 & . & 0\\
\mathrm{K}_2^{1,-1} & \mathrm{K}_2^{2,-1} & \mathrm{K}_2^{3,-1} & . & 0\\
. & . & . & . & .\\
\mathrm{K}_2^{1,1} & \mathrm{K}_2^{2,1} & \mathrm{K}_2^{3,-1} & . & \mathrm{K}_2^{T,-1}\\
. & . & . & . & .\\
. & . & . & . & .\\
\mathrm{K}_s^{1,-1} & 0 & 0 & . & 0\\
\mathrm{K}_s^{1,-1} & \mathrm{K}_s^{2,-1} & 0 & . & 0\\
\mathrm{K}_s^{1,-1} & \mathrm{K}_s^{2,-1} & \mathrm{K}_s^{3,-1} & . & 0\\
. & . & . & . & .\\
\mathrm{K}_s^{1,-1} & \mathrm{K}_s^{2,-1} & \mathrm{K}_s^{3,-1} & . & \mathrm{K}_s^{T,-1}\\
. & . & . & . & .\\
. & . & . & . & .\\
\mathrm{K}_S^{1,-1} & 0 & 0 & . & 0\\
\mathrm{K}_S^{1,-1} & \mathrm{K}_S^{2,-1} & 0 & . & 0\\
\mathrm{K}_S^{1,-1} & \mathrm{K}_S^{2,-1} & \mathrm{K}_S^{3,-1} & . & 0\\
. & . & . & . & .\\
\mathrm{K}_S^{1,-1} & \mathrm{K}_S^{2,-1} & \mathrm{K}_S^{3,-1} & . & \mathrm{K}_S^{T,-1}
\end{bmatrix} \tag{4.34}$$

$$\mathrm{B}_{Vprec2} = \begin{bmatrix} \mathrm{K}_1^{1,1} & 0 & 0 & . & 0 \\ 0 & \mathrm{K}_1^{2,1} & 0 & . & 0 \\ 0 & 0 & \mathrm{K}_1^{3,1} & . & 0 \\ . & . & . & . & . \\ 0 & 0 & 0 & . & \mathrm{K}_1^{T,1} \\ \mathrm{K}_2^{1,1} & 0 & 0 & . & 0 \\ 0 & \mathrm{K}_2^{2,1} & 0 & . & 0 \\ 0 & 0 & \mathrm{K}_2^{3,1} & . & 0 \\ . & . & . & . & . \\ 0 & 0 & 0 & . & \mathrm{K}_2^{T,1} \\ . & . & . & . & . \\ . & . & . & . & . \\ \mathrm{K}_s^{1,1} & 0 & 0 & . & 0 \\ 0 & \mathrm{K}_s^{2,1} & 0 & . & 0 \\ 0 & 0 & \mathrm{K}_s^{3,1} & . & 0 \\ . & . & . & . & . \\ 0 & 0 & 0 & . & \mathrm{K}_s^{T,1} \\ . & . & . & . & . \\ . & . & . & . & . \\ \mathrm{K}_S^{1,1} & 0 & 0 & . & 0 \\ 0 & \mathrm{K}_S^{2,1} & 0 & . & 0 \\ 0 & 0 & \mathrm{K}_S^{3,1} & . & 0 \\ . & . & . & . & . \\ 0 & 0 & 0 & . & \mathrm{K}_S^{T,1} \end{bmatrix} \tag{4.35}$$

$$\mathbf{E}_{Vprec3} = \begin{bmatrix} \mathbf{K}_1^{1,1} & \mathbf{G}_1^{2,-1} & \mathbf{0} & . & \mathbf{0} \\ \mathbf{0} & \mathbf{K}_1^{2,1} & \mathbf{G}_1^{2,-1} & . & \mathbf{0} \\ . & . & . & . & . \\ \mathbf{0} & . & \mathbf{K}_1^{T-3,1} & \mathbf{G}_1^{T-2,-1} & \mathbf{0} \\ \mathbf{0} & . & \mathbf{0} & \mathbf{K}_1^{T-2,1} & \mathbf{G}_1^{T-1,-1} \\ . & . & . & . & . \\ . & . & . & . & . \\ \mathbf{K}_S^{1,1} & \mathbf{G}_S^{2,-1} & \mathbf{0} & . & \mathbf{0} \\ \mathbf{0} & \mathbf{K}_S^{2,1} & \mathbf{G}_S^{2,-1} & . & \mathbf{0} \\ . & . & . & . & . \\ \mathbf{0} & . & \mathbf{K}_S^{T-3,1} & \mathbf{G}_S^{T-2,-1} & \mathbf{0} \\ \mathbf{0} & . & \mathbf{0} & \mathbf{K}_S^{T-2,1} & \mathbf{G}_S^{T-1,-1} \end{bmatrix} \tag{4.36}$$

4.3.2.6 Number of New Clusters and Drawpoints

At the cluster-level and the drawpoint-level formulations, this constraint is controlled using two equations for each model. One equation is applied to period

one and the other is applied to the rest of the mine life. Equation (4.37) illustrates the structure of this constraint at the cluster-level and the drawpoint-level formulations. Matrices U_{new}, A_{new}, and Z_{new} are $T\times(D\times T)$ that all the elements of U_{new} and A_{new} are zero. Equation (4.38) illustrates the structure of matrix Z_{new}. K^{t}_{one} is a $1\times CL$ and $1\times D$ vector of ones at the cluster-level and the drawpoint-level formulations, respectively. This vector is placed in the related column to the considered period. 0 is a $1\times CL$ and $1\times D$ vector with all the elements equal to zero at the cluster-level and the drawpoint-level formulations, respectively. Lb_{new} and Ub_{new} are $T\times 1$ vectors. Each row represents a period and is based on the geotechnical conditions it can be changed. The elements of vector Lb_{new} are the minimum acceptable number of the clusters or drawpoints according to the considered model. In vector Ub_{new}, the first element is equal to the maximum number of the acceptable active clusters or drawpoints based on the considered model.

$$\left[Lb_{new}\right]\le\left[U_{new}\quad A_{new}\quad Z_{new}\right]\le\left[Ub_{new}\right] \tag{4.37}$$

$$Z_{new}=\begin{bmatrix} K^{1}_{one} & 0 & 0 & 0 & . & 0 \\ 0 & K^{2}_{one} & 0 & 0 & . & 0 \\ 0 & 0 & K^{3}_{one} & 0 & . & 0 \\ 0 & 0 & 0 & . & . & 0 \\ 0 & 0 & 0 & 0 & . & K^{T}_{one} \end{bmatrix} \tag{4.38}$$

At the drawpoint-and-slice-level formulation, this constraint is controlled using Equations (3.43) and (3.44). Equation (4.39) illustrates the structure of this constraint for this formulation. The X_{new} and B_{new} matrices are $T\times(S\times T)$. The E_{new} and C_{new} matrices are $T\times(D\times T)$. All the elements of matrices X_{new}, B_{new}, and C_{new} are zero. In matrix E_{new}, the first row represents Equation (3.44) and the rest represent Equation (3.43). The structure of matrix E_{new} is shown in Equation (4.40). K^{t}_{one} and G^{t}_{-one} are $1\times D$ vectors with all the elements equal to 1 and -1, respectively. Lb_{new} and Ub_{new} are $T\times 1$ vectors which are created in a way

defined for the cluster-level and the drawpoint-level formulations. After creating the coefficient matrix and lower and upper bound vectors of Equations (4.37) and (4.39), each row of the matrix and vectors is divided by the norm of the same row of the coefficient matrix.

$$\left[\mathrm{Lb}_{new}\right] \le \left[\mathrm{X}_{new} \quad \mathrm{B}_{new} \quad \mathrm{E}_{new} \quad \mathrm{C}_{new}\right] \le \left[\mathrm{Ub}_{new}\right] \tag{4.39}$$

$$\mathrm{E}_{new} = \begin{bmatrix} \mathrm{K}^{1}_{one} & 0 & 0 & . & 0 & 0 \\ \mathrm{G}^{1}_{-one} & \mathrm{K}^{2}_{one} & 0 & . & 0 & 0 \\ 0 & \mathrm{G}^{2}_{-one} & \mathrm{K}^{3}_{one} & . & 0 & 0 \\ 0 & 0 & 0 & . & 0 & 0 \\ 0 & 0 & 0 & . & \mathrm{G}^{T-1}_{-one} & \mathrm{K}^{T}_{one} \end{bmatrix} \tag{4.40}$$

4.3.2.7 Draw rate

At the cluster-level formulation, the amount of the material that can be extracted from each cluster varies with the number of the draw columns in the cluster. This constraint is controlled using Equation (3.12). Equation (4.41) illustrates the structure of this constraint at the cluster-level formulation. U_{DR}, A_{DR}, and Z_{DR} are $(CL \times T) \times (CL \times T)$ matrices and all the elements of Z_{DR} are equal to zero. Equation (4.42) illustrates the structure of matrix U_{DR}. $\mathrm{K}^{t}_{cl,Ton_{cl}}$ is a $1 \times CL$ vector with all the elements equal to zero except the $cl\,th$ element, which is equal to the tonnage of cluster cl. This vector is placed in the related column under the considered period. Equation (4.43) illustrates the structure of matrix A_{DR}. $\mathrm{G}^{t}_{cl,-DR_{cl}}$ is a $1 \times CL$ vector with all the elements equal to zero except the $cl\,th$ element, which is equal to multiplying the number of draw columns in the cluster by the minimum acceptable draw rate of a drawpoint. In both Equations (4.42) and (4.43), 0 is a $1 \times CL$ vector with all the elements equal to zero. Lb_{DR} and Ub_{DR} are $(CL \times T) \times 1$ vectors. All the elements of the lower bound vector are zero. In the upper bound vector, the first T rows belong to cluster 1, the second T rows belong to cluster 2, and so on. Therefore, the upper bound of each cluster which is a $T \times 1$ vector is calculated using Equation (4.44). NDP_{cl} is the number of draw columns

in the cluster. $\overline{DR}_t$ and $\underline{DR}_t$ are the maximum and minimum draw rates of the drawpoints in the cluster. At the drawpoint-level formulation, the similar method is applied with the difference being that here, NDP_{cl} is equal to 1.

$$\left[\mathrm{Lb}_{DR}\right] \le \left[\mathrm{U}_{DR} \quad \mathrm{A}_{DR} \quad \mathrm{Z}_{DR}\right] \le \left[\mathrm{Ub}_{DR}\right] \tag{4.41}$$

$$\mathrm{U}_{DR} = \begin{bmatrix} \mathrm{K}^{1}_{1,Ton_1} & 0 & 0 & . & 0 & 0 \\ 0 & \mathrm{K}^{2}_{1,Ton_1} & 0 & . & 0 & 0 \\ 0 & 0 & \mathrm{K}^{3}_{1,Ton_1} & . & 0 & 0 \\ . & . & . & . & . & . \\ 0 & 0 & 0 & . & \mathrm{K}^{T-1}_{1,Ton_1} & 0 \\ 0 & 0 & 0 & . & 0 & \mathrm{K}^{T}_{1,Ton_1} \\ . & . & . & . & . & . \\ . & . & . & . & . & . \\ \mathrm{K}^{1}_{CL,Ton_{CL}} & 0 & 0 & . & 0 & 0 \\ 0 & \mathrm{K}^{2}_{CL,Ton_{CL}} & 0 & . & 0 & 0 \\ 0 & 0 & \mathrm{K}^{3}_{CL,Ton_{CL}} & . & 0 & 0 \\ 0 & 0 & 0 & . & 0 & 0 \\ 0 & 0 & 0 & . & \mathrm{K}^{T-1}_{CL,Ton_{CL}} & 0 \\ 0 & 0 & 0 & . & 0 & \mathrm{K}^{T}_{CL,Ton_{CL}} \end{bmatrix} \tag{4.42}$$

$$\mathrm{A}_{DR} = \begin{bmatrix} \mathrm{G}^{1}_{1,-DR_1} & 0 & . & . & 0 \\ 0 & \mathrm{G}^{2}_{1,-DR_1} & . & . & 0 \\ 0 & 0 & \mathrm{G}^{3}_{1,-DR_1} & . & 0 \\ . & . & . & . & . \\ 0 & 0 & 0 & . & \mathrm{G}^{T}_{1,-DR_1} \\ . & . & . & . & . \\ . & . & . & . & . \\ \mathrm{G}^{1}_{CL,-DR_{CL}} & 0 & 0 & . & 0 \\ 0 & \mathrm{G}^{2}_{CL,-DR_{CL}} & 0 & . & 0 \\ 0 & 0 & \mathrm{G}^{3}_{CL,-DR_{CL}} & . & 0 \\ . & . & . & . & . \\ 0 & 0 & 0 & . & \mathrm{G}^{T}_{CL,-DR_{CL}} \end{bmatrix} \tag{4.43}$$

$$\left[\mathrm{Ub}^{cl}_{DR}\right]_{T\times 1} = NDP_{cl} \times \left(\overline{DR}_t - \underline{DR}_t\right) \tag{4.44}$$

The draw rate constraint is controlled at the drawpoint-and-slice-level formulation using Equation (3.45). To create the required matrices, this equation is simplified to two inequalities (4.45) and (4.46). Constraint (4.47) represents the structure of this constraint at the drawpoint-and-slice-level formulation. Indices 1 and 2

represent inequalities (4.45) and (4.46), respectively. All the matrices – X_{DR1}, X_{DR2}, B_{DR1}, B_{DR2}, E_{DR1}, E_{DR2}, C_{DR1}, and C_{DR2} – have $D \times T$ rows. All the elements of matrices B_{DR1}, E_{DR1}, C_{DR1}, and B_{DR2} are equal to zero. Equation (4.48) illustrates the structure of matrix X_{DR1}. $K^{t}_{S^{ds},ton}$ is a $1 \times S$ vector with all the elements equal to zero except the elements whose IDs are equal to the IDs of the slices within the draw column associated with drawpoint d.

$$\sum (Ton_n).X_{n,t} \le \overline{DR}_{d,t} \tag{4.45}$$

$$\left(E_{d,t} - C_{d,t}\right).\underline{DR}_{d,t} - \sum (Ton_n).X_{n,t} \le 0 \tag{4.46}$$

$$\forall d \in \{1,...,D\},\ t \in \{1,...,T\},\ n \in S^{ds}$$

$$\begin{bmatrix} Lb_{DR1} \\ Lb_{DR2} \end{bmatrix} \le \begin{bmatrix} X_{DR1} & B_{DR1} & E_{DR1} & C_{DR1} \\ X_{DR2} & B_{DR2} & E_{DR2} & C_{DR2} \end{bmatrix} \le \begin{bmatrix} Ub_{DR1} \\ Ub_{DR2} \end{bmatrix} \tag{4.47}$$

The values of these elements are equal to the tonnage of the related slices. 0 is a $1 \times CL$ vector with all the elements equal to zero. Lb_{DR1} and Ub_{DR1} are $(D \times T) \times 1$ vectors with all the elements equal to -infinity and the maximum acceptable draw rate, respectively. Matrix X_{DR2} is similar to matrix X_{DR1} with the difference being that in matrix X_{DR2}, all the tonnage must be multiplied by -1. Equation (4.49) illustrates the structure of matrix E_{DR2}.

$K^{t}_{d,\underline{DR_d}}$ is a $1 \times D$ vector with all the elements equal to zero except the $d\,th$, which is equal to the minimum draw rate of drawpoint d. 0 is a $1 \times D$ vector with all the elements equal to zero. Matrix C_{DR2} is similar to matrix E_{DR2} with the difference being that in this matrix, the minimum draw rate of the drawpoint must be multiplied by -1. Lb_{DR2} and Ub_{DR2} are $(D \times T) \times 1$ vectors with all the elements equal to -infinity and zero, respectively. After creating the coefficient matrix and

lower and upper bound vectors of Equations (4.41) and (4.47), each row of the matrix and vectors is divided by the norm of the same row of the coefficient matrix.

$$X_{DR1} = \begin{bmatrix} K^{1}_{S^{1s},ton} & 0 & . & 0 & 0 \\ 0 & K^{2}_{S^{1s},ton} & . & 0 & 0 \\ . & . & . & . & . \\ 0 & 0 & . & K^{T-1}_{S^{1s},ton} & 0 \\ 0 & 0 & . & 0 & K^{T}_{S^{1s},ton} \\ . & . & . & . & . \\ . & . & . & . & . \\ K^{1}_{S^{ds},ton} & 0 & . & 0 & 0 \\ 0 & K^{2}_{S^{ds},ton} & . & 0 & 0 \\ . & . & . & . & . \\ 0 & 0 & . & K^{T-1}_{S^{ds},ton} & 0 \\ 0 & 0 & . & 0 & K^{T}_{S^{ds},ton} \end{bmatrix} \tag{4.48}$$

$$E_{DR2} = \begin{bmatrix} K^{1}_{1,\underline{DR_1}} & 0 & . & 0 & 0 \\ 0 & K^{2}_{1,\underline{DR_1}} & . & 0 & 0 \\ . & . & . & . & . \\ 0 & 0 & . & K^{T-1}_{1,\underline{DR_1}} & 0 \\ 0 & 0 & . & 0 & K^{T}_{1,\underline{DR_1}} \\ . & . & . & . & . \\ . & . & . & . & . \\ K^{1}_{D,\underline{DR_D}} & 0 & . & 0 & 0 \\ 0 & K^{2}_{D,\underline{DR_D}} & . & 0 & 0 \\ . & . & . & . & . \\ 0 & 0 & . & K^{T-1}_{D,\underline{DR_D}} & 0 \\ 0 & 0 & . & 0 & K^{T}_{D,\underline{DR_D}} \end{bmatrix} \tag{4.49}$$

4.3.2.8 Reserves

Equation (4.50) illustrates the structure of this constraint at the cluster-level and the drawpoint-level formulations. U_{res}, A_{res}, and Z_{res} are $CL \times CL$ and $D \times D$ matrices at the cluster level and the drawpoint level formulations, respectively. All the elements of matrices A_{res} and Z_{res} are zero. Equation (4.51) illustrates the structure of the U_{res} for the cluster level formulation. $K^{t,1}_{r}$ is a $1 \times CL$ and $1 \times D$ vector at the cluster level and the drawpoint level formulations, respectively. All the elements of these vectors are zero except the $r\,th$ element, which is equal to 1.

r represents the ID number of the cluster or drawpoint at the related formulation. Lb_{res} and Ub_{res} are $CL \times 1$ and $D \times 1$ vectors of ones at the cluster-level and the drawpoint-level formulations, respectively.

$$\left[\mathrm{Lb}_{res}\right] \leq \left[\mathrm{U}_{res} \quad \mathrm{A}_{res} \quad \mathrm{Z}_{res}\right] \leq \left[\mathrm{Ub}_{res}\right] \tag{4.50}$$

$$\mathrm{U}_{res} = \begin{bmatrix} \mathrm{K}_1^{1,1} & \mathrm{K}_1^{2,1} & . & \mathrm{K}_1^{T-1,1} & \mathrm{K}_1^{T,1} \\ \mathrm{K}_2^{1,1} & \mathrm{K}_2^{2,1} & . & \mathrm{K}_2^{T-1,1} & \mathrm{K}_2^{T,1} \\ . & . & . & . & . \\ . & . & . & . & . \\ . & . & . & . & . \\ . & . & . & . & . \\ \mathrm{K}_r^{1,1} & \mathrm{K}_r^{2,1} & . & \mathrm{K}_r^{T-1,1} & \mathrm{K}_r^{T,1} \end{bmatrix} \tag{4.51}$$

Equation (4.52) illustrates the structure of this constraint at the drawpoint-and-slice-level formulation. X_{res} and B_{res} are $S \times (S \times T)$ matrices, and E_{res} and C_{res} are $S \times (D \times T)$ matrices. All the elements of matrices B_{res}, E_{res}, and C_{res} are zero. The structure of matrix X_{res} is similar to that of matrix U_{res} in Equation (4.51). The lower and upper bounds are $CL \times 1$ vectors of ones.

$$\left[\mathrm{Lb}_{res}\right] \leq \left[\mathrm{X}_{res} \quad \mathrm{B}_{res} \quad \mathrm{E}_{res} \quad \mathrm{C}_{res}\right] \leq \left[\mathrm{Ub}_{res}\right] \tag{4.52}$$

4.3.3 Multiple Mines

For multiple mine problems, similar structures are used. As explained in Figure 4.3 and Figure 4.4, the coefficient vector of the objective function and constraints' coefficient matrix are divided into different areas based on the existing decision variables in each model. Then each area is divided into periods. According to the selected level of resolution, each period consists of clusters, drawpoints, or drawpoints and slices. For multiple mine problems, each period consists of clusters, drawpoints, or drawpoints and slices for different mines. Figure 4.5 illustrates this concept for multiple mines.

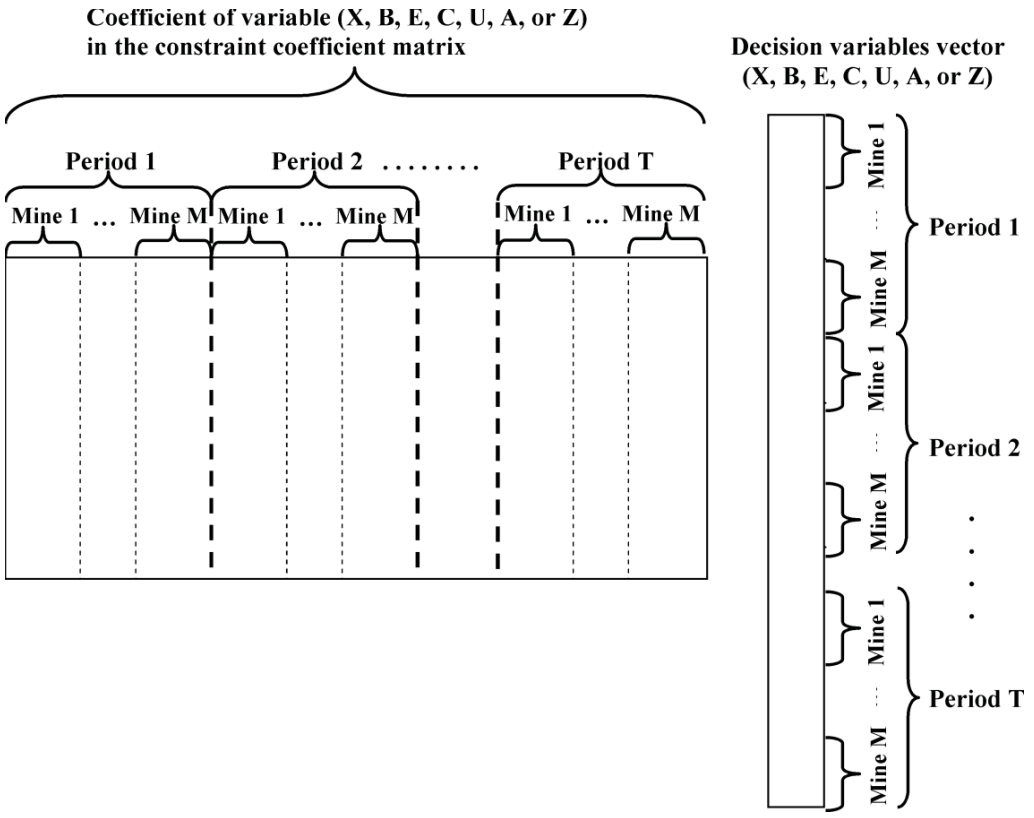

Figure 4.5. The structure of each variable in the constraint coefficient matrix and decision variable vector for multiple mines problem

4.4 Implementation of an Efficient MILP Model

We have progressively developed an efficient and robust MILP models for long-term block cave production scheduling (Pourrahimian et al., 2012a; Pourrahimian et al., 2012b; Pourrahimian et al., 2012c). This leads to a large-scale optimization problem with numerous decision variables and constraints that leads to significant memory overhead and time to solve. We implemented a practical mine production sequencing program using the advancement direction and modified hierarchical clustering algorithms based on an algorithm presented by Tabesh and Askari-Nasab (2011) which resulted in reduced number of binary variables to be solved for during optimization. We have further developed techniques to reduce the number of non-zero decision variables.

4.4.1 Implementation of MILP Model with Fewer Binary Decision Variables

The most common problem in the MILP formulation is the size of the branch-and-cut tree. The tree becomes so large that insufficient memory remains to solve the LP sub-problems. The size of the branch-and-cut tree can actually be affected by the specific approach one takes in performing the branching, and by the structure of each problem. So, there is no way to determine the size of the tree before solving the problem. But, the number of decision variables in each formulation affects the size of the branch-and-cut tree. The general strategy in formulating the MILP for block-cave production scheduling is therefore to reduce the number of decision variables, thereby reducing the solution time significantly. Variable reduction techniques are used to improve the solution time. These techniques endeavor to limit the search space by eliminating certain variables or by a priori setting the values of other variables.

As mentioned before, the general form of the MILP formulation can be represented by Equation (4.1), subject to constraints of the MILP model. The objective functions for long-term block-cave production scheduling, as stated by Equations (3.3), (3.16), and (3.29), for three levels of resolution. At each level of resolution, the objective function coefficient vector, $\mathbf{c}$, is a column vector containing the discounted cash flows in all periods. The objective function decision variables vector, $\mathbf{r}$, is a column vector containing non-zero elements to be solved in the MILP model during optimization. Reducing the number of non-zero decision variables in vector $\mathbf{r}$ results in a production-scheduling problem with a smaller size.

Clustering reduces the number of variables, especially binary variables in the MILP formulation, to make the formulation computationally tractable. The size of the problem and number of the binary decision variables are managed at the clustering level formulation using the defined number of clusters.

After solving the problem at the cluster level, the earliest period that each cluster can be reached and the cluster life, if all the constraints are satisfied, are known. On the other hand, it is assumed that the portion scheduled to be extracted from each cluster is taken from all the drawpoints, based on the ratio of each draw column's tonnage in the cluster. The drawpoints of each cluster are known, so the earliest start time and the cluster life allow elimination from the drawpoint level model of any variables that would mine each drawpoint before its earliest start time. Two years flexibility for the earliest start time is assumed at the drawpoint level. For this purpose, if, at the cluster level, the extraction of a drawpoint is started in period t with the cluster life of n, at the drawpoint level any variables that would mine this drawpoint before period $t-2$ and after $(t+n)+2$ are eliminated. This is done by changing the related decision variables in vector $\mathbf{r}$ to zero.

Theoretically, this variable reduction technique decreases the solution space for the optimization problem. Thus during optimization, some of the branches in the branch-and-cut tree are eliminated, ensuring that the solution for the practical production scheduling problem is reached faster.

The results of the drawpoint level are used at the drawpoint-and-slice-level formulation to eliminate the unnecessary variables. The same concept is used to eliminate the variables related to the drawpoints. In addition to eliminating the variables related to the drawpoints, some of the variables related to the slices can also be eliminated. These variables are eliminated based on the earliest extraction time of each slice as well. According to the maximum-allowed draw rate, the earliest extraction time for each slice is defined. For this purpose, each draw column is divided into groups based on the maximum allowable draw rate from the drawpoint. The total tonnage of slices within each group must be equal to or greater than the maximum allowable draw rate from the drawpoint. Then these groups are numbered from bottom to top. The numbers are added to the starting period of the drawpoint to obtain the earliest starting time of each group and,

consequently, the earliest starting time of each slice. For example, in Figure 4.6, the draw column associated with drawpoint D50 has 20 slices.

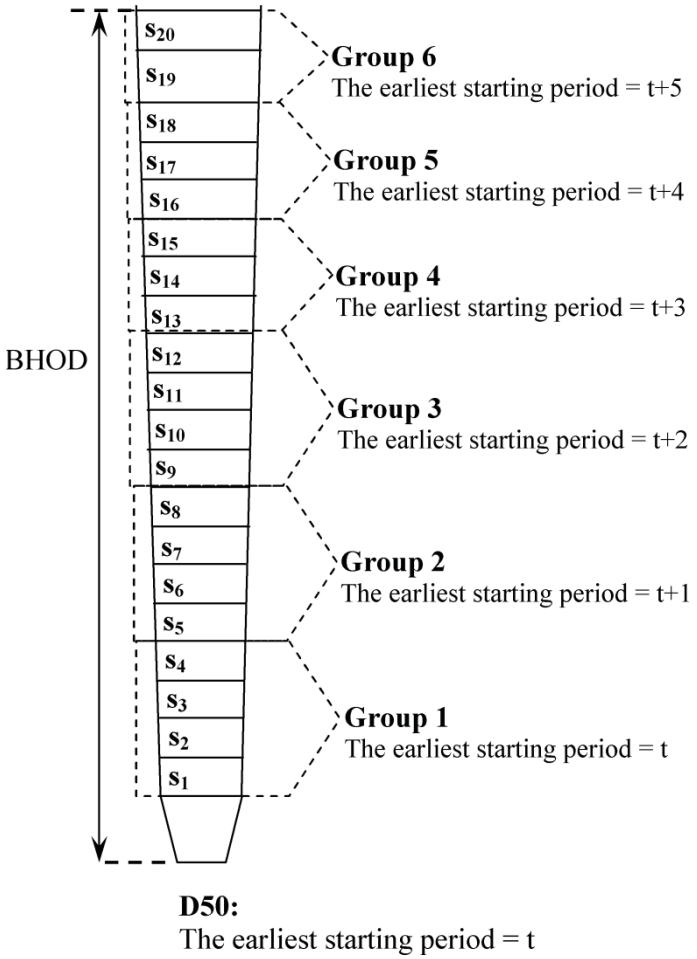

Figure 4.6. Elimination of the variables related to the slices

Based on the maximum allowable draw rate, this draw column is divided into six groups, which are numbered from bottom to top. This means if extraction from drawpoint D50 is started in period t, only the slices within group 1 can be extracted in period t; the earliest starting time for the slices within group 2 is $t+1$ and so on. This concept makes it possible to eliminate from the drawpoint-and-cluster level any variables that would mine each slice before its earliest start time.

4.5 Summary and Conclusion

In summary, the mathematical models and theoretical architecture developed in Chapter 3 were used as the basis for the MILP formulation framework development in the first part of this chapter. The models involve the interactions of the objective function and the constraints in an optimization framework to achieve the objective. The main objective is to maximize the mining operation's NPV.

The numerical model of the MILP formulations is developed in MATLAB (Math Works Inc, 2011), with the generalized structure used by TOMLAB/CPLEX (Holmstrom, 2011) in solving large-scale MILP problems. After creating all requirements such as vectors and matrices, the resulting numerical model is passed on to TOMLAB/CPLEX for optimization. The second part of this chapter explores further numerical modeling techniques needed to implement an efficient, practical MILP model for block-cave long-term production planning.

CHAPTER 5

VERIFICATION, EXPERIMENTS, AND DISCUSSION OF RESULTS

Chapter 6 presents experimentation with the MILP model framework and DSBC software. This includes case studies and verification of the models. The models for different levels of the resolution cluster level, drawpoint level, and drawpoint-and-slice level are discussed separately. A modified hierarchical clustering algorithm based on the algorithm presented by Tabesh and Askari-Nasab (2011) for long-term production scheduling of block caving is applied on the data. A multi-step case study is carried out to verify the models and generate a near-optimal realistic mine plan in a reasonable CPU time.

5.1 Introduction

The study proceeded with the application and verification of the models. This chapter will include discussions about the application of the methodology using the models on a dataset, and the results. In order to develop the models proposed in this research, the main dataset was obtained from Gemcom. This is the sample dataset in PCBC. The small dataset is a part of the main dataset. The slice file, drawpoints coordinates, and best height of draw (BHOD) were used as the input data for the MILP models for long-term production scheduling of block-cave mines. First, different models were applied on the small dataset to explain the single-step method. Then, the results were analyzed. To describe the multi-step approach, the method was explained using the main dataset, and the results were discussed.

5.2 Main Dataset

The main dataset contained 298 drawpoints. The minimum and maximum numbers of slices, which were 10m, were 29 and 36 within draw columns, respectively. There were 9790 slices within the main dataset. Figure 5.1 illustrates a plan view of the drawpoint configuration based on the relevant coordinates.

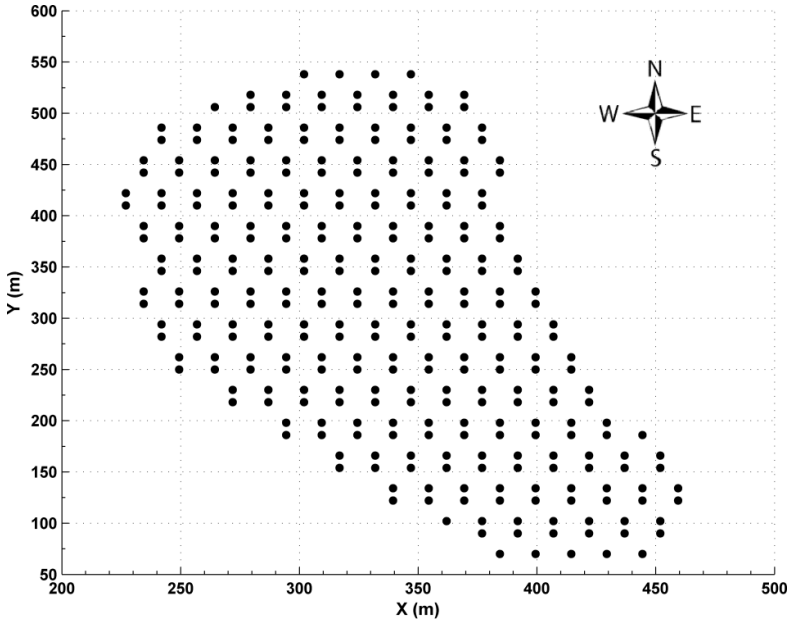

Figure 5.1. Plan view of 298 drawpoints

The total tonnage of material in the slice file was almost 66 Mt with an average density of 2.7 (t/m^3). The tonnage from individual drawpoints varied between 184 and 362kt. Figure 5.2 shows the tonnage distribution for draw columns. Only twenty-six percent of the columns contained more than 220kt of ore.

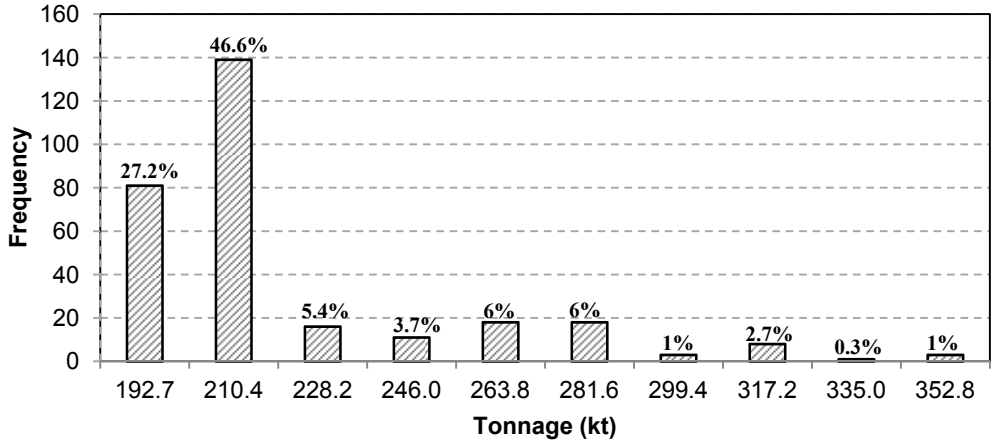

Figure 5.2. Draw columns tonnage distribution

Figure 5.3 shows the surface created from the initial height of draw columns based on the slice file. It is obvious that the draw columns located at the south end of the mine have a higher elevation than the other draw columns. Figure 5.4 shows the surface created from the weighted average grade of slices in each draw column. This shows that maximum area of the mine has a grade between 1.2% and 1.4%.

5.3 Application of the MILP Models using the Single-step Method

The performance of the proposed MILP models was analyzed based on the net present value (NPV), smoothness and practicality of the generated schedules, number of new drawpoints that must be opened in each period, and number of active drawpoints.

The application of the models was implemented on a Dell Precision T7500 computer at 2.7 GHz, with 24GB of RAM. The goal was to maximize the NPV at a discount rate of 12%, while assuring that all constraints were satisfied during the mine-life.

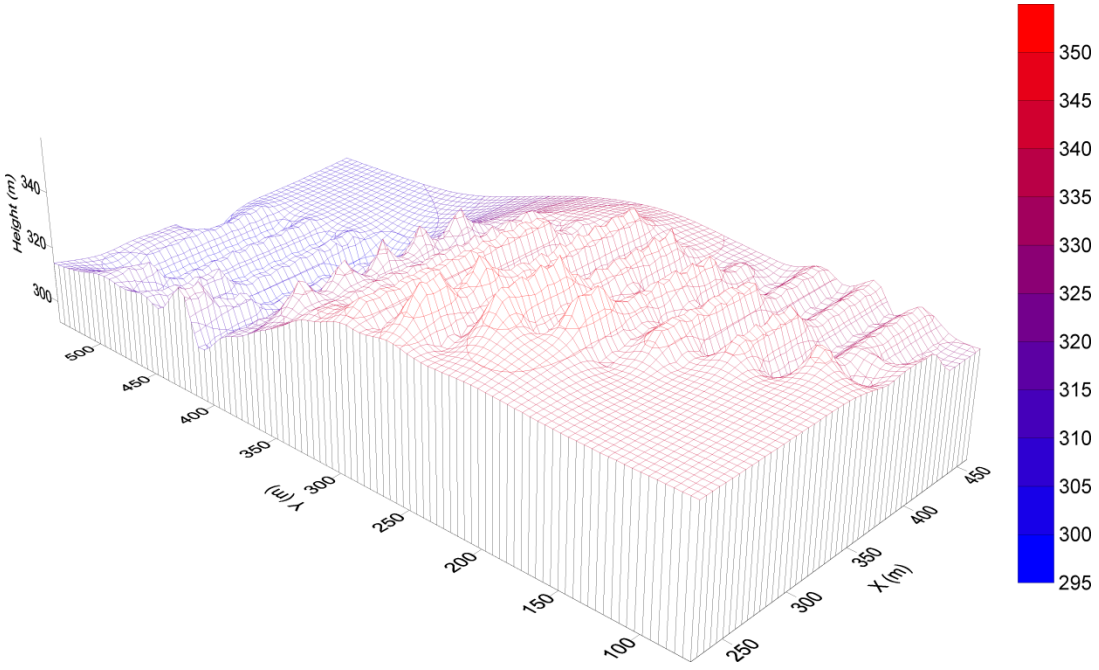

Figure 5.3. Height profile based on the main database

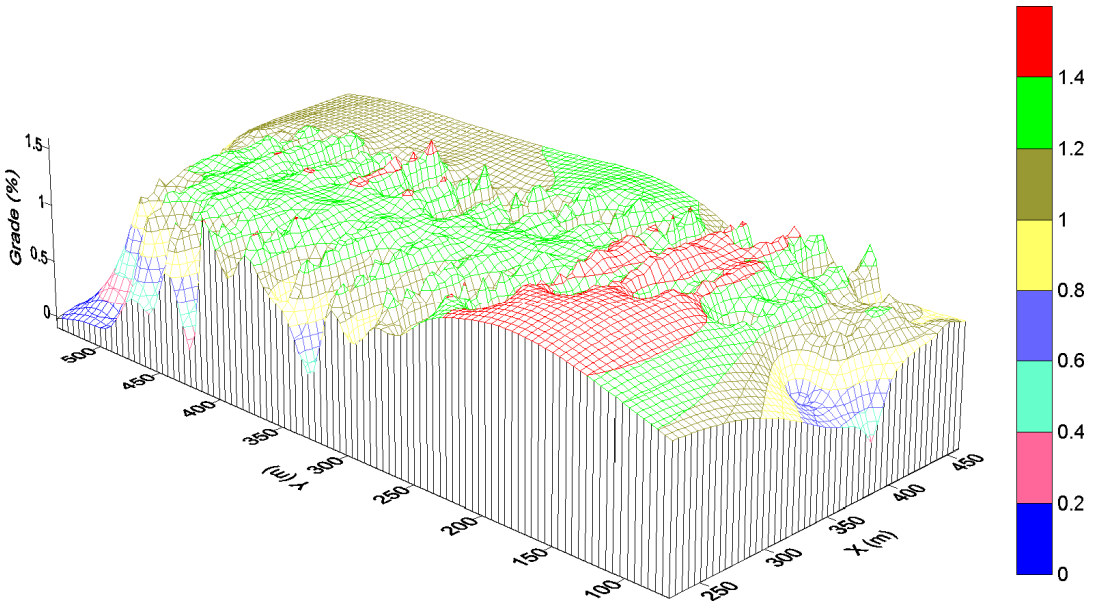

Figure 5.4. Grade profile based on the average grade of each draw column

A part of the main dataset containing 102 drawpoints with the slice height of 10 meters was considered. Figure 5.5 illustrates a plan view of the drawpoint configuration based on the relevant coordinates and distance between the center-lines of draw columns.

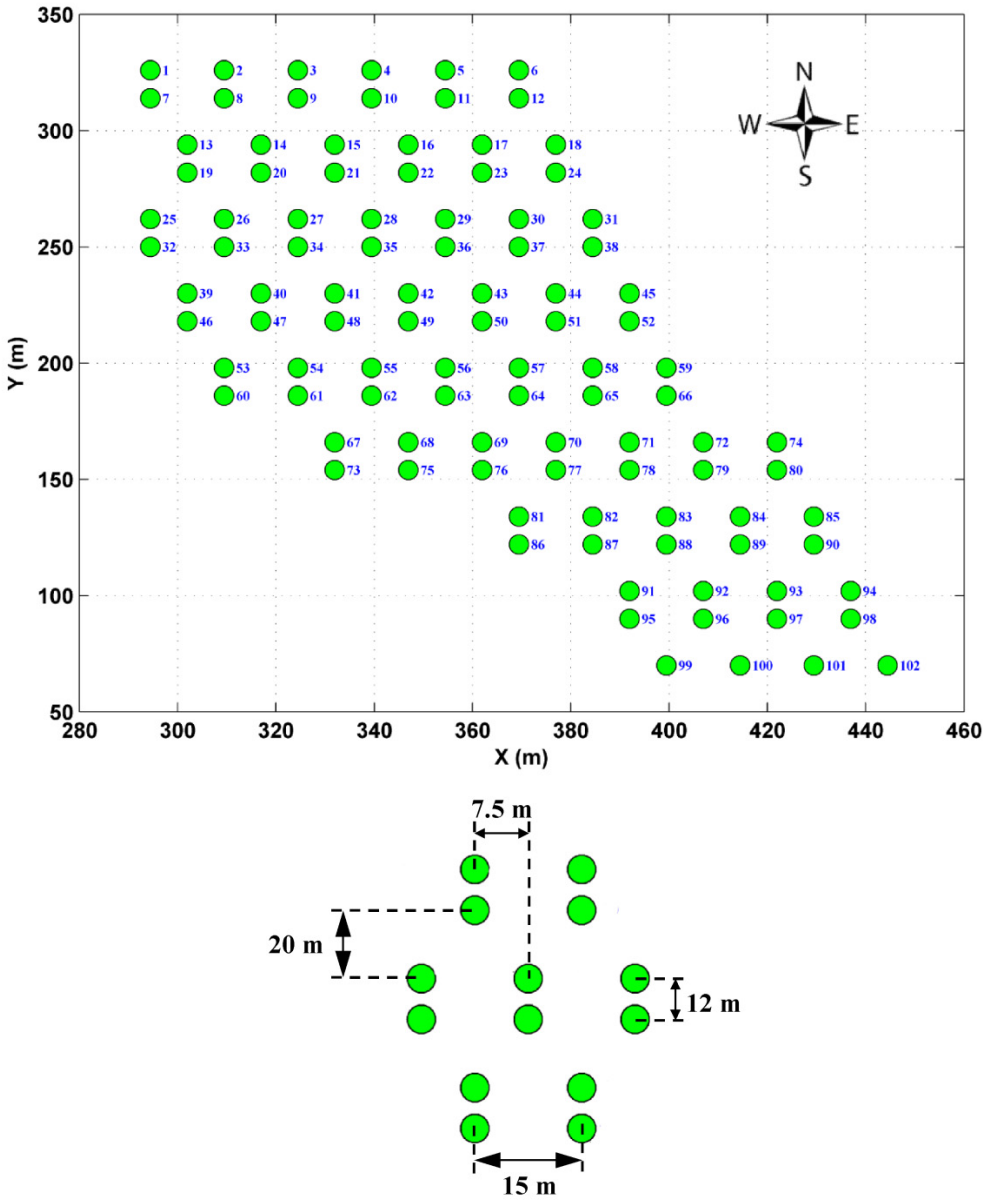

Figure 5.5. Plan view of 102 drawpoints

The minimum and maximum numbers of slices within draw columns were 33 and 36, respectively. The initial slice file contained 3470 slices, of which 1412 were eliminated after applying the BHOD. The BHOD was limited to not less than 50 m and at least 50 m of the drawpoints with the BHOD of zero was extracted. After applying this assumption, minimum and maximum heights of the draw column were 50m and 290m, respectively.

Figure 5.6 illustrates a 3D view of the draw columns after applying the BHOD. The total tonnage of material to be extracted was almost 13.5 Mt. The tonnage from individual drawpoints after applying the BHOD varied between 28.1kt and 220.5kt. The deposit was scheduled over 15 periods, equivalent to 15 years.

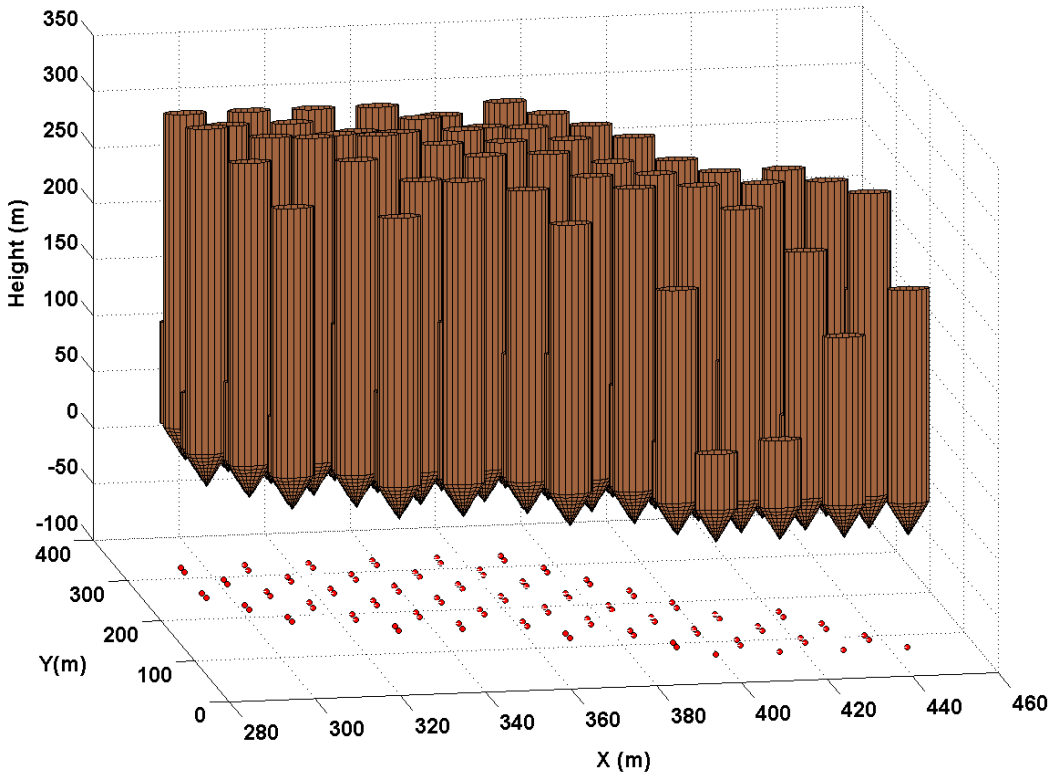

Figure 5.6. 3D view of draw columns after applying the BHOD (102 draw columns)

5.3.1 Application of the Single-step Method at the Cluster Level

To aggregate the draw columns, the advancement lines which distinguish the phases were defined for each direction. These phases control practical cave advancement. We tested models with no phases defined and the solutions were not practical. After the test, clustering was done within the phases for each direction. Figure 5.7 shows the created clustering phases for four advancement directions: west to east (WE), east to west (EW), north to south (NS), and south to north (SN). We ran different scenarios to choose the best possible solution among the different possible directions.

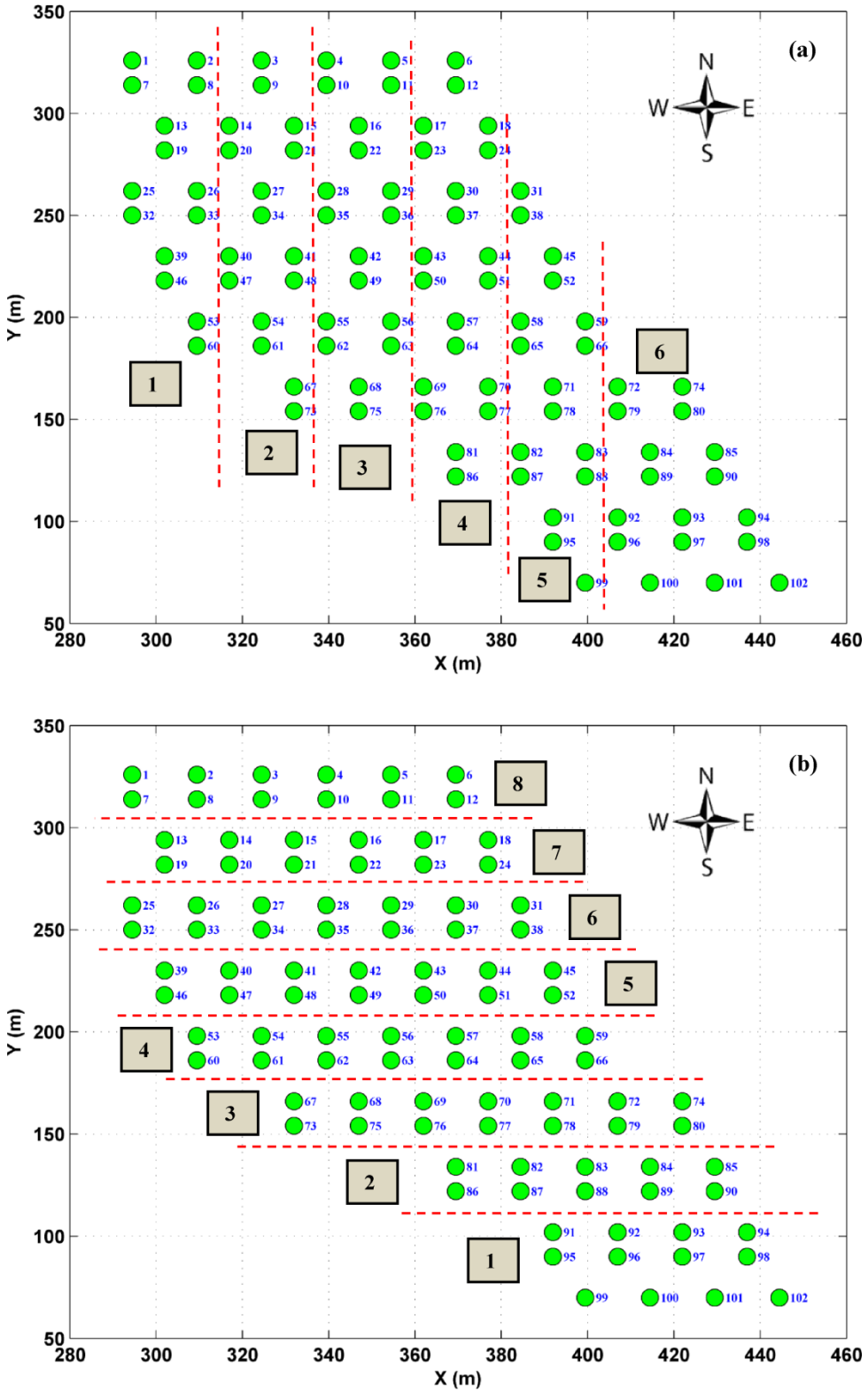

Figure 5.7. Defined advancement lines to create clustering phases: (a) west to east or east to west direction, and (b) north to south or south to north direction.

The tonnage of material within each phase is shown in Figure 5.8. The total tonnage of material was calculated for each phase based on the tonnage of draw columns within the phase. For clustering, the maximum number of clusters that could be created was set to 17. The weight factors of the tonnage, average grade, and distance between the draw columns were set to 0.05, 0.05, and 5. The maximum number of draw columns in each cluster could not be more than 10.

Figure 5.9 and Figure 5.10 illustrate the clusters in cardinal directions with tonnage value, dollar value, and average grade for each cluster. The total tonnage of material to be extracted was almost 13.5 Mt.

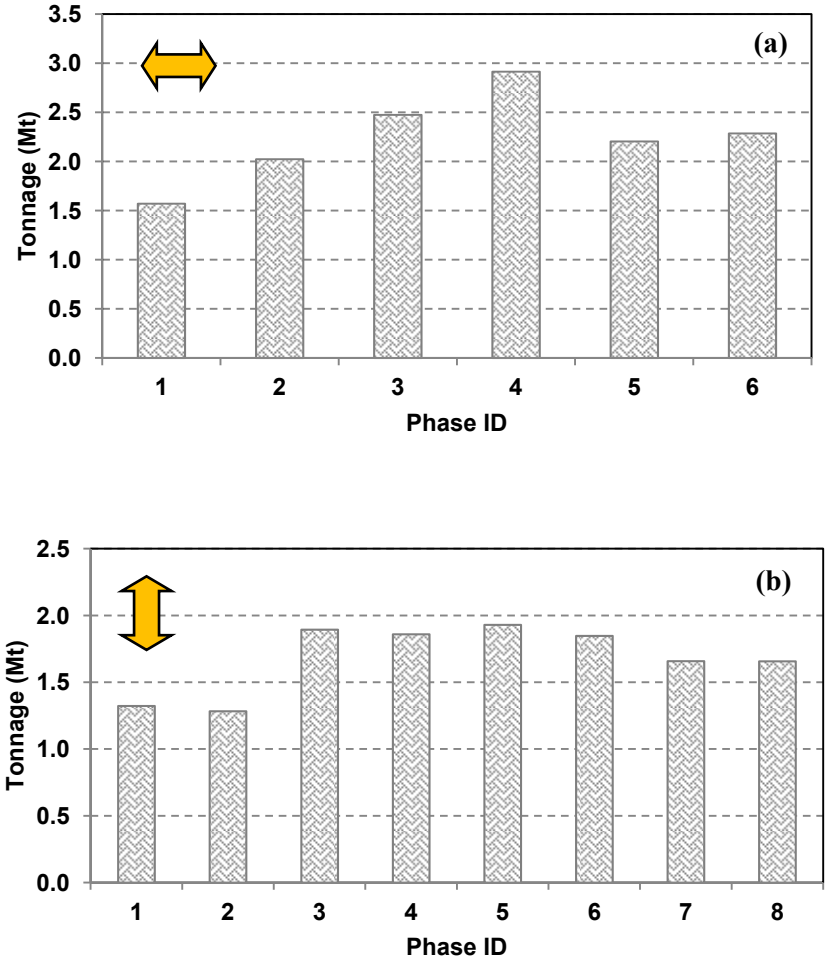

Figure 5.8. Available tonnage within each phase for different advancement directions: (a) WE/EW, and (b) NS/SN

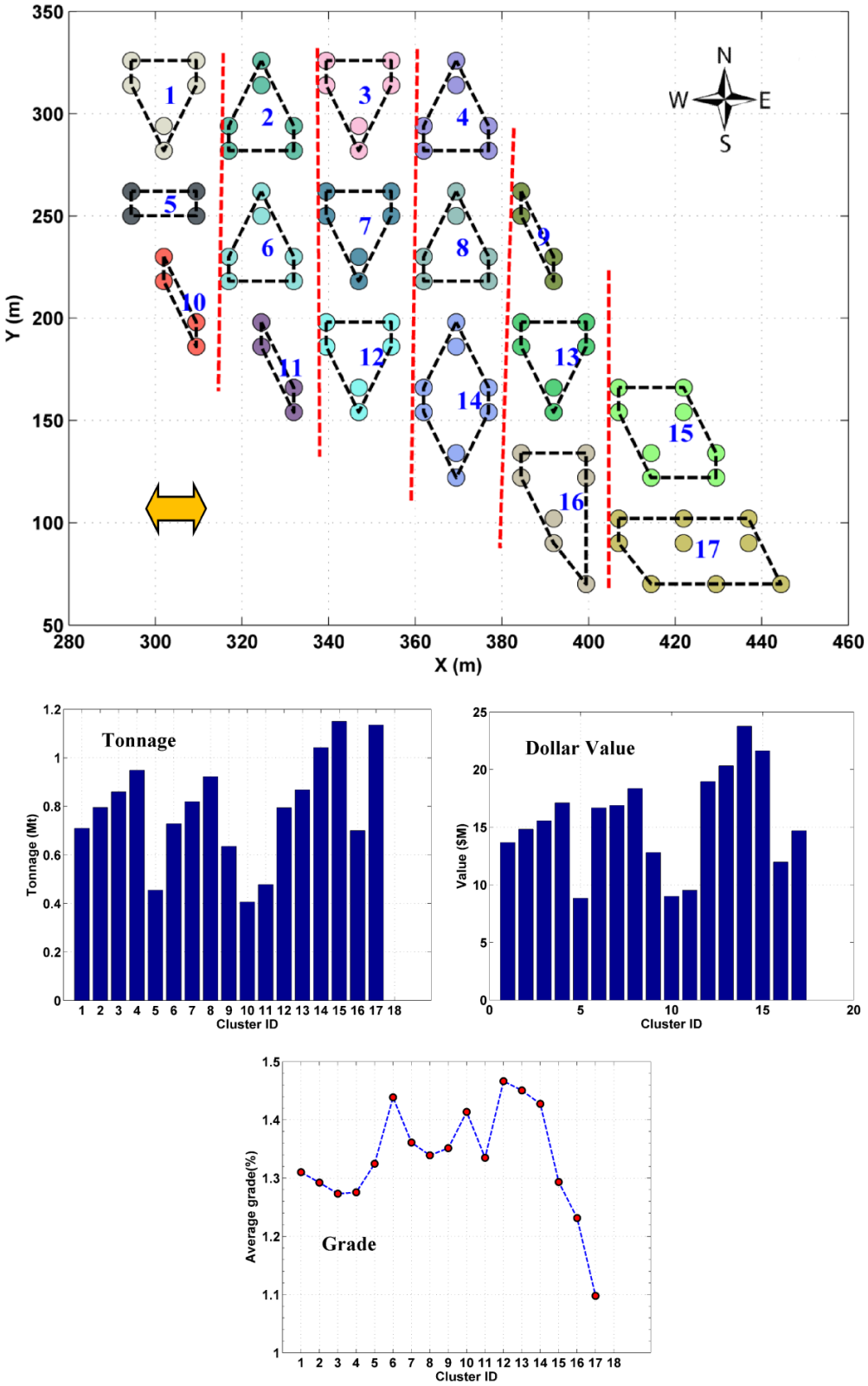

Figure 5.9. Clusters and their information in WE and EW directions

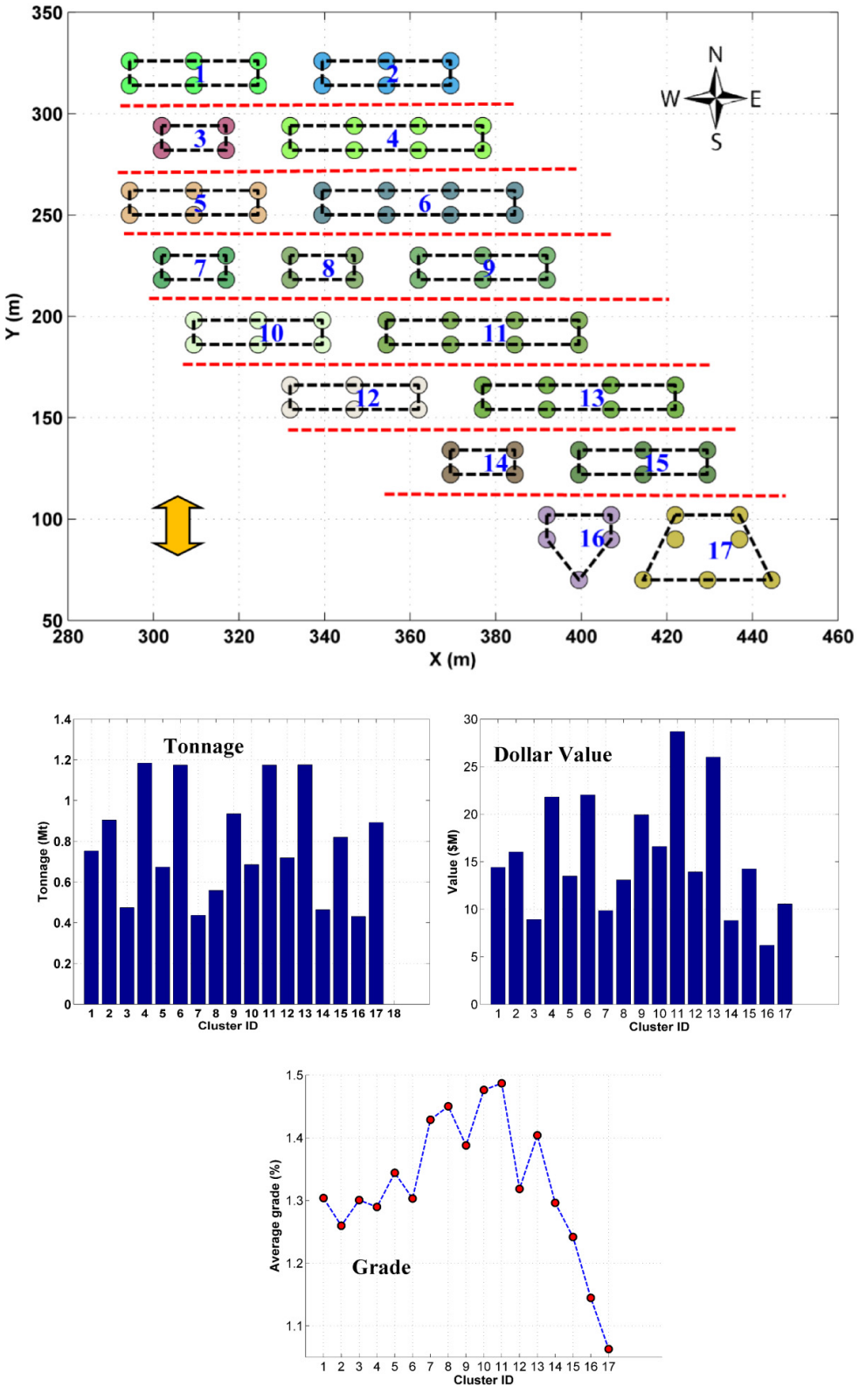

Figure 5.10. Clusters and their information in NS and SN directions

A capacity of 900kt/yr was considered as the upper bound on the mining capacity for the cluster level formulation. The maximum number of active clusters in each period was set to five. The maximum number of the new clusters which could be opened in each period was set to two. The lower and upper bounds of the draw rate for drawpoints were set to 10kt/yr/per drawpoint and 40kt/yr/per drawpoint. The draw rate bounds for each cluster were calculated based on number of the draw columns within the cluster. An EPGAP of 1% was set for the optimization at cluster level. Table 5.1 shows the summary of the parameters. Table 5.2 shows the number of decision variables and constraints for each direction at the cluster level.

Table 5.3 shows a summary of the results for each direction at the cluster level. The results show that the maximum NPV was gained in the west to east direction. A comparison between the difference in percent from the maximum NPV shows that the difference in percent for east to west and south to north was more than the defined EPGAP.

Table 5.1. Production scheduling parameters at cluster level

Parameter	Value
Total tonnage of material (Mt)	13.5
Number of periods	15
Discount rate (%)	12
Maximum mining capacity (kt/yr)	900
Maximum number of active clusters	5
Maximum number of new clusters	2
Draw rate (lower / upper) (kt/yr/per drawpoint)	10 / 40

Table 5.2. Number of variables and constraints for cluster level with 17 clusters

Direction	Number of clusters	Number of constraints	Decision variables		
			Total	Continuous	Binary
WE	17	1,429	765	255	510
EW	17	1,429	765	255	510
NS	17	1,444	765	255	510
SN	17	1,399	765	255	510

Table 5.3. Numerical result for cluster level formulation with 17 clusters

Direction	CPU time 8 CPUs @ 2.7 GHz	EPGAP (%)	Optimality GAP (%)	NPV ($M)	Difference from Max. (%)
WE	00:01:24	1	0.99	123.21	0
EW	00:02:57	1	1.00	121.71	1.22
NS	00:00:50	1	0.82	121.98	1.0
SN	00:00:47	1	0.99	121.28	1.57

Figure 5.11 to Figure 5.16 show that all assumed constraints were satisfied for the cluster-level formulation. Figure 5.11 shows the tonnage of production in each period for different directions. It is obvious that the formulation tried to keep the mining capacity at the upper bound.

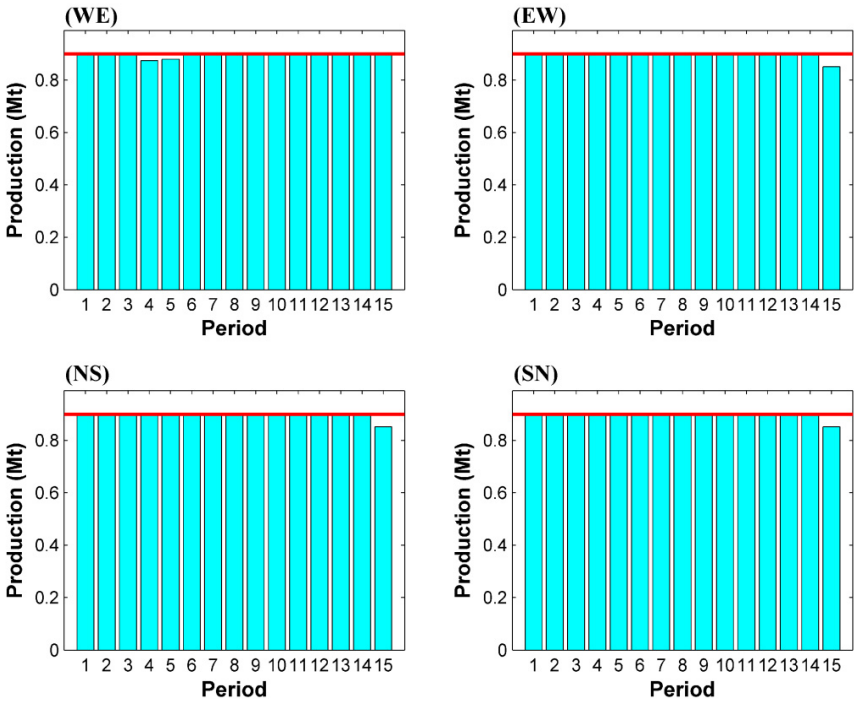

Figure 5.11. Production tonnage for different directions at the cluster level over the mine life

Figure 5.12 and Figure 5.13 illustrate the maximum number of active clusters and drawpoints in each period for the different advancement directions, respectively. In Figure 5.12, in the west to east direction during the first four years, the maximum allowable number of clusters was activated, while in the east to west direction from year three, there were five active clusters.

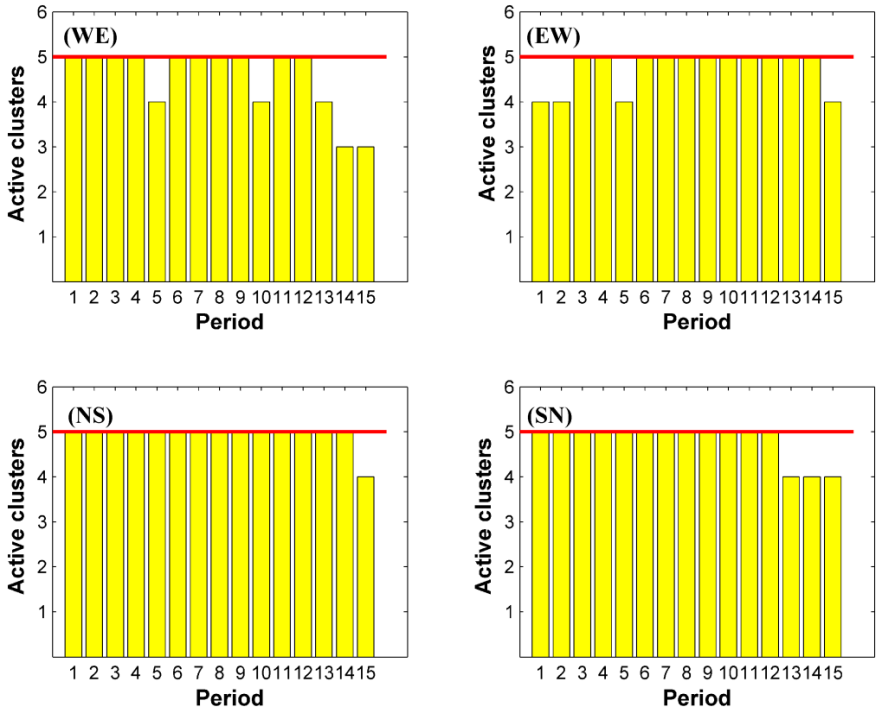

Figure 5.12. Number of active clusters for different directions at the cluster level over the mine life

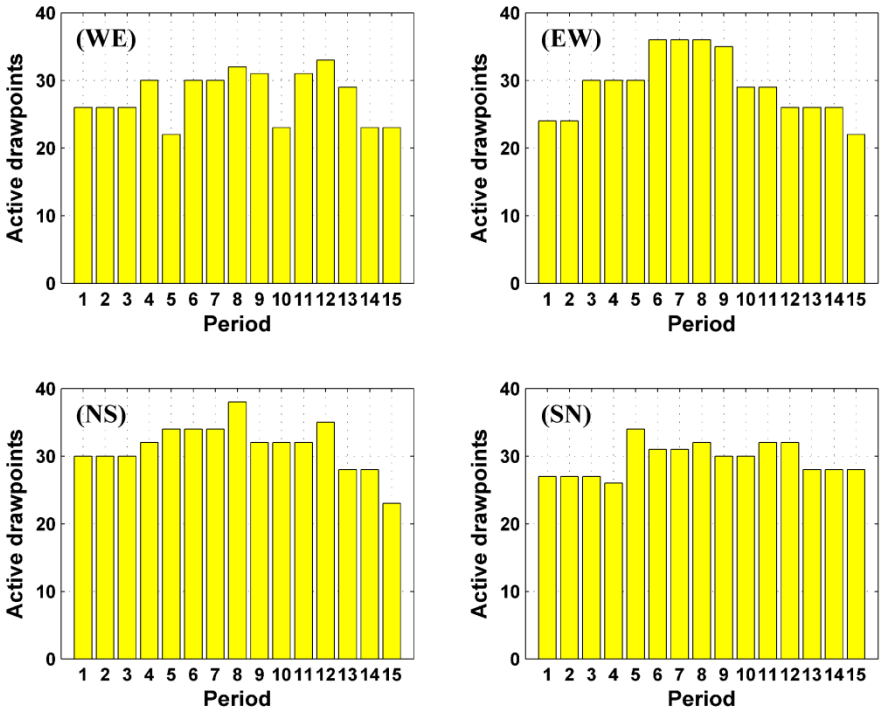

Figure 5.13. Number of active drawpoints for different directions at the cluster level over the mine life

In the west to east direction, from periods 12 to 15, the number of active drawpoints gradually decreased. For mining in the north to south and south to north directions, the maximum allowable numbers of clusters were activated. Period 15 had the least number of active clusters in all advancement directions.

Figure 5.14 shows the number of new clusters which had to be opened in each period for different advancement directions. The number of new clusters opened in period one could be equal to the maximum allowable number of active clusters to reach the required production in this period. In all directions except east to west, the number of clusters opened was equal to the maximum allowable number of active clusters. Also, in these three directions, there was no need to open new clusters in periods two and three. In all directions, in periods seven, 14, and 15, the clusters that had already been opened were extracted and a new cluster was not opened in these periods.

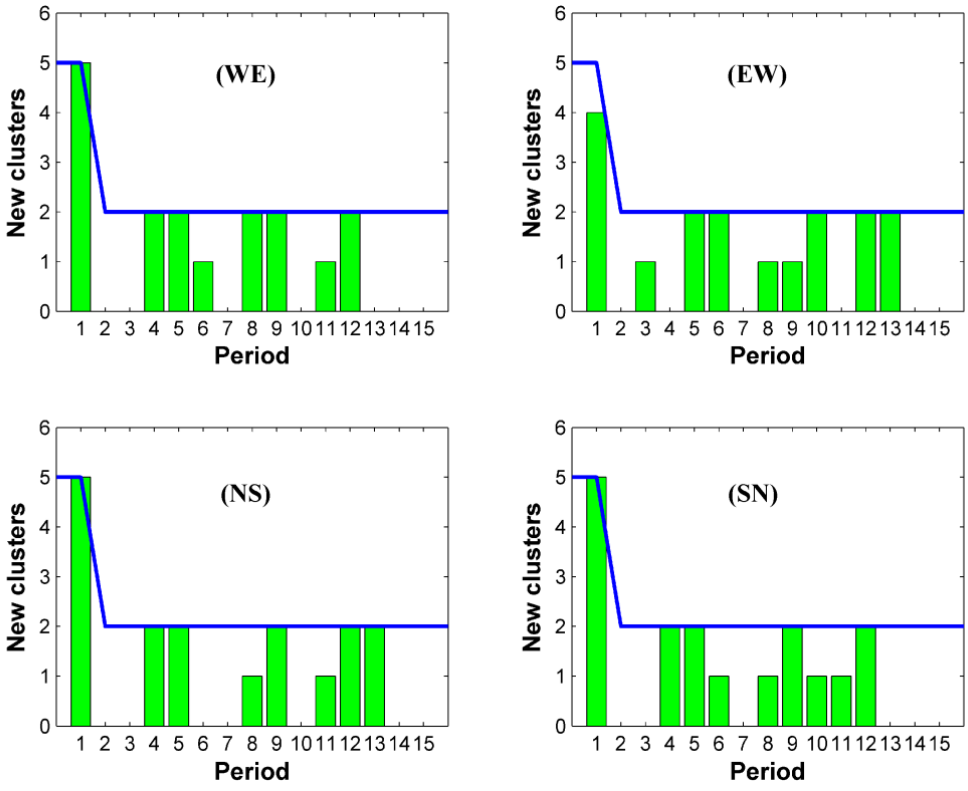

Figure 5.14. Number of new clusters that must be opened for different directions at the cluster level over the mine life

Figure 5.15 and Figure 5.16 show the tonnage extracted from clusters two, eight, and 17 in different directions. The lower and upper bounds of the draw rate for drawpoints were known and these boundaries were defined for each cluster according to the number of draw columns within the cluster. In other words, the lower and upper bounds of the draw rate for each cluster were equal to the number of the draw columns within the cluster, times the minimum or maximum draw rate, respectively.

Figure 5.15 shows that cluster eight, which contained six drawpoints, was mined in six periods from period eight to period 13 in the west to east direction. This cluster was mined in four periods from period one to period four in the east to west direction. In the west to east direction, extraction from cluster eight was started with 60kt/period in period eight and gradually increased to near the 240kt/period until period 11. It then reached 60kt/period again in period 13. But in the east to west direction, extraction from this cluster had to be started with the maximum allowable draw rate. Extraction from cluster 17, which contained nine drawpoints, was started with 90kt/period in both the west to east and east to west directions, but the life of the cluster in the east to west direction was more than in the west to east direction. In the west to east direction, the draw rate of cluster 17 increased after the first period of extraction, while it was mined with a uniform draw rate of 90kt/period during the first five periods in the east to west direction.

Figure 5.16 compares the extraction amount from clusters two and 17 in the north to south and south to north directions. The life of cluster two in both directions was four periods and it had the exact same behavior. Extraction from cluster 17, which contained seven drawpoints, was started with 70kt/period and finished with 280kt/period after four periods in the north to south direction. In the south to north direction, this cluster was extracted with a draw rate of 100kt/period in periods one and two. Then the draw rate increased to 280kt/period in period four. The extraction finished with the draw rate of 160kt/period in period five.

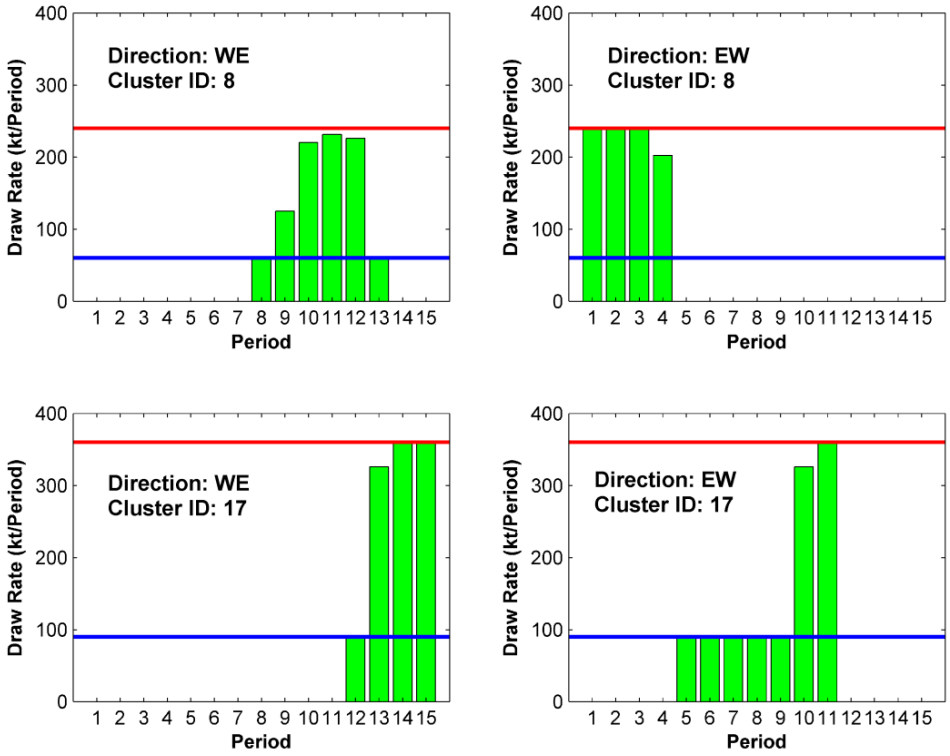

Figure 5.15. Amount of depletion from clusters 8 and 17 in the WE and EW directions

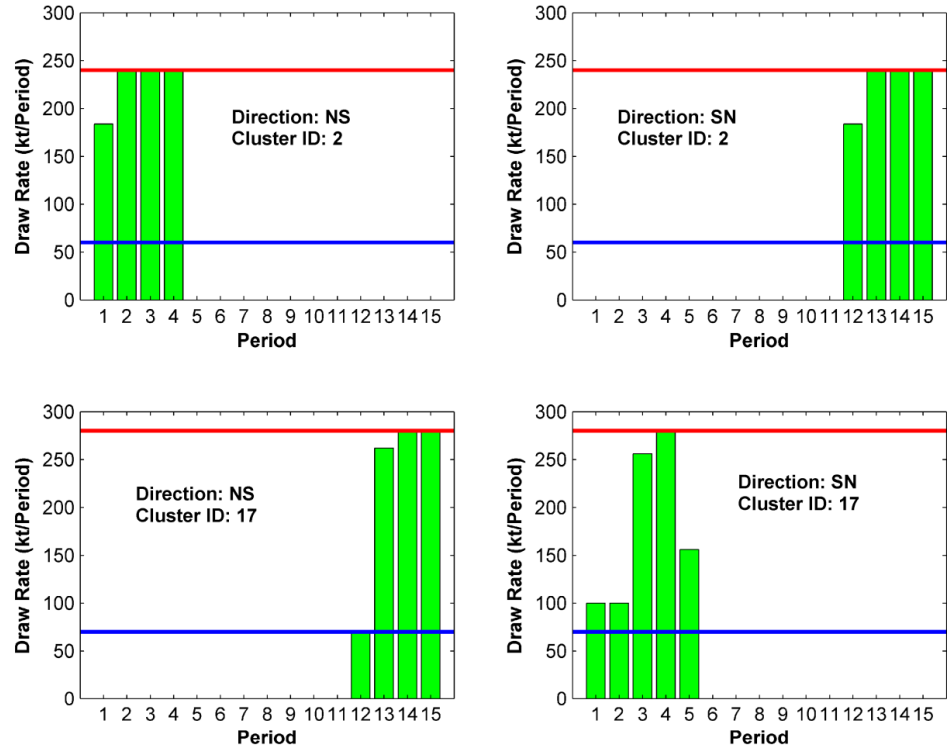

Figure 5.16. Amount of depletion from clusters 8 and 17 in the NS and SN directions

Figure 5.17 illustrates the cumulative discounted cash flow and discounted cash flow for different directions. It is obvious that in period one, the west to east direction had the maximum discounted cash flow and in the last period, the north to south direction had the minimum one.

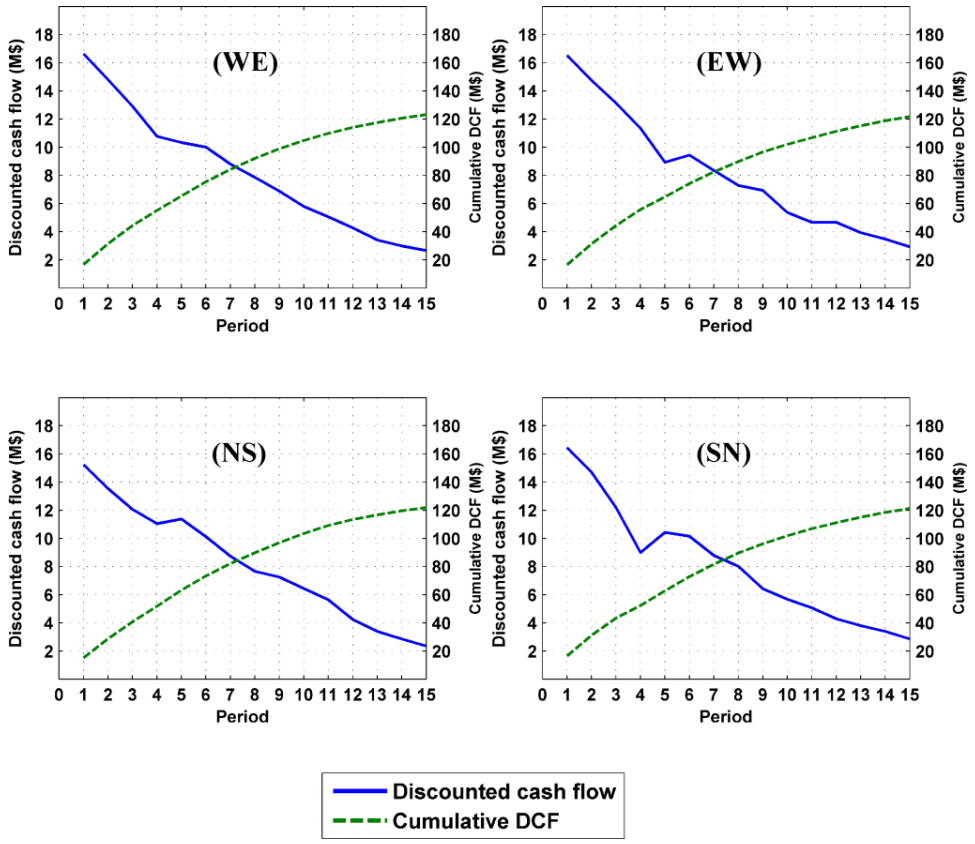

Figure 5.17. Discounted cash flow and cumulative DCF for different directions at the cluster level over the mine life

Figure 5.18 illustrates the opening pattern at the cluster level for the west to east direction, which has the maximum NPV. If the mine was divided into two parts, west and east, it is obvious that all drawpoints within the west area were opened during the first five periods. All drawpoints were opened before period 12 and after that extraction continued by extracting the material from the active drawpoints.

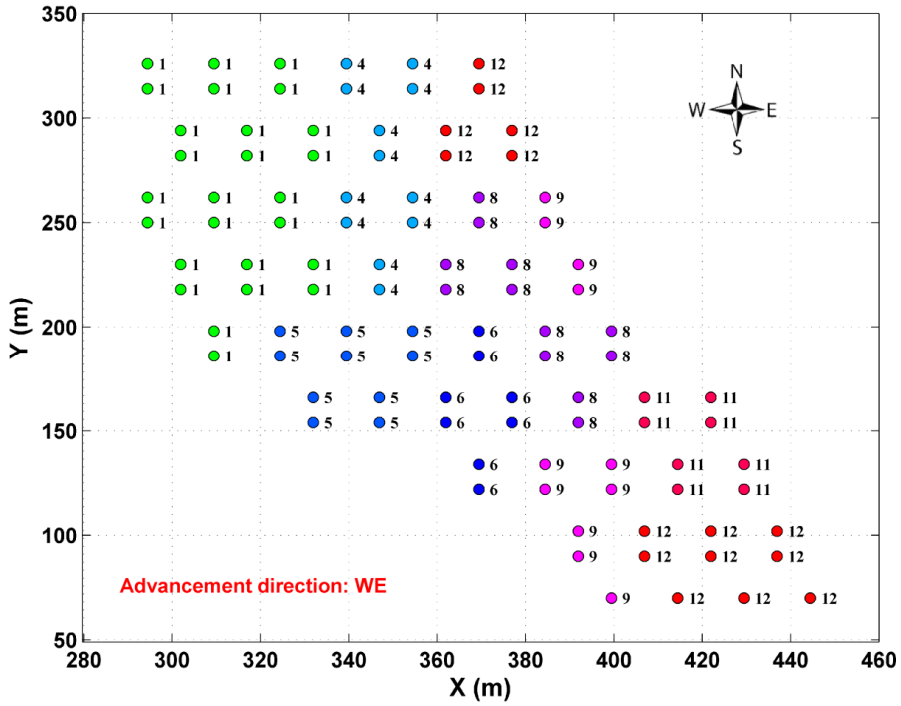

Figure 5.18. Opening pattern using the cluster-level formulation in the WE direction

5.3.2 Application of the Single-Step Method at the Drawpoint Level

This formulation was implemented on the same dataset with 102 drawpoints. The total tonnage of material to be extracted was almost 13.5 Mt. A capacity of 900kt/yr was considered as the upper bound on the mining capacity for the drawpoint level formulation. The maximum number of active drawpoints in each period was set to 40. The maximum number of the new clusters which could have been opened in each period was set to 15. The lower and upper bounds of the draw rate for drawpoints were set to 10kt/yr/per drawpoint and 40kt/yr/per drawpoint, respectively. The summary of the parameters are illustrated in Table 5.4. An EPGAP of 3% was set for the optimization at the drawpoint level. The drawpoint level formulation had a 4590-decision variable in which 3060 were binary variables.

Table 5.5 shows the number of constraints and a summary of the results for each direction at the drawpoint level. The results show that the maximum NPV was gained in the west to east direction.

Table 5.4. Production scheduling parameters at drawpoint level

Parameter	Value
Total tonnage of material (Mt)	13.5
Number of periods	15
Discount rate (%)	12
Maximum mining capacity (kt/yr)	900
Maximum number of active drawpoints	40
Maximum number of new drawpoints	15
Draw rate (lower / upper) (kt/yr/per drawpoint)	10 / 40

Table 5.5. Numerical results for the drawpoint level formulation

Direction	Number of constraints	CPU time 8 CPUs @ 2.7 GHz	EPGAP (%)	Optimality GAP (%)	NPV ($M)
WE	19,854	00:30:56	3	2.72	125.27
EW	19,884	00:49:46	3	2.98	124.70
NS	20,874	00:27:46	3	2.93	124.31
SN	19,284	01:03:17	3	2.99	124.78

It is obvious that due to the increase in the number of the constraints, despite the increased value assumed for EPGAP, the CPU time increased compared to the cluster level formulation. Figure 5.19 to Figure 5.23 show that all assumed constraints were satisfied for the drawpoint level formulation.

Figure 5.19 shows the tonnage of production in each period for different directions. The formulation tried to keep mining capacity at the upper bound. For all directions, the tonnage of mined material was equal to the maximum allowable capacity in all periods except the last period. In the last period, only the remaining reserve was extracted and this was less than the defined higher bound for the mining capacity.

Figure 5.20 illustrates the maximum number of active drawpoints in each period for the different advancement directions. In all directions, the number of active drawpoints decreased between periods 11 and 15. Only in the first period of the south to north direction was the number of active drawpoints fewer than 30.

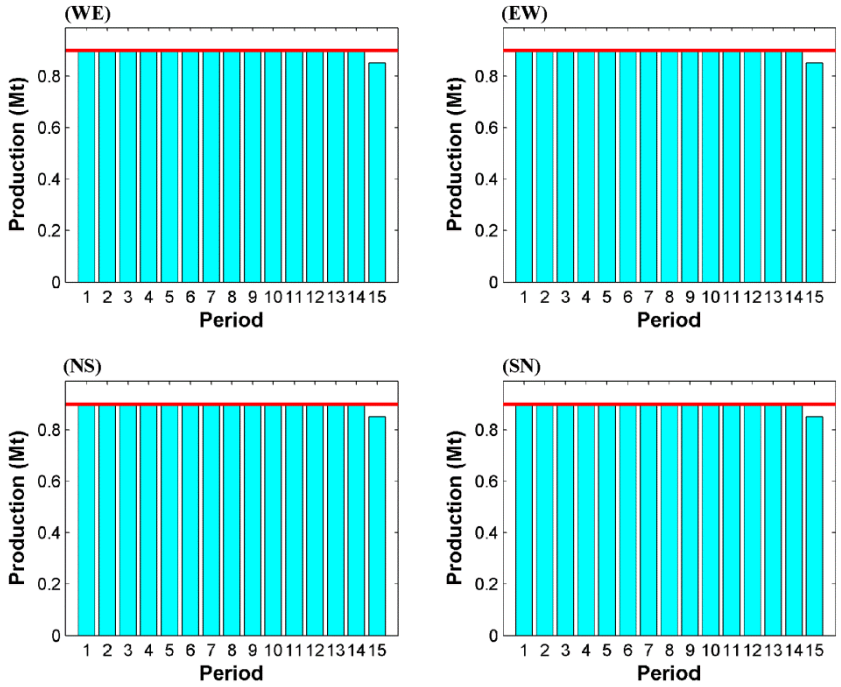

Figure 5.19. Production tonnage for different directions at the drawpoint level over the mine life

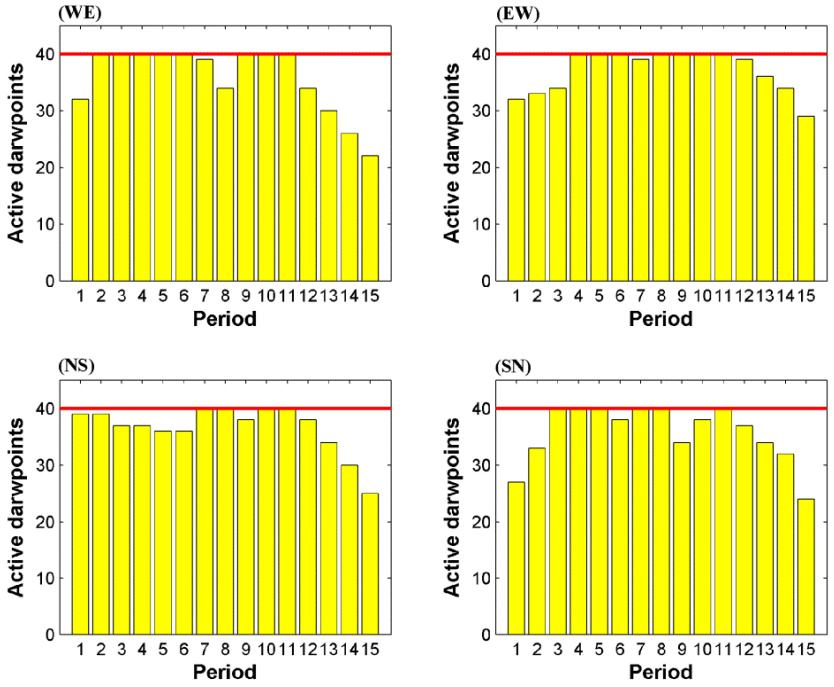

Figure 5.20. Number of active drawpoints for different directions at the drawpoint level over the mine life

Figure 5.21 shows the number of new drawpoints that were opened in each period for different advancement directions. The number of new drawpoints opened in period one could be equal to the maximum allowable number of active drawpoints in this period to reach the required production. It can be seen that only in the first period of the north to south direction, the number of new drawpoints that had to be opened was close to the maximum allowable number of active drawpoints. In the west to east direction, the number of new drawpoints reduced from 32 drawpoints in the first period to two drawpoints in the fifth period. Then, 13 new drawpoints were opened in period six and, after this period, the number of new drawpoints that had to be opened was fewer than 13. In the west to east direction, the last drawpoints were opened in period 13 and, after that, the extraction continued from the active drawpoints.

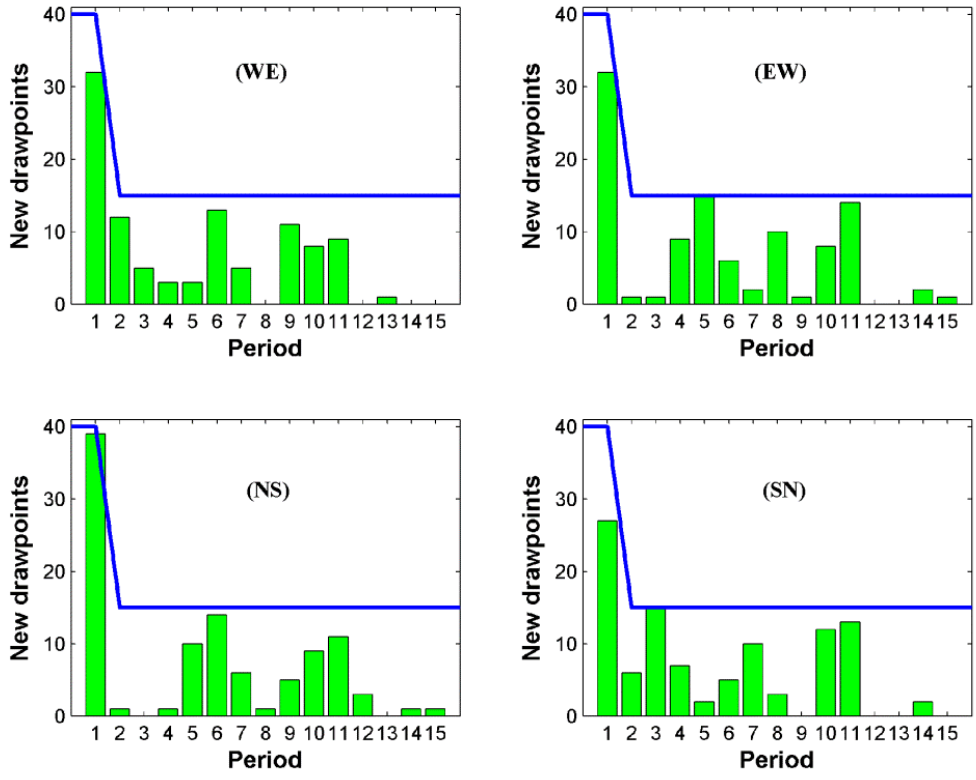

Figure 5.21. Number of new drawpoints that must be opened for different directions at the drawpoint level over the mine life

Figure 5.22 and Figure 5.23 show the tonnage which must be extracted from drawpoints 96, 80, and 57 in different directions. Figure 5.22 shows that drawpoint 96 was mined in six periods from periods 10 to 15 in the west to east direction. But it was mined in seven periods between periods four and 10 in the east to west direction. In both directions, the extraction was started with 10kt/period and increased gradually to 40kt/period. It continued with the maximum allowable draw rate during the last three periods of the drawpoint life. In the west to east direction, extraction from drawpoint 80 was started with a draw rate greater than the minimum draw rate and then it increased and reached the maximum draw rate from the second period of extraction. But in the east to west direction, drawpoint 80 was extracted with the minimum draw rate during the first three periods. Figure 5.23 shows that extraction from drawpoint 57 is started in period six in both directions, north to south and south to north. In the north to south direction, the extraction is started with the minimum draw rate of 10kt/yr, while in the south to north direction; it is started with a draw rate of 20kt/yr.

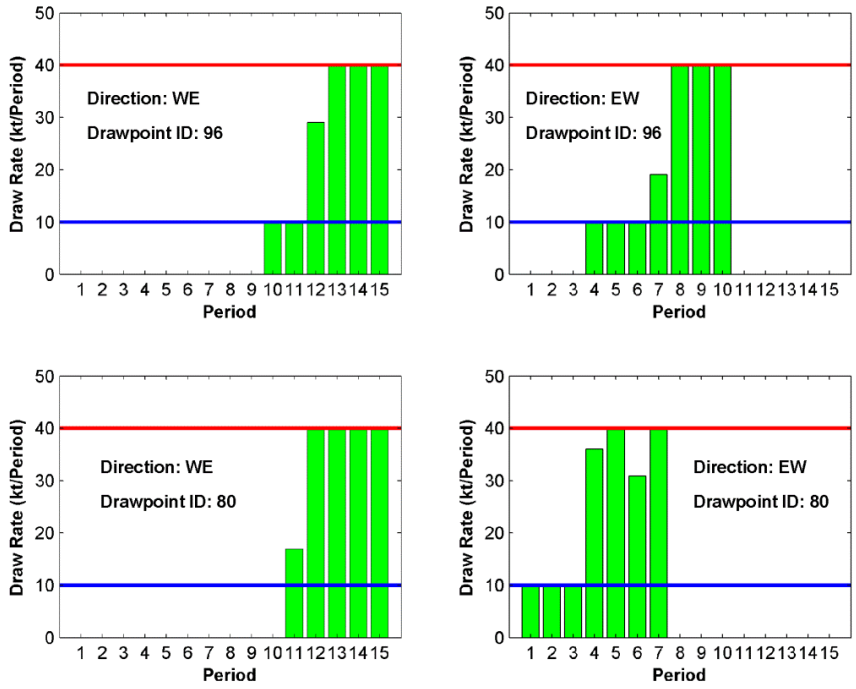

Figure 5.22. Amount of depletion from drawpoints 96 and 80 in the WE and EW directions

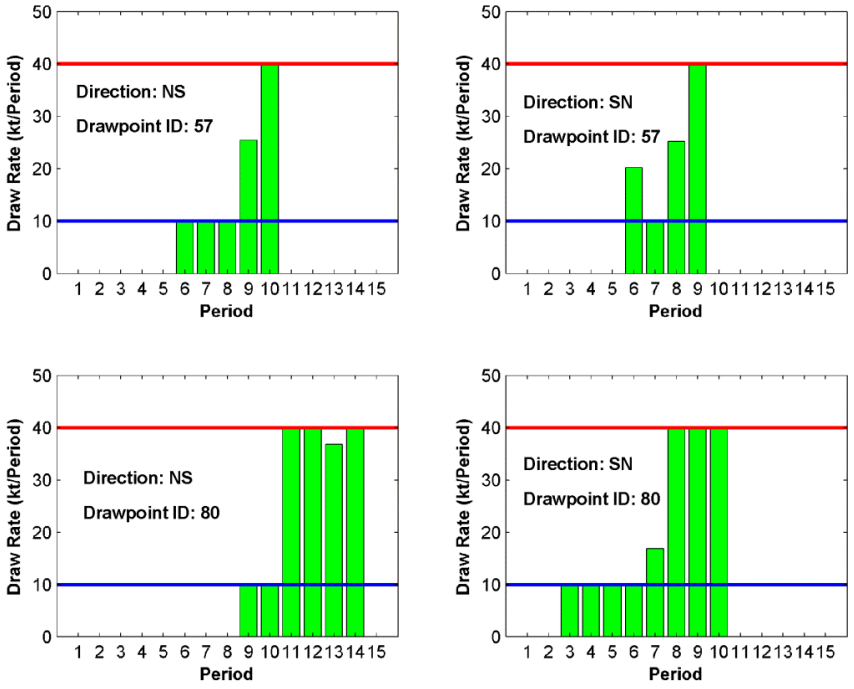

Figure 5.23. Amount of depletion from drawpoints 57 and 80 in the NS and SN directions

Figure 5.24 illustrates the cumulative discounted cash flow and discounted cash flow for different directions. In the west to east direction, the discounted cash flow for period two was more than period one, because of the number of new drawpoints opened in this period. Figure 5.25 illustrates the opening pattern at the drawpoint level for the west to east direction, which has the maximum NPV. If the mine was divided into two parts, west and east, it is obvious that the greatest part of the drawpoints within the west area opened before period six. The last drawpoint opened in period 13 and after that the extraction continued from the active drawpoints. It is obvious that practicality the obtained opening pattern from the cluster level formulation was better than at the drawpoint level. At the cluster level, the formulation dealt with bigger mining units than at the drawpoint level. Consequently, when a cluster was opened, a number of drawpoints were opened. But, at the drawpoint level, the model dealt with drawpoints and it was possible that only one drawpoint be opened. It should be noted that the time horizon for the drawpoint level formulation can vary as a subset of the mine-life.

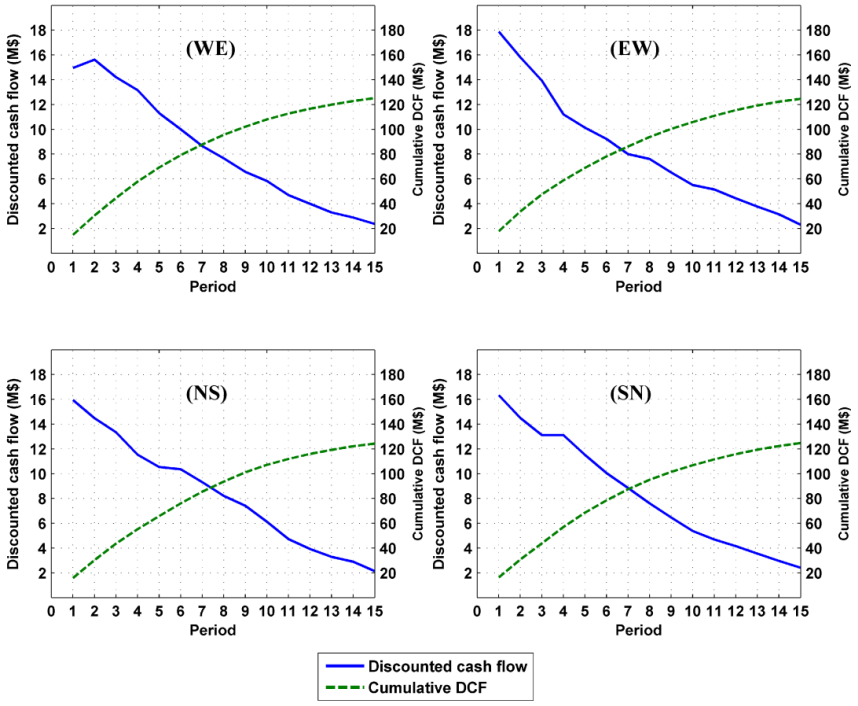

Figure 5.24. Discounted cash flow and cumulative DCF for different directions at the drawpoint level over the mine life

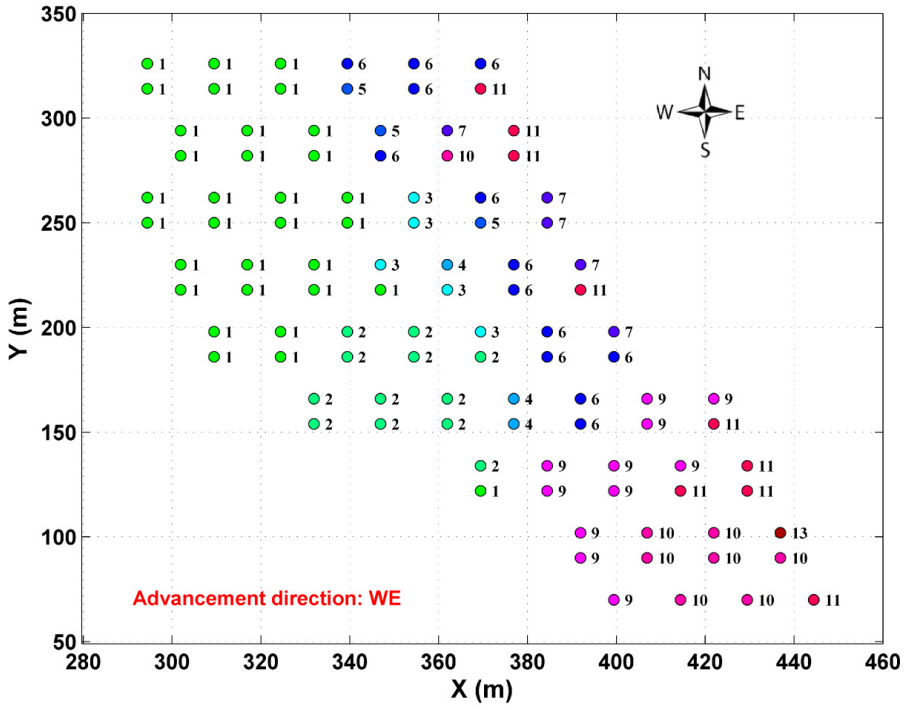

Figure 5.25. Opening pattern using the drawpoint level formulation in the WE direction

The drawpoint-level method can be used to control the size of the MILP formulation when the sequence of extraction of the drawpoints for a mine with a large number of drawpoints is going to be optimized at the drawpoint level.

5.3.3 Application of the Single-Step Method at the Drawpoint-and-Slice Level

The scheduling parameters at this level of resolution were the same as at the drawpoint level. In addition, this level of resolution had a constraint to control the average grade of production per period. The lower and upper bounds of the average grade were set to 0.7% and 1.6%. An EPGAP of 5% was set for the optimization run. The problem was only solved for the west to east (WE) and south to north (SN) directions because these were shown to generate the highest NPV at the drawpoint resolution level. Table 5.6 shows the number of decision variables and the number of constraints for the WE and SN directions at the drawpoint-and-slice level formulation. There are many binary variables, and consequently, more CPU time must be spent to solve the problem.

Table 5.7 shows a summary of the results for the WE and SN directions at the drawpoint-and-slice level.

Table 5.6. Number of variables and constraints at the drawpoint-and-slice level formulation with 102 drawpoints and 2,058 slices

Direction	Number of DP/SL	Number of constraints	Decision variables		
			Total	Continuous	Binary
WE	102 / 2,058	115,146	64,800	30,870	33,930
SN	102 / 2,058	114,576	64,800	30,870	33,930

Table 5.7. Numerical result for the drawpoint-and-slice level formulation with 102 drawpoints and 2,058 slices

Direction	CPU time 8 CPUs @ 2.7 GHz	EPGAP (%)	Optimality GAP (%)	NPV ($M)
WE	110:43:26	5	5	131.63
SN	124:31:18	5	5	126.63

The resulting NPVs of the drawpoint-and-slice level were \$131.63M and \$126.63M in the WE and SN directions, respectively. The obtained optimality gap for both directions was 5%. The results show that even to solve the small-size problem at the drawpoint-and-slice level, a long CPU time is required.

Figure 5.26 to Figure 5.29 show that all assumed constraints were satisfied at the drawpoint-and-slice level formulation in the considered directions. Figure 5.26 illustrates the production tonnage in each period. In both directions, the formulation tried to extract the maximum allowable amount of material.

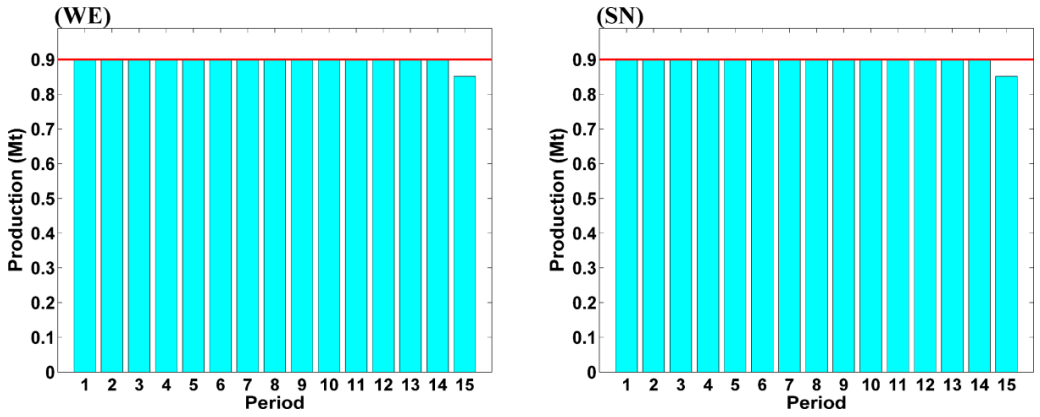

Figure 5.26. Production tonnage in the WE and SN directions at the drawpoint-and-slice level over the mine life

Figure 5.27 illustrates the number of active drawpoints in each period. In both directions, the number of active drawpoints in period one was fewer than 40. In the west to east direction, the number of active drawpoints gradually increased, from 33 in period one to 40 in period four. Then, the mine worked with the maximum number of active drawpoints until period 13 and after that the number of active drawpoints reduced. In the south to north direction, the mine worked with the maximum number of active drawpoints from periods two to 12. In the last years of the mine life, the number of active drawpoints in the south to north direction was less than in the west to east direction.

Figure 5.28 illustrates the number of drawpoints that had to be opened in each period. The number of new drawpoints that could be opened in the first period was

set to 40. From period two to period 15, a maximum of 15 new drawpoints could be opened. In both directions, the number of new clusters from period two to period 15 was less than 15 except in period 11 of south to north direction in which 15 new drawpoints had to be opened. In the west to east direction, the last drawpoints were opened in period 13 while a number of new drawpoints were opened in period 14 in the north to south direction.

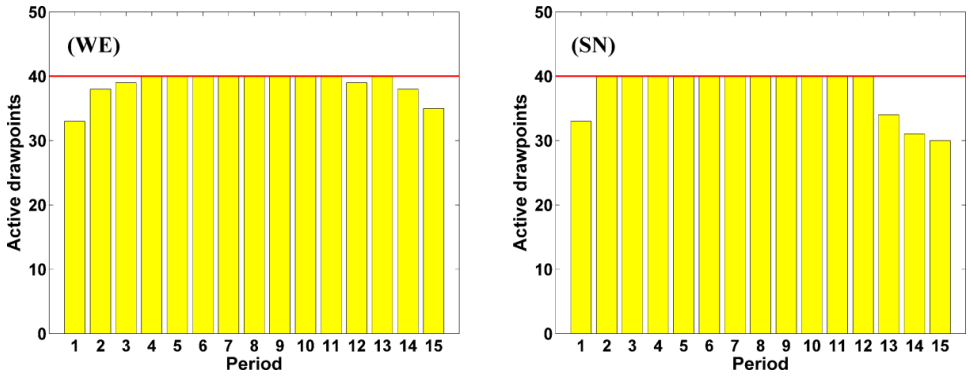

Figure 5.27. Number of active drawpoints in the WE and SN directions at the drawpoint-and-slice level over the mine life

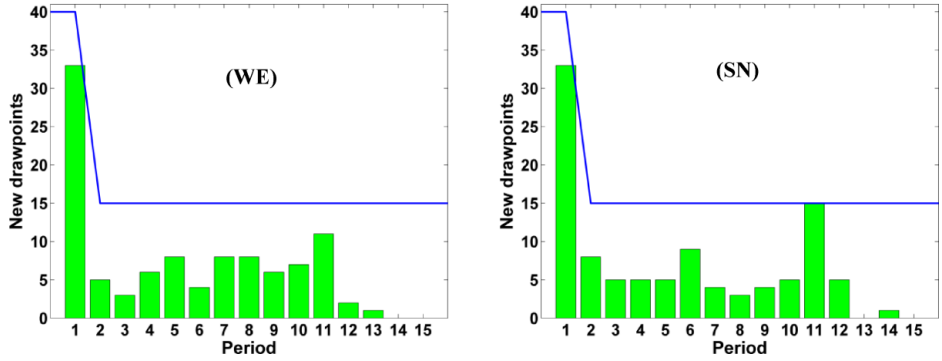

Figure 5.28. Number of new drawpoints that must be opened in the WE and SN directions at drawpoint-and-slice level over the mine life

Figure 5.29 illustrates the average grade of production. In the west to east direction, during the first three periods the average grade of the production was higher than the south to north direction. In both directions, during the mine life the average grade of the production was higher than 1 % except the last period. In the west to east direction, the average grade of production had a downward trend. After period 11, the average grade of production increased. In the south to north

direction, the average grade of production increased significantly. This was because of the high grade draw columns located at the north side of the mine.

Figure 5.30 and Figure 5.31 show the opening pattern of the drawpoints in the west to east and south to north directions.

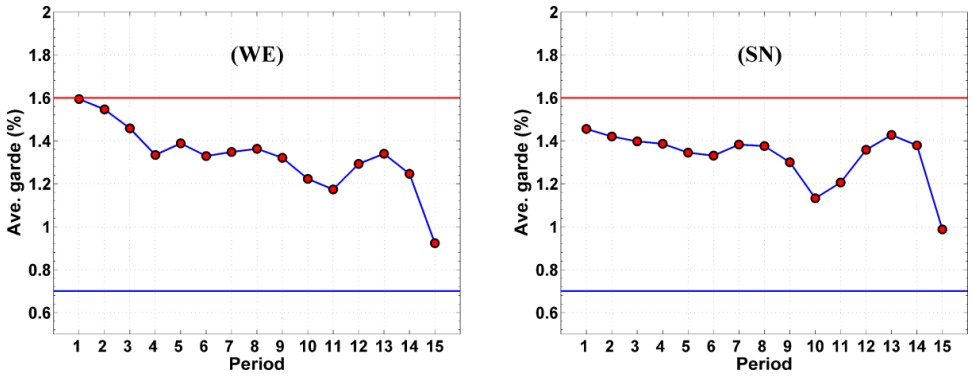

Figure 5.29. Average grade of production in the WE and SN directions at the drawpoint-and-slice level over the mine life

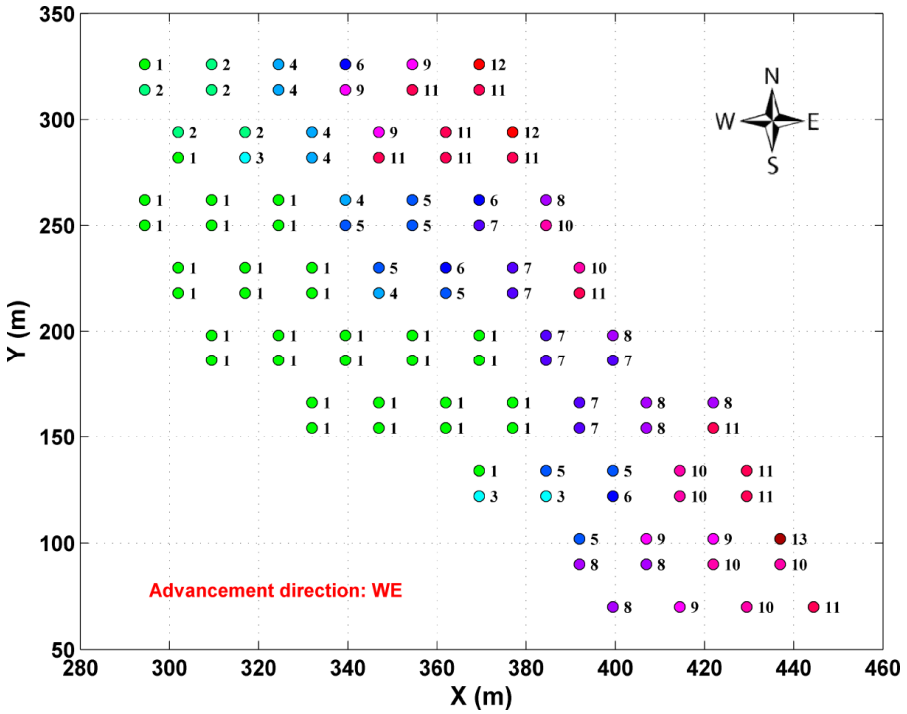

Figure 5.30. Opening pattern using the drawpoint-and-slice level formulation in the WE direction

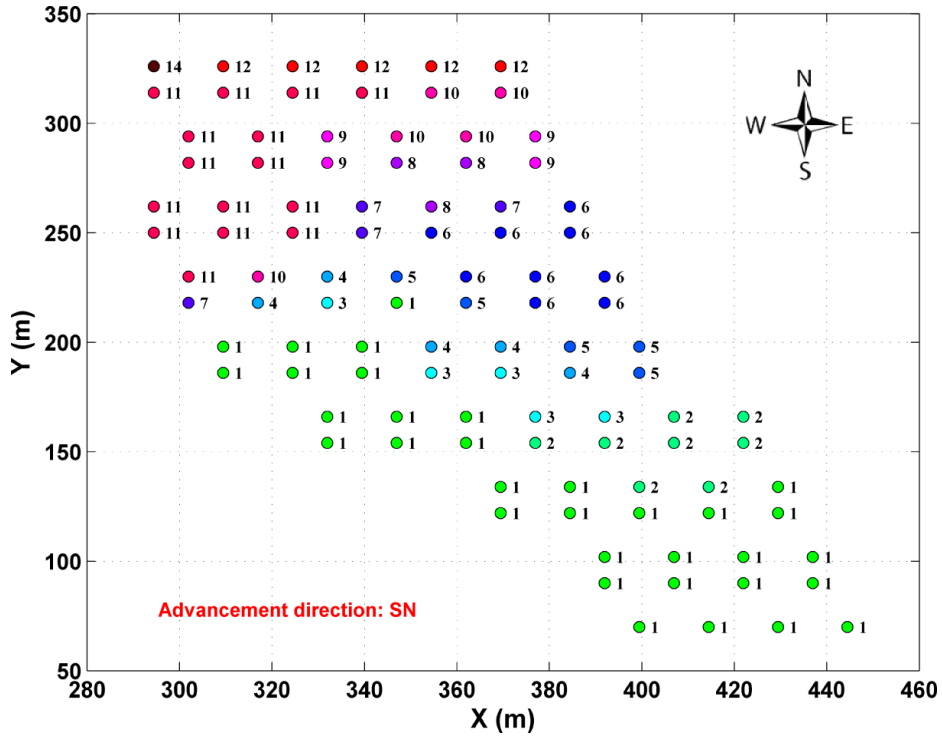

Figure 5.31. Opening pattern using the drawpoint-and-slice level formulation in the SN direction

In the west to east direction, if the mine was divided into two sections, west and east, most of the drawpoints in the west section were opened during the first five periods. In west to east direction, if the mine was divided into two sections north and south, most of the drawpoints in the south section were opened during the first five periods.

5.3.4 Summary and Comparison of Results of Three Different Levels of Resolution

The MILP formulations for three levels of problem resolution -- cluster level, drawpoint level, and drawpoint-and-slice level -- were applied independently on a dataset containing 102 drawpoints and 2,058 slices.

At the cluster level, the optimal life-of-mine multi-period block-cave production schedule is generated. This is the strategic yearly production schedule with the objective of NPV maximization. The strategic plan honors mining capacity and uniform feed to the processing plant. At the drawpoint level, the optimal long-term

block cave production schedule is generated. The time horizon for this model can vary as a subset of the life-of-mine to control the size of the MILP to be solved.

At drawpoint-and-slice level, the optimal long-term plan at the drawpoint level, including slices, is generated. The time horizon for this detailed 3D model could vary as a subset of the time horizons chosen in the previous levels.

In all the levels, the problem was solved over the mine life and the same input scheduling parameters were considered. The results showed that all the considered constraints had been satisfied and the models worked properly. The obtained NPVs were the optimal values that could be reached based on the obtained optimality gap.

Table 5.8 summarizes the results of three levels of resolution for the single-step method. It is obvious that the number of the constraints and variables increased from the cluster level to the drawpoint-and-slice level and, consequently, the solving time increased.

To solve the problem at these three levels of resolution, the EPGAP was set to 1%, 3%, and 5% at the cluster, drawpoint, and drawpoint-and-slice levels, respectively. Despite the higher obtained optimality gap for the drawpoint-and-slice level, the solving time for this level was significantly longer than for others. The obtained NPV at the drawpoint-and-slice level was more than at the drawpoint level, and drawpoint level's NPV was more than at the cluster level.

In the west to east direction, the NPV of the drawpoint-and-slice level was 4.8% and 6.4% more than the drawpoint and cluster levels, respectively. But, the solving time of the problem at the drawpoint-and-slice level for this direction was 4745 times more than cluster level and 215 times more than drawpoint level.

It is obvious that it is not possible to solve a real-size problem at the drawpoint and drawpoint-and-slice levels in a reasonable CPU time. So, to overcome the size problem of mathematical programming models and to generate a robust practical near-optimal schedule, a multi-step method is explained in the next section.

Table 5.8. Comparison of results of the three levels of resolution for the single-step method

Level of resolution	Dir.	Number of CL/DP/SL	Number of Constraints & variables	Opt. GAP (%)	CPU time 8 CPUs @ 2.7 GHz	NPV ($M)	Diff. from the best (%)
Cluster level	WE	17 / 0 / 0	1,429 765	0.99	00:01:24	123.21	-6.4
	EW	17 / 0 / 0	1,429 765	1.00	00:02:57	121.71	-7.54
	NS	17 / 0 / 0	1,444 765	0.82	00:00:50	121.98	-7.33
	SN	17 / 0 / 0	1,399 765	0.99	00:00:47	121.28	-7.86
Drawpoint level	WE	0 / 102 / 0	19,854 4,590	2.72	00:30:56	125.27	-4.83
	EW	0 / 102 / 0	19,884 4,590	2.98	00:49:46	124.70	-5.26
	NS	0 / 102 / 0	20,874 4,590	2.93	00:27:46	124.31	-5.56
	SN	0 / 102 / 0	19,284 4,590	2.99	01:03:17	124.78	-5.2
Drawpoint-and-slice level	WE	0 / 102 / 2,058	115,146 64,800	5	110:43:26	131.63	The best
	SN	0 / 102 / 2,058	114,576 64,800	5	124:31:18	126.63	-3.8

5.4 Application of the MILP Models using the Multi-Step Method

In a multi-step method, the performance of the proposed models was analyzed based on the NPV, mining production, and practicality of the generated schedules. The models were tested on a Dell Precision T7500 computer at 2.7 GHz, with 24GB of RAM. The goal was to maximize the NPV at a discount rate of 12%, while assuring that all constraints were satisfied during the mine life. In this method, the results of each level were used to reduce the number of variables in the next level. The main dataset containing 298 drawpoints with the slice height of 10 meters was considered. The minimum and maximum numbers of slices within draw columns were 29 and 36, respectively. The initial slice file contained 9790 slices, of which 4251 were eliminated after applying the BHOD. The BHOD was limited to not less than 50m. After applying this assumption, the minimum and

maximum heights of the draw column were 50m and 290m, respectively. The models were optimized on a dataset containing 298 drawpoints and 5539 slices over 15 periods in four different advancement directions. Figure 5.32 illustrates a 3D view of the draw columns after applying the BHOD. The total tonnage of material to be extracted was almost 37 Mt. The tonnage from individual drawpoints after applying the BHOD varied between 28kt and 233kt.

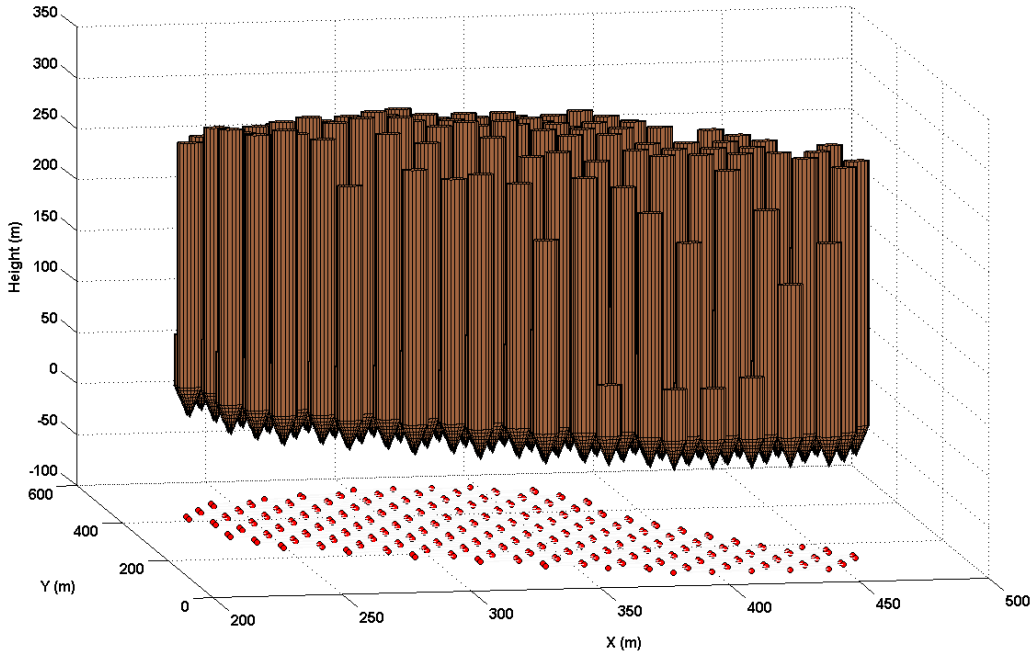

Figure 5.32. 3D view of the draw columns after applying the BHOD (298 draw columns)

In this method, the problem was solved at the beginning for different advancement directions, using the cluster level formulation. Then, based on the results, the best advancement direction was recognized.

At the drawpoint and the drawpoint-and-slice level models, the problem was only optimized for the recognized best advancement direction. Using the starting period of drawpoints and the cluster life in the best advancement direction, all the variables that would mine each drawpoint before its earliest start time were eliminated at the drawpoint level model. Then, the problem was optimized at this level of resolution. Afterwards, based on the results of the drawpoint level formulation, all the variables that would mine each drawpoint before its obtained

earliest start time from the drawpoint level model were eliminated at the drawpoint-and-slice level model. Theoretically, this variable reduction technique decreased the solution space for the optimization problem. Thus, during optimization, some of the branches in the branch-and-cut tree were eliminated, ensuring that the solution for the practical production scheduling problem was reached faster. In addition to the elimination of the variables related to the drawpoints, some of the variables related to the slices were eliminated based on the earliest extraction time of each slice, which was calculated using the maximum allowed draw rate and the earliest start time of the drawpoint.

To aggregate the draw columns, the advancement lines for each direction were defined. Afterwards, clustering was done between lines for each direction. Figure 5.33 shows the created clustering phases for four advancement directions: west to east (WE), east to west (EW), north to south (NS), and south to north (SN). The tonnage of material within each phase is shown in Figure 5.34. The total tonnage of material was calculated for each phase based on the tonnage of draw columns within the phase. For clustering, the maximum number of clusters was set to 35. The weight factors of the tonnage, average grade, and distance between the draw columns were set to 0.1, 0.1, and 5, respectively. The maximum number of draw columns in each cluster could not be more than 15.

Figure 5.35 and Figure 5.36 illustrate the clusters in cardinal directions with tonnage value, dollar value, and average grade for each cluster. A capacity of 2.5Mt/yr was considered as the upper bound on the mining capacity for all formulations. The maximum number of active clusters in each period was set to 15. The maximum number of the new clusters which could be opened in each period was set to 5. The lower and upper bounds of the draw rate for drawpoints were set to 10kt/yr/per drawpoint and 50kt/yr/per drawpoint. The draw rate bounds for each cluster were calculated based on number of the draw columns within the cluster. The summary of the parameters is illustrated in Table 5.9. An EPGAP of 1% was set for the optimization at the cluster level.

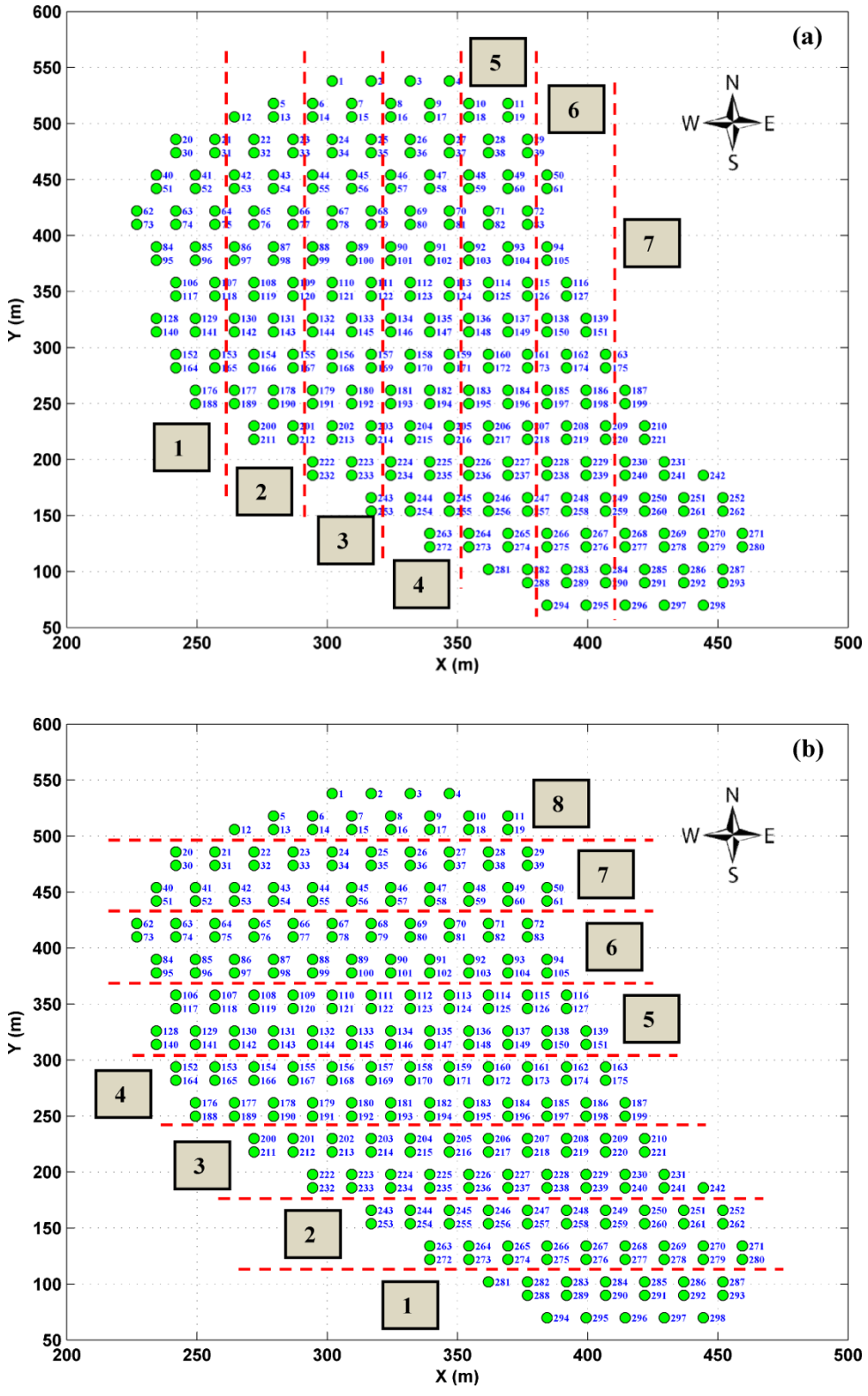

Figure 5.33. Defined advancement lines to create clustering phases: (a) west to east or east to west direction (WE/EW), and (b) north to south or south to north direction (NS/SN).

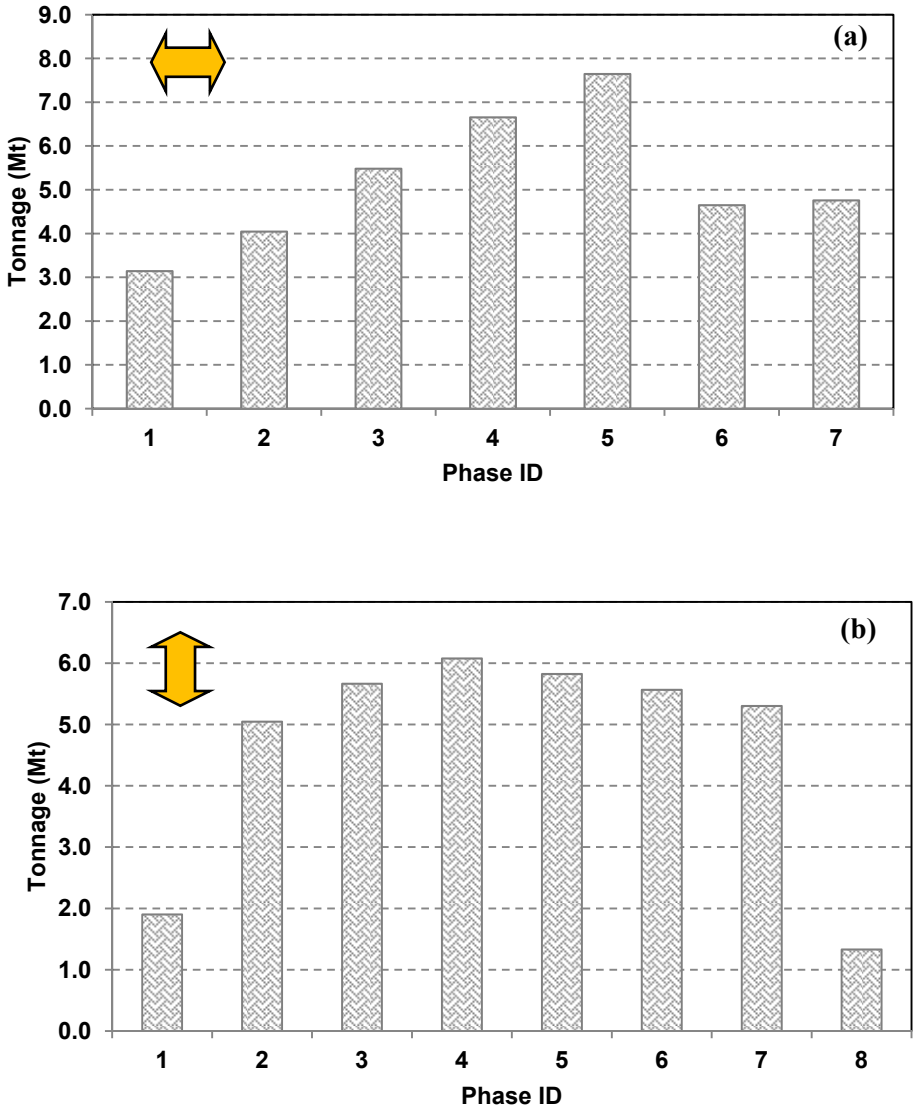

Figure 5.34. Available tonnage within each phase for different advancement directions: (a) WE/EW, and (b) NS/SN

Table 5.10 shows the number of decision variables and the number of constraints for each direction at the cluster level. Table 5.11 shows a summary of the results for each direction at the cluster level. The maximum NPV was gained in the west to east direction. A comparison between the difference in percent from the maximum NPV shows that the difference in percentage for the east to west and north to south directions was more than the defined EPGAP, while for the south to north direction it was less than the defined EPGAP.

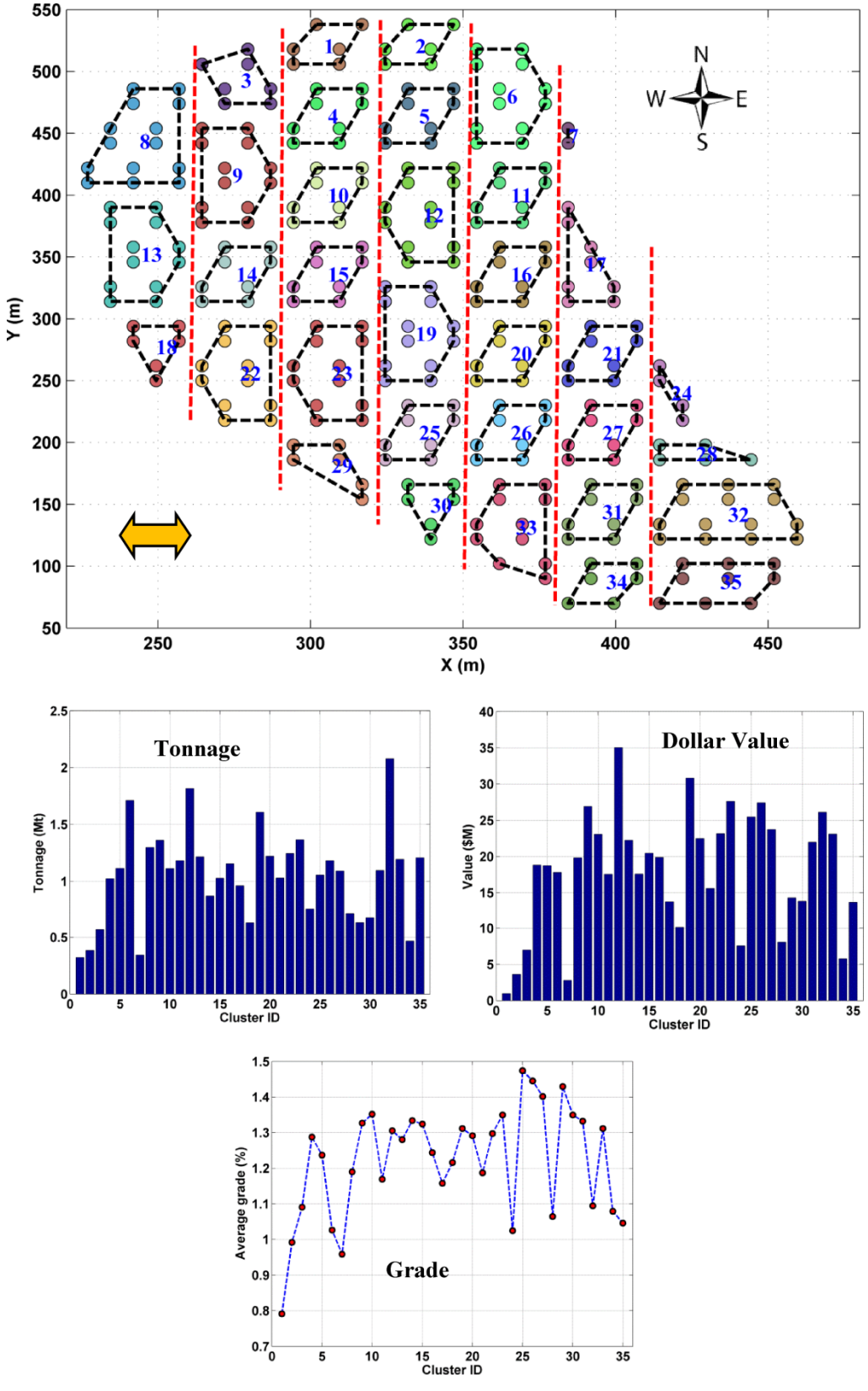

Figure 5.35. Clusters and their information in the WE and EW directions

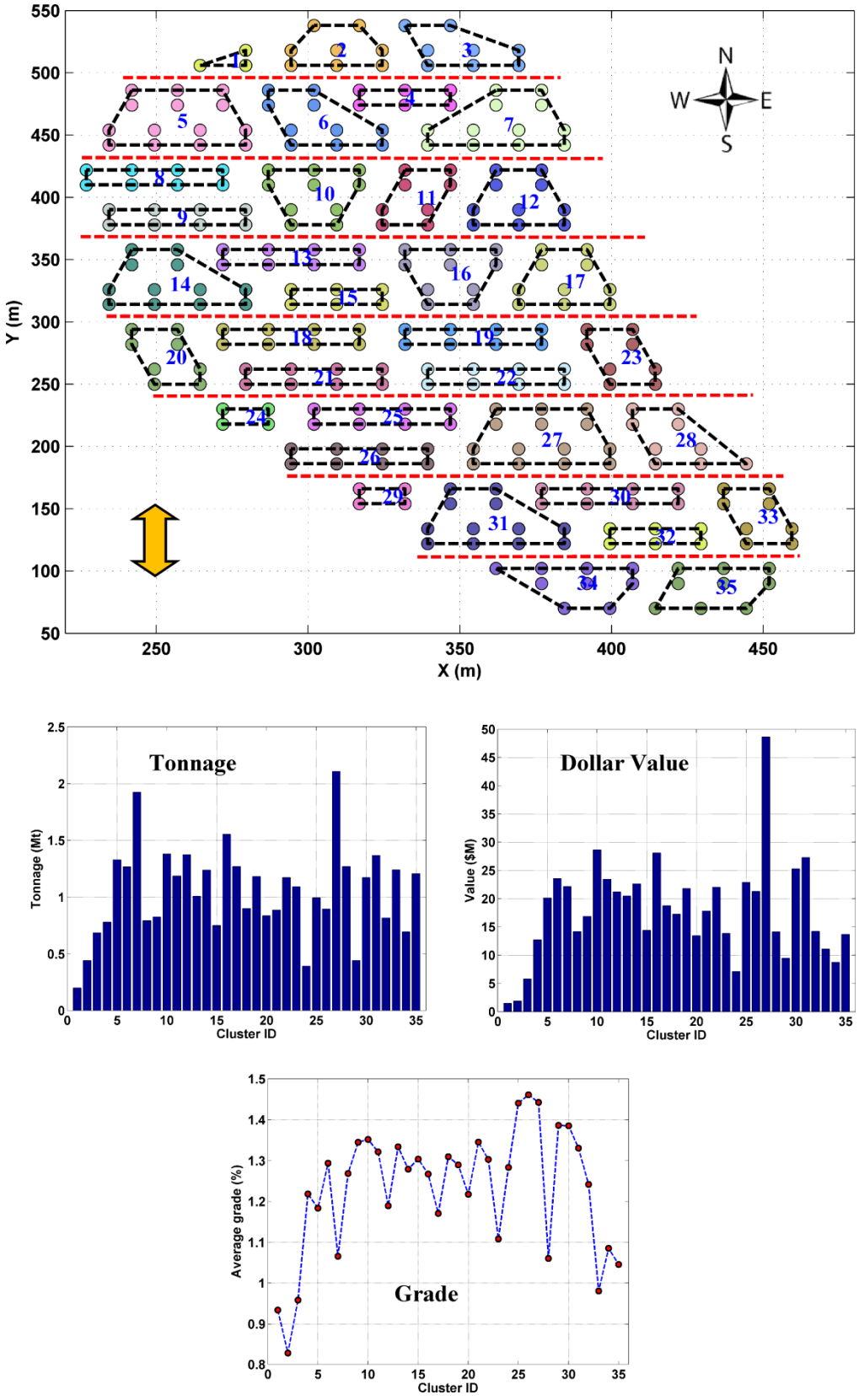

Figure 5.36. Clusters and their information in the NS and SN directions

Table 5.9. Production scheduling parameters at cluster level

Parameter	Value
Total tonnage of material (Mt)	37
Number of periods	15
Discount rate (%)	12
Maximum mining capacity (Mt/yr)	2.5
Maximum number of active clusters	15
Maximum number of new clusters	5
Draw rate (lower / upper) (kt/yr/per drawpoint)	10 / 50

Table 5.10. Number of variables and constraints for cluster level with 35 clusters

Direction	Number of clusters	Number of constraints	Decision variables		
			Total	Continuous	Binary
WE	35	2,935	1,575	525	1,050
EW	35	2,965	1,575	525	1,050
NS	35	2,950	1,575	525	1,050
SN	35	3,070	1,575	525	1,050

Table 5.11. Numerical result for cluster level formulation with 35 clusters

Direction	CPU time 8 CPUs @ 2.7 GHz	EPGAP (%)	Optimality GAP (%)	NPV ($M)	Difference from Max. (%)
WE	00:00:05	1	0.74	313.56	0
EW	18:47:07	1	1.00	306.56	2.2
NS	00:36:28	1	0.94	300.01	4.3
SN	00:00:13	1	0.68	312.54	0.3

As a result, only the WE and SN directions had the potential to be considered as mining directions based on the obtained NPVs. Therefore, the results of these two directions were compared.

Figure 5.37 to Figure 5.41 show that all assumed constraints were satisfied for the cluster level formulation. Figure 5.37 shows the tonnage of production in each period for different directions. It is obvious that the formulation tried to keep mining capacity at the upper bound.

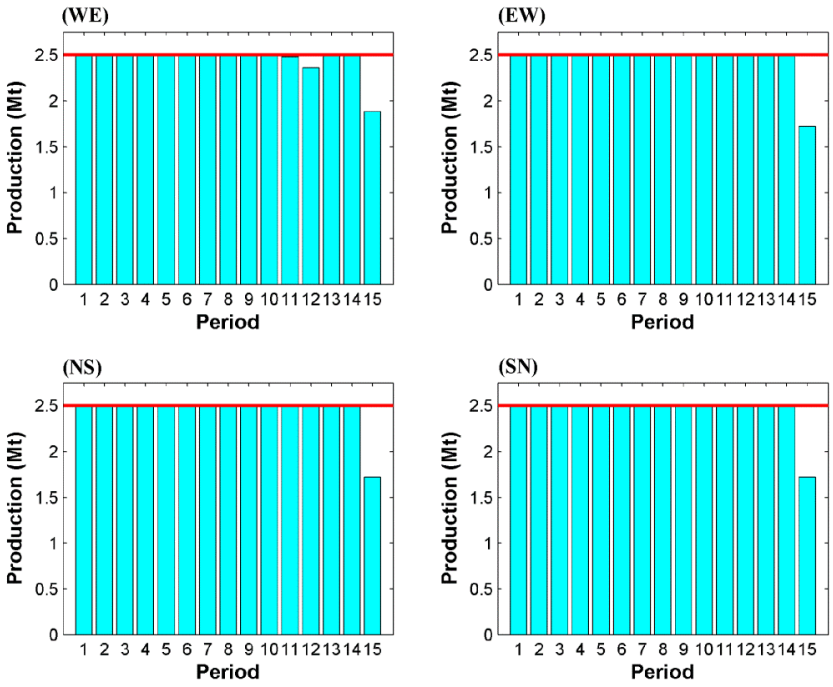

Figure 5.37. Production tonnage for different directions at the cluster level over the mine life

Figure 5.38 illustrates the maximum number of active clusters in each period for the different advancement directions. In the west to east direction, the numbers of active clusters never reached the maximum allowable number, while in the south to north direction 15 clusters were active in period four. On the other hand, between periods two and nine, the number of active drawpoints in the south to north direction was more than in the west to east direction. After period nine, there were more active clusters in the west to east direction than in the south to north direction.

Figure 5.39 shows the number of new clusters which had to be opened in each period for different advancement directions. The blue line represents the upper bound for this constraint. The number of new clusters opened in period one was equal to the maximum allowable number of active clusters in this period to reach the required production. From period two to the end of the mine life, the maximum number of new clusters which could be opened in each period was equal to five.

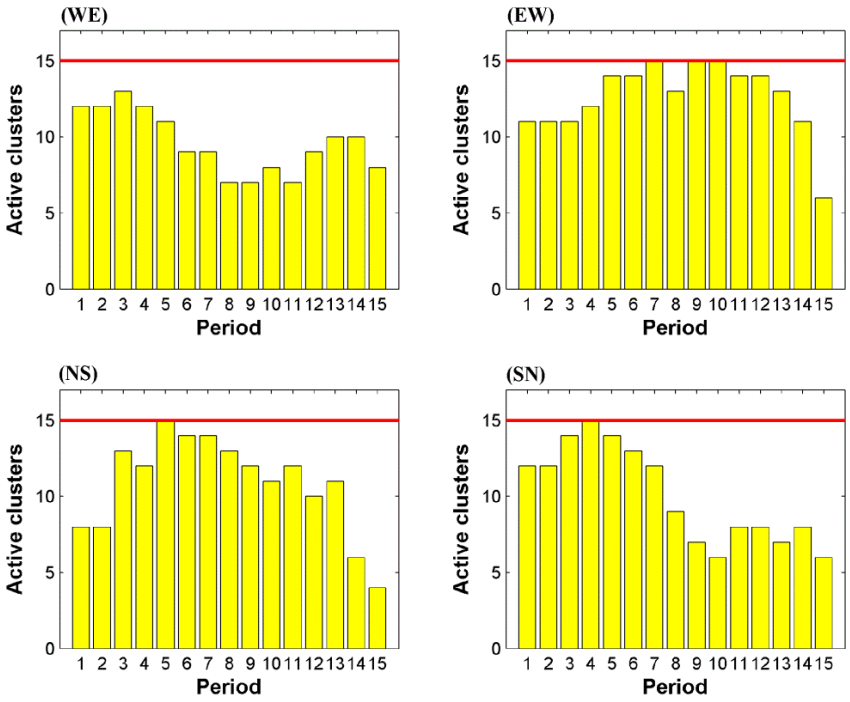

Figure 5.38. Number of active clusters for different directions at the cluster level over the mine life

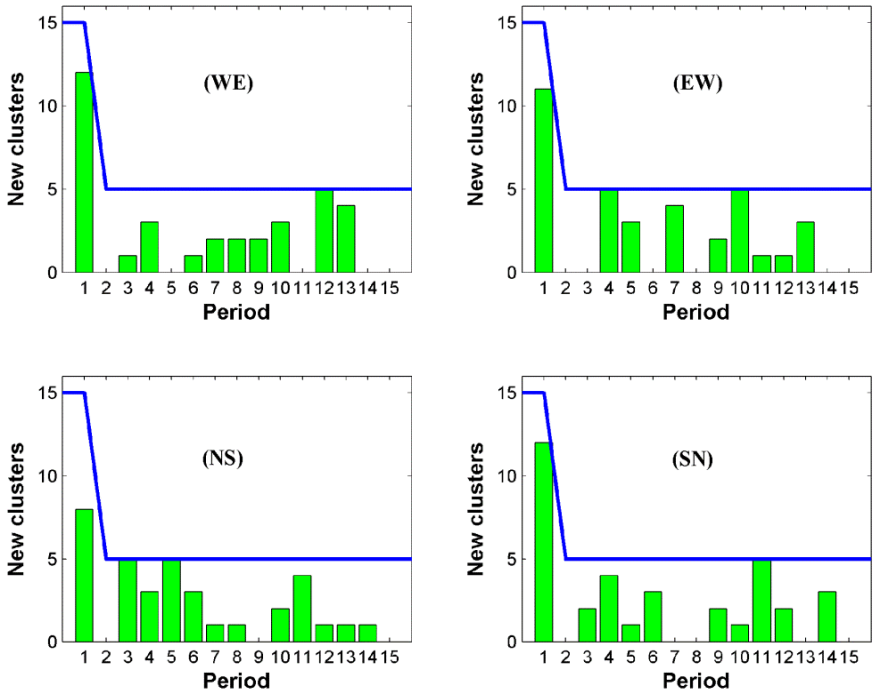

Figure 5.39. Number of new clusters that must be opened for different directions at the cluster level over the mine life

In the west to east direction, all the clusters were opened by period 13. However, in the south to north direction, this happened by period 14. In the west to east direction, from period six to period 10, at least one new cluster had to be opened, while in south to north direction there was no need to open a new cluster in periods seven and eight.

Figure 5.40 and Figure 5.41 show the amount of tonnage which could be extracted from different clusters in the WE/EW and NS/SN directions. The lower and upper bounds of the draw rate for each cluster were equal to the number of the draw columns within the cluster times, the minimum or maximum draw rate, respectively. Figure 5.40 shows the draw rate of clusters 10 and 22 in the west to east direction and clusters 20 and 35 in east to west direction. Cluster 10 contained eight drawpoints and was mined in four periods, from period one to period four, in the west to east direction. Extraction from cluster 10 was started with 240kt/period in period one and gradually increased to 400kt/period in period three, continuing with 200kt/period in period four.

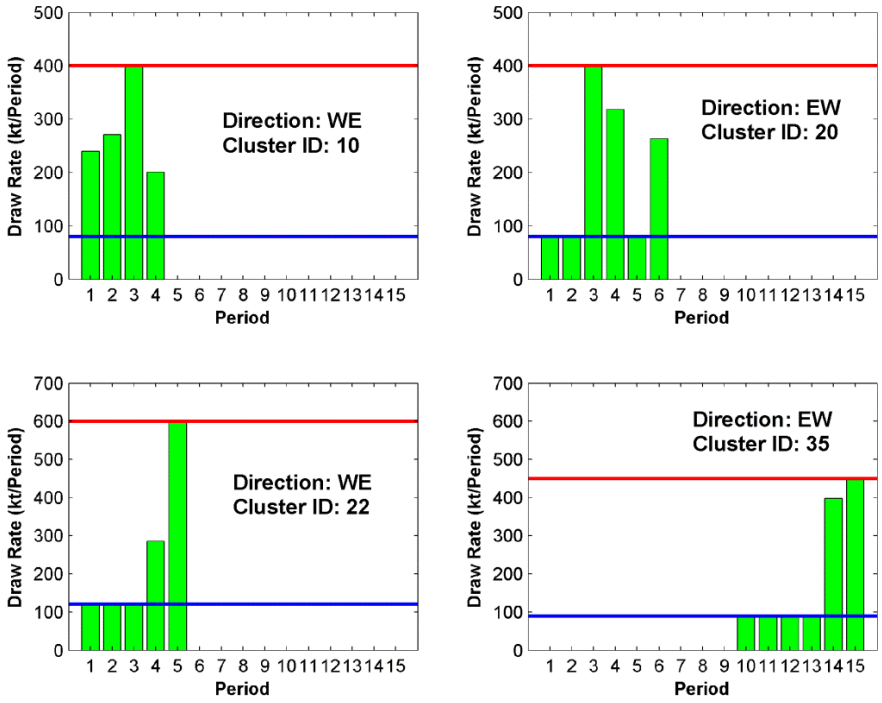

Figure 5.40. Amount of depletion from clusters 10, 20, 22, and 35 in the WE and EW directions

Cluster 22, with 12 drawpoints, was extracted during the first five periods. Extraction from this cluster was started with a draw rate of 120kt/period and continued up to period three. After period three, the draw rate increased in period four, reaching 600kt/period in period five. Cluster 35, with nine drawpoints, was extracted in six periods from period 10 to period 15. Cluster 20, with eight drawpoints, was extracted during the first six periods. After two years of extraction with a draw rate of 80kt/period, extraction from this cluster continued with a draw rate 400kt/period in period three. The draw rate decreased and reached 80kt/period in period five.

Figure 5.41 shows the draw rate of clusters 20 and 28 in the north to south direction, and clusters 16 and 33 in the south to north direction. In the south to north direction, extraction from clusters 16 and 33 started with the minimum allowable draw rate and gradually increased to reach the maximum allowable draw rate of each cluster.

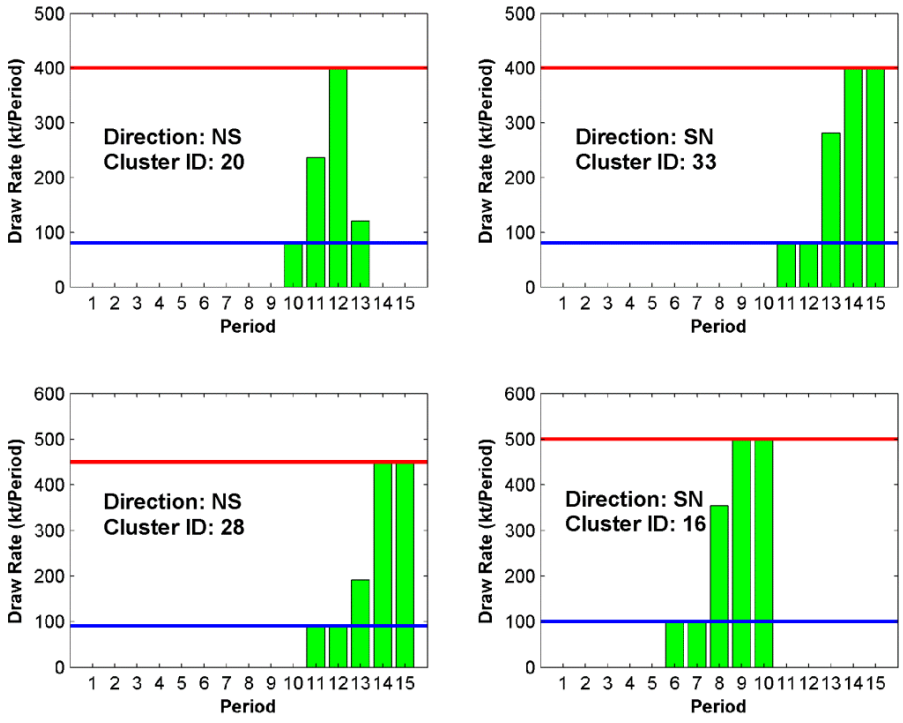

Figure 5.41. Amount of depletion from clusters 16, 20, 28, and 33 in NS and SN directions

Figure 5.42 illustrates the cumulative discounted cash flow and discounted cash flow for different directions. Figure 5.43 and Figure 5.44 illustrate the opening pattern at the cluster level for the west to east and south to north directions, respectively. In both directions, it is obvious that most of the drawpoints located around the right side and top boundaries were opened after period 10.

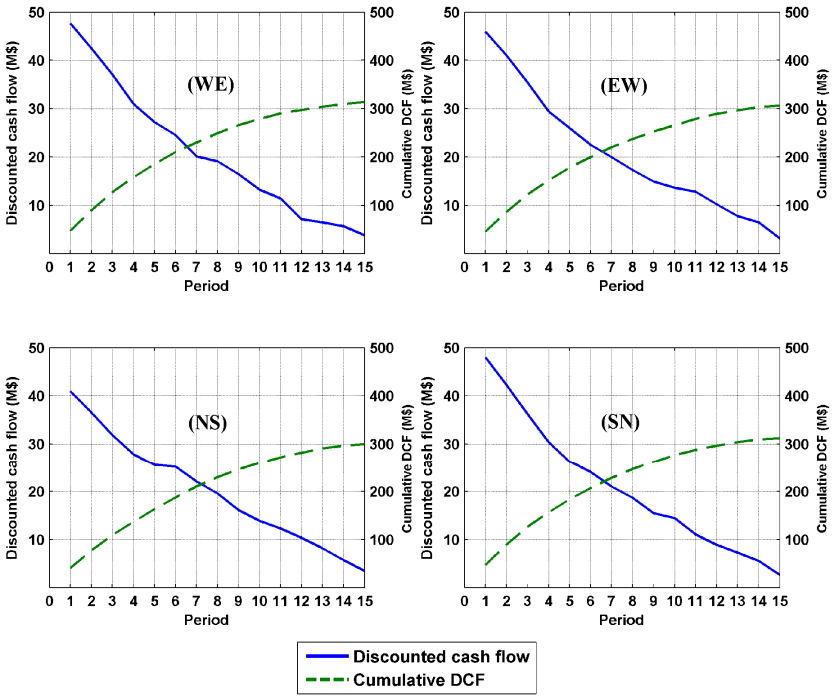

Figure 5.42. Discounted cash flow and cumulative DCF for different directions at the cluster level over the mine life

To solve the problem at the drawpoint level, both the west to east (WE) and south to north (SN) directions were selected because of the close NPV. In other words, percentage difference between the NPVs of these two directions is less than the assumed EPGAP. To solve the problem at the drawpoint level in the west to east (WE) and south to north (SN) directions, the solution from the previous stage was used, based on the early start and late finish, to eliminate the variables. As mentioned before, theoretically, this variable reduction technique decreased the solution space for the optimization problem. Thus during optimization, some of the branches in the branch-and-cut tree were eliminated, ensuring that the solution for the practical production scheduling problem was reached faster.

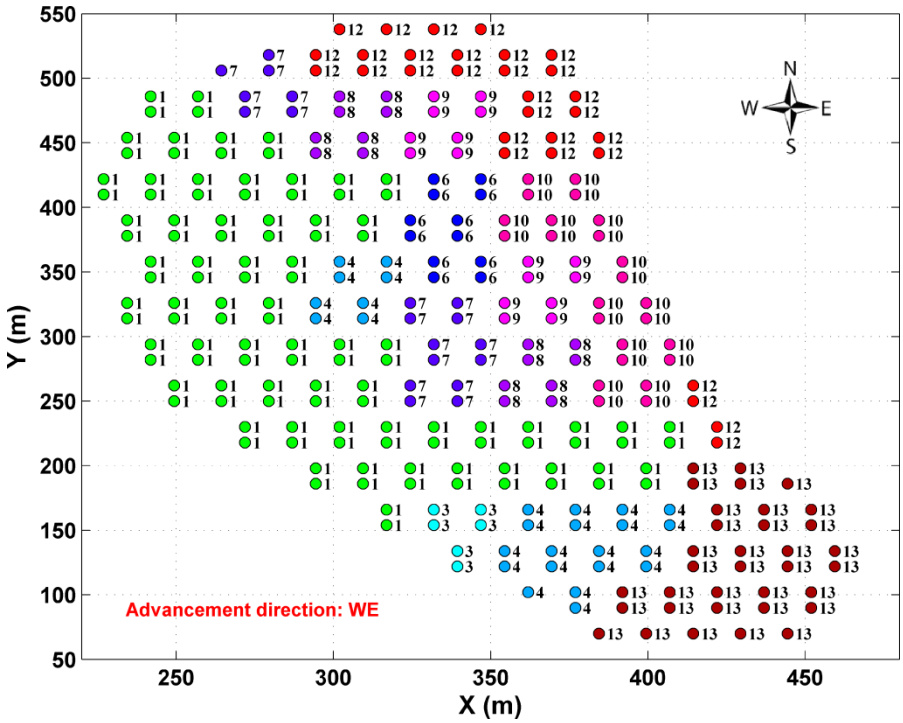

Figure 5.43. Opening pattern using the cluster level formulation in the WE direction for 298 drawpoints

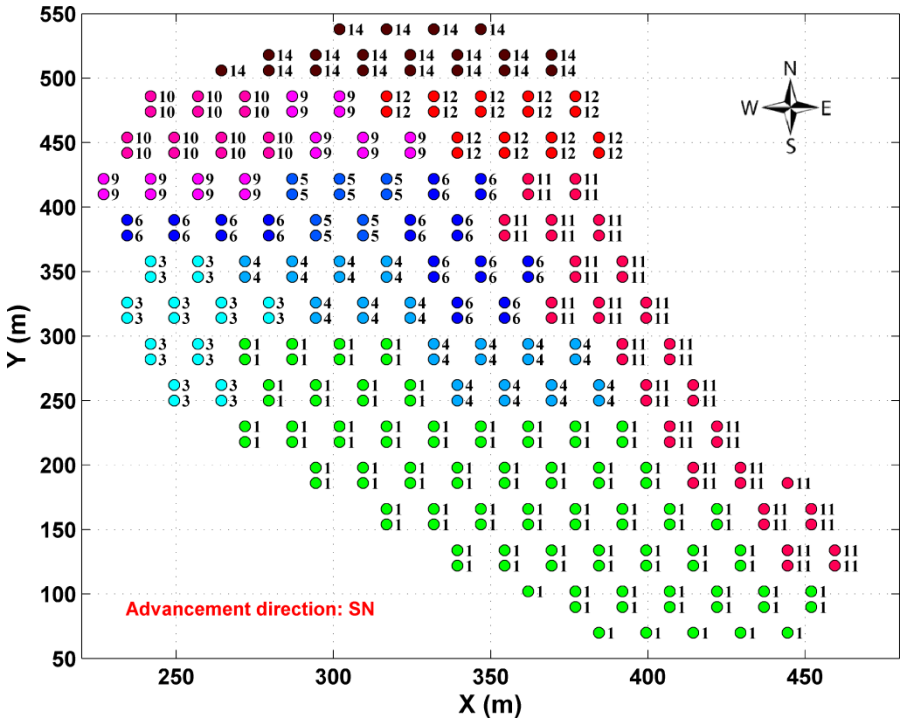

Figure 5.44. Opening pattern using the cluster level formulation in the SN direction for 298 drawpoints

Table 5.12 shows the number of decision variables and the number of constraints for the WE and SN directions at the drawpoint level. There are 8,940 binary decision variables in both directions.

Table 5.12. Number of variables and constraints at the drawpoint level with 298 drawpoints

Direction	Number of drawpoints	Number of constraints	Decision variables		
			Total	Continuous	Binary
WE	298	79,046	13,410	4,470	8,940
SN	298	89,336	13,410	4,470	8,940

The number of decision variables was reduced using the obtained starting periods from the cluster level solution. Two years flexibility was assumed for the earliest start time at the drawpoint level. For this purpose, if at the cluster level, the extraction of a drawpoint was started in period t with the cluster life of n, at the drawpoint level any variables that would mine this drawpoint before period $t-2$ and after $(t+n)+2$ were eliminated. This was done by changing the related decision variables in the decision variables vector to zero.

In the west to east direction, the total number of variables, 13410, was reduced to 8860, of which the 1093 were from continuous variables and the 3457 were from binary variables. In the north to south direction, the total number of variables, 13410, was reduced to 8969, of which the 1065 were from continuous variables and the 3376 were from binary variables. The problem was solved for two different EPGAPs of 4% and 1%.

Table 5.13 shows a summary of the results for these directions at the drawpoint level. The problem was solved in 15 and 31 minutes for the WE and SN directions for an EPGAP of 4%, respectively. The obtained NPVs for these directions were almost \$312M. To solve the problem with an EPGAP of 1%, more CPU time was spent in comparison to the EPGAP of 4%. As a result, the NPV was improved almost 1.7% in both directions. The reason for the higher NPV for this level was the resolution of the level. In other words, when the problem was solved at the drawpoint level, the economic value of each draw column was taken into account.

Therefore, the model tried to mine the draw columns with higher economic values earlier than other draw columns.

Table 5.13. Numerical result for drawpoint level formulation with 298 drawpoints

Direction	CPU time 8 CPUs @ 2.7 GHz	EPGAP (%)	Optimality GAP (%)	NPV ($M)	Improvement (%)
WE	00:15:40	4	2.92	312.38	--------
SN	00:31:45		3.23	311.52	--------
WE	06:58:47	1	1	317.60	1.65
SN	210:22:29		1	317.09	1.77

Figure 5.45 to Figure 5.48 show that all assumed constraints were satisfied for this level of resolution. Figure 5.45 illustrates the tonnage of production in each period for directions WE and SN. The formulation wanted to maximize the NPV so it tried to keep the mining capacity at the upper bound. This resulted in the same yearly production for both directions.

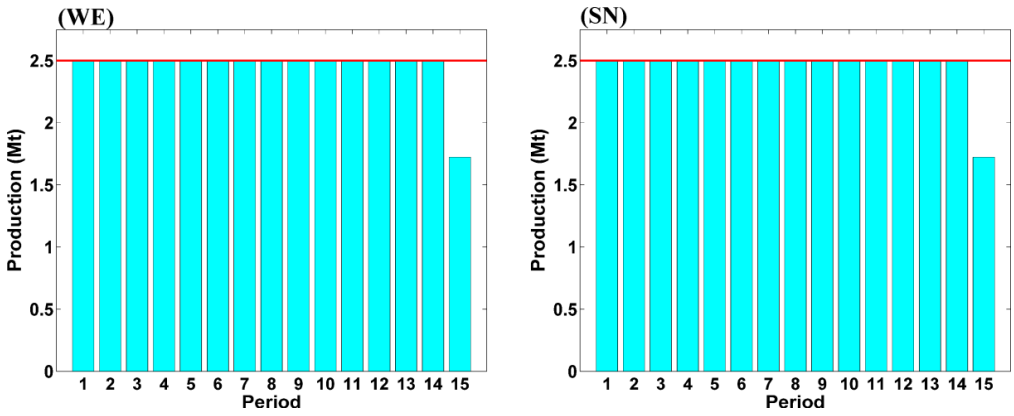

Figure 5.45. Production tonnage for WE and SN directions at the drawpoint level over the mine life

Figure 5.46 shows the number of active drawpoints for WE and SN directions. During the early years, the number of active drawpoints in the west to east direction was less than that in the north to south direction. Although in both directions the maximum allowable tonnage was produced in each period, the number of active drawpoints did not reach the defined maximum allowable number. In both directions after period 11, the number of active drawpoints

gradually decreased. In both directions, period 15 had the minimum number of active drawpoints, but this number for the SN direction was more than the number for the WE direction.

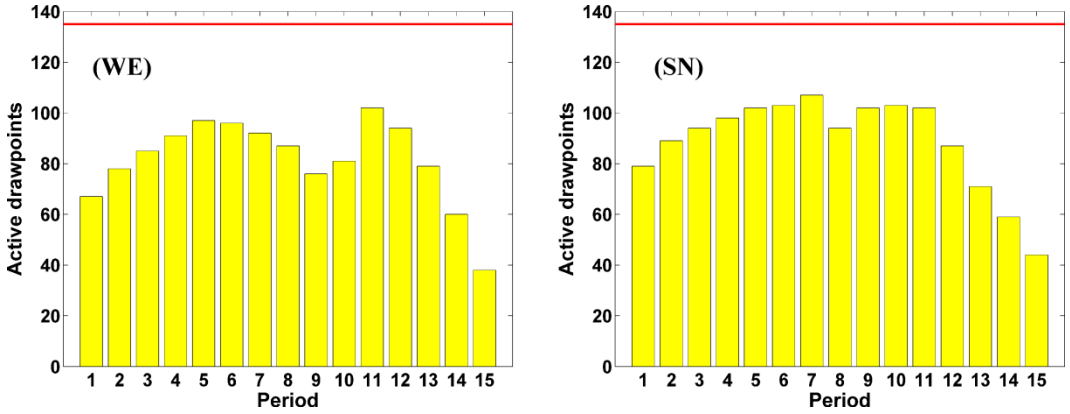

Figure 5.46. Number of active drawpoints in WE and SN directions at the drawpoint level over the mine life

Figure 5.47 illustrates the number of new drawpoints that were opened in each period. The extraction started with more drawpoints in the south to north direction compared to the west to east direction. In the west to east direction, 296 drawpoints were opened by period 12. After this period the extraction continued, using the available active drawpoints. In all periods of the south to north direction, there was at least one drawpoint that had to be opened, but in none of the periods did the number of new drawpoints reach the maximum allowable number.

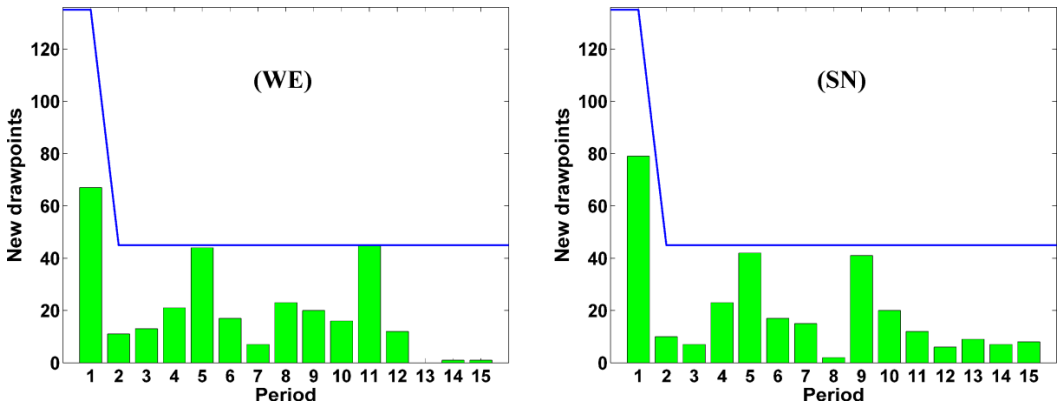

Figure 5.47. Number of new drawpoints that must be opened in the WE and SN directions at the drawpoint level over the mine life

Figure 5.48 illustrates the draw rate of drawpoint 123 in WE and SN directions. This drawpoint is located almost in the middle of the mine. The drawpoint life in the SN direction is one period less than that in the WE direction, but it behaves in a manner similar to that of the draw rate point of view in both directions. The extraction started with the draw rate of 10kt/period, which is the minimum acceptable draw rate for an active drawpoint. In the west to east direction, the extraction from this drawpoint continued with a draw rate of 10kt/period during the next two periods. The draw rate then increased to reach 50kt/period, which was the maximum allowable draw rate. In the south to north direction, after the first period, the draw rate increased and reached 50kt/period in the third period of the extraction.

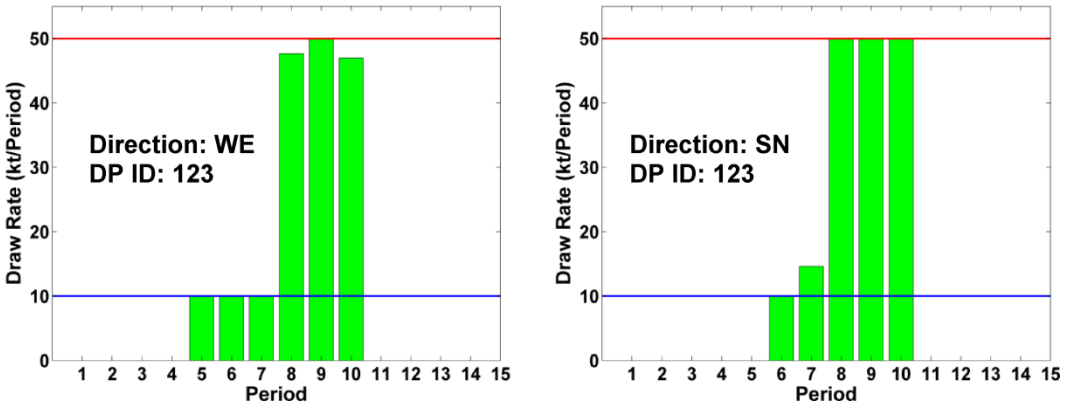

Figure 5.48. Amount of depletion from drawpoint 123 in the WE and SN directions

Figure 5.49 and Figure 5.50 illustrate the opening patterns in WE and SN directions, respectively. In both directions, it is obvious that most of the drawpoints, which are located around the right side and top boundaries, were opened after period nine.

According to the obtained NPVs and satisfied constraints, both WE and SN directions can be considered as the mining directions. But, to solve the problem at the drawpoint-and-slice level formulation, the WE direction was considered. An EPGAP of 5% was set for optimization. Unlike the cluster level and drawpoint level formulations, the grade of production was considered at the drawpoint-and-slice level formulation.

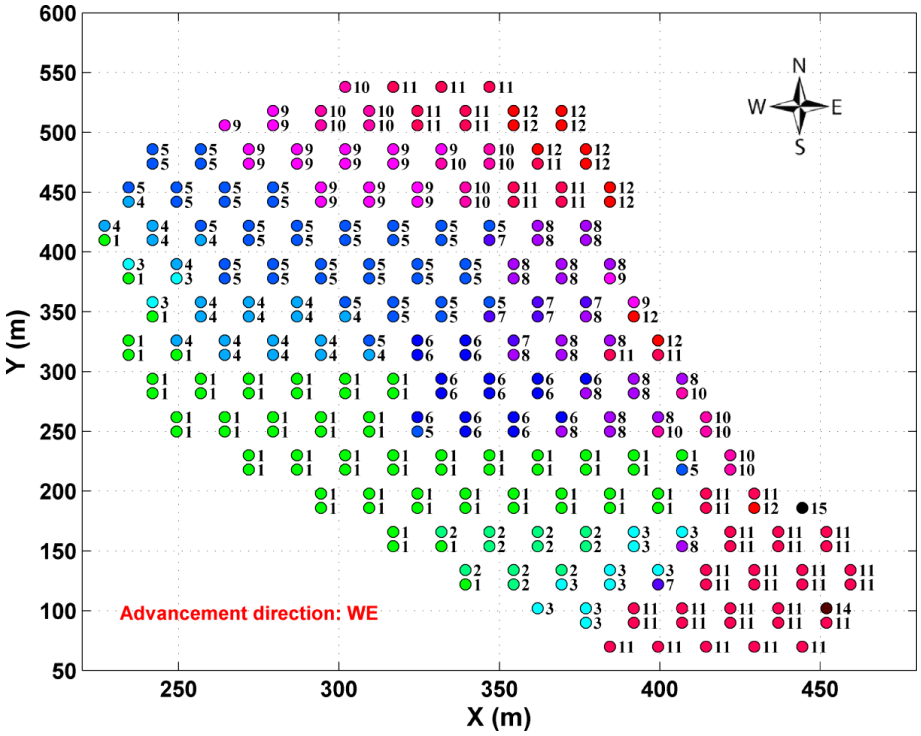

Figure 5.49. Opening pattern using the drawpoint level formulation in the WE direction for 298 drawpoints (multi-step method)

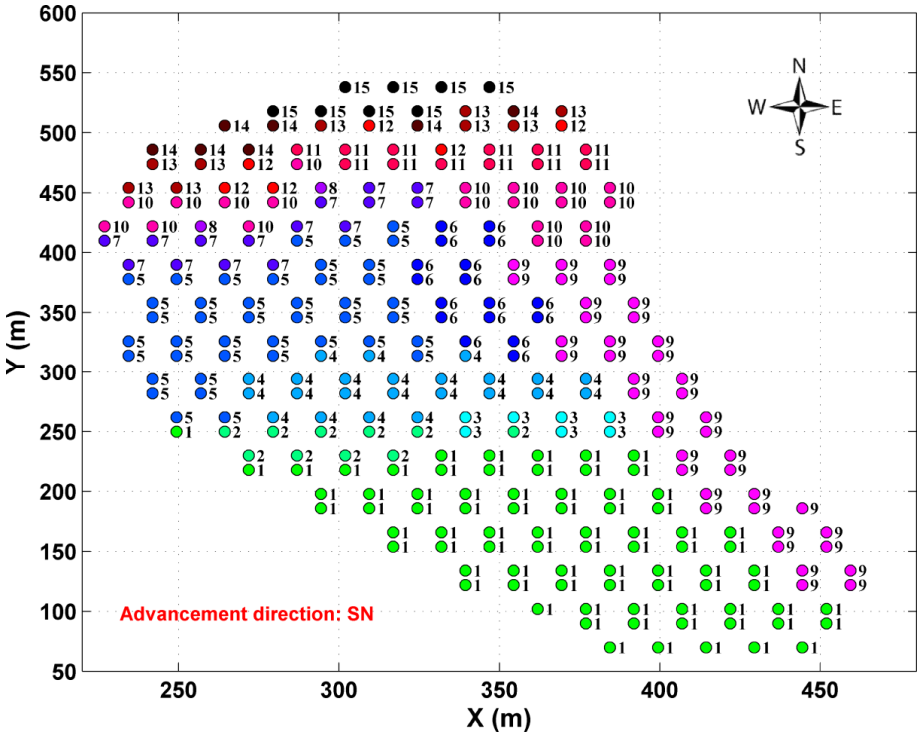

Figure 5.50. Opening pattern using the drawpoint level formulation in the SN direction for 298 drawpoints (multi-step method)

The lower and upper bounds of the average grade were set to 0.7% and 1.6%. For this level also, the solution from the drawpoint level was used based on the early start and late finish to eliminate the variables. Table 5.14 shows the number of decision variables and the number of the constraints for the WE direction at the drawpoint-and-slice level formulation.

Table 5.14. Number of variables and constraints at the drawpoint-and-slice level formulation with 298 drawpoints and 5,539 slices

Direction	Number of DP/SL	Number of constraints	Decision variables		
			Total	Continuous	Binary
WE	298/5,539	336,079	175,110	83,085	92,025

The solution from the drawpoint level was used based on the early start and late finish to eliminate the variables at the drawpoint-and-slice level formulation. Consequently, the total number of variables of 175,110 was reduced to 125,708, of which 23,675 were continuous variables and 25,727 were binary.

It is obvious that even after eliminating 28% of the binary decision variables, there are still a large number of decision variables in the model. Table 5.15 shows a summary of the results for these directions at the drawpoint-and-slice level. The resulting NPV of the drawpoint-and-slice level was $324.42M, with an optimality gap of 4.9%. The obtained NPV for the west to east direction at the drawpoint-and-slice level was 3.4% and 2.1% more than at the cluster level and drawpoint level, respectively.

Table 5.15. Numerical result for the drawpoint-and-slice level formulation with 298 drawpoints and 5,539 slices

Direction	CPU time 8 CPUs @ 2.7 GHz	EPGAP (%)	Optimality GAP (%)	NPV ($M)
WE	16:34:23	5	4.9	324.42

The reason for the higher NPV at the drawpoint-and-slice level is the resolution of the level. In other words, when the problem is solved at the drawpoint-and-slice level, the method deals with the slices. The economic value of each slice is taken into account. Therefore, the model tries to mine slices with higher economic values and grades, earlier than other slices. But, at the drawpoint level, all the

slices within a draw column are grouped, and the summation of the economic value of slices is considered as the draw column economic value, which is a constant value for each draw column. At the cluster level, the summation of the economic value of the draw columns which are within the cluster is considered to be the cluster economic value and is a constant value for each draw column.

Figure 5.51 shows that all defined constraints were satisfied. The number of active drawpoints increased gradually until period five. Afterwards, during the next six periods, the mine will work with maximum allowable active drawpoints. From periods 12 to 15, this number gradually decreases. Figure 5.51c shows that until period 12 at least five new drawpoints were opened in each period. Figure 5.51d shows the average grade of production in each period. It can be seen that the model tried to mine the slices with a higher grade earlier so that the average grade of production had a descending trend. During the last periods, because of more dilution, the average grade of production was less than that of previous years. During the first ten periods, the average grade of production was greater than 1.2%. Only in two periods 12 and 15 was the average grade of production less than 1%.

Figure 5.52 shows how to extract the material from the draw column associated with drawpoint 56. Figure 5.52a shows the extraction periods and depletion tonnages from this drawpoint during its life. Figure 5.52b shows the percentage extracted from each slice located within the draw column associated with drawpoint 56. In Figure 5.52b, the vertical axis represents the ID number of slices located within the considered draw column. The numbers in front of each slice indicate the percentage extracted from that slice in the related period. It is obvious that there is a continuous extraction order between slices, and the defined precedence between slices of a draw column is observed. For instance, 21% of slice 849 was extracted in period nine, so extraction from slice 850 would not start until the rest of the material was extracted from slice 849 in period 10.

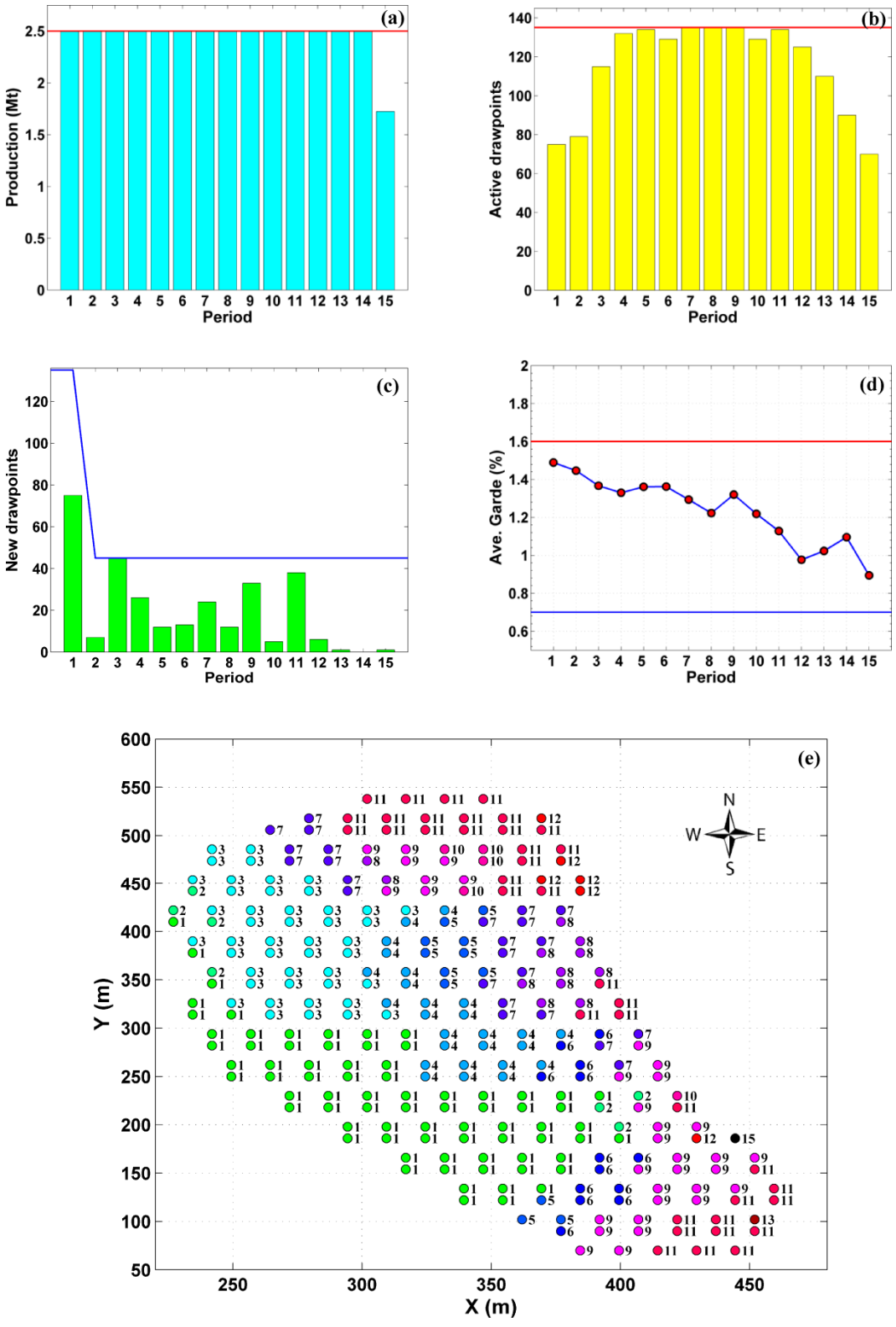

Figure 5.51. Satisfied constraints and opening pattern of drawpoints based on the drawpoint-and-slice level solution for the west to east direction

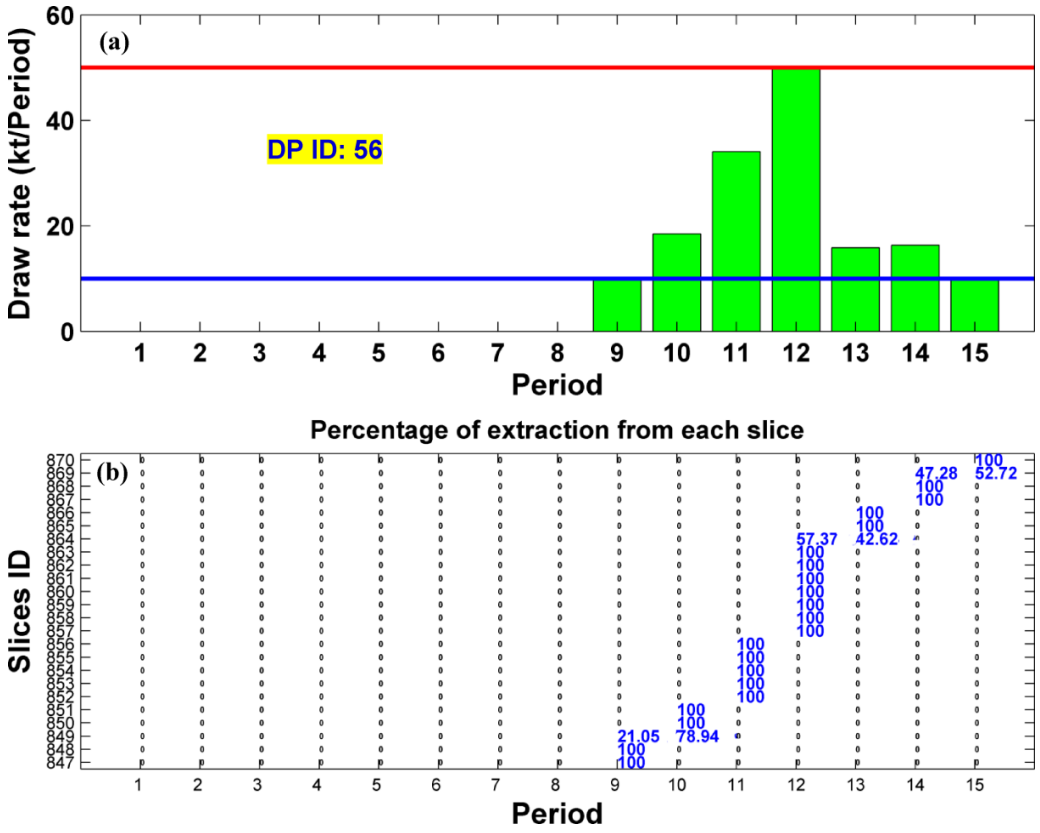

Figure 5.52. How to extract from drawpoint 56: (a) draw rate, and (b) percentage extraction from each slice within draw column associated with drawpoint 56

The discounted cash flow (DCF) over the mine life and the cumulative discounted cash flow for the three levels of resolution are shown in Figure 5.53. It is obvious that the DCF during the first two years of the mine life for the drawpoint-and-slice level formulation was greater than the other levels, but it fluctuated between periods two and 15. The resulting NPV for the drawpoint-and-slice level was greater than that for other levels in the west to east direction. At the drawpoint-and-slice level, the model extracted slices with a higher economic value earlier than other slices. But at the drawpoint level, the method dealt with a draw column whose economic value was a weighted average of slices within the related draw column. The economic values of draw columns were used to calculate the cluster economic value. In addition, the defined flexibility for the starting period helped the model to mine earlier the drawpoints or slices with higher economic values.

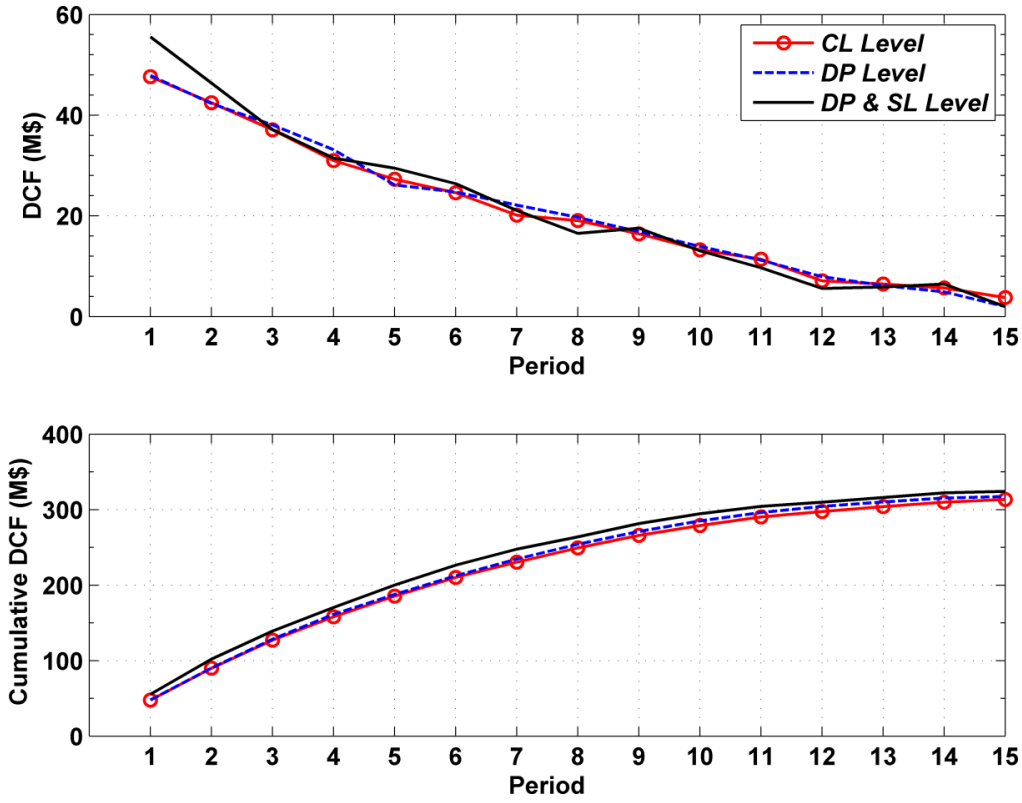

Figure 5.53. Comparison of the discounted cash flow for three levels of resolution in the west to east direction using the multi-step method

5.4.1 Summary of the Multi-Step Method

The multi-step method was applied on a dataset containing 298 drawpoints and 5,539 slices over 15 periods. Table 5.16 shows a summary of the results for the multi-step method. After defining the advancement lines and phases, the draw columns within each phase were clustered. Then, the problem was solved in four directions at a cluster level with an EPGAP of 1%. Based on the results, directions west to east and south to north with an NPV of $313.56M and $312.54M, respectively, were selected as directions in which to solve the problem at the drawpoint level. Then, the solution from the previous stage was used based on the early start and late finish to eliminate the variables. Consequently, the number of decision variables was reduced by 34% in the both directions. Then the problem was solved in the both directions with two EPGAPs of 4% and 1%. Based on the results, the NPV of both directions was $317M. For the last step, the west to east direction was selected.

Table 5.16. Results of the three levels of resolution for the multi-step method

Level of resolution	Dir.	Number of CL/DP/SL	Number of constraints &variables	Opt. GAP (%)	CPU time 8 CPUs @ 2.7 GHz	NPV ($M)	Diff. from the best (%)
Cluster level	WE	35 / 0 / 0	2,935 1,575	0.74	00:00:05	313.56	-3.35
	EW	35 / 0 / 0	2,965 1,575	1.00	18:47:07	306.56	-5.51
	NS	35 / 0 / 0	2,950 1,575	0.94	00:36:28	300.01	-7.52
	SN	35 / 0 / 0	3,070 1,575	0.68	00:00:13	312.54	-3.66
Drawpoint level	WE	0 / 298 / 0	79,046 13,410	2.92	00:15:40	312.38	-3.71
	SN	0 / 298 / 0	89,336 13,410	3.23	00:31:45	311.52	-3.98
	WE	0 / 298 / 0	79,046 13,410	1	06:58:47	317.60	-2.1
	SN	0 / 298 / 0	89,336 13,410	1	210:22:29	317.09	-2.26
Drawpoint-and-slice level	WE	0 / 298 / 5,539	336,079 175,110	4.9	16:34:23	324.42	The Best

After eliminating 28% of the decision variables based on the solution of the drawpoint level, the problem was solved at the drawpoint-and-slice level with an EPGAP of 5%. The NPV was $324.4M. In the west to east direction, the NPV of drawpoint-and-slice level was 2.1% and 3.4% more than drawpoint level and drawpoint-and-slice level, respectively.

At all levels, all the defined constraints were satisfied and the models worked properly. It is obvious that the small EPGAPs increase the CPU time. From the cluster level to drawpoint-and-slice level, increasing the number of constraints and decision variables increases the solution time.

5.4.2 Sensitivity Analysis

Impact of changes in constraints on the NPV and CPU time was investigated for each level of resolution. For this purpose three constraints were only considered, because some of the constraints such as mining capacity, continuous mining, and

precedence between clusters or drawpoints are not changeable. Considered constraints included draw rate, the maximum number of active clusters/drawpoints in each period and the maximum number of new clusters/drawpoints that need to be constructed in each period. The sensitivity analysis was done for the dataset containing 102 drawpoints using one-at-a-time approach. In this method a sensitivity ranking is obtained by increasing each parameter while leaving all others constant, quantifying the change in model output. Table 5.17 shows the main production scheduling parameters. Table 5.18, Table 5.19, and Table 5.20 show production scheduling parameters for different scenarios according to changes in draw rate, the maximum number of active clusters or drawpoints, and the maximum number of new clusters or drawpoints, respectively. According to the Table 5.18, Table 5.19, and Table 5.20, the problem solved for 31 different conditions. Figure 5.54 to Figure 5.62, show the results. In these figures the blue bars, red lines, and black lines represent NPV, amount of CPU time and percentage difference from the optimal solution based on results' EPGAP, respectively.

Table 5.17. Production scheduling parameters for main scenario

Common parameters	Value
Number of periods	15
Discount rate (%)	12
Maximum mining capacity (kt/yr)	900
Cluster level	
Maximum number of active clusters	5
Maximum number of new clusters	2
Draw rate (lower / upper) (kt/yr/per drawpoint) × NDP_{cl}	(10 / 40) × NDP_{cl}
Drawpoint and drawpoint-and-slice levels	
Maximum number of active drawpoints	40
Maximum number of new drawpoints	15
Draw rate (lower / upper) (kt/yr/per drawpoint)	10 / 40

Table 5.18. Different scenarios according to changes in draw rate

	Scenarios			
Cluster level	1	2	3	4
Maximum number of active clusters	5	5	5	5
Maximum number of new clusters	2	2	2	2
Draw rate (lower / upper) (kt/yr/per drawpoint) × NDP_{cl}	**10/40**	**10/50**	**10/55**	**10/60**
Drawpoint and drawpoint-and-slice levels				
Maximum number of active drawpoints	40	40	40	40
Maximum number of new drawpoints	15	15	15	15
Draw rate (lower / upper) (kt/yr/per drawpoint)	**10/40**	**10/50**	**10/55**	**10/60**

Table 5.19. Different scenarios according to changes in the maximum number of active clusters or drawpoints

	Scenarios			
Cluster level	1	2	3	4
Maximum number of active clusters	**5**	**6**	**7**	**8**
Maximum number of new clusters	2	2	2	2
Draw rate (lower / upper) (kt/yr/per drawpoint) × NDP_{cl}	10/40	10/40	10/40	10/40
Drawpoint and drawpoint-and-slice levels				
Maximum number of active drawpoints	**40**	**50**	**60**	----
Maximum number of new drawpoints	15	15	15	----
Draw rate (lower / upper) (kt/yr/per drawpoint)	10/40	10/40	10/40	----

Figure 5.54 to Figure 5.56 show impact of changes in draw rate on the NPV and CPU time at three levels of resolution. At all levels of resolutions the NPV increased with increasing the upper bound of the draw rate. Unlike cluster and drawpoint-and-slice levels, at drawpoint level, the amount of CPU time increased with increasing the upper bound of the draw rate. At cluster and drawpoint-and-slice levels, percent changes of CPU time from maximum draw rate of 40 (kt/yr/per drawpoint) to 50 (kt/yr/per drawpoint) were 74% and 82%, respectively.

Table 5.20. Different scenarios according to changes in the maximum number of new clusters or drawpoints

	Scenarios		
Cluster level	1	2	3
Maximum number of active clusters	5	5	5
Maximum number of new clusters	**2**	**3**	**4**
Draw rate (lower / upper) (kt/yr/per drawpoint) × NDP_{cl}	10/40	10/40	10/40
Drawpoint and drawpoint-and-slice levels			
Maximum number of active drawpoints	40	40	40
Maximum number of new drawpoints	**15**	**20**	**30**
Draw rate (lower / upper) (kt/yr/per drawpoint)	10/40	10/40	10/40

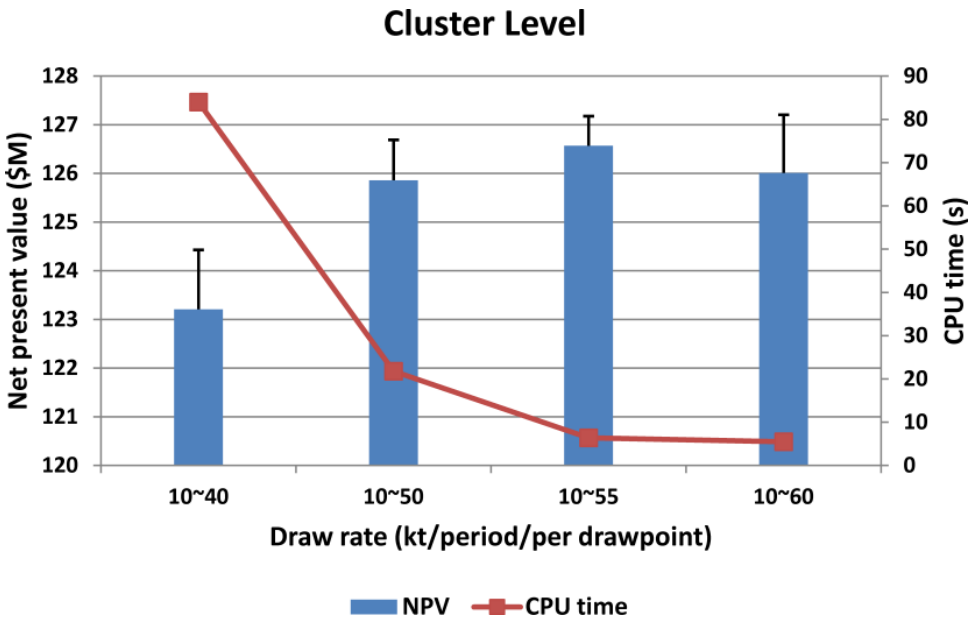

Figure 5.54. Impact of changes in the draw rate on the NPV and CPU time at the cluster level

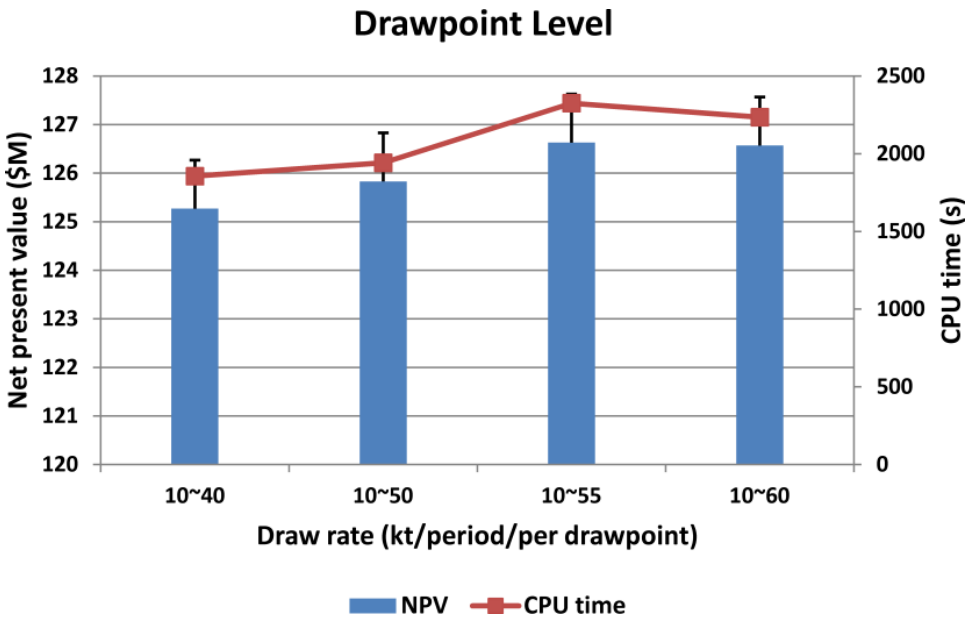

Figure 5.55. Impact of changes in the draw rate on the NPV and CPU time at the drawpoint level

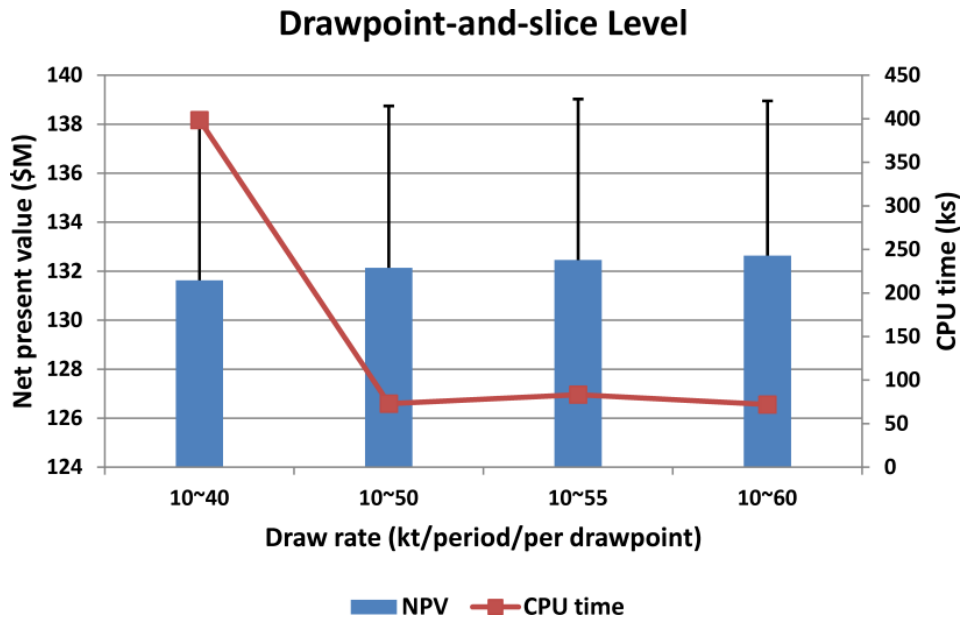

Figure 5.56. Impact of changes in the draw rate on the NPV and CPU time at the drawpoint-and-slice level

Figure 5.57 to Figure 5.59 show impact of changes in the maximum number of active clusters and drawpoints on the NPV and CPU time at three levels of resolution. At all levels of resolution, with increasing the upper bound, the NPV increased, while amount of CPU time decreased. At the cluster level, with changing the number of active clusters from five to six, amount of CPU time decreased 98%. Despite the increase in the NPV from six to eight active clusters, there was no significant change in the amount of CPU time. Figure 5.60 to Figure 5.62 show impact of changes in the maximum number of new clusters and drawpoints on the NPV and CPU time at three levels of resolution. At all levels of resolution the NPV increased with increasing the upper bound. At cluster level amount of CPU time decreased from two to three new clusters, but it increased from three to four new clusters. Amount of CPU time had a same situation at drawpoint-and-slice level with higher percent changes.

It must be mentioned that the constraints of each level of resolution have a complicated interaction, therefore changing of the parameters, changes the structure of the problem.

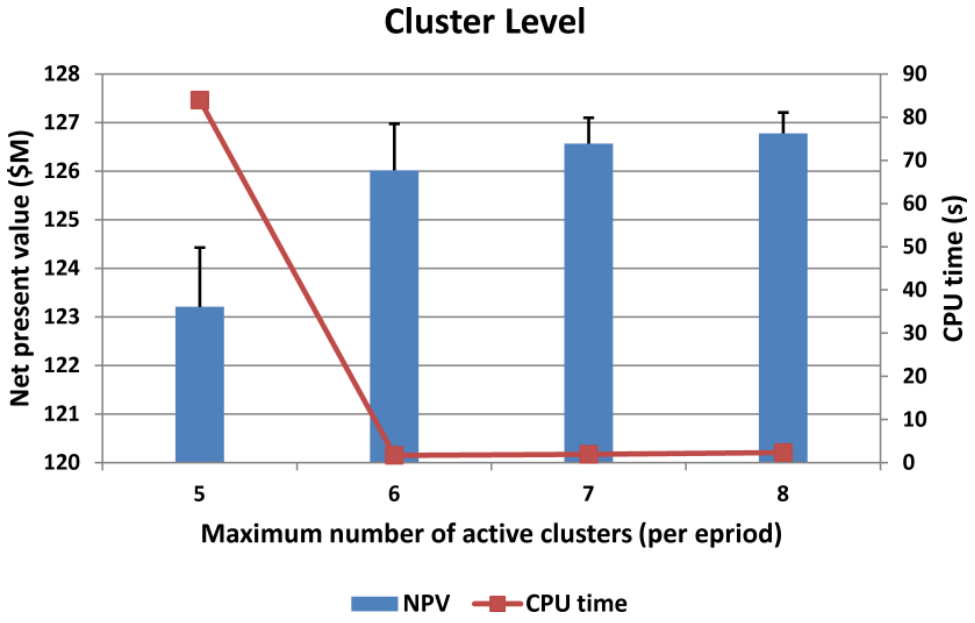

Figure 5.57. Impact of changes in the maximum number of active clusters on the NPV and CPU time at the cluster level

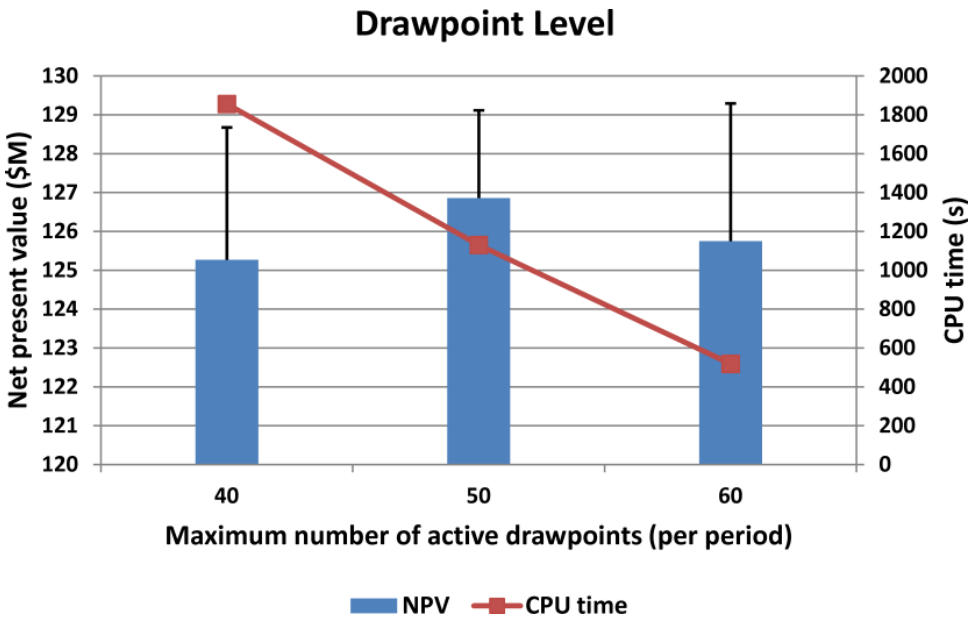

Figure 5.58. Impact of changes in the maximum number of active drawpoints on the NPV and CPU time at the drawpoint level

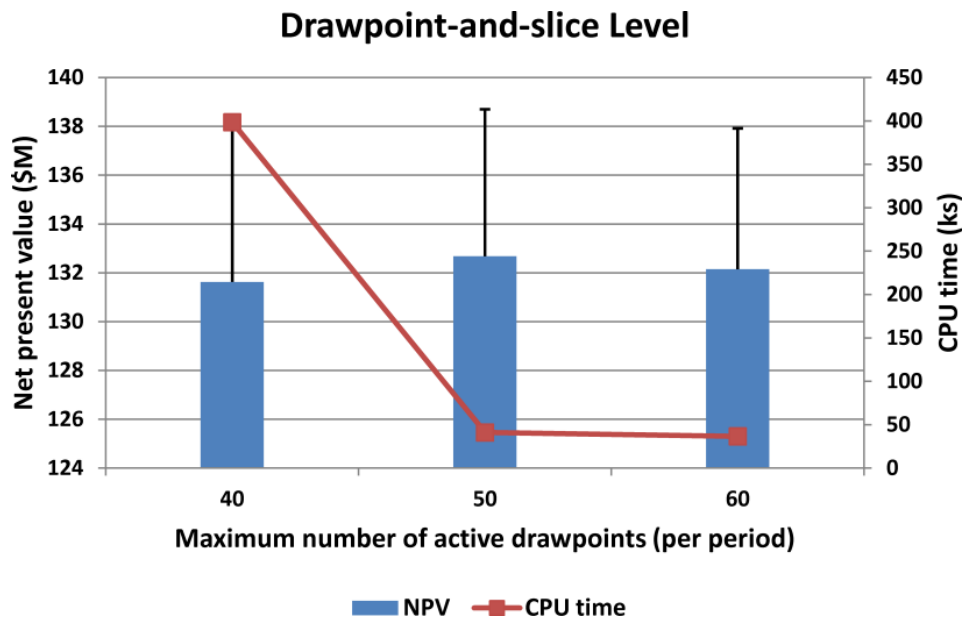

Figure 5.59. Impact of changes in the maximum number of active drawpoints on the NPV and CPU time at the drawpoint-and-slice level

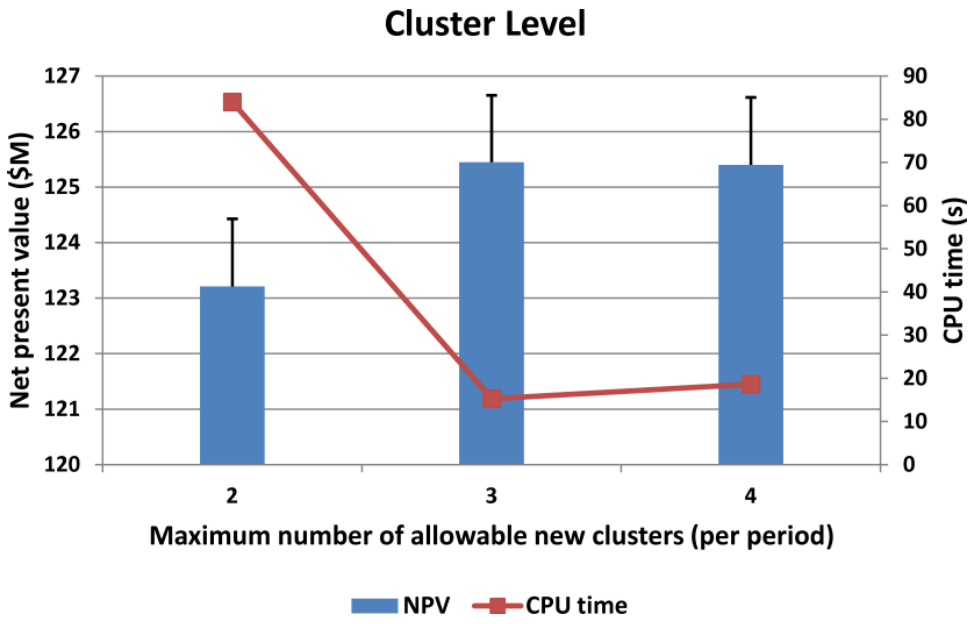

Figure 5.60. Impact of changes in the maximum number of allowable new clusters on the NPV and CPU time at the cluster level

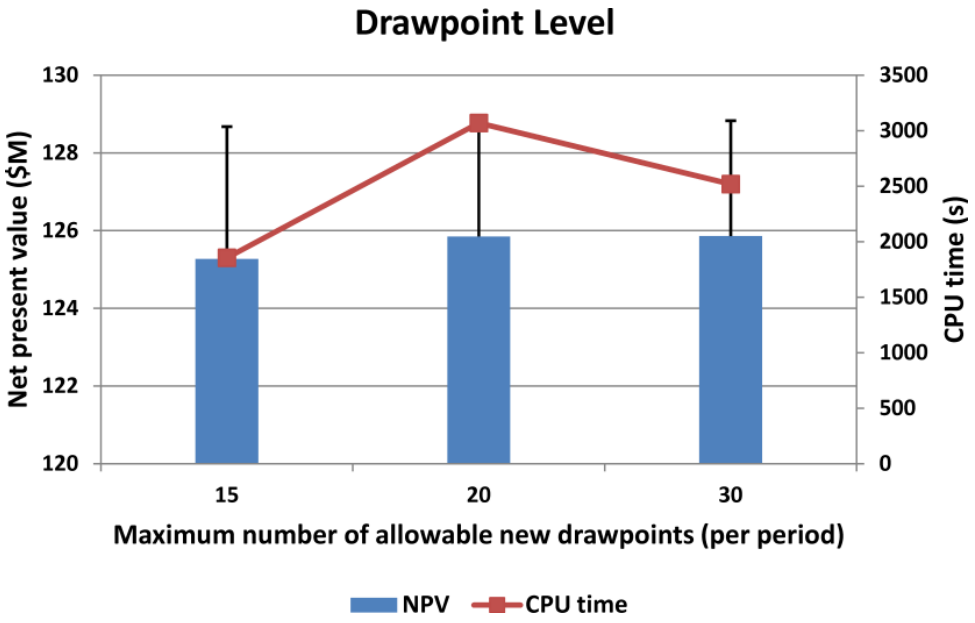

Figure 5.61. Impact of changes in the maximum number of allowable new drawpoints on the NPV and CPU time at the drawpoint level

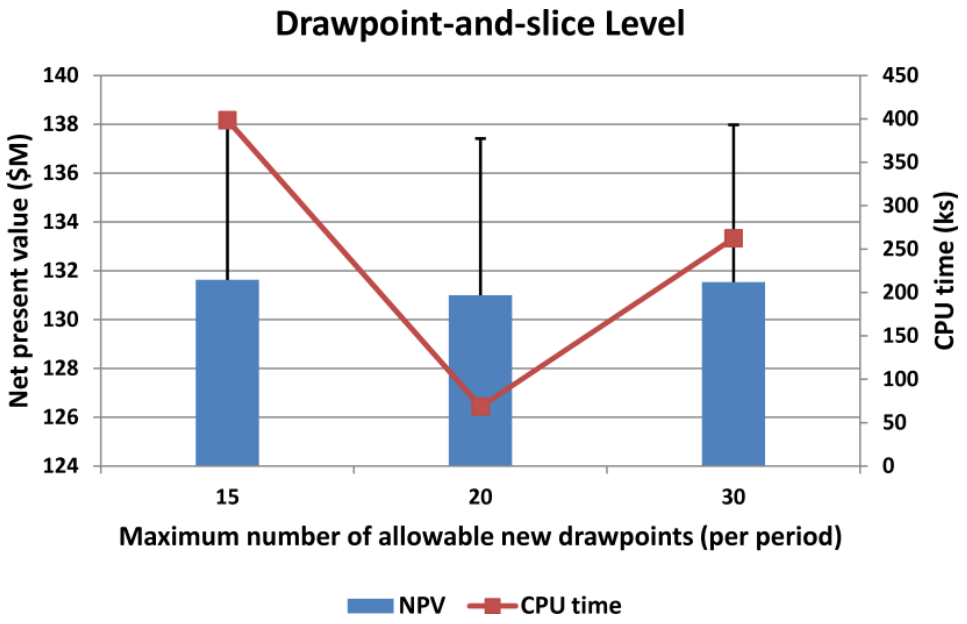

Figure 5.62. Impact of changes in the maximum number of allowable new drawpoints on the NPV and CPU time at the drawpoint-and-slice level

5.4.3 Effectiveness of Multi-Step Method

To demonstrate the effectiveness of the multi-step method, two different datasets were solved using the single-step and multi-step methods in the west to east direction. For each dataset the same input scheduling parameters were used to solve the problem using single-step and multi-step methods. Table 5.21 summarizes the results.

For dataset containing 102 drawpoints, in the single-step method at the drawpoint level, the EPGAP was set to 3%. At the drawpoint level, the solve time for the multi-step method with optimality gap of 0.55% was 68 times faster than the single-step method. At the drawpoint-and-slice level, the solve time for the multi-step method with optimality gap of 4.7% was 17 times faster than the single-step method with the optimality gap of 5%, while percentage difference between the NPVs was only 0.34%.

For dataset containing 298 drawpoints, in the single-step method the EPGAP was set to 5%. At the drawpoint level, the solve times for the multi-step method with optimality gaps of 1% and 2.92% were 6.8 times and 183 times faster than the

single-step method, respectively. At the drawpoint-and-slice level, the single-step method was still running after six days without any feasible solution. This comparison showed the effectiveness of the proposed method. A higher number of drawpoints increased the execution time of the problem exponentially, and reduced the probability of finding a near-optimal solution.

Table 5.21. Comparison of the results of MILP formulations for multi-step and single-step methods

Dir.	Level of formulation	Multi-step			Single-step			Diff. between methods' NPV (%)
		CPU time 8 CPUs 2.7 GHz	NPV ($M)	Optimality GAP (%)	CPU time 8 CPUs 2.7 GHz	NPV ($M)	Optimality GAP (%)	
	102 drawpoints and 2,058 slices							
WE	Cluster	00:01:24	123.21	0.99	00:01:24	123.21	0.99	0
	Drawpoint	00:00:27	126.84	0.55	00:30:56	125.27	2.72	1.24
	DP & Slice	06:24:37	132.07	4.7	110:43:26	131.63	5	0.34
	298 drawpoints and 5,539 slices							
WE	Cluster	00:00:05	313.56	0.74	00:00:05	313.56	0.74	0
	Drawpoint	06:58:47	317.60	1	47:38:43	310.25	4.8	2.4
		00:15:40	312.38	2.92				0.68
	DP & Slice	16:34:23	324.42	4.9	I stopped running after six days.			-------

The multi-step method made it possible to solve the problem with a smaller EPGAP in a reasonable amount of time. The method presented here can solve large-scale problems. At the cluster level, the optimal life-of-mine multi-period block cave production schedule is generated. The time horizon for the drawpoint level can vary as a subset of the life-of-mine. At the drawpoint-and-slice level, the time horizon for this detailed 3D model can vary as a subset of the time horizons chosen in the previous levels.

Figure 5.63 shows a schematic comparison of the multi-step and single-step methods from solution time and quality point of view. At the cluster level, the solution time and quality for both methods are same. It is obvious that at the drawpoint and drawpoint-and-slice levels the solution time of single-step method

is more than multi-step method. In multi-step and single-step methods, the solution time increases from cluster level to drawpoint-and-slice level and the solution quality improves so that the maximum NPV is obtained at drawpoint-and-slice level.

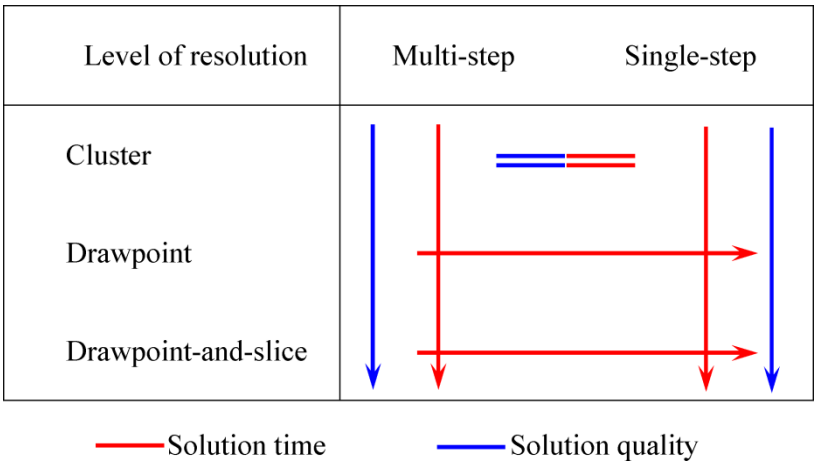

Figure 5.63. Schematic comparison of the methods and levels of resolutions in terms of solution time and solution quality

Production scheduling of any mining system has an enormous effect on the economics of the operation. The scheduling problems are complex due to the nature and variety of the constraints acting upon the system. In the available block-cave scheduling software, the mining sequence is controlled manually and, consequently, cannot yield an optimum solution for the problem. A series of opening sequences are evaluated and the results used to try to create an opening sequence that improves on the highest achieved net present value. This trial-and-error approach cannot be guaranteed to deliver a schedule with the highest NPV. Also, it is not possible to estimate or put bounds on the highest NPV for a given problem using trial-and-error methods. Hence, relying only on manual planning methods or computer software based on heuristic algorithms will lead to mine schedules that are not the optimal global solution.

All the presented MILP formulations for three levels of problem resolution -- cluster level, drawpoint level, and drawpoint-and-slice level -- guarantee that a practical schedule with the best NPV will be delivered for the assessed directions

because the exact algorithms are used. The MILP formulations use a solver developed based on exact solution methods for optimization where an optimization termination criterion is set up to define how far our generated solution is from the optimal solution. The solution is subject to practical and technical mining constraints that include (i) mining capacity, (ii) draw rate, (iii) mining precedence, (iv) maximum number of active drawpoints, (v) number of new drawpoints in each period, (vi) continuous mining, and (vii) total reserves.

The production scheduler defines the best starting point and advancement direction based on optimization. Also, the scheduler defines the opening and closing time of each drawpoint and cluster, the draw rate from each drawpoint and cluster, the number of new drawpoints and clusters that need to be constructed, and the sequence of extraction from the drawpoints and clusters to support a given production target.

5.5 Summary and Conclusion

This chapter covered the case studies and verification of the MILP formulations for three levels of problem resolution: (i) cluster level, (ii) drawpoint level, and (iii) drawpoint-and-slice level. All formulations maximized the NPV subject to several constraints such as the vertical mining rate, lateral mining rate and mining capacity, and the maximum number of active drawpoints or clusters. These formulations could be used in two ways: (i) single-step, and (ii) multi-step. In both methods, to solve the problem at the cluster level, after defining the advancement lines and phases, the draw columns within each phase were clustered using a modified hierarchical clustering algorithm based on the algorithm presented by Tabesh and Askari-Nasab (2011).

First, the MILP formulations for three levels of problem resolution were applied independently on a dataset containing 102 drawpoints and 2,058 slices. The goal was to maximize the NPV at a discount rate of 12%, while assuring that all constraints were satisfied during the mine life. The BHOD was limited to not less than 50m. The total tonnage of material which had to be extracted was almost 13.5

Mt. The deposit was scheduled over 15 periods. Details of the results have been summarized in Table 5.8.

The performance of the proposed models was analyzed based on NPV, mining production, and practicality of the generated schedules. At all the levels, the maximum NPV was obtained in the west to east direction. The cluster level, drawpoint level and drawpoint-and-slice level formulations generated production schedules which yielded NPVs of $123.2M, $125.2M, and $131.6M over a 15-year mine life at an annual discount rate of 12% in the west to east direction. The NPV of the drawpoint-and-slice level formulation was 4.8% and 6.4% more than that of the drawpoint and cluster levels, respectively.

The obtained NPVs are near-optimal values that can be reached based on the obtained optimality gap. In the standard industry software currently used for block-cave production scheduling, there is no measure of the quality of the solution against the upper bound of the theoretical optimum. At each of the levels of resolution, the opening pattern is gained based on the optimal solution, while in the industry software it is assumed that the opening pattern is known.

At the cluster level, any number of drawpoints can be handled according to the defined number of clusters and the number of draw columns within each cluster. However, solving a real-size problem at the drawpoint level and drawpoint-and-slice level in a reasonable amount of CPU time is not possible. To overcome the size problem of mathematical programming models and to generate a robust practical near-optimal schedule, the multi-step method was introduced.

The multi-step method was applied on a large dataset containing 298 drawpoints and 5,539 slices. The goal was to maximize the NPV at a discount rate of 12%, while assuring that all constraints were satisfied during the mine life. The BHOD was limited to not less than 50m. The total tonnage of material to be extracted was almost 37 Mt. In this method, the results of each level were used to reduce the number of variables in the next level. In multi-step method, the performance of the proposed models was analyzed based on NPV, mining production, and practicality

of the generated schedules. At the beginning, 35 clusters were created and the problem was solved for different advancement directions at the cluster level. Based on the results, the west to east and south to north directions had the maximum NPVs. Then, the solution from the previous stage was used based on the early start and late finish to eliminate the variables. Almost 34% of decision variables were eliminated in both directions. After solving the problem at drawpoint level, using the solution of this level and two years flexibility, the number of decision variables was reduced by 28% at the drawpoint-and-slice level formulation in the west to east directions. In this direction, the multi-step method generated production schedules which yielded NPVs of $313.5M, $317.6M, and $324.4M over a 15-year mine life at an annual discount rate of 12%. The NPV of the drawpoint-and-slice level formulation was 2.1% and 3.4% more than drawpoint and cluster levels, respectively.

In both the single-step and multi-step methods, the resulting NPVs for the drawpoint-and-slice level were greater than those for other levels. At the drawpoint-and-slice level, the method uses the slices' economic value. The model extracts slices with a higher economic value earlier than other slices. But at the drawpoint level, the method uses a draw column whose economic value is a weighted average of slices within the related draw column.

CHAPTER 6

SUMMARY, CONCLUSIONS AND RECOMMENDATIONS

Chapter 7 contains the thesis summary and concluding statements. The benefits and contributions of this research are highlighted, as well as recommendations for future work in integrated mine planning and production scheduling.

6.1 Summary of Research

As the mining industry is faced with lower grades and marginal reserves, production scheduling algorithms are continually coming to the forefront as one of the important methods for determining the viability of mining projects. A production schedule must provide a mining sequence that takes into account the physical limitations of the mine and, to the extent possible, meets the demanded quantities of each raw ore type at each time period throughout the mine-life. The economics of today's mining industry are such that the major mining companies are increasing the use of massive mining methods. Among the mining methods available, caving methods are favored because of their low cost and high production rates. Caving methods have become the underground bulk mining method of choice, a trend that is expected to continue in the foreseeable future. The optimal production schedules play an important role in generating economic returns from the block-caving method because it is not possible to change the mining method once the cave is initiated and the loss of large amounts of the deposit if production is carried out with poor draw practice. Currently, the software packages use simulation and heuristic methods to determine feasible rather than optimal production schedules. These methods rapidly provide different schedules for review by a planner, but they suffer from their inability to provide an optimal solution.

Because of the improvement in both computer processing power and optimization solution algorithms, the ability to find an optimum schedule has been increased. Many efforts have been made recently to address open pit optimization and production scheduling problems. But the literature on underground mining is more recent. In summary, the major shortcomings of the current production scheduling methods in block caving are: a) limitations in solving large-scale problems; b) treatment of stochastic variables as deterministic processes; c) the trial-and-error process to find the mining start point and advancement direction; d) integration of fewer geotechnical constraints into real-scale production

scheduling. These inadequacies can cause distortions in the mine plans, resulting in sustainability, regulatory and profitability issues.

To solve the limitations in dealing with large-scale problems, the trial-and-error process to find the mining start point and advancement direction, and integration of fewer geotechnical constraints into real-scale production scheduling, this research has developed a mixed-integer linear programming (MILP) mine planning framework to address long-term optimal block-cave production scheduling. Figure 6.1 shows a summary of the workflow for completing a case study based on the developed models.

The objective of this research is to develop, implement, and verify a theoretical optimization framework for block-cave long-term production scheduling, whereby a mineral is extracted and prepared at a desired market specification, with the maximum economic return measured by NPV, and within acceptable technical and operational constraints. These constraints are the development rate, vertical mining rate (production rate per drawpoint), lateral mining rate (rate of opening new drawpoints), mining capacity, maximum number of active drawpoints, cave draw strategies, and advancement direction.

Three MILP formulations were introduced for three levels of problem resolution: (i) cluster level, (ii) drawpoint level, and (iii) drawpoint-and-slice level. At the cluster level, the optimal life-of-mine multi-period block-cave production schedule is generated. This is the strategic yearly production schedule with the objective of net present value (NPV) maximization. At the drawpoint level, the optimal long-term block-cave production schedule is generated. The time horizon for this model can vary as a subset of the life-of-mine to control the size of the MILP to be solved. At drawpoint-and-slice level, the optimal long-term mine plan at the drawpoint level, including slices, is generated. The time horizon for this detailed 3D model can vary as a subset of the time horizons chosen in the previous levels.

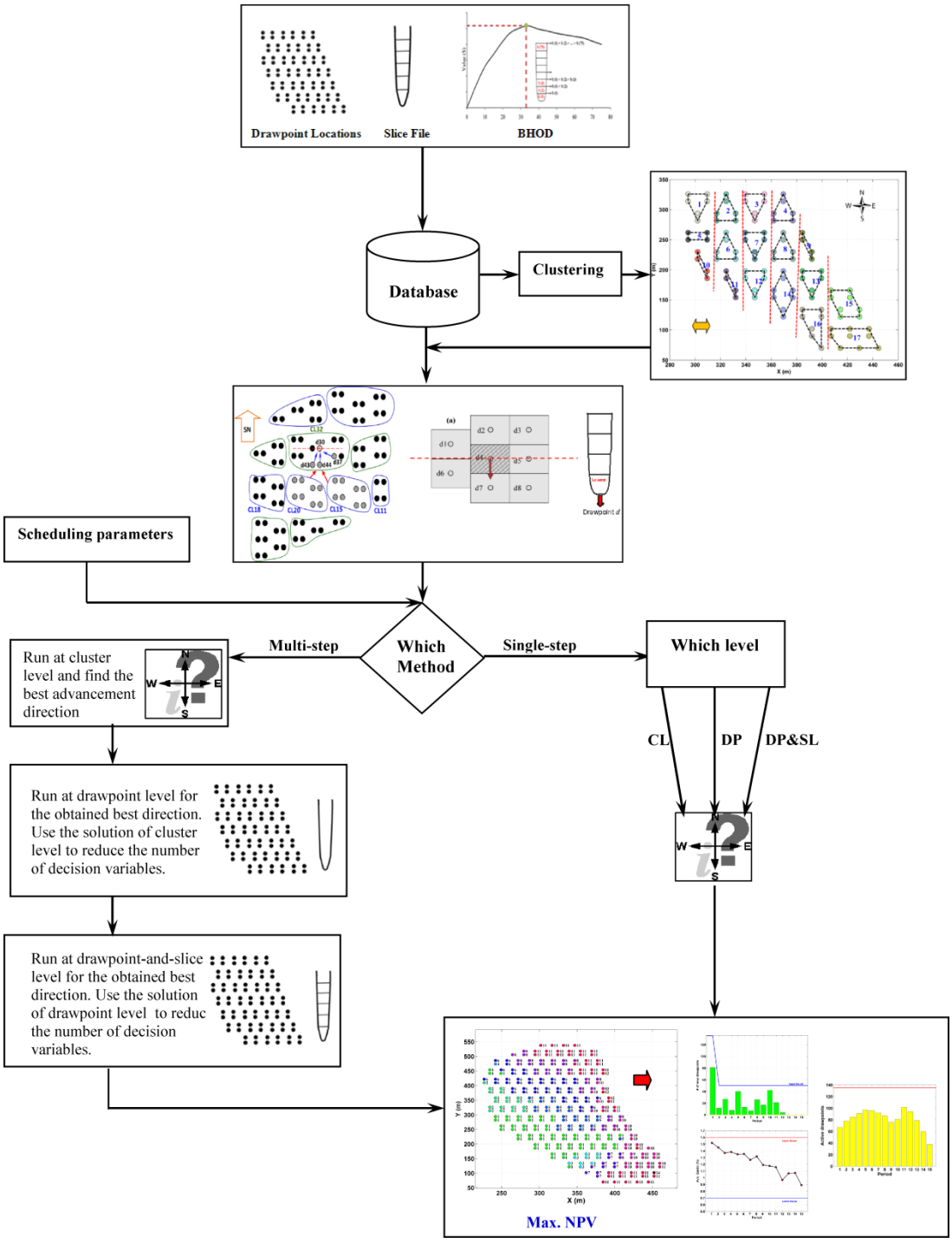

Figure 6.1. Summary of the research methods

These formulations can be used in two ways: (i) as a single-step method in which each of the formulations is used independently, (ii) or as a multi-step method in

which each step's solution is used to reduce the number of variables in the next level and consequently generate a practical block-cave schedule in a reasonable CPU runtime for large-scale problems.

In both methods, to solve the problem at the cluster level, after defining the advancement lines and phases, the draw columns within each phase are clustered using a modified hierarchical clustering algorithm based on the algorithm presented by Tabesh and Askari-Nasab (2011).

In general, the development and implementation of the MILP optimization model framework was undertaken in different stages. The results at each stage were published to facilitate continuous feedback from the research community and mining industry experts to improve the research methodology and models (Pourrahimian and Askari-Nasab, 2009a; Pourrahimian and Askari-Nasab, 2010a; Pourrahimian and Askari-Nasab, 2011; Pourrahimian et al., 2012a; Pourrahimian et al., 2012b; Pourrahimian et al., 2012c).

MATLAB (Math Works Inc, 2011) programming platform was used to capture the MILP model framework. The model's main components include the objective function and constraints. These components interact with the draw columns' slices through the user input scheduling parameters. TOMLAB/CPLEX (Holmstrom, 2011), which is a large-scale optimization solver developed based on the branch-and-cut algorithm, was used for this research.

The MILP formulations for three levels of problem resolution were applied independently on a data set containing 102 drawpoints and 2,058 slices. At all the levels, the problem was solved over 15 periods and the same input scheduling parameters were considered. The results showed that all the considered constraints had been satisfied and the models worked properly. The obtained NPVs were the optimal values that could be reached based on the obtained optimality gap. The number of the constraints and variables increased from the cluster level to the drawpoint-and-slice level and, consequently, the solving time increased. To solve the problem at these three levels of resolution, the EPGAP was set to 1%, 3%, and

5% at the cluster level, drawpoint level, and drawpoint-and-slice level, respectively. Despite the higher obtained optimality gap for the drawpoint-and-slice level, the solving time of this level was significantly more than at other levels. The obtained NPV at the drawpoint-and-slice level was more than at the drawpoint level. The NPV of the drawpoint level was more than at the cluster level. The cluster level, drawpoint level and drawpoint-and-slice level formulations generated production schedules which yielded a NPV of $123.2M, $125.2M, and $131.6M in the west to east direction, which was the best advancement direction. The NPV of the drawpoint-and-slice level was 4.8% higher than that of the drawpoint level and 6.4% more than the cluster level. However, the solving time of the problem at drawpoint-and-slice level for this direction was 4745 times more than cluster level and 215 times more than drawpoint level.

The results of single step showed that solving a real-size problem at the drawpoint level and drawpoint-and-slice level in a reasonable CPU time is not possible. To overcome the size problem of mathematical programming models and to generate a robust practical near-optimal schedule, a multi-step method was introduced.

The multi-step method was applied on a dataset containing 298 drawpoints and 5,539 slices over 15 periods. After defining the advancement lines and phases, the draw columns within each phase were clustered. Then, the problem was solved in four directions at the cluster level with an EPGAP of 1%. Based on the results, the directions west to east and south to north with NPVs of $313.56M and $312.54M were selected as directions to solve the problem at the drawpoint level. Then, the solution from the previous stage was used, based on the early start and late finish, to eliminate the variables. Consequently, the number of decision variables was reduced 34% in the both directions. This variable reduction technique decreased the solution space for the optimization problem. Thus during optimization, some of the branches in the branch-and-cut tree were eliminated, ensuring that the solution for the practical production scheduling problem was reached faster. Then, the problem was solved in the both directions with two EPGAPs of 4% and 1%.

Based on results, the NPV of both directions was $317M. For the last step, the west to east direction was selected. After eliminating 28% of the decision variables based on the solution of the drawpoint level, the problem was solved at the drawpoint-and-slice level with the EPGAP of 5%. The NPV was $324.4M. At all levels, all the defined constraints had been satisfied and the models worked properly. Table 6.1 shows a summary of the results for both the single-step and multi-step.

Table 6.1. Summary of results from numerical application for single-step and multi-step methods

Level of resolution	Dir.	Number of CL/DP/SL	Number of constraints variables	Opt. GAP (%)	CPU time 8 CPUs @ 2.7 GHz	NPV ($M)	Diff. from the best (%)
Single-step Method (102 drawpoints)							
Cluster level	WE	17 / 0 / 0	1,429 / 765	0.99	00:01:24	123.21	-6.4
	EW	17 / 0 / 0	1,429 / 765	1.00	00:02:57	121.71	-7.54
	NS	17 / 0 / 0	1,444 / 765	0.82	00:00:50	121.98	-7.33
	SN	17 / 0 / 0	1,399 / 765	0.99	00:00:47	121.28	-7.86
Drawpoint level	WE	0 / 102 / 0	19,854 / 4,590	2.72	00:30:56	125.27	-4.83
	EW	0 / 102 / 0	19,884 / 4,590	2.98	00:49:46	124.70	-5.26
	NS	0 / 102 / 0	20,874 / 4,590	2.93	00:27:46	124.31	-5.56
	SN	0 / 102 / 0	19,284 / 4,590	2.99	01:03:17	124.78	-5.20
Drawpoint-and-slice level	WE	0 / 102 / 2,058	115,146/64,800	5	110:43:26	131.63	The best
	SN	0 / 102 / 2,058	114,576/64,800	5	124:31:18	126.63	-3.8
Multi-step Method (298 drawpoints)							
Cluster level	WE	35 / 0 / 0	2,935 / 1,575	0.74	00:00:05	313.56	-3.35
	EW	35 / 0 / 0	2,965 / 1,575	1.00	18:47:07	306.56	-5.51
	NS	35 / 0 / 0	2,950 / 1,575	0.94	00:36:28	300.01	-7.52
	SN	35 / 0 / 0	3,070 / 1,575	0.68	00:00:13	312.54	-3.66
Drawpoint level	WE	0 / 298 / 0	79,046 / 13,410	2.92	00:15:40	312.38	-3.71
	SN	0 / 298 / 0	89,336 / 13,410	3.23	00:31:45	311.52	-3.98
	WE	0 / 298 / 0	79,046 / 13,410	1	06:58:47	317.60	-2.1
	SN	0 / 298 / 0	89,336 / 13,410	1	210:22:29	317.09	-2.26
Drawpoint-and-slice level	WE	0 / 298 / 5,539	336,079/175,110	4.9	16:34:23	324.42	The best

To demonstrate the effectiveness of the multi-step method, the problem was solved using a single-step method for the same input scheduling parameters in the west to east direction. In the single-step method, the EPGAP was set to 5%. At the drawpoint level, the solving time for the multi-step method with an optimality gap of 1% was six times faster than the single-step method. With an optimality gap of 2.92%, it was 183 times faster.

The multi-step method made it possible to solve the problem with a smaller EPGAP in a reasonable CPU time. At the drawpoint-and-slice level, the single-step method was still running after six days without any feasible solution. The increase in the number of drawpoints increased the run time of the model exponentially and reduced the probability of finding a near-optimal solution.

The method presented here can solve large-size problems. At the cluster level, the optimal life-of-mine, multi-period block-cave production schedule is generated. The time horizon for the drawpoint level can vary as a subset of the life-of-mine. At the drawpoint-and-slice level, the time horizon for this detailed 3D model can vary as a subset of the time horizons chosen in the previous levels.

6.2 Conclusions

In pursuing this research, the literature review conducted established the limitations in the current body of knowledge in production scheduling optimization. These limitations can affect the viability as well as other aspects of mining projects, emphasizing the need for optimization tools that take into consideration these deficiencies. Consequently, it is important that robust models are developed to address these challenges. In addition, relying only on manual planning methods or computer software based on heuristic algorithms will lead to mine schedules that are not the optimal global solution. In this research we developed a theoretical framework for long-term production schedule optimization of block-cave mines using MILP. The theoretical framework was implemented and verified on a real dataset. The research objectives outlined in Chapter 1 have been achieved within the research scope. The following

conclusions were drawn from the implementation of the MILP model framework for block-cave production scheduling:

- The presented MILP models maximize the NPV of the mining operations while enforcing production control constraints.

- The MILP models generate production schedules for large-scale block-caving projects using clustering and multi-step techniques.

- The presented MILP models can generate production schedules at three levels of problem resolution: (i) cluster level, (ii) drawpoint level, and (iii) drawpoint-and-slice level.

- The cluster-level model generates the optimal life-of-mine multi-period block-cave production schedule. This is the strategic, yearly production schedule with the objective of NPV maximization.

- The drawpoint-level model generates the optimal long-term block cave production schedule. The time horizon for this model can vary as a subset of the life-of-mine to control the size of the MILP to be solved.

- The drawpoint-and-slice level model generates the optimal medium-term plan at the drawpoint level, including slices. The time horizon for this detailed 3D model could vary as a subset of the time horizons chosen for the previous levels.

- The MILP models provide a fast and flexible production scheduling optimization approach through the use of the multi-step method. In the considered case study, at the drawpoint level, the solving time for the multi-step method with an optimality gap of 1% was 6 times faster than the single-step method with a larger optimality gap of 4.8%. With an optimality gap of 2.92%, it was 183 times faster. Also, the obtained NPV for the multi-step method was 2.3% more than single-step method. The single-step method was

not able to reach a feasible solution at the drawpoint-and-slice level, while the multi-step method generated a schedule with a NPV of $324.4M.

- The MILP models generate a production schedule with the maximum NPV.
- The MILP models show the starting point and advancement direction needed to reach the maximum NPV.

6.3 Contributions of PhD Research

This research has developed mathematical, MILP models for block-cave production scheduling. The resulting formulations and methodology offer the following significant improvements over the previous research in the context of mathematical programming models for block-cave production scheduling:

- Proposition of three MILP production scheduling models and their implementation as prototype software with a graphical user interface at three levels of detailed resolution: (i) cluster level, (ii) drawpoint level, and (iii) drawpoint-and-slice level.
- Consideration of a multistage solution methodology using the three above-mentioned MILP models to generate a practical block-cave schedule in a reasonable CPU runtime.
- Proposition of using a hierarchical clustering algorithm based on the cave advancement direction to aggregate drawpoints into selective mining units of scheduling. The contribution of drawpoint aggregation is twofold: (a) it generates a practical mining schedule that follows a selective mining unit; and (b) reduces the number of variables, especially binary variables in the MILP formulation, to make it computationally tractable.
- Introduction of the concept of different cave advancement directions to find the best single operation direction or combination thereof, and the best starting location. Since the caving industry is now moving towards the next generation of caving geometries and scenarios, super caves, this concept will be useful.

- The models provide the starting point and the advancement direction to use in the commercial software packages in which the opening pattern is defined manually.

6.4 Recommendations for Future Research

Although models developed in this thesis have provided new methods and formulations for block-cave production scheduling, there is still the need for continued investigation into using mathematical programming models in production scheduling of block-cave mines. The following recommendations could improve and add to the body of knowledge in this research area.

- The MILP models assumed that data from geologic block models were deterministic values. As a result, no attribute uncertainties were considered. It also assumed that future cost and price data used for the slice economic value were constant. This assumption means that as cost and price change in the future, there will be a need to re-optimize the production schedules. To overcome these limitations, the MILP model framework should be extended to include stochastic variables like grade and mineral prices during optimization.
- In addition to the assumed constraints in this research, there are other mine planning parameters that are a function of the rock mass. Future research will need to define all these parameters and the relationships between them to establish a more comprehensive production-scheduling model.
- The MILP models assumed that there was no material mixing between blocks as a function of draw. The dilution modeling was carried out in PCBC at the slice level, prior to using this static model. Future research will need to consider material mixing during optimization.

BIBLIOGRAPHY

[1] Akaike, A. and Dagdelen, K. (1999). *A strategic production scheduling method for an open pit mine*. in Proceedings of 28th International Symposium on the Application of Computers and Operations Research in the Mineral Industry, Colorado School of Mines, Littleton, USA, pp. 729-738.

[2] Alford, C., Brazil, M., and Lee, D. H. (2007). Optimisation in Underground Mining. in *Handbook Of Operations Research In Natural Resources*, Vol. 99, *International Series in Operations Research & Management Science*, Springer US, pp. 561-577.

[3] Askari-Nasab, H. (2006). Intelligent 3D interactive open pit mine planning and optimization. Ph.D. Thesis, University of Alberta, Edmonton, Pages 167.

[4] Askari-Nasab, H. and Awuah-Offei, K. (2009). Open pit optimization using discounted economic block values. *Transactions of the Institution of Mining and Metallurgy, Section A*, *118* (1), 1-12.

[5] Askari-Nasab, H., Pourrahimian, Y., Ben-Awuah, E., and Kalantari, S. (2011). Mixed integer linear programming formulations for open pit production scheduling. *Journal of Mining Science, © Springer, New York, NY 10013-1578, United States*, *47* (3), 338-359.

[6] Barbaro, R. W. and Ramani, R. V. (1986). Generalized multiperiod MIP model for production scheduling and processing facilities selection and location. *Mining Engineering*, *38* (2), 107-114.

[7] Barlett, P. J. (1992). *The design and operation of mechanized cave at Premier Diamond mine*. in Proceedings of Massmin 1992, South African Institute of Mining Metallurgy: Johannesburg, Johannesburg, pp. 227-232.

[8] Barraza, M. and Crorkan, P. (2000). *Esmeralda mine exploration project*. in Proceedings of MassMin 2000, The Australasian Institute of Mining and Metallurgy: Melburne, Brisbane, pp. 267-278.

[9] Boland, N., Dumitrescu, I., Froyland, G., and Gleixner, A. M. (2009). LP-based disaggregation approaches to solving the open pit mining production scheduling problem with block processing selectivity. *Computers and Operations Research*, *36* (4), 1064-1089.

[10] Brazil, M., Lee, D. H., Rubinstein, D. A., Weng, J. F., and Wormald, N. C. (2000). *Network optimization of underground mine design*. in Proceedings of The Australasian Institute of Mining and Metallurgy, pp. 57-65.

[11] Brazil, M., Lee, D. H., Van Leuven, M., Rubinstein, J. H., Thomas, D. A., and Wormald, N. C. (2003). Optimising declines in underground mines. *Mining Technology*, *112* (3), 164-170.

[12] Brown, E. T. (2003). *Block caving geomechanics*. Indooroopilly, Queensland : Julius Kruttschnitt Mineral Research Centre, The University of Queensland, Brisbane, Pages 516.

[13] Burgher, K. E. and Erickson, E. (1984). The optimization of coal mine production schedules using linear programming: An example that determines the effect of reclamation costs and interest rates. *Mining Science And Technology*, *2* (1), 69-78.

[14] Butcher, R. J. (1999). Design rules for avoiding draw horizon damage in deep level block caves. *The Journal of The SOuth African Institute of Mining and Metallurgy*, *99* (2), 151-156.

[15] Caccetta, L. (2007). Application of Optimisation Techniques in Open Pit Mining. in *Handbook Of Operations Research In Natural Resources*, Vol. 99, *International Series In Operations Research amp; Mana*, A. Weintraub, C. Romero, T. Bjørndal, R. Epstein, and J. Miranda, Eds., Springer US, pp. 547-559.

[16] Caccetta, L. and Hill, S. P. (2003). An Application of branch and cut to open pit mine scheduling. *Journal of Global Optimization*, *27* (2), 349-365.

[17] Carlyle, W. M. and Eaves, B. C. (2001). Underground planning at Stillwater mining company. *INTERFACES*, *31* (4), 50-60.

[18] Chacon, J., Gopfert, H., and Ovalle, A. (2004). *Thirty tears evolution of block caving in Chile*. in Proceedings of MassMin 2004, Santiago, Chile.

[19] Chanda, E. C. K. (1990). An application of integer programming and simulation to production planning for a stratiform ore body. *Mining Science and Technology*, *11* (2), 165-172.

[20] Chanda, E. K. C. and Dagdelen, K. (1995). Optimal blending of mine production using goal programming and interactive graphics systems. *International Journal of Surface Mining, Reclamation and Environment*, *9* (4), 203-208.

[21] Chitombo, G. P. (2010). *Cave mining-16 years after Laubscher's 1994 paper 'cave mining-state of the art'*. in Proceedings of Caving 2010, Australian centre for geomechanics, Perth, Australia, pp. 45-61.

[22] Dagdelen, K. and Johnson, T. B. (1986). *Optimum open pit mine production scheduling by lagrangian parameterization*. in Proceedings of 19th Application of Computers and Operations Research in the Mineral Industry Proceedings, Society of Mining Engineers of the American Institute of Mining, Metallurgical, and Petroleum Engineers, Inc., Littleton, Colorado., pp. 127-142.

[23] Dagdelen, K. and Kawahata, K. (2007). Oppurtunities in multi-mine planning through large scale mixed-integer linear programming optimization. in *33rd International Symposium on Computer Application in the Minerals Industry (APCOM)*. Santiago, Chile.

[24] Datamine Corporate Limited (2008). NPV Scheduler. Ver. 4, Beckenham, UK.

[25] De Wolfe, V. (1981). Draw control in principle and practice at Henderson mine. in *Design and operation of caving and sublevel stopping mines*, D. R. Stewart, Ed. New York, Society of Mining Engineers of the American Institute of Mining, Metallurgical, and Petroleum Engineers, Inc. , pp. 729-735.

[26] Denby, B. and Schofield, D. (1994). Open-pit design and scheduling by use of genetic algorithms. *Transactions of the IMM Section A*, *103* A(21-26).

[27] Denby, B. and Schofield, D. (1995). Inclusion of risk assessment in open pit design and planning. *Institution of Mining and Metallurgy*, *104* (A), 67-71.

[28] Diering, T. (2000). *PC-BC: A block cave design and draw control system*. in Proceedings of MassMin 2000, The Australasian Institute of mining and Metallurgy: melburne, Brisbane, pp. 301-335.

[29] Diering, T. (2004). *Computational considerations for production scheduling of block cave mines*. in Proceedings of MassMin 2004, Santiago, Chile, , pp. 135-140.

[30] Diering, T. (2012). *Quadratic programming applications to block cave scheduling and cave management*. in Proceedings of 6th International Conference & Exhibition on Mass Mining (MassMin 2012), Paper No: 6809, Sudbury, ON, Canada.

[31] Diering, T. and Villa, D. (2007). Working notes to use PCBC (revision 1.0). Vancouver: Gemcom Software International Inc., pp. 60.

[32] Doepken, W. G. (1982). The Henderson Mine. in *Underground Mining Methods Handbook*, Vol. 1, W. A. Hustrulid, Ed. New York, Society of Mining Engineers of the American Institute of Mining, Metallurgical, and Petroleum Engineers, Inc. , pp. 990-997.

[33] Epstein, R., Gaete, S., Caro, F., Weintraub, A., Santibanez, P., and Catalan, J. (2003). Optimizing long-term planning for underground copper mines. in *Copper 2003, 5th International Conference*, vol. I. Santiago, Chili: CIM and the Chilean Institute of Mining, pp. 265-279.

[34] Feng, L., Qiu, M.-H., Wang, Y.-X., Xiang, Q.-L., Yang, Y.-F., and Liu, K. (2010). A fast divisive clustering algorithm using an improved discrete particle swarm optimizer. *Pattern Recognition Letters*, *31* (11), 1216-1225.

[35] Flores, G., Karzulovic, A., and Brown, E. T. (2004). *Current practices and trends in cave mining*. in Proceedings of MassMin 2004, Chilean Engineering Institute: Santiago., Santiago, pp. 83-90.

[36] GemcomSoftwareInternational (2012). Ver. 6.2.4, Vancouver, BC, Canada.

[37] Gemcom Software International (2012). Whittle strategic mine planning software. Ver. 4.4, Vancouver.

[38] Gerling, R. and Helms, W. (1986). *A model for long range scheduling of the mining sequence for flat lying orebodies*. in Proceedings of 19 Application of Computers and Operations Research in the Mineral Industry, Society of Mining Engineers of the Amwrica Institute of Mining, Metallurgical, and Petroleum Engineers, Inc., New York, pp. 333-342.

[39] Gershon, M. (1987). Heuristic approaches for mine planning and production scheduling. *Geotechnical and Geological Engineering*, *5* (1), 1-13.

[40] Gershon, M. E. (1983). Mine scheduling optimization with mixed integer programming. *Mining Engineering*, *35* 351-354.

[41] Gonzalez, T. F. (1982). On the Computational Complexity of Clustering and Related Problems. *System Modeling and Optimization*, *38* 174-182.

[42] Guest, A., VanHout, G. J., Von, J. A., and Scheepers, L. F. (2000). *An application of linear programming for block cave draw control*. in Proceedings of Massmin 2000, The Australian Institute of Mining and Metallurgy: Melbourne., Brisbane, Australia.

[43] Hanson, B. D. and Selim, A. A. (1975). Probabilistic simulation of underground production systems. *Transactions of the Institution of Mining and Metallurgy*, *258* (3), 19-24.

[44] Heslop, T. G. and Laubscher, D. H. (1981). Draw control in caving operations on sSouthern African Chrysotile asbestos mines. in *Design and operation of caving and sublevel stoping mines*, D. R. Stewart, Ed. New York, Society of Mining Engineers of the American Institute of Mining, Metallurgical, and Petroleum Engineers, Inc. , pp. 755-774.

[45] Holmstrom, K. (2011). TOMLAB/CPLEX, ver. 11.2. Ver. Pullman, WA, USA: Tomlab Optimization.

[46] Horst, R. and Hoang, T. (1996). *Global optimization : deterministic approaches.* Springer, New York, 3rd ed, Pages xviii, 727 p.

[47] Horst, R. and Hoang, T. (1996). *Global optimization: Deterministic approaches.* Springer, New York, 3rd ed, Pages 727.

[48] Huang, Y. and Kumar, U. (1994). Optimizing the number of load-haul-dump machines in a Swedish mine by using Queuing theory- A case study. *International Journal of Surface Mining, Reclamation and Environment*, *8* (3), 171-174.

[49] IBM (2009). ILOG CPLEX. Accessed April 1, 2010, http://www-01 .ibm.com/ software/integration/optimization/cplex.

[50] Johnson, S. (1967). Hierarchical clustering schemes. *Psychometrika*, *32* (3), 241-254.

[51] Johnson, T. B. (1969). *Optimum open-pit mine production scheduling*. in Proceedings of 8th International Symposium on Computers and Operations Research, Salt Lake City, Utah, USA.

[52] Jordi, K. C. and Curin, D. C. (1979). *Goal programming for strategic planning*. in Proceedings of 16th Application of Computers and Operations Research in the Mineral Industry Proceedings, SOciety of Mining Engineers of the American Institute of Mining, Metallurgical, and Petroleum Engineers, Inc., New York, pp. 296-303.

[53] Julin, D. E. (1992). Block caving, Chapter. 20.3. in *SME Mining Engineering Handbook*, H. L. Hartman, Ed. Littleton, Colo. : Society for Mining, Metallurgy, and Exploration, Inc., pp. 1815-1836.

[54] Julin, D. E. and Tobie, R. L. (1973). Block caving - characteristics, advantages and disadvantages type. in *SME Mining Engineering Handbook*, Society of Mining Engineers of the American Institute of Mining, Metallurgical, and Petroleum Engineers, Inc. , pp. 162-167.

[55] Kim, Y. C. and Zhao, Y. (1994). *Optimum open pit production sequencing - The current state of the art*. in Proceedings of SME Annual Meeting Preprint #94-224, Socity for Mining, Matallurgy and Exploration, Inc., Littleton, Colorado, pp. 1-8.

[56] Kuchta, M., Newman, A., and Topal, E. (2004). Implementing a production schedule at LKAB 's Kiruna Mine. *Interfaces*, *34* (2), 124-134.

[57] Laubscher, D. H. (1994). Cave mining - the state of the art. *Journal of The South African Institute of Mining and Metallurgy*, *94* (10), 279-293.

[58] Maitra, S., Rao, P. V., Sengupta, D., and Rao, V. S. (1994). *Optimal production scheduling using operations research techniques in a large opencast iron ore mine*. in Proceedings of Mine Planning and Equipment Selection Istanbul, Turkey, pp. 87-91.

[59] MathWorksInc (2011). MATLAB (R2011b). Ver. 7.13.0.564, MathWorks, Inc.

[60] Maxwell, A. S. (1978). Underground production mining at Chingola, with emphasis on a computerized ore-reserve calculation, depletion, and prediction system. in *11th Commonwealth Mining and Metallurgical Congress*. Hong Kong: The Institution of Mining and Metallurgy, Hong Kong, pp. 507-524.

[61] Muge, F. H., Santos, N., Vierira, J. L., and Cortez, L. (1992). *Dynamic programming in mine planning and production scheduling*. in Proceedings of 23rd Application of Computers and Operations Research in the Mineral Industry, Society of mining Engineering of the American Institute of Mining,

Metallurgical, and Petroleum Engineers, Inc. Littleton, Colorado., Littleton, Colorado, USA.

[62] Newman, A. M. and Kuchta, M. (2007). Using aggregation to optimize long-term production planning at an underground mine. *European Journal of Operational Research*, *176* (2), 1205-1218.

[63] Newman, A. M., Rubio, E., Caro, R., Weintraub, A., and Eurek, K. (2010). A review of operations research in mine planning. *Interfaces*, *40* 222-245.

[64] Osanloo, M., Gholamnejad, J., and Karimi, B. (2008). Long-term open pit mine production planning; a review of models and algorithms. *International Journal of Surface Mining, Reclamation and Environment*, *22* (1), 3-35.

[65] Owen, K. C. and Guest, A. R. (1994). *Underground mining of Kimberlite pipes*. in Proceedings of XV CMMI Congress, South African Institute of Mining Metallurgy: Johannesburg, Johannesburg, pp. 207-218.

[66] Parkinson, A. F. (2012). Essay on sequence optimization in block cave mining and inventory policies with two delivery size. PhD Thesis, University of British Colombia, Vancouver, Pages 188.

[67] Peele, R. (1941). *Mining Enginners' Handbook.* John Wiley & Sons, New York, 3rd ed.

[68] Pourrahimian, Y. and Askari-Nasab, H. (2009a). Optimizing block extraction sequence with MIP method and investigating the effect of road condition on truck cycle time. Mining Optimization Laboratory (MOL) Research Report One, University of Alberta (ISBN: 978-1-55195-279-6), Edmonton, AB, Canada, pp. 168-188.

[69] Pourrahimian, Y. and Askari-Nasab, H. (2009b). A review of open pit mine production scheduling and a guide for using Excel Solver in modeling MIP problems. Mining Optimization Laboratory (MOL) Research Report One, University of Alberta (ISBN: 978-1-55195-279-6), Edmonton, AB, Canada, pp. 189-206.

[70] Pourrahimian, Y. and Askari-Nasab, H. (2010a). A mathematical programming formulation for block cave production scheduling. Mining Optimization Laboratory (MOL) Reserch Report Two, University of Alberta (ISBN: 978-1-55195-280-2) Edmonton, AB, Canada, pp. 134-156.

[71] Pourrahimian, Y. and Askari-Nasab, H. (2010b). An overview of block caving operation and available methods for production scheduling of block cave mines. Mining Optimization Laboratory (MOL) Reserch Report Two, University of Alberta (ISBN: 978-1-55195-280-2) Edmonton, AB, Canada, pp. 116-133.

[72] Pourrahimian, Y. and Askari-Nasab, H. (2011). Block cave production scheduling optimization using mixed integer linear programming. Mining Optimization Laboratory (MOL) Research Report Three, University of Alberta (ISBN: 978-1-55195-281-9), Edmonton, AB, Canada, 3, pp. 75-98.

[73] Pourrahimian, Y., Askari-Nasab, H., and Tannant, D. (2009c). *Production scheduling with minimum mining width constraints using mathematical programming* in Proceedings of Mine Planning and Equipment Selection (MPES) CD-ROM, Banff, AB, Canada, pp. 646-653.

[74] Pourrahimian, Y., Askari-Nasab, H., and Tannant, D. (2012a). Mixed-integer linear programming formulation for block-cave sequence optimisation. *Int. J. Mining and Mineral Engineering*, *4* (1), 26-48.

[75] Pourrahimian, Y., Askari-Nasab, H., and Tannant, D. (2012b). *Block cave production scheduling optimization using mathematical programming*. in Proceedings of 6th International Conference & Exhibition on Mass Mining (MassMin), Sudbury, ON, Canada, pp. (papaer No. 6799).

[76] Pourrahimian, Y., Askari-Nasab, H., and Tannant, D. (2012c). A multi-step approach for block cave production scheduling optimization. *International Journal of Mining Science and Technology*, *Elsevier, Under Review, August 4, 2012* (23 pages).

[77] Pretorius, D. D. and Ngidi, S. (2008). *Cave management ensuring optimal life of mine at Palabora*. in Proceedings of MassMin 2008 Lulea, Sweden, pp. 63-71.

[78] Rahal, D. (2008). The use of mixed integer linear programming for long-term scheduling in block caving mines. PhD Thesis, The University of Queensland, Brisbane, Queensland, Australia, Pages 312.

[79] Rahal, D., Smith, M., Van Hout, G. J., and Von Johannides, A. (2003). *The use of mixed integer linear programming for long-term scheduling in block caving mines*. in Proceedings of 31st International Symposium on the Application of Computers and operations Research in the Minerals Industries (APCOM), Cape Town, South Africa.

[80] Ramazan, S. (2007). *Large-scale production scheduling with the fundamental tree algorithm - model, case study and comparisons*. in Proceedings of Orebody Modelling and Strategic Mine Planning, Perth, Western Australia.

[81] Ramazan, S., Dagdelen, K., and Johnson, T. B. (2005). Fundamental tree algorithm in optimising production scheduling for open pit mine design. *Mining Technology : IMM Transactions section A*, *114* (1), 45-54.

[82] Ramazan, S. and Dimitrakopoulos, R. (2004a). *Recent applications of operations research and efficient MIP formulations in open pit mining*. in Proceedings of SME Annual Meeting, SME, Cincinnati, Ohio, pp. 73-78.

[83] Ramazan, S. and Dimitrakopoulos, R. (2004b). Traditional and new MIP models for production scheduling with in-situ grade variability. *International Journal of Surface Mining, Reclamation & Environment*, *18* (2), 85-98.

[84] Rech, W., Keskimaki, K. W., and Stewart, D. S. (2000). *An update on cave development and draw control at the Henderson*. in Proceedings of MassMin

2000, The Australasian Institute of Mining and Metallurgy: Melbourne, Brisbane, pp. 495-505.

[85] Rojas, E., Molina, R., Bonani, A., and Constanzo, H. (2000). *The pre-undercut caving method at the E1 Teniente mine, Codelco Chile*. in Proceedings of MassMin 2000, The Australasian Institute of mining and Metallurgy:Melbourne., Brisbane, pp. 261-266.

[86] Rubio, E. (2002). Long-term planning of block caving operations using mathematical programming tools. MSc Thesis, University of British Columbia, Vancouver, Canada, Pages 116.

[87] Rubio, E. (2006). Block cave mine infrastructure reliability applied to production planning. PhD Thesis, University of British Columbia, Vancouver, Pages 132.

[88] Rubio, E., Caceres, C., and Scoble, M. (2004b). *Towards an integrated approach to block cave planning*. in Proceedings of MassMin 2004, Santiago, Chile, pp. 128-134.

[89] Rubio, E. and Diering, T. (2004a). *Block cave production planning using operations research tools*. in Proceedings of MassMin 2004, Santiago, Chile, pp. 141-149.

[90] Runge Limited (2009). XPAC Autoscheduler. Ver. 7.8.

[91] Russell, F., M. (1987). *Application of a PC-based network analysis program to mine scheduling*. in Proceedings of 20 Internationa Symposium on the Application of Computers and Mathematics in the Mineral Industries, SAIMM, Johannesburg, South Africa, pp. 123-1312.

[92] Sherer, H. E. and Gentry, D. W. (1982). *Use of an interactive dynamic program system as an aid to mine valuation*. in Proceedings of 17 Application of Computers and Operations Research in the Mineral Industry, Society of Mining Engineers of the Amwrica Institute of Mining, Metallurgical, and Petroleum Engineers, Inc., New York, pp. 161-169.

[93] Smith, M. L. (1999). Optimizing inventory stockpiles and mine production: an application of separable and goal programming to phosphate mining using AMPL/CPLEX. in *CIM Bulletin*, vol. 92, pp. 61-64.

[94] Smith, M. L., Sheppard, I., and Karunatillake, G. (2003). *Using MIP for strategic life-of-mine planning of the lead/zinc stream at Mount Isa Mines*. in Proceedings of 24th international symposium, Application of computers in the mineral industry(APCOM), Cape Town, South Africa, pp. 465-474.

[95] Song, X. (1989). *Caving process simulation and optimal mining sequence at Tong Kuang Yu mine, China*. in Proceedings of 21st Application of Computers and Operations Research in the Mineral Industry, Society of mining Engineering of the American Institute of Mining, Metallurgical, and Petroleum Engineers, Inc. Littleton, Colorado., Las Vegas, NV, USA, pp. 386-392.

[96] Su, Y. L. (1986). *A computer solution to the Queuing problem at a mine-mill interface*. in Proceedings of 19th Application of Computers and Operations Research in the Mineral Industry, Society of mining Engineering of the American Institute of Mining, Metallurgical, and Petroleum Engineers, Inc. Littleton, Colorado., Pennsylvania State University, USA, pp. 394-400.

[97] Summers, J. (2000). *Analysis and management of mining risk*. in Proceedings of MassMin2000, The Australasian Institute of Mining and Metallurgy:Melbourne, Brisbane, Australia, pp. 63-82.

[98] Tabesh, M. and Askari-Nasab, H. (2011). Two-stage clustering algorithm for block aggregation in open pit mines. *Mining Technology*, *120* (3), 158-169.

[99] Tobie, R. L. and Julin, D. E. (1982). Block caving: Chapter 1, general description. in *Underground Mining Methods Handbook*, W. A. Hustrulid, Ed. New York, Society of Mining Engineers of the American Institute of Mining, Metallurgical, and Petroleum Engineers, Inc. , pp. 967-972.

[100] Topal, E. (2008). Early start and late start algorithms to improve the solution time for long-term underground mine production scheduling. *Journal of The South African Institute of Mining and Metallurgy*, *108* (2), 99-107.

[101] Trout, L. P. (1995). *Underground mine production scheduling using mixed integer programming*. in Proceedings of 25th international symposium, Application of computers in the mineral industry (APCOM), Brisbane, Australia, pp. 395-400.

[102] Van As, A. and Van Hout, G. J. (2008). *Implications of widely spaced drawpoints*. in Proceedings of MassMin 2008, Lulea University of Technology Press, Lulea, Sweden, pp. 147-154.

[103] Weintraub, A., Pereira, M., and Schultz, X. (2008). A priori and a posteriori aggregation procedures to reduce model size in MIP mine planning models. *Electronic Notes in Discrete Mathematics*, *30* (0), 297-302.

[104] Winkler, B. M. (1996). *Using MILP to optimize period fix costs in complex mine sequencing and scheduling problems*. in Proceedings of 26th International Symposium, Application of Computers and Operations Research in the Mineral Industry(APCOM), Socity of Mining Engineers of the American Institute of Mining, Metallurgical, and Petroleum Engineers, Inc, Littleton, Colorado, pp. 441-446.

[105] Winkler, B. M. (1998b). *System for quality oriented mine production planning with MOLP*. in Proceedings of 27th International Symposium, Application of Computers in the Mineral Industry (APCOM), Royal School of Mines, London, United Kingdom, pp. 53-59.

[106] Winkler, B. M. and Griffin, P. (1998). *Mine production scheduling with linear programming-development of a practical tool*. in Proceedings of 27th International Symposium, Application of Computers in the Mineral Industry

(APCOM), Institution of Mining and Metallurguy, London, United Kingdom, pp. 673-679.

[107] Wolsey, L. A. (1998). *Integer programming.* J. Wiley, New York, Pages 264.

[108] Wooller, R. (1992). Production scheduling system. *Transactions of the Institution of Mining and Metallurgy, Section A*, *101* 47-554.

APPENDIX

CONFIGURATION OF DSBC FOR BLOCK-CAVE PRODUCTION SCHEDULING (DSBC: Drawpoint Scheduling in Block-Caving)

This appendix introduces the open-source software application with a graphical user interface called drawpoint scheduling in block-caving (DSBC). This appendix explains how the sequence of extraction in a block cave mine can be optimized using the mixed-integer linear programming (MILP) formulations in the DSBC. This appendix presents the workflow and documentation on how to use DSBC software. The prototype software helps transfer knowledge and optimization technology developed in this research to practitioners and end-users in the field of block-cave production scheduling.

1 Introduction

The main industrial contribution of this research includes development and testing of a prototype open-source software application with a graphical user interface, DSBC. The prototype software helps transfer knowledge and optimization technology developed in this research to practitioners and end-users in the field of block-cave production scheduling.

The mining concepts and strategy, clustering, and mathematical formulations outlined in Chapter 3 were developed as numerical models representing the MILP framework application in Chapter 4. In this appendix, an open-source software application with a graphical user interface called drawpoint scheduling in block-caving (DSBC) is introduced. The appendix also explains how the sequence of extraction in a block-cave mine can be optimized using the MILP formulations in the DSBC.

All stages before scheduling, from creating a block model to converting a slice file, are done using GEMS and PCBC (Gemcom Software International, 2012). These stages include:

1. Creating a block model using GEMS.
2. Importing drawpoints data such as coordinates, dip, and azimuth.
3. Creating a slice file using PCBC.
4. Calculating the best height of draw (BHOD).

After creating the slice file, all the clustering and optimization steps are done using the DSBC. These steps are as follows:

1. Importing the slice file, the BHOD file, and coordinates of drawpoints into DSBC.

2. Creating all required databases and sets to use in the developed MILP models.

3. Clustering the draw columns based on the similarity of the draw column's tonnage, average grade, and physical location.

4. Defining the scheduling parameters.

5. Creating the objective function and constraints for three levels of resolution: cluster level, drawpoint level, and drawpoint-and-slice level.

6. Solving the problem using one of the methods: either single-step or multi-step.

7. Plotting the results.

2 Required Software to Run the DSBC

To run the DSBC, at the beginning MATLAB and TOMLAB/CPLEX must be installed on the computer. MATLAB is a high-level language and interactive environment for numerical computation, visualization, and programming. Using MATLAB, the user can analyze data, develop algorithms, and create models and applications. The language, tools, and built-in math functions enable users to explore multiple approaches and reach a solution faster than with spreadsheets or traditional programming languages, such as C/C++ or Java. TOMLAB is a general-purpose development and modeling environment in MATLAB for research, teaching, and finding practical solutions to optimization problems. TOMLAB/CPLEX integrates the solver package CPLEX with MATLAB and TOMLAB.

3 Experiments Framework for the MILP Models

The methodology applied to the block-cave production scheduling problem in the MILP framework includes a solution scheme that is based on the branch-and-cut optimization algorithm (Horst and Hoang, 1996) implemented in TOMLAB/CPLEX (Holmstrom, 2011). To be able to obtain reliable experimental results, the solution scheme employed in solving the problem should be able to capture the complete definition of the block-cave production scheduling problem.

The assumptions are based on the framework for applying operations research methods in mining. Figure 1 shows the general workflow of database creation in the DSBC. After creating the database, based on the selected level of resolution, the problem is solved. These levels include the cluster level, drawpoint level, and drawpoint-and-slice level.

The three MILP formulations for three levels of problem resolution -- cluster level, drawpoint level, and drawpoint-and-slice level -- can be used in two ways: (i) single-step, in which each formulations is used independently; and (ii) multi-step, in which each step's solution is used to reduce the number of variables in the next level and consequently generate a practical block-cave schedule in a reasonable CPU runtime for large-scale problems. Figure 2 and Figure 3 show the general workflow for single-step and multi-step methods, respectively. It should be mentioned that the MILP formulations use a solver developed based on exact solution methods for optimization. In this solver, an optimization termination criterion is set up to stop the algorithm when an integer feasible solution has been proved to be within a specific percentage of optimality, subject to the practical and technical mining constraints.

4 Input Data

To solve the problem we use the PCBC's slice file. Three Excel files with the following information have to be prepared:

- *Coordinates*: This file contains two sheets titled "Drawpoints" and "Tunnels." Figure 4 shows the order of these Excel sheets. The order of columns in the sheet titled Drawpoints is record, drawpoint's name, X, Y, and depth. In the sheet titled Tunnels, the coordinates of the start point and endpoint of each tunnel are defined.

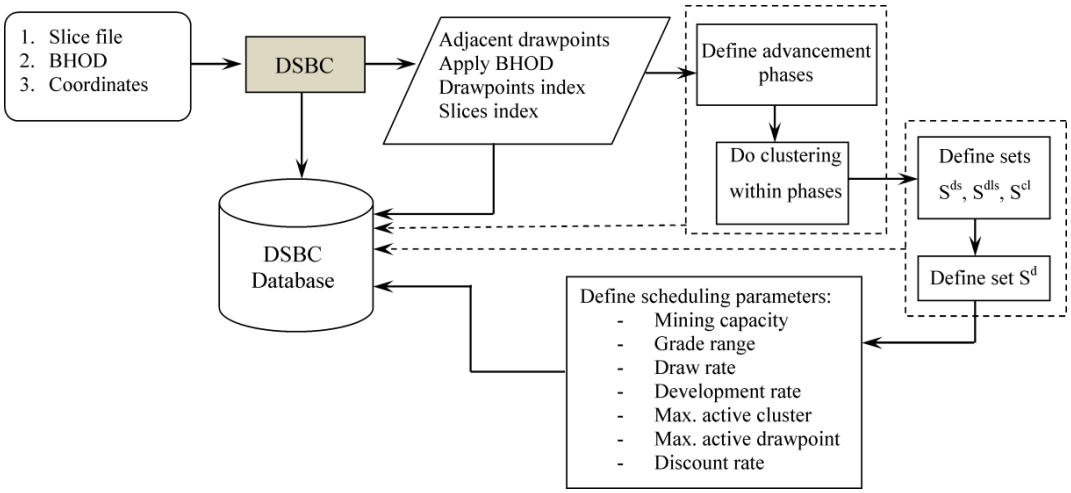

Figure 1. Database creation in the DSBC

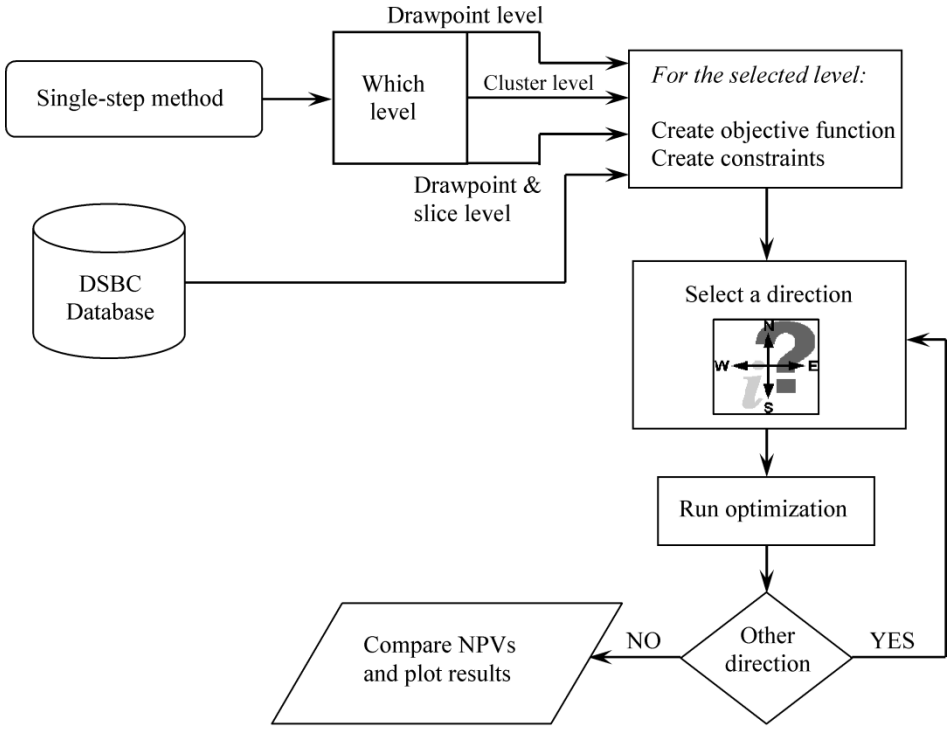

Figure 2. General workflow for single-step method

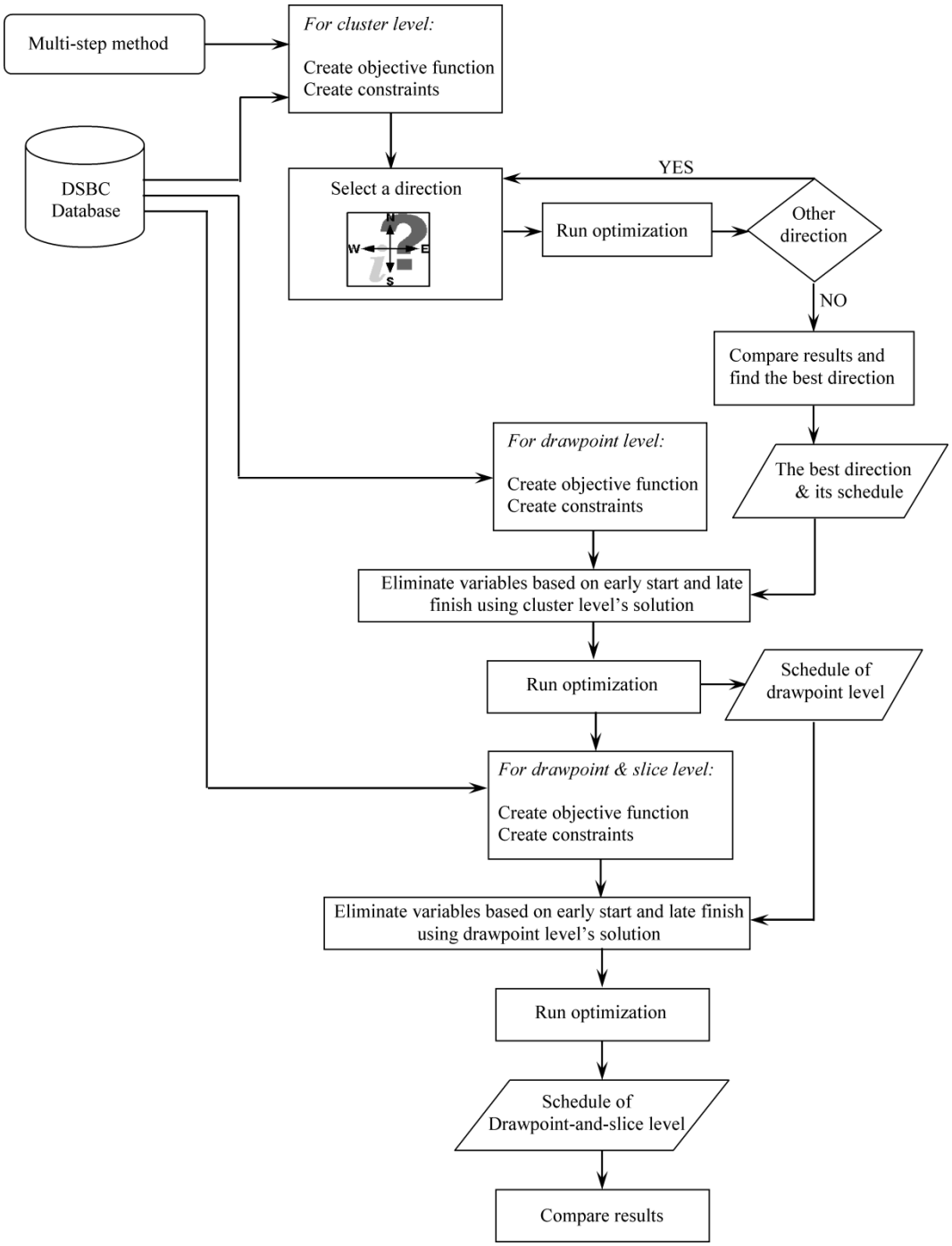

Figure 3. General workflow for multi-step method

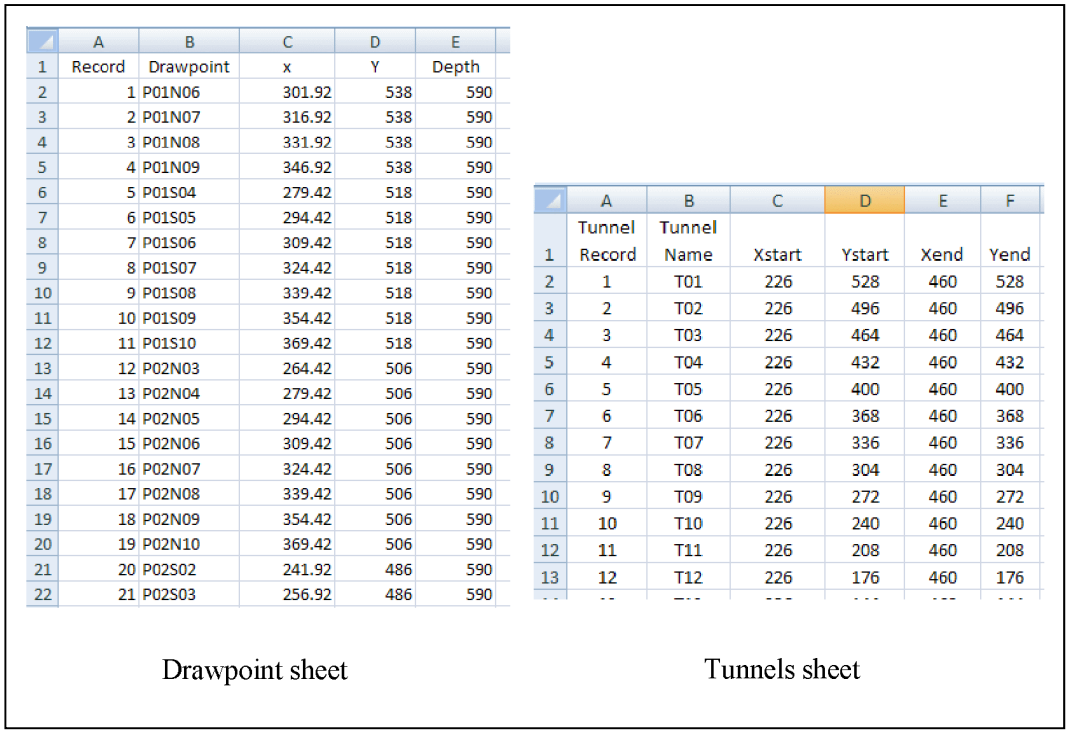

	A	B	C	D	E
1	Record	Drawpoint	x	Y	Depth
2	1	P01N06	301.92	538	590
3	2	P01N07	316.92	538	590
4	3	P01N08	331.92	538	590
5	4	P01N09	346.92	538	590
6	5	P01S04	279.42	518	590
7	6	P01S05	294.42	518	590
8	7	P01S06	309.42	518	590
9	8	P01S07	324.42	518	590
10	9	P01S08	339.42	518	590
11	10	P01S09	354.42	518	590
12	11	P01S10	369.42	518	590
13	12	P02N03	264.42	506	590
14	13	P02N04	279.42	506	590
15	14	P02N05	294.42	506	590
16	15	P02N06	309.42	506	590
17	16	P02N07	324.42	506	590
18	17	P02N08	339.42	506	590
19	18	P02N09	354.42	506	590
20	19	P02N10	369.42	506	590
21	20	P02S02	241.92	486	590
22	21	P02S03	256.92	486	590

Drawpoint sheet

	A	B	C	D	E	F
1	Tunnel Record	Tunnel Name	Xstart	Ystart	Xend	Yend
2	1	T01	226	528	460	528
3	2	T02	226	496	460	496
4	3	T03	226	464	460	464
5	4	T04	226	432	460	432
6	5	T05	226	400	460	400
7	6	T06	226	368	460	368
8	7	T07	226	336	460	336
9	8	T08	226	304	460	304
10	9	T09	226	272	460	272
11	10	T10	226	240	460	240
12	11	T11	226	208	460	208
13	12	T12	226	176	460	176

Tunnels sheet

Figure 4. Structure of drawpoints and tunnels sheets in the Excel file

- *Slice info:* This file contains information about slices within each draw column. These data include dilution, density, tonnage, dollar value, and percentage of the elements within each slice. Figure 5 shows the order of parameters in this file.
- *BHOD:* This file contains the BHOD information for draw columns and other economic information. Figure 6 shows the order of this file.

5 Guideline on Running DSBC

The DSBC folder contains sub-folders, .tif and .m files (see Table 1). Within the folder DSBC, right click on the *DSBC_Login.m*, and then open it in MATLAB. In MATLAB, run the opened text file. If you have been asked to change the directory, accept it and change the directory. In the opened login window, enter User name and Password. Then press **Login** (see Figure 7). The main window of DSBC comes up (see Figure 8).

	A	B	C	D	E	F	G	H	I	J
1	Record	Slice Name	Descriptic	Height	Dil %	Density	Tons	$val	CU	AU
2	1	P07S03	... Vmix10	10.00	0	2.80	3,007.59	25.95	1.48	0.50
3				20.00	1	2.80	5,790.37	24.73	1.47	0.43
4				30.00	4	2.80	6,438.14	22.97	1.42	0.41
5				40.00	8	2.79	6,702.38	20.89	1.36	0.38
6				50.00	13	2.79	6,676.88	18.16	1.27	0.35
7				60.00	20	2.78	6,675.91	14.94	1.17	0.32
8				70.00	26	2.77	6,639.00	11.39	1.06	0.28
9				80.00	33	2.77	6,696.08	7.68	0.94	0.25
10				90.00	41	2.76	6,731.95	3.84	0.82	0.22
11				100.00	49	2.75	6,605.59	(0.09)	0.70	0.18
12				110.00	57	2.74	6,491.40	(3.86)	0.58	0.15
13				120.00	65	2.73	6,414.18	(7.30)	0.47	0.12
14				130.00	72	2.73	6,396.01	(10.30)	0.37	0.10
15				140.00	78	2.72	6,417.30	(12.85)	0.29	0.08
16				150.00	83	2.72	6,406.64	(15.00)	0.22	0.06
17				160.00	87	2.71	6,390.34	(16.77)	0.17	0.04
18				170.00	91	2.71	6,390.87	(18.18)	0.12	0.03
19				180.00	94	2.71	6,409.45	(19.27)	0.09	0.02
20				190.00	96	2.70	6,380.00	(20.10)	0.06	0.02
21				200.00	97	2.70	6,428.43	(20.70)	0.04	0.01
22				210.00	98	2.70	6,493.94	(21.12)	0.03	0.01
23				220.00	99	2.69	6,513.13	(21.41)	0.02	0.00
24				230.00	99	2.68	6,472.15	(21.60)	0.01	0.00
25				240.00	99	2.67	6,478.63	(21.72)	0.01	0.00
26				250.00	100	2.66	6,507.08	(21.79)	0.01	0.00
27				260.00	100	2.65	6,520.76	(21.83)	0.01	0.00
28				270.00	100	2.63	6,482.01	(21.84)	0.01	0.00
29				280.00	100	2.61	6,505.49	(21.84)	0.01	0.00
30				290.00	100	2.59	6,062.47	(21.83)	0.01	0.00
31				300.00	100	2.57	6,069.73	(21.81)	0.01	0.00
32				310.00	100	2.55	6,071.42	(21.79)	0.01	0.00
33				320.00	100	2.54	6,071.42	(21.77)	0.01	0.00
34				330.00	100	2.54	6,071.42	(21.77)	0.01	0.00
35				334.50	100	2.50	2,439.55	(21.86)	0.00	0.00
36										
37	2	P08N03	... Vmix10	10.00	1	2.80	3,007.59	27.37	1.57	0.42
38				20.00	3	2.80	5,790.37	24.71	1.48	0.40

Figure 5. Structure of the slice file

	A	B	C	D	E	F	G	H	I	J
1	Record	Draw Point	OK?	Best HOD	Ave_Dol	Net_Dol	Tot_Dol	Tonnage	CU	AU
2	1	P07S03	OK	90	15.95049	882.9919	882.9919	55358.29	1.198847	0.337136
3	2	P08N03	OK	80	14.90038	723.4717	723.4717	48553.92	1.173203	0.311591
4	3	P07S04	OK	160	19.85667	2037.188	2037.188	102594.6	1.3276	0.360297
5	4	P08N04	OK	140	19.59518	1744.636	1744.636	89033.96	1.323794	0.348382
6	5	P07S05	OK	220	21.16943	3000.261	3000.261	141726.1	1.372936	0.363632
7	6	P08N05	OK	210	20.68158	2789.119	2789.119	134860.1	1.358006	0.358263
8	7	P07S09	OK	280	20.46782	3713.835	3713.835	181447.5	1.344116	0.371735
9	8	P08N09	OK	280	21.31608	3871.473	3871.473	181622.1	1.378115	0.363758
10	9	P07S10	OK	280	17.35229	3178.504	3178.504	183174.9	1.244121	0.347454
11	10	P08N10	OK	280	19.56856	3588.879	3588.879	183400.3	1.320371	0.353706
12	11	P07S11	OK	270	12.15976	2116.752	2116.752	174078.4	1.073345	0.315853
13	12	P08N11	OK	280	15.41513	2786.104	2786.104	180738.3	1.184623	0.326591
14	13	P08S04	OK	100	14.25443	879.1486	879.1486	61675.44	1.151218	0.309256

Figure 6. Structure of the file containing the BHODs

Table 1. Existing sub-folders, photos and MATLAB files within the DSBC's folder

Folders	.tif files	.fig files	.m files
1. FUNCTION	1. BlockCave1	1. DSBC_Login	1. DSBC_Login
2. IMPORT	2. BlockCave2		
3. Input Data	3. BlockCave3		
4. MODELS			
5. REPORTS			
6. RESULTS			
7. TOMLAB Input			
8. TOMLAB Output			

Figure 7. DSBC's login window

The components of the main window are menu bar, system information area, and date and time information area. The menu bar contains File, Preparation, Clustering, Display, Sets, Models, Variable Elimination, Run, and Solution Analysis.

In the system information area, useful information about the computer which the DSBC is running on that and version of the MATLAB are presented. Under the system information area, the date and time of the current and previous login is displayed.

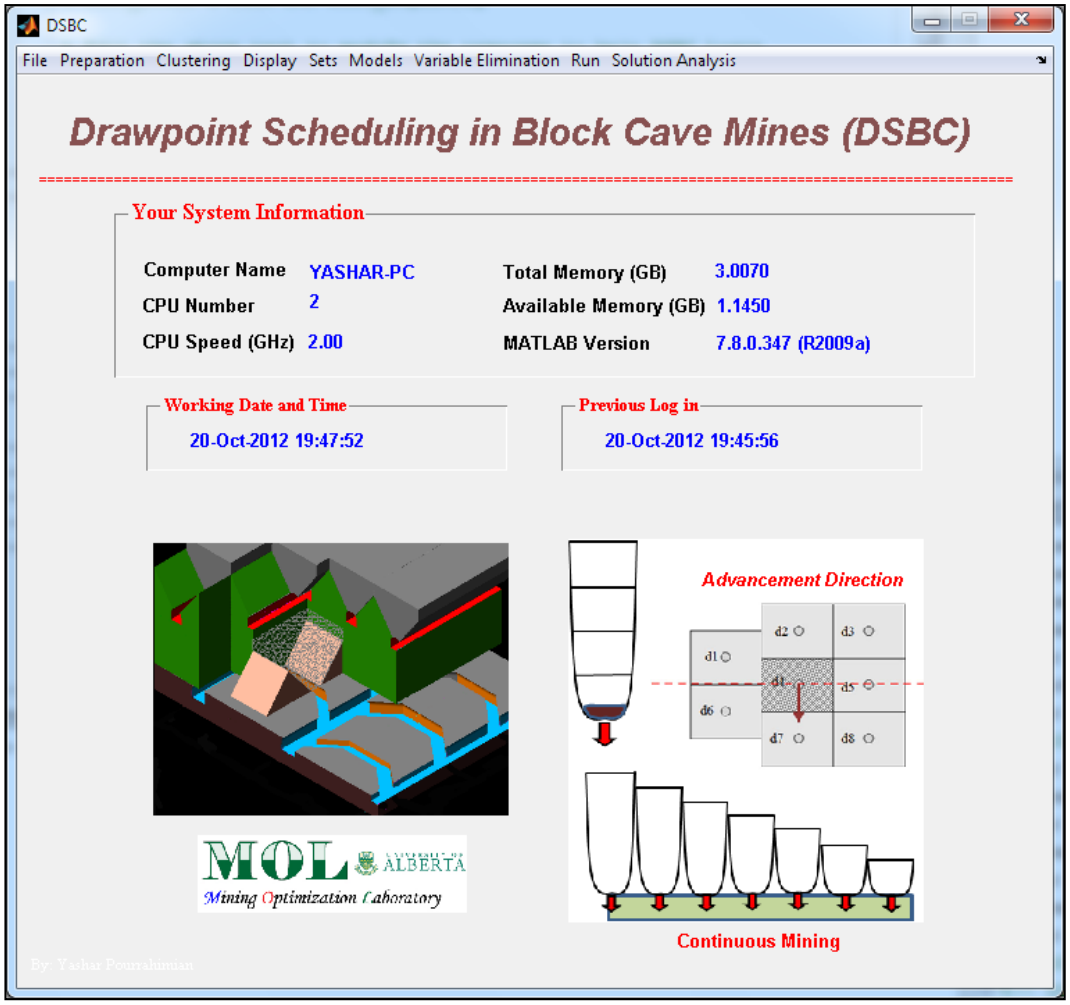

Figure 8. Main window of the DSBC

5.1 Database Preparation

After executing the DSBC, to create a new project, go to:

File > Set New Problem

If there is another project, this option makes a back up from that project and then creates a new project. To import the three main Excel files into the DSBC, go to **File > import .xls to DSBC**. In the opened window, import the Excel files one by one. Then press **OK** (see Figure 9). After the Excel files are imported, they have to be converted to the MATLAB format. For this purpose, go to **File > Convert To .mat**.

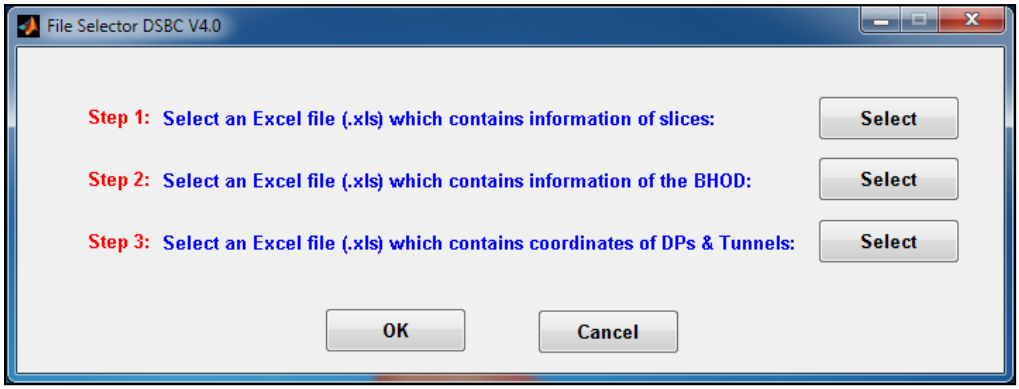

Figure 9. Import window

A window titled **Excel 2 MATLAB** comes up (see Figure 10). In this window you have to follow the steps. After each step the window is updated at the left bottom corner, and green lines appear.

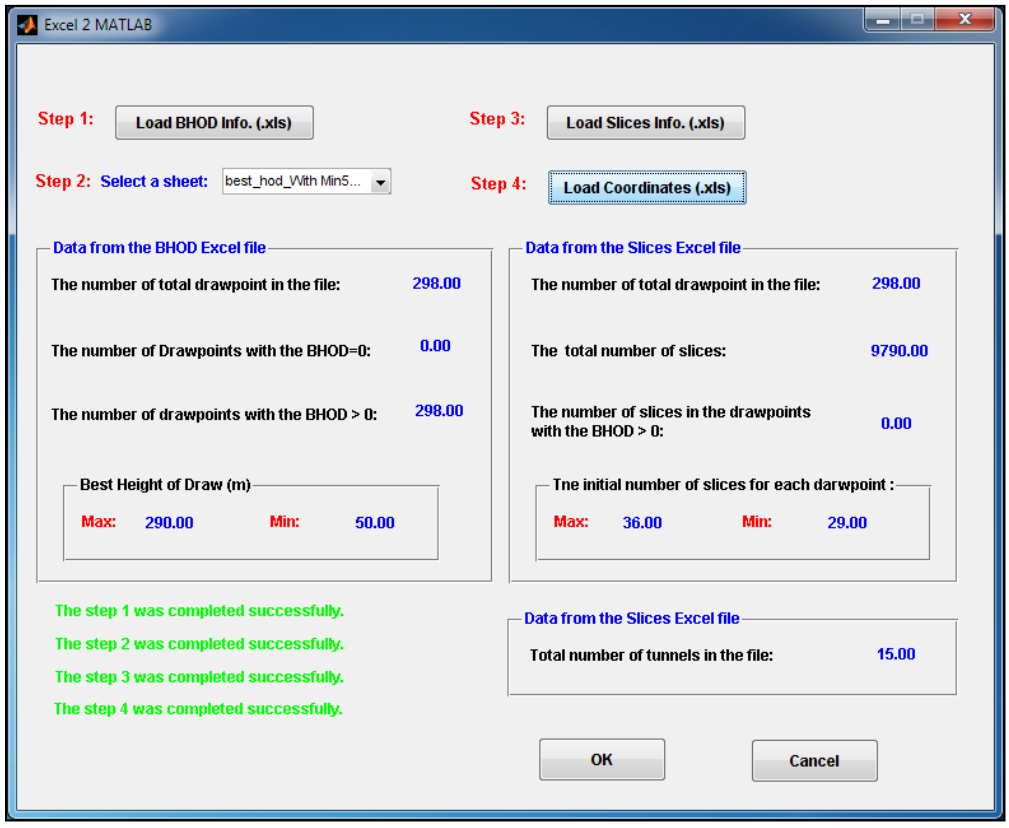

Figure 10. Excel 2 MATLAB window to convert .xls files to .mat

In the Excel 2 MATLAB window, Press **Load BHOD Info. (.xls)**. Then, from the pop-up menu in front of Step 2, select the sheet which contains the BHODs (see Figure 11).

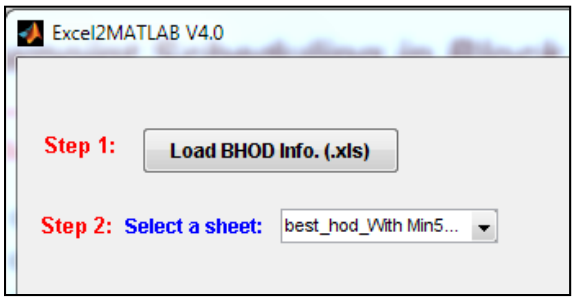

Figure 11. Selection of the sheet which contains the BHOD information

Press **Load Slice Info. (.xls)** to convert the slices info, and then Press **Load Coordinates (.xls)**. Check the data. Then press **OK**.

As the next step, the adjacent drawpoints and the drawpoints located between tunnels are recognized. Also, for each drawpoint-and-slice, an index is defined and the BHODs are applied on the initial draw columns. All this is done using the **Preparation** menu. Under this menu, there are five options. Select these options in the following order. After each step a dialog box is opened and displays useful information about the step.

1. **Preparation > Find Adjacent Drawpoints**
2. **Preparation > Create Index for Drawpoints**

In the opened window, enter the height of the slices.

3. **Preparation > Find Drawpoints Between Tunnels**
4. **Preparation > Apply BHOD on Slice file**
5. **Preparation > Create Index for Slices**

The **Display** menu allows a user to show the plan view of drawpoints, 3D view of draw columns, initial height of draw columns, and height of draw columns after applying the BHOD. To show these views, go to the **Display** menu and select the

related option. If there is a draw column with BHOD = 0 in the data, it can be displayed using the last option under the **Display** menu.

5.2 Clustering and Creating the Sets

The next step is clustering. Before clustering, the advancement directions must be defined. For this purpose, go to **Clustering > Advancement Areas**. In the opened window, select a direction and press **APPLY**. This will display the plan view of the drawpoints and tunnels. Now, based on the advancement direction, the boundary of phases must be created in the following order:

- WE or EW: the lines should be created from left to right.
- NS or SN: the lines should be created from bottom to top.
- SWNE or NESW: the lines should be created from the left bottom corner to the right top corner.
- NWSE or SENW: the lines should be created from the right bottom corner to the left top corner.

Each line has two points. These points must be out of the black dash-line boundary. To pick the start and end points of the lines, use the LEFT click on the mouse. However, for the last line, the last point MUST be selected by the RIGHT click on the mouse. Figure 12 shows the advancement lines for the west to east (WE) and east to west (EW) directions. There are seven lines for the WE and EW directions. To define the phases boundaries for other directions, press **CLEAR** and then select another direction and press **APPLY**. Then, repeat the steps described in the previous sentence. Finally, press **OK**. The next step is the clustering of the draw columns within each phase. However, before clustering, the data must be prepared. For this purpose, go to **Clustering > Preparation**.

To cluster the draw columns within each phase using the hierarchical clustering method, go to **Clustering > Method > DPs Clustering Hierarchical**. Then, select a direction for clustering and press **Plot**.

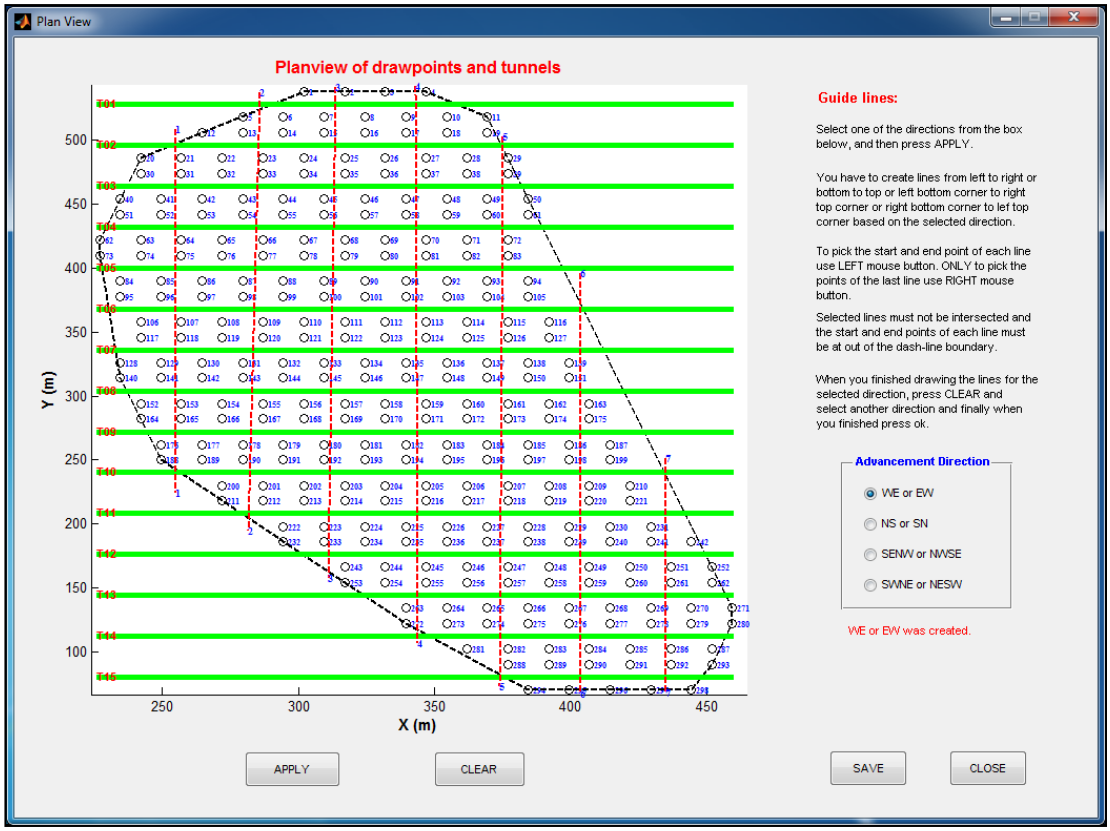

Figure 12. The window for advancement line selection with the phases boundaries for the WE or EW directions

Afterwards, the clustering parameters input window comes up; in this window type the required numbers (see Figure 13). If you press **OK**, the clusters in the selected direction appear. To find the best weights that create practical clusters, you have to repeat the clustering with different weights.

After clustering, you can analyze the clusters or display them. For this purpose, go to **Clustering > Display**.

Two options are available (see Figure 14). Using **DP Clusters**, you can display the clusters in the selected direction. Using **DP Clusters Analysts**, you can obtain useful information about the clusters and drawpoints within each cluster. This information includes tonnage, average grade, economic value, and number of drawpoints within each cluster. Go to **Clustering > Display > DP Clusters Analysts**.

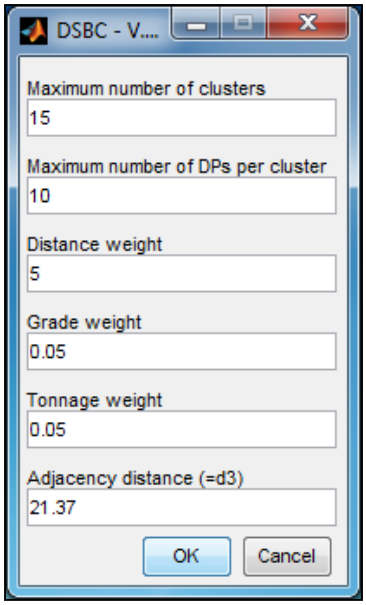

Figure 13. The clustering parameters input window

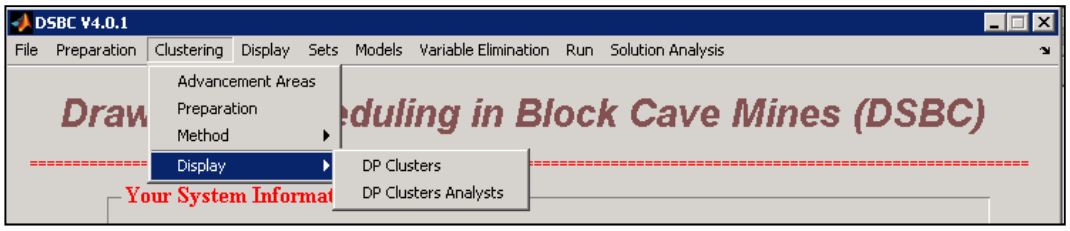

Figure 14. Available options for cluster displaying and analyzing in the DSBC

The DP Cluster Analysts window comes up. Select one of the existing directions and then press **PLOT**. The window on the left will display clusters from the selected direction. The window on the right will display tonnage, average grade, economic value, and number of draw columns for each cluster. At the bottom of the main window, each cluster can be analyzed based on tonnage, grade, and the economic value of the draw columns within the cluster. Figure 15 illustrates the DP Cluster Analysts window.

All the required sets explained in Chapter 3 are created through the **Sets** menu. To create sets S^{ds}, S^{dls}, S^{adj}, S^{CL}, and S^{d}, go to the menu called **Sets** (see Figure 16) and then select the options in the following order:

Sets > Create Sds, Sdls, Sadj

Sets > Create SCL

Sets > Create Sd

Figure 15. Cluster analysts window

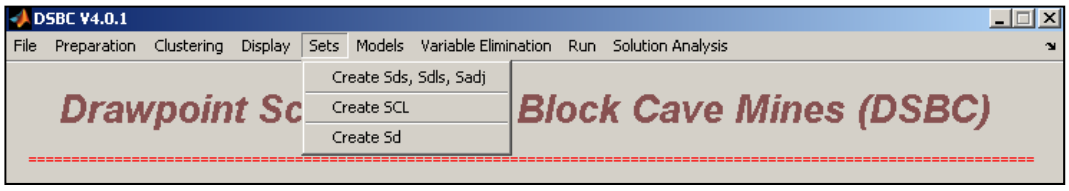

Figure 16. Sets menu to create all the required sets

5.3 MILP Models Preparation

To create the MILP models, the first step is to define of all the scheduling parameters based on the considered model. For this purpose there are two options. To define the scheduling parameters for the clustering-level model, go to

Models > Scheduling Parameters > Model With Cluster

In the opened window, select a direction and then press the **Schedule** button. A window will come up in which to enter the scheduling parameters for the clustering-level model (see Figure 17).

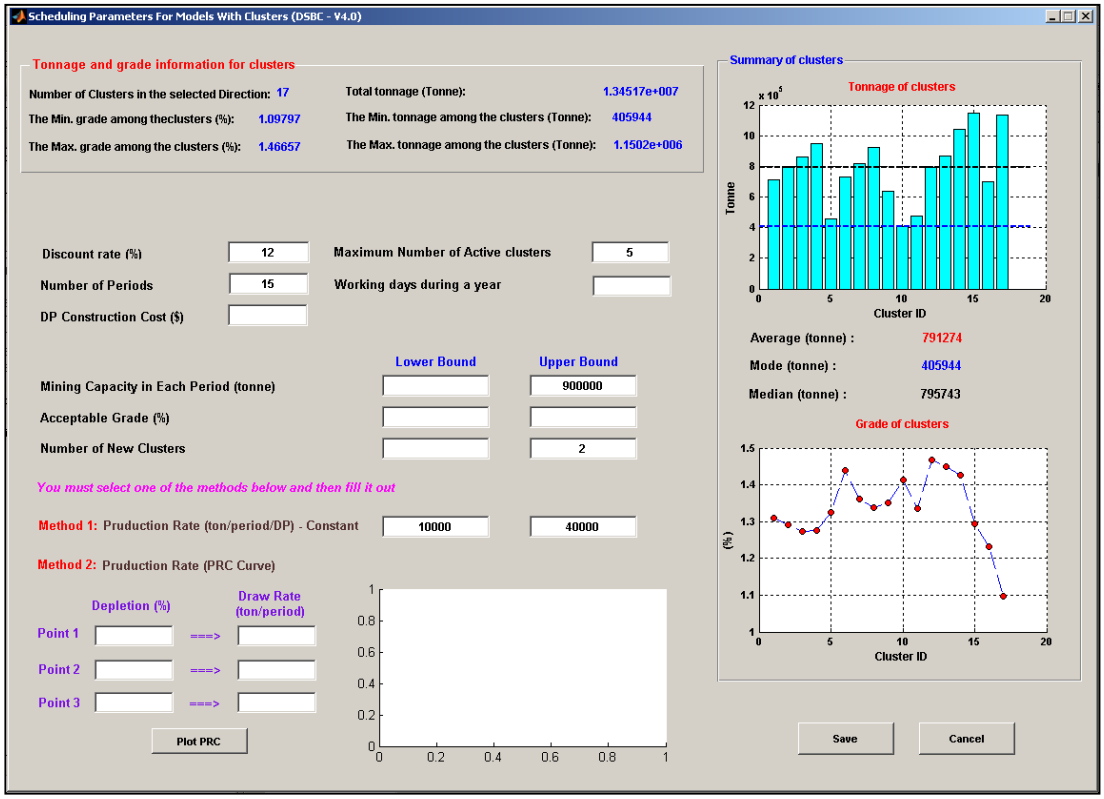

Figure 17. Scheduling parameters definition window for the cluster-level model

At the top part of this window, there is a summary about the minimum and maximum grade and tonnage among the clusters. Displayed on the right side of the window are the average grade of each cluster and its tonnage with the average, mode, and median lines. Fill out the blank boxes based on the project requirements. At the cluster-level model, user does not need to define the acceptable grade. For the draw rate, two different methods can be applied: (i) constant range, and (ii) production rate curve (PRC). Enter the drawpoint production rate in method 1. It will be automatically calculated for each cluster.

Finally press the **SAVE** button. The summary of the entered data will appear; review the summary. If it is correct, press **OK**.

To define the scheduling parameters for the other models, go to

Models > Scheduling Parameters > Model Without Cluster

At the top of the open window, a summary of the useful data about the drawpoints and slices is presented. The right-hand side of the window displays the histograms related to the mentioned data (see Figure 18).

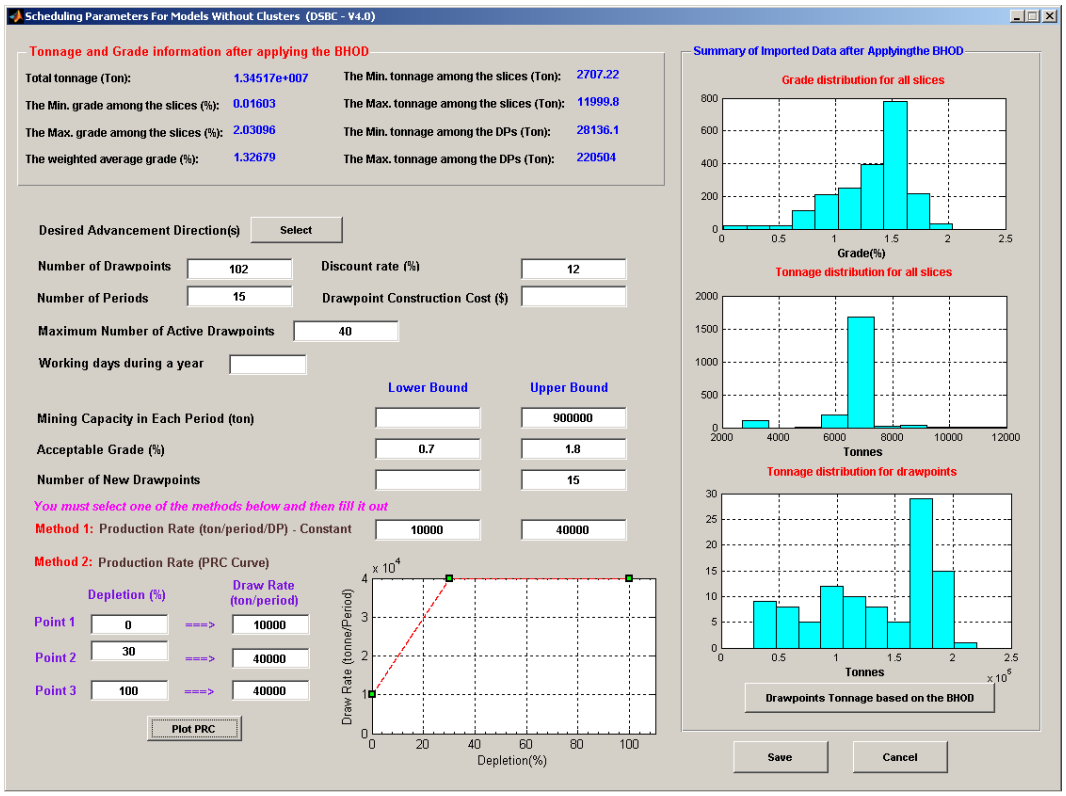

Figure 18. Scheduling parameters definition window for the drawpoint level and drawpoint-and-slice level models

Press the **Select** button in front of Desired Advancement Direction(s) and then select the scheduling directions. Then, press **OK** (see Figure 19). Fill out the blank boxes according to the project requirements. This time the acceptable grade must be defined. Finally, press the **SAVE** button. The summary of the entered data will appear. Check for accuracy. If everything is correct, press **OK**.

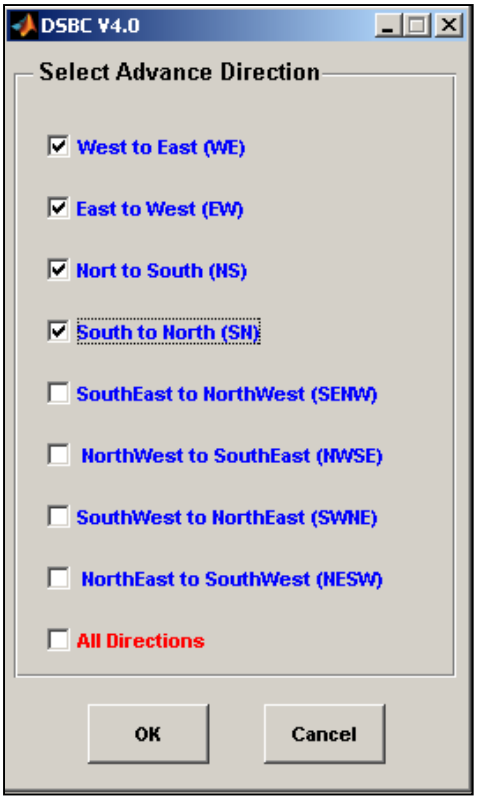

Figure 19. Direction selection window

After defining the scheduling parameters and in order to create the models go to **Models > Create** and select the level of resolution needed to solve the problem. For example, to solve the problem at the cluster level, go to **Models > Create > Clustered DPs**. A mathematical model creator window will appear (see Figure 20). To see the formulation in detail, press the **Display Model** button. Create objective function and constraint in the order that has been appeared.

To create the draw rate constraint, select the **Lower and Upper Bounds option**. For the mining precedence, at the cluster level select **Set_SCL.mat** from the folder **SetSCL**. At the drawpoint level, select **Set_Sd.mat** from the folder **SetSd**. Finally, press **OK**.

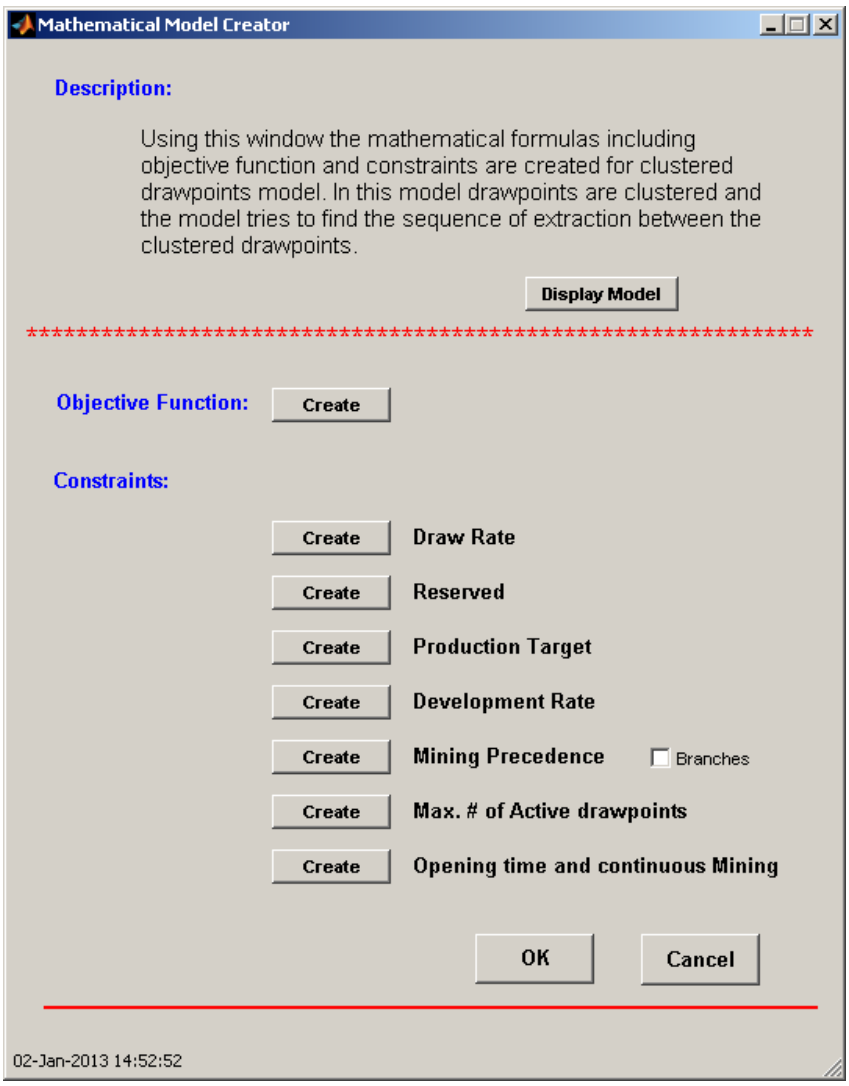

Figure 20. Mathematical model creator window for the cluster-level model

5.4 Scheduling Optimization

The MILP formulations presented for three levels of problem resolution -- cluster level, drawpoint level, and drawpoint-and-slice level -- can be used in two ways: (i) a single-step method in which each of the formulations is used independently, and (ii) a multi-step method in which each step's solution is used to reduce the number of variables in the next level and consequently generate a practical block-cave schedule in a reasonable CPU runtime for large-scale problems.

- **Single-Step Method**

After the model for each level of resolution has been created, it can be solved using the **Run** menu. For this purpose, go to **Run > Export to TOMLAB**. Select the model that you have created, and press the **Export** button. Then go to **Run > Solve the Model**.

TOMLAB/CPLEX is executed automatically. Then, a window comes up (see Figure 21). In this window, select the model and the advancement direction for optimization. Then enter the relative tolerance on the gap between the best integer objective and the objective of the best node remaining. For example, for the EPGAP of 1%, type 1 in the box. Finally, based on the number of available CPUs on your computer, enter the number of required CPUs to solve the selected model and press **Solve**.

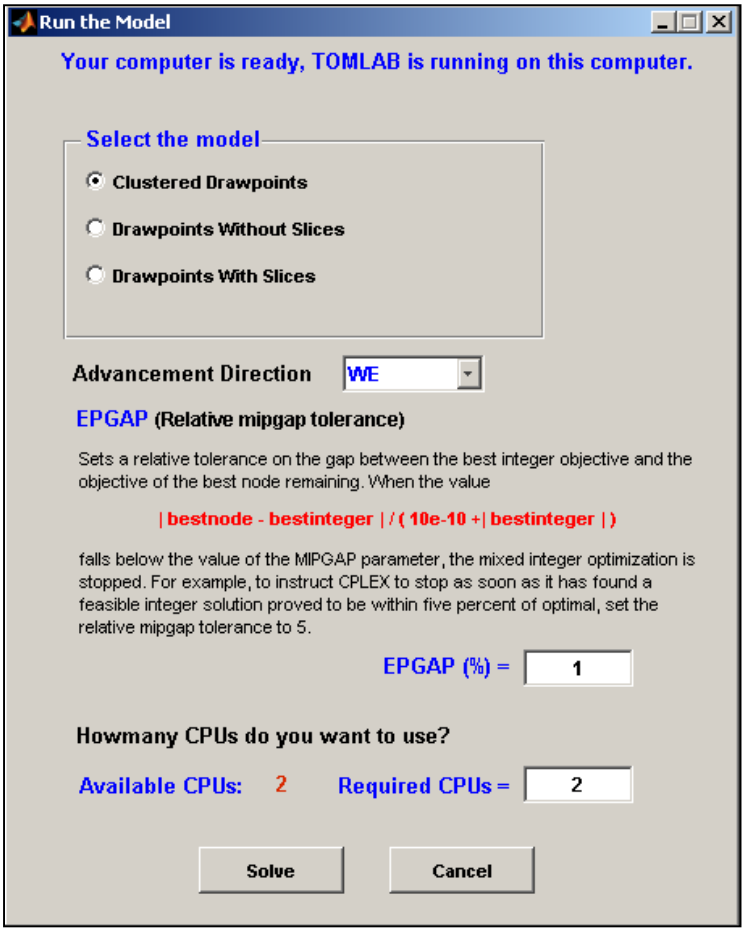

Figure 21. The window for defining the optimization criteria

After solving the problem in the selected advancement direction, to display the obtained results, go to **Solution Analysis > Results Preparation** and then select the related model and prepare it. To plot the results, go to **Solution Analysis > Plot Results**.

- **Multi-Step Method**

To solve the problem using the multi-step method, create all models. After creating the models, go to **Run > Export to TOMLAB**.

Select the cluster level model and export it. Then go to **Run > Solve the Model**. Select **Clustered Drawpoints** as a model and a direction to run the optimization. Enter the proper numbers for the EPGAP and the number of required CPUs. When the problem was solved, select another direction and solve the problem in that direction. Using **Plot Wizard**, recognize the best advancement direction for the obtained solutions in the selected directions. For this purpose, go to **Solution Analysis > Results Preparation** and then select the cluster-level model and prepare it. Afterwards, go to **Solution Analysis > Plot Results** and analyze the results to find the best advancement direction.

Then, go to **Variable Elimination > Cluster to Drawpoint Level**. Afterwards, go to **Run > Export to TOMLAB**. Select **Drawpoint Without Slices** and export it. Then, go to **Run > Solve the Model**. Select **Drawpoint Without Slices** as the model. The advancement direction must be the direction which had the maximum net present (NPV) value at the cluster level. Enter the proper numbers for EPGAP and the number of required CPUs and then solve the problem. After solving the problem at the drawpoint level, in order to solve it at the drawpoint-and-slice level, go to **Solution Analysis > Results Preparation** and select **Drawpoint Without Slices** and prepare it. Afterwards, go to **Variable Elimination > Drawpoint to Slice Level**. Select the solution of the drawpoint level as the starting period. Then, go to **Run > Export to TOMLAB**. Select **Drawpoint With Slices** and export it. Solve the problem at the drawpoint-and-slice level. The advancement direction must be that direction which had the maximum NPV at the

cluster level. Enter the proper numbers for EPGAP and the number of required CPUs and then solve the problem.

After solving the problem, using the **Plot Wizard** you can analyze the results and compare different models.

5.5 Result Analysis

After solving the problem, results must be prepared for display. For this purpose, go to **Solution Analysis > Results Preparation** and select the related model and prepare it. Next, to plot the results, go to **Solution Analysis > Plot Results**. The **Plot Wizard** window will appear (see Figure 22). Select a model and then plot the results based on available options.

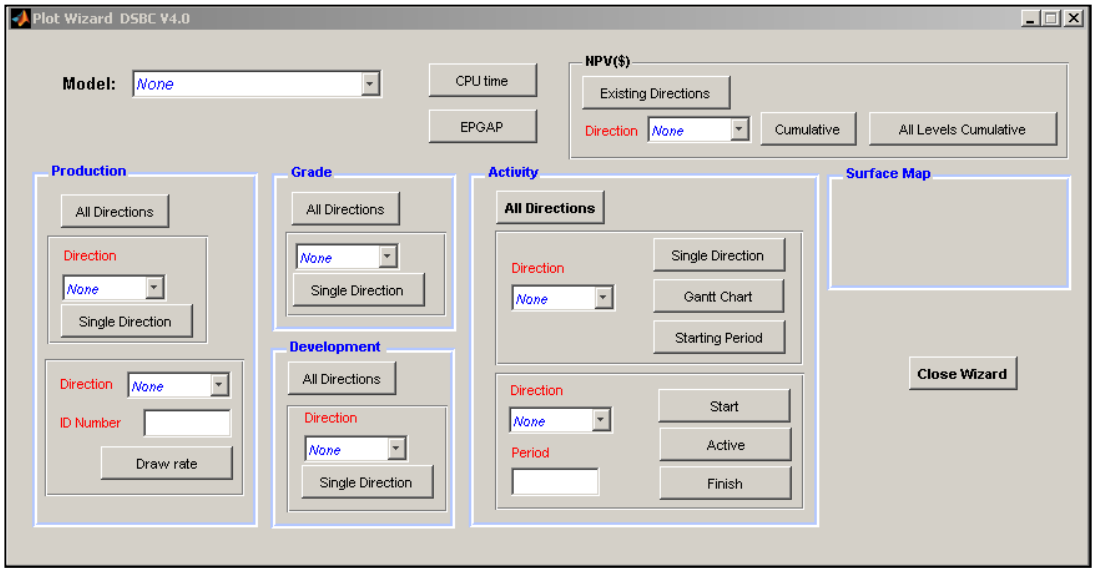

Figure 22. Plot wizard window